UNCLASSIFIED

AD 402 358

Reproduced
by the

DEFENSE DOCUMENTATION CENTER

FOR

SCIENTIFIC AND TECHNICAL INFORMATION

CAMERON STATION, ALEXANDRIA, VIRGINIA

UNCLASSIFIED

NOTICE: When government or other drawings, specifications or other data are used for any purpose other than in connection with a definitely related government procurement operation, the U. S. Government thereby incurs no responsibility, nor any obligation whatsoever; and the fact that the Government may have formulated, furnished, or in any way supplied the said drawings, specifications, or other data is not to be regarded by implication or otherwise as in any manner licensing the holder or any other person or corporation, or conveying any rights or permission to manufacture, use or sell any patented invention that may in any way be related thereto.

402 358

ANALYSIS AND EVALUATION OF SEISMIC DATA FOR ON-SITE INSPECTION PROJECT VELA

FINAL REPORT
CONTRACT No. AF33(600)-43368

Roland F. Beers, Inc. 2/23/63

By

Lawrence B. Luhrs
Lawrence L. Davis

ASTIA
APR 30 1963
TISIA A

Distribution List

FINAL REPORT

CONTRACT NO. AF33(600)-43368

Recipient	Address	No. Copies
Vela Seismic Information Analysis Center	University of Michigan P. O. Box 618 Ann Arbor, Michigan	2
RAND Corporation Attn: Dr. Richard Latter	1700 Main Street Santa Monica, California	1
Seismological Laboratory California Institute of Tech. Attn: Dr. Hugo Benioff	220 North San Rafael Street Pasadena, California	1
Columbia University Lamont Geological Observatory Attn: Professor Jack Oliver	Palisades, New York	1
Coast and Geodetic Survey Attn: Geophysics Division	U. S. Department of Commerce Washington 25, D. C.	1
Field Laboratory Coast and Geodetic Survey	Sandia Base Albuquerque, New Mexico	1
U. S. Atomic Energy Commission Division of Military Applications	Washington 25, D. C.	1
Defense Atomic Support Agency Blast and Shock Division	Washington 25, D. C.	1
U. S. Arms Control and Disarmament Agency Attn: Mr. Charles Gellner	Department of State Washington 25, D. C.	2
Lawrence Radiation Laboratory Attn: Dr. Roland Herbst	Livermore, California	1
Shell Development Company Attn: Dr. Sidney Kaufman	P. O. Box 481 Houston 1, Texas	1
Dr. Clark Goodman Prengle, Dukler and Crump, Inc.	5417 Crawford Street Houston, Texas	1

Distribution List (Cont'd.)

FINAL REPORT

CONTRACT NO. AF33(600)-43368

Recipient	Address	No. Copies
Institute for Defense Analyses Research and Engineering Support Division	1825 Connecticut Ave., N.W. Washington 9, D. C.	1
Air Force Cambridge Research Laboratories Attn: CRZGW	L. G. Hanscom Field Bedford, Massachusetts	1
Air Force Office of Scientific Research Attn: SRPG	Temporary Building D Washington 25, D. C.	1
Armed Services Technical Information Agency	Arlington Hall Station Arlington 12, Virginia	2
U. S. Geological Survey Division of Experimental Geology	Department of Interior Washington 25, D. C.	1
VELA UNIFORM Data Analysis and Technique Development Center	314 Montgomery Street Alexandria, Virginia	1
Air Force Technical Applications Center	Headquarters U. S. Air Force Washington 25, D. C.	2
Nuclear Test Detection Office Advanced Research Projects Agency	Department of Defense Washington 25, D. C.	5
Stanford Research Institute Attn: Dr. Robert Vaile	Palo Alto, California	1

ANALYSIS AND EVALUATION OF SEISMIC DATA FOR ON-SITE INSPECTION - PROJECT VELA

FINAL REPORT
CONTRACT NO. AF 33(600)-43368

Table of Contents

		Page No.
1.0	Introduction	1
2.0	Conclusions	3
3.0	Stratigraphy and Structure of Rainier Mesa	7
	3.1 Generalized Stratigraphic Section of Oak Spring Formation, Rainier Mesa, Nye County, Nevada as Delineated by the U.S.G.S.	8
	3.2 Summary of the Average Mineral Composition (Percent by Volume) of Oak Spring Formation (at Rainier Test Site), Nevada Test Site, Nye County, Nevada as Determined by the U.S.G.S	10
4.0	Pre-Shot Physical Properties of the Oak Spring Formation, Rainier Site	11
	4.1 Average Values for Some Physical Properties of Units of the Oak Spring Formation at Rainier Test Site as Determined by the U.S.G.S	12
	4.2 Pre-Rainier Velocities Hagestad Location Reported by the U.S.G.S	15
	4.3 Interval Velocities from U.S.G.S. Velocity Survey of UCRL Drill Hole 3, Rainier Site	16
	4.4 Pre-Shot Values of Physical Properties of Tos_3 Lithologic Unit at Blanca Site	16
	(Figures 4.1 through 4.5)	
5.0	Post-Shot Physical Properties, Oak Spring Formation and Subsurface Effects	18
	5.1 Average Velocities Observed 325 Feet West of Evans Ground Zero by U.S.G.S. Following Rainier Event	20
	5.2 Average Velocities Observed at Evans Zero Location by U.S.G.S. Following Rainier Event	21
	(Figures 5.1 through 5.6)	
6.0	Structural Changes	22
	(Figures 6.1a through 6.2b)	
7.0	Instrumentation	25
	(Figures 7.1 through 7.15)	

Table of Contents (Continued)

		Page No.
8.0	Uphole Velocity Surveys..... (Figures 8.1 through 8.7)	27
9.0	Near-Surface Velocity Profiling..... (Figures 9.1 through 9.50)	32
10.0	First Arrival Amplitudes..... (Figures 10.1 through 10.30)	38
11.0	Horizontal Seismic Ranging..... (Figures 11.1 through 11.17)	41
12.0	Tatum Salt Dome..... (Figures 12.1 through 12.7)	47

Enclosure 1 Topographic Map of Rainier Mesa Showing Location of Near Surface Velocity Profiles and Uphole Velocity Surveys and Average Vertical Velocites of the Upper 75 to 100 Feet of Oak Spring Tuff

Enclosure 2 Topographic Map of Rainier Mesa Showing Results of Horizontal Seismic Ranging Survey

Enclosure 3 UED Seismic Profiles Across Tatum Salt Dome

Enclosure 4 Time Section of Tatum Salt Dome, Line I

Enclosure 5 Time Section of Tatum Salt Dome, Line II

1.0 Introduction

This report covers work performed in compliance with Air Force Technical Applications Center Project VELA T/1133/S/AMC entitled "Analysis and Evaluation of Seismic Data for On-Site Inspection - Project VELA". The contract calls for a review of seismic data and evaluation of their significance for purposes of on-site inspection.

The data were furnished by the Project Officer, A.F.T.A.C., Headquarters, U. S. Air Force, Washington 25, D. C. They included field records and ancillary notes from experimental seismic investigations conducted for A.F.T.A.C. by United Electro Dynamics, Inc. in the vicinity of and subsequent to the PLUMBOB and HARDTACK Underground Nuclear Test Programs at the Nevada Test Site and reflection records from a seismic survey of the Tatum Salt Dome in Mississippi.

The U.E.D., Inc. seismic investigations at the Nevada Test Site involve the use of near-surface velocity profiling (calibrated short spread reverse profile refraction shooting) and a new method, akin to echo ranging, known as horizontal seismic ranging to detect the effects and/or cavities produced by underground explosions.

The survey program on Rainier Mesa using near-surface profiling consisted of running three lines on top of the mesa and one line below the rim, on the mesa face, in such manner as to provide a sampling of undisturbed as well as intensely fractured tuff. The survey program using horizontal seismic ranging consisted of several shots fired at each of three H.S.R. locations distributed across the top of the mesa using different settings of horizontal directional response. Uphole velocity data were acquired in conjunction with these investigations at five locations, four of which were located on top of the mesa and one near the east rim.

The objective of the near-surface velocity survey was to delineate anomalous horizontal velocity variations and attenuation of first arrival energy in the shallow Oak Spring tuff due to explosion-produced fracturing and/or faulting. The development and use of horizontal seismic ranging, represents an effort to apply the underlying concepts of echo ranging as used in anti-submarine warfare in the ocean, to the problem of detecting cavities at long range from the surface of the ground.

To enable a complete evaluation of the seismic results, it is required to know the probable range and magnitude of the effects of the explosions on the mechanical and physical properties of the tuff. To provide a basis for such evaluation, available data on the tuff were collected and collated.

The reflection seismograph survey of Tatum Salt Dome consists of two lines, one northeast and the other southwest, across the dome. The purpose of this survey is to define the configuration of the top of the salt and other major stratigraphic units in sufficient detail to enable evaluation of the structural effects of subsequent nuclear testing.

2.0 Conclusions

The uphole velocity data acquired by U.E.D., Inc. are largely concentrated in the western part of Rainier Mesa and encompass only the upper 200 feet of the welded Tos_8 tuff. They indicate a well-defined velocity stratification, which varies laterally in both thickness and velocity. These velocity data also indicate velocity inversion at a depth corresponding to, but not necessarily identified with, any one zone of fracturing. Lateral variation in the velocity and thickness of this zone are commensurate with (if not greater than) that which occurs in adjacent layers. It is not certain that the zone of velocity inversion is continuous or parallel to the velocity stratification. Neither is it known with certainty what the relationship is between velocity stratification in the shallow section and surface topography.

Examination of the deep vertical velocity data acquired below the welded Tos_8 tuff (in conjunction with the nuclear test program on Rainier Mesa) disclosed appreciable areal velocity variation--equivalent to that observed in the shallow section and additional velocity reversals.

Since no "test program" velocity data were obtained (at locations other than the Rainier site) before and after the tests, the maximum range at which the explosions produced a detectable alteration in vertical velocity is unknown. Neither is there means for evaluating whether the vertical velocities were altered at the range of distances at which U.E.D., Inc. seismic investigations were conducted. This is so because no pre-test velocity measurements were made and all but one of the U.E.D., Inc. uphole velocity surveys are located in the western part of the mesa.

The objective of near-surface velocity profiling (short spread reverse profile refraction shooting) on Rainier Mesa was to delineate anomalous horizontal variation in the welded Tos_8 tuff, attributable to the effects of underground nuclear tests. At the horizontal ranges where the near-surface velocity survey on top of Rainier Mesa was conducted (from the LOGAN and BLANCA Events), horizontal velocity probably should be effected only by fracturing and/or faulting of the tuff. At the Rainier site, the effect of interlayer spalling and fracturing should influence horizontal velocity.

Observed refraction velocities in the area on top of and along the east rim of Rainier Mesa (where the fracturing and faulting of the welded Tos_8 tuff were most severe) are neither as high nor as low as refraction velocities observed in what is believed

to be undisturbed tuff. Salient features of the refraction velocity profile (constructed for the north-south line surveyed along the east rim of the mesa) are: a reduction in velocity from north to south, commensurate with reduction in average uphole velocity (determined from deep NSVP shot of each profile); generally lower refraction velocities than one should expect, for transmission in high velocity layers which have been delineated by uphole velocity surveys; abrupt transition from low to higher velocities midway of the line.

To evaluate the significance of variation in observed refraction velocities (where there is velocity reversal at depth), it is first required to know the position of the shot with respect to such reversal, and paths taken by first-arrival energy in reaching the surface on each profile. Since one assumption made in all refraction methods is that there is no decrease in velocity with depth, the depth and correlation of refractors could not be delineated from profile to profile on the basis of refraction data alone. Consequently, there was no way of evaluating the variation in horizontal velocity of refractors along the survey line.

The degree of uncertainty in deriving horizontal velocity from the first refraction arrival times (recorded with near-surface velocity profiles on Rainier Mesa) is of the order of ten per cent. Since post-shot U.S.G.S. evaluation of the effect of the Rainier Event on physical properties of the tuff disclosed a ten per cent velocity reduction 100 feet from the weapon point, it is doubted that detection is possible of the alteration in horizontal velocity attributable to test-produced fracturing.

Although the first refraction arrivals (recorded on a number of near-surface velocity profiles) indicate faulting, such information is of dubious value without knowing the history of the fault. If this history is known, one need not use seismic methods to locate the fault.

Also investigated by U.E.D., Inc. was variation in the attenuation of first arrival energy attributable to the effects of the tests. At the distance at which the amplitude measurements were made from the sites of the underground tests, one should only observe cumulative attenuation of amplitude deriving from the effect of fracturing and/or faulting. Alteration of the intrinsic physical properties of the tuff at these distances should be too small to produce an effect on recorded amplitudes distinguishable from that deriving from other sources.

Variations in the peak recorded amplitude of the first arrival energy are ascribed to changes in the source and source conditions, changes in the medium and the effects of geophone plant. Consequently, evaluation of the variation in peak recorded amplitudes of the direct and refraction arrivals along the line and with proximity to the sites of the LOGAN, BLANCA and RAINIER Events was unfeasible.

Evaluation of variation in the attenuation of first arrival energy due to changes in the mechanical properties of the medium along the line of survey is prevented by ambiguity in the correlation and depth of the refractors delineated by the near-surface velocity survey. Variations in gross rates of attenuation indicate extensive changes in geology but do not provide a basis for comparison.

Investigations with horizontal seismic ranging, employing a technique akin to echo ranging, to detect cavities at long range from the surface gave negative results.

The computed locations of the reflections recorded at the array show no greater concentration in the areas known to have been effected by he explosions than elsewhere. However, uncertainty in identifying valid events and indeterminate lateral velocity variations probably had a substantial effect on the results.

Uncertainty in identifying valid events may have led to some fallacious alignments. The lateral velocity variations known to exist from the uphole velocity surveys should have produced substantial error in the location of the points of reflection over and above that deriving from the need to neglect the depth component.

Since no provision is made for deriving the depth at which a reflection originated, there is no way of evaluating the depth of section examined, except from indirect evidence. On the basis of the apparent velocities determined from the move-outs of recorded events, one is inclined to conclude that no signals were recorded from below the high velocity layer constituting the base of the welded Tos_8 tuff. At this depth of penetration, no reflections would be obtained from the chimneys or cavities created by the underground test, but should derive from structural variation in the shallow section, particularly areas of intense fracturing and faulting.

The seismic survey of Tatum Salt Dome was made for the purpose of defining the configuration of the top of the salt, the top of the anhydrite and the top of the limestone in sufficient detail that the structural effects of subsequent nuclear testing might be delineated at a later date.

Despite generally poor records, it was possible to delineate the configurations of the above-mentioned horizons for all but the edges of the dome in time and depth. While there is a progressive mis-tie with depth between the calculated depths of the seismic mapping horizons and the depths of these same units identified in core holes located along the seismic survey lines, it is sufficiently small as not to qualify the interpretation and correlations.

Conversion from time to depth was made using the velocity function $V_z = 6100 + .7z$ for the sediments, 9000 feet per second for the limestone and 19,000 feet per second for the anhydrite.

While the configuration of the edge of the dome could not be evaluated from the seismic data, this is not abnormal considering the dips involved. Since the point of deterioration in record quality coincides with the edge of the dome as delineated by the U.S.G.S. and reported in Technical Letter: DRIBBLE I, this configuration was adopted.

So far as use of seismic methods for on-site detection of the effects of underground explosions is concerned, the results are inconclusive. This is particularly true of the near-surface velocity profiling (calibrated short spread reverse profile refraction shooting). What the results do illustrate is that the field techniques acceptable for conventional structural surveys are inadequate, and that half measures cannot be employed where it is desired to delineate variation in the physical properties (mechanical or intrinsic) of the medium.

The method of horizontal seismic ranging presents problems which, it is believed, cannot be resolved without a program of controlled experiments under more favorable environmental conditions. However, until these problems are fully resolved, use of this method for the detection of underground cavities presents unsurmountable difficulties.

3.0 Stratigraphy and Structure of Rainier Mesa

Rainier Mesa is a prominent topographic feature in the northwest part of the Nevada Test Site composed of the Oak Spring formation of Tertiary age. In the vicinity of the RAINIER, LOGAN and BLANCA events, this formation is about 1900 feet thick and is divided into eight lithologic units which are designated, in ascending order, Tos_1 to Tos_8. The thicknesses of these units together with their lithologic descriptions at the RAINIER site are given in Table 3.1. Information concerning the thickness and lithology of these units at the LOGAN site was limited to the deeper units, see Table 3.1. The lithologic unit Tos_8 which caps Rainier Mesa and is the thickest welded tuff, is underlain largely by non-welded tuffaceous friable, to compact indurated rocks which are rhyolitic in composition.

The average mineral composition of the two uppermost lithologic units Tos_8 and Tos_7 of the Oak Spring formation at the Rainier site is given in Table 3.2. The stratigraphic units of the Oak Springs formation at the RAINIER site strike north 55° - 83° E. and dip 5° - 28° N.W., while at LOGAN, the beds appear to have a more northerly strike with similar general direction of dip. At the RAINIER location structure consists of northeast trending folds, with amplitudes of 50 to 120 feet, and north to northwest trending faults, with vertical displacements of up to 50 feet. In the tunnel at LOGAN, faults strike north to northeast with an average bearing of N. 30° E. and dip 75° to the southeast. These faults parallel the northeast set of joints and are probably related to them.

Joints are most numerous in the welded tuff. The joint sets at the RAINIER and LOGAN sites trend predominately north and northwest and dip steeply. Northeast trending joints are vertical or dip southeast.

Table 3.1 Generalized stratigraphic section of Oak Spring formation, Rainier Mesa, Nye County, Nevada as delineated by the U.S.G.S.

Lithologic Unit	Thickness (Feet) Rainier	Logan	Description
Tos_8	270		At the Rainier location Tos_8 consists of two ash flows of welded tuff. The lower 130 to 140 feet is quartz latitic tuff, which grades downward into coarse pumiceous nonwelded tuff of Tos_7. The upper part, which is rhyolitic welded tuff, caps Rainier Mesa. The welded tuffs are resistant to erosion and crop out as cliffs. Near vertical joints are abundant.
Tos_7	720		Tos_7 at the Rainier location has been divided into 3 subunits designated from youngest to oldest as a, b, and c. Subunit a is about 50 feet thick; and is poorly sorted, massive fine to coarse indurated pumiceous tuff. Subunit b is about 490 feet thick, and consists of granular tuff and interbedded gray tuffaceous sandstones in which pumice fragments are abundant. The rocks are soft, friable and poor to well bedded in outcrops which appear along the east slope of Rainier Mesa. Subunit c is about 180 feet thick consisting of granular, fine to coarse, indurated tuff. The Rainier explosion chamber is in subunit c.
Tos_6	0-75		Tos_6 at the Rainier location consists of fine to coarse, well-bedded welded rhyolitic tuff, which unconformably underlies Tos_7.
Tos_5	98-125		Tos_5 at the Rainier location consists of fine to coarse, well-bedded pumiceous tuff, which unconformably underlies Tos_6.

Table 3.1 Generalized stratigraphic section of Oak Spring formation, Rainier Mesa, Nye County, Nev. (Con't)

Lithologic Unit	Thickness (Feet) Rainier	Logan	Description
Tos_4	285		Tos_4 at the Rainier location consists of fine to medium nonwelded pumiceous tuff in beds from 2 to 15 feet thick.
Tos_3	100	170	Tos_3 at the Rainier location consists of nonwelded pumiceous tuff with some tuffaceous sandstones. The basal bed forms a blocky outcrop. Most beds are 12 to 35 feet thick. Locally Tos_3 is as much as 170 feet thick. At Logan Tos_3 is divided into four subunits, A through D. A is basal unit. Subunit A is a 34 foot thick massive coarse, hard locally soft or friable. Subunit B is a 23 foot thick fairly well bedded coarse tuff with luminae and beds of 4 foot thickness. Subunit C is approximately 75 feet thick. Fine grained tuff makes up about one-third this unit. The tuffs of this unit vary from soft to hard. Subunit D is some 33 feet thick and is coarse hard to medium tuff.
Tos_2	120	120	Tos_2 at Rainier is a fine to coarse, bedded to massive, nonwelded tuff; a thick bedded tuffaceou sandstone forms at top of unit. At Logan lower Tos_2 contains three beds pisolite.
Tos_1	210	210	Tos_1 at Rainier location is a fine nonwelded tuff Conglomerate, up to 5 feet thick locally forms the base of the unit. At Logan site subunit K and basal part subunit I are firmly cemented. These tuffs are well bedded and range in thickness from 1 to 5 feet. Scour and fill structure are prominent in subunit G.

Table 3.2 Summary of the average mineral composition (percent by volume) of Oak Spring formation (at Rainier Test Site), Nevada Test Site, Nye County, Nevada as determined by the U.S.G.S.

Lithologic unit	Tos_8	Tos_7 1/	
		a b	c
Number of analyses	5		47
Phenocrysts	16.4		14.7
Quartz	4.9		1.5
Alkali feldspar	7.4		5.0
Plagioclase	3.8		5.9
Biotite	.2		1.7
Pyroxene and amphibole	2/		.12
Magnetite	.15		.48
Xenoliths			4.9
Shards and lapilli	83.63/		74.6
Heulandite			27.0
Quartz	Dominant		
Montmorillonite			15.9
B - cristobalite	Present		9.8
Feldspar	Dominant		
Biotite			.5
Amorphous material	Present		21.4
Vesicles	3.5		5.8

1/ Tos_7 a. Upper indurated tuff
b. Middle friable tuff
c. Lower indurated tuff

2/ Not present

3/ Quartz and feldspar are the dominant minerals; glass comprises most of the amorphous material.

4.0 Pre-Shot Physical Properties of the Oak Spring Formation, RAINIER Site

Average values of the physical properties of the Oak Spring formation are tabulated in Table 4.1. The USGS estimates the accuracy of the tabulated data to be as follows:

Porosity ± 25%, bulk Density ± 5%, grain Density ± 3%
Permeability ± 100%, velocity ± 5% and strength ± 40%

The data are most complete for welded and non-welded tuff. It should be noted that each property varies considerably within each of the eight stratigraphic units, hence, small differences between the averages in Table 4.1 have little significance. However, the greatest differences occur between the welded tuff of Tos_6 and Tos_8 and the other stratigraphic units. The welded tuffs have higher strengths, higher elastic moduli, higher velocities (when unfractured), and lower porosities, than the other units. While the permeability to fluid is low, the bulk permeability due to fractures is high. The welded tuff (Tos_8) has a porosity of about one-half that of the bedded friable tuff or 14 percent. The water content is probably more on the order of 30 percent than (the measured) 15 percent indicated for most of the unweathered friable tuffs. The strength of tuff in place is probably represented more closely by the maximum value than the average value. In the natural state, the strength of tuff is estimated to be 80 percent higher than the average, or 2,200 psi. Above 10,000 psi hydrostatic pressure, non-welded tuff will deform to strains of at least 20 percent without rupture. Deformation of the order of 20 percent will increase density by 8 percent. Other strengths are probably 30 to 50 percent higher than the average. Figures 4.1 and 4.2 show the variation in velocity with axial pressure for the principal types of tuff in the Oak Spring formation. The uniformity of the velocity with pressure and strength of the welded tuff is such that the nuclear events probably did not produce a significant change in velocity via alteration of the density at appreciable distances from the detonation.

Table 4.1 Average values for some physical properties of units of the Oak Spring formation at Rainier Test Site as determined by the U.S.G.S.

Lithologic unit	Tos_8	Tos_7 1/ a	b	c	Tos_6	Tos_5	Tos_4	Tos_3	Tos_2	Tos_1
Number of samples	31		76		4	40	118	53	9	
Porosity (percent) K/ 2/	14		36	28	19	40	39	38	35	
Wet bulk density (g/cc) K/	2.3		1.9		2.2	1.8	1.9	1.9	1.9	
Dry bulk density (g/cc) K/	2.2		1.5	1.65	2.0	1.4	1.5	1.5	1.6	
Grain density (g/cc) K/	2.6		2.4	2.3	2.5	2.3	2.4	2.4	2.5	
Natural state bulk GEM/ density (g/cc)				1.92						
Water content by GEM/ volume (g/cc)				0.286						
Water content by GEM/ weight (percent)				15						
Permeability to air K/ (millidarcies)	0.66 (10)		6 (5)			21.0 (9)	0.98 (9)	0.81 (4)	0.89 (12)	0.46 (3)
(cal/deg cm sec)	2.2		1.6		2.2	1.9	1.9	2.0	1.4	
Velocity /in situ/ (ft/sec)	5/ 11,000	5/ 5,600	5/ 7,500	6/ 8,300	7/ 5,650	7/ 8,200	7/ 8,700	7/ 10,400	7/ 11,500	12,000
Compressive strength, R/ 8/ natural state (psi)				1,200						
- E (10^6 psi)				0.18						
Compressive strength R/ natural state, under hydrostatic pressure = 10^3 (psi)				5,100						
- No. samples										
- E (10^6 psi)				0.37						

Table 4.1 Average values for some physical properties of units of the Oak Spring formation at Rainier Test Site determined by the U.S.G.S. (Con't)

Lithologic unit	Tos_8	Tos_7 1/ a	b	c	Tos_6	Tos_5	Tos_4	Tos_3	Tos_2	Tos_1
Number of samples	31		76		4	40	118	53	9	
Compressive strength M/ air dry (psi)	21,100			4,700					6,100	
- No samples (strength)										
- No samples (moduli)				(5)						
- P				0.11						
- E (10^6 psi)				1.11						
- G* (10^6 psi)				0.50						
Tensile strength, M/ air dry (psi)	330			165					100	
- No samples										
- P	0.12			0.12					0.08	
- E (10^6 psi)	1.69			0.46					0.88	
- G* (10^6 psi)	0.78			0.22					0.26	
Dynamic elastic M/ moduli										
- No samples	(4)			(1)					(3)	
- E*	1.48			0.45					0.66	
- G*	0.59			0.24					0.32	

1/ Tos_7 a. Upper indurated tuff. b. Middle friable tuff. c. Lower indurated tuff; subunit c has been further subdivided during mapping of Rainier and lateral tunnels into lithologic units designated A to Z.

2/ Measurements taken from following sources: K = G. V. Keller, L = A. H. Lachenbruch, GEM = G. E. Manger, M. = U. S. Bureau of Mines, R = E. C. Robertson, RAR = R. A. Robie.

3/ Computed from average chemical composition assuming 16 percent water; average value for lithologic units T, U, and V.

4/ Average velocities taken from continuous velocity log (Schlumberger Well Surveying Corp.) in drill hole through Tos_8 and Tos_7, 800 feet from Rainier ground zero. The velocity near the surface is low (about 3,000 ft/sec) because of many open fractures.

5/ Average velocities from refraction measurement in Rainier tunnel.

6/ These velocities are average velocities taken from a continuous velocity log (Seismograph Service Corp.) in drill hole through the entire Oak Spring formation and 1 mile from the Rainier site. The velocities are to some extent dependent on overburden so they will not apply to the units where they are exposed or have shallow cover.

7/ All strength and elastic measurements were uniaxial in air except as noted. Symbols for elastic moduli: P = Poisson's ratio, E = Young's modulus, G = rigidity modulus; symbols are starred where calculated with elasticity theory.

Pre-Rainier Velocity measurements were made in the Hagestad hole southwest of the RAINIER site and, in UCRL drill hole 3, 80 feet from RAINIER ground zero.

At the Hagestad location a total of 1450 feet of Oak Spring formation was logged commencing 452 feet below the surface (165 feet below the top of Tos_7) and extending to a depth of 1943 feet. Observed interval velocities are listed in Table 4.2 and the velocity log is shown in Figure 4.3.

Table 4.2 Pre-RAINIER Velocities Hagestad Location Reported by the U.S.G.S.

Geologic Unit	Depth (ft) From	To	Velocity Range (ft/s) From	To	Average Velocity (ft/s)
Tos_7	450	1050	5000	14000	6300
Tos_6	1050	1115	5300	5700	5600
Tos_5	1115	1330	7500	10000	9000
Tos_4	1330	1510	7100	9700	9000
Tos_3	1510	1750	9000	11400	10000
Tos_2	1750	1870	10500	14400	12000
Tos_1	1870	1900	10300	11000	10500

At UCRL drill hole 3 the velocities of the different lithologic units were measured using a procedure similar to one generally employed by the petroleum industry for deep well velocity surveys. With this method shots were fired in a separate shot hole, which in this case was located 185 feet distant, and arrival times are recorded at detectors lowered down the survey hole.

The procedure provides good results when the detectors are located at considerable depth. However, as the detector nears the surface, seismic travel paths deviate appreciably from the vertical. Corrections for slant path assumed straight line travel paths and equal horizontal and vertical velocities. As a consequence of these assumptions, there is some reservation as to the accuracy of reduced velocities above 400 feet where travel paths show greatest deviation from vertical.

The interval velocities recorded at UCRL drill hole 3, by the U.S.G.S. are listed in Table 4.3.

Table 4.3 Interval Velocities from U.S.G.S. Velocity Survey of UCRL Drill Hole 3, RAINIER Site

Depth (Feet)	Interval Velocity (Ft/s)
230-270	7,150
270-310	13,700
310-395	6,650
395-525	7,070
525-675	7,180
675-775	5,850

The travel paths from shot to detector and time-depth curve obtained by U.S.G.S. are shown in Figure 4.4.

The variation in porosity, bulk density, and grain density with depth in the upper part of UCRL drill hole 3 is shown in Figure 4.5.

Although the velocity survey at UCRL drill hole 3 did not log the uppermost 100 feet of hole, the variation in porosity and bulk density from the surface to a depth of 125 feet should produce appreciable variation in interval velocity.

BLANCA Site

At the BLANCA site pre-shot evaluation of the physical properties of the Oak Spring formation was confined to the immediate vicinity of the explosion chamber which was located in the Tos_3 unit. Values of the measured physical properties of the tuff (as determined by the U.S.G.S.) are listed in Table 4.4.

Table 4.4 Pre-Shot Values of Physical Properties of Tos_3 Lithologic Unit at BLANCA Site

Percent Water Content	18.0%
Water Content by Volume	0.34 g/cc
Grain Density	2.3 g/cc

Natural State Bulk Density	1.9 g/cc
Dry Bulk Density	1.5 g/cc
Porosity	33.4%

Comparison of the physical properties measured at BLANCA with their counterparts measured at the RAINIER site discloses that for the properties measured, the principal difference was in porosity.

LOGAN Site

No physical properties appear to have been evaluated at the LOGAN site. However, since BLANCA and LOGAN are in close proximity, the values of the physical properties measured at BLANCA probably also apply reasonably well at LOGAN.

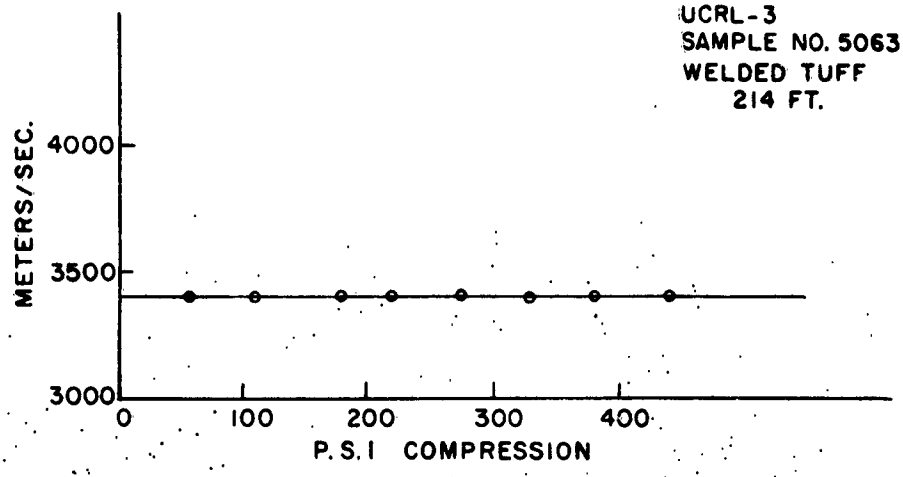

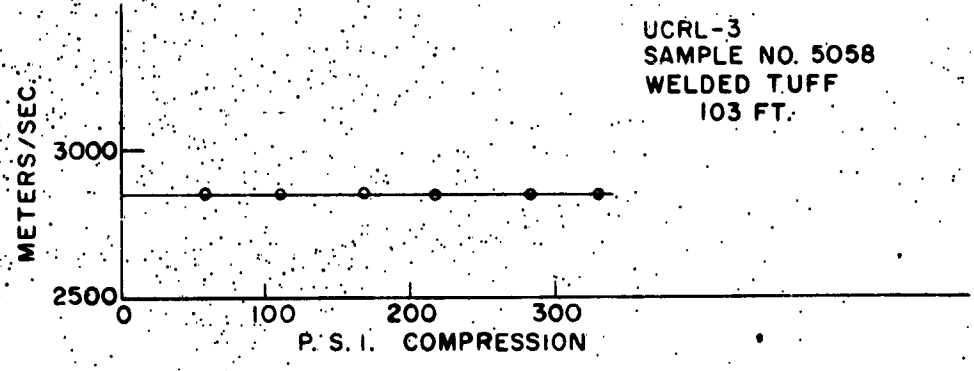

DILATIONAL VELOCITY VERSUS AXIAL PRESSURE

FIGURE 4.1

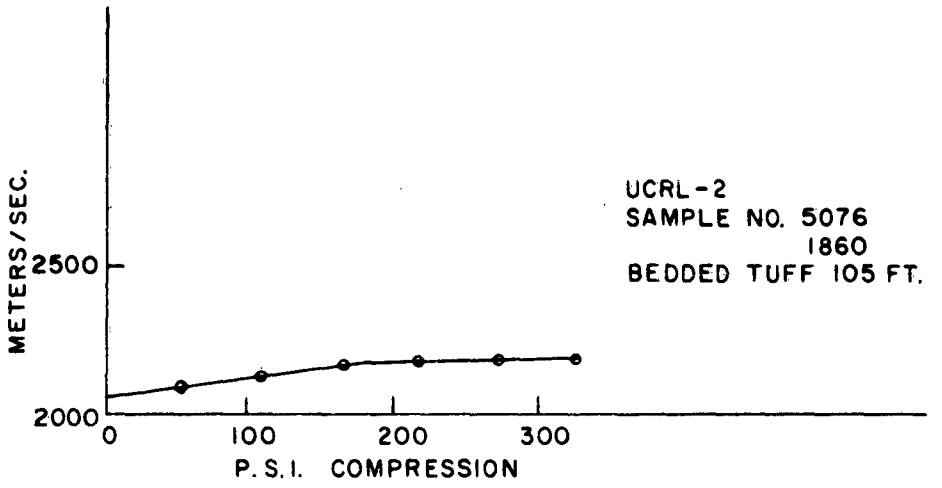

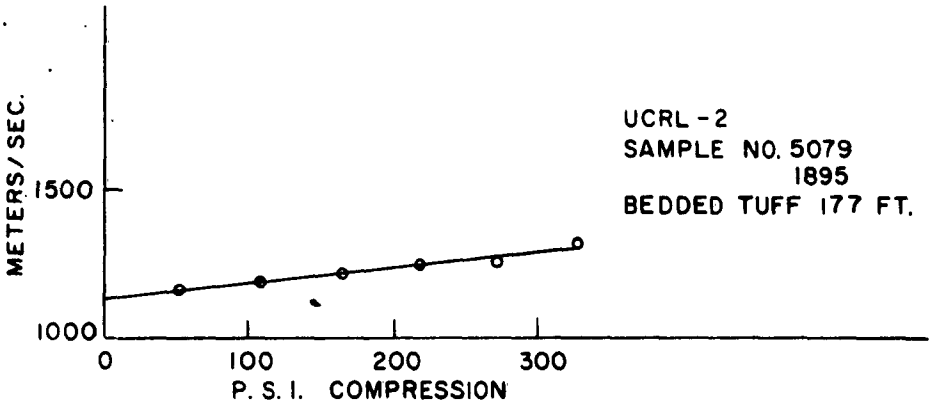

DILATIONAL VELOCITY VERSUS AXIAL PRESSURE

FIGURE 4.2

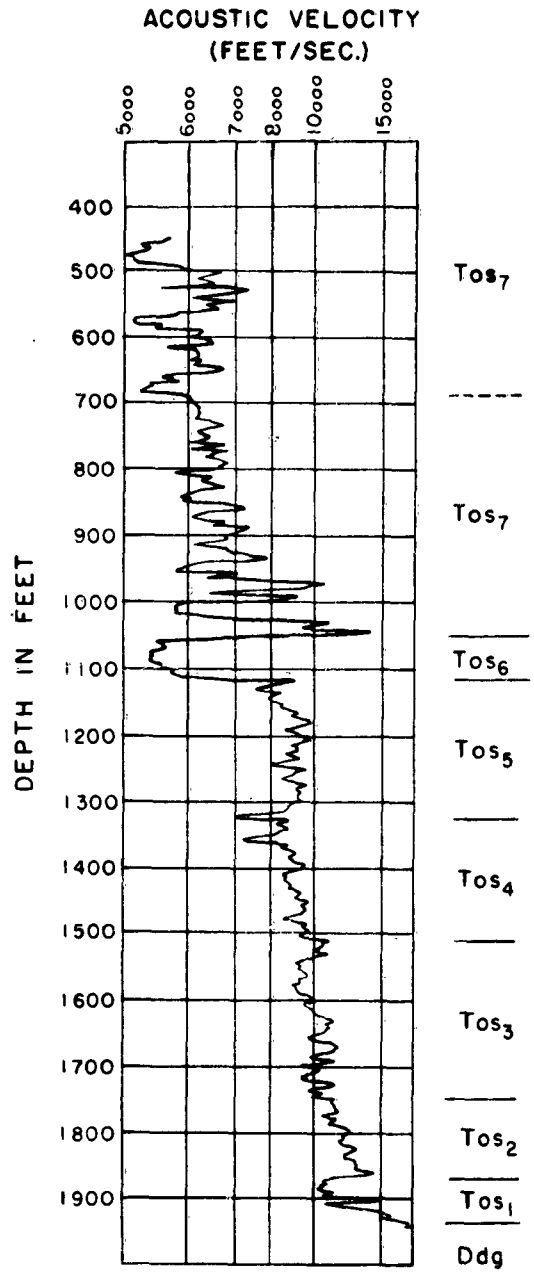

FIGURE 4.3 ACOUSTIC LOG
HAGESTADT HOLE

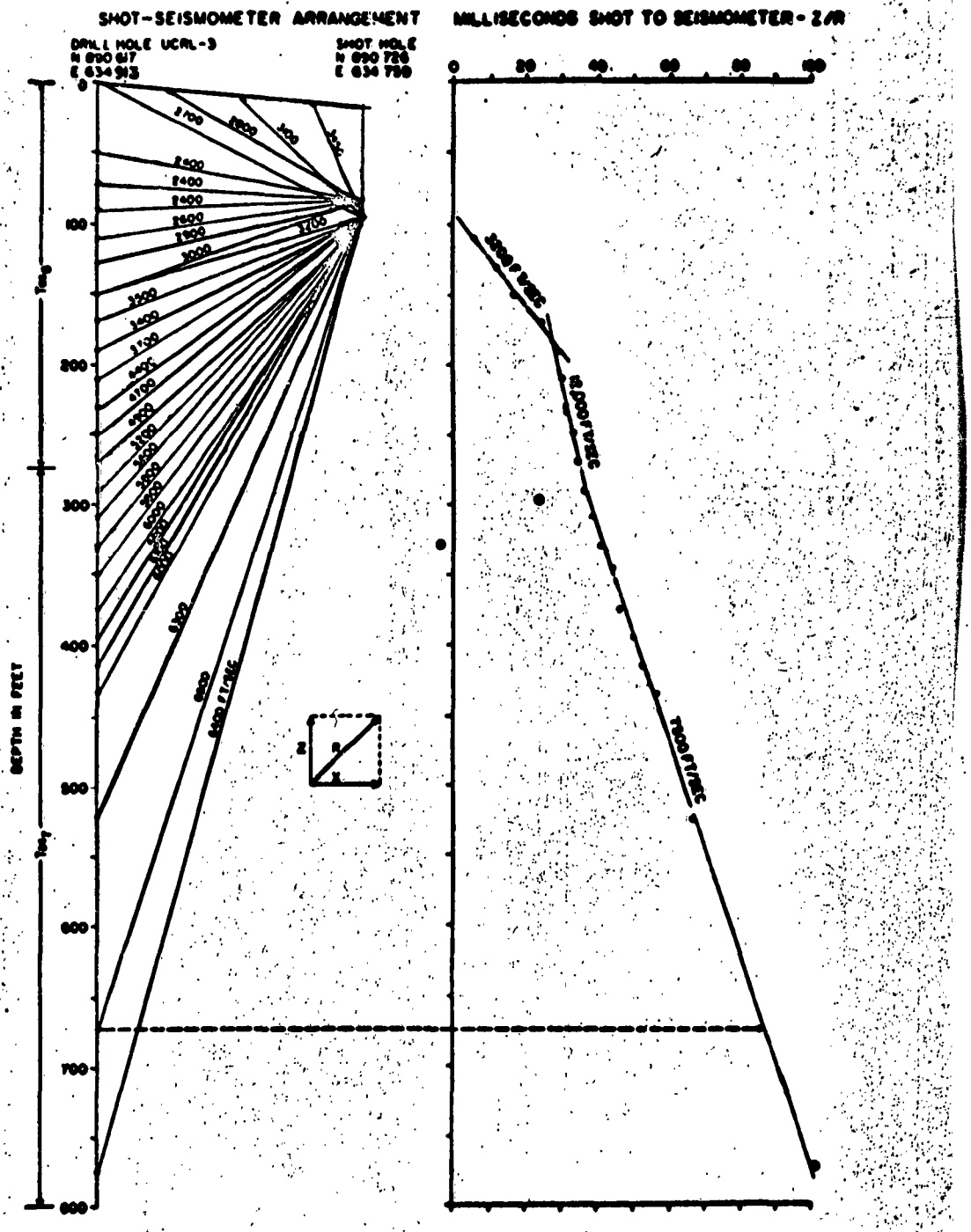

Fig. 4.4 Pre-Rainier velocity survey in drill hole UCRL-3, Nevada Test Site

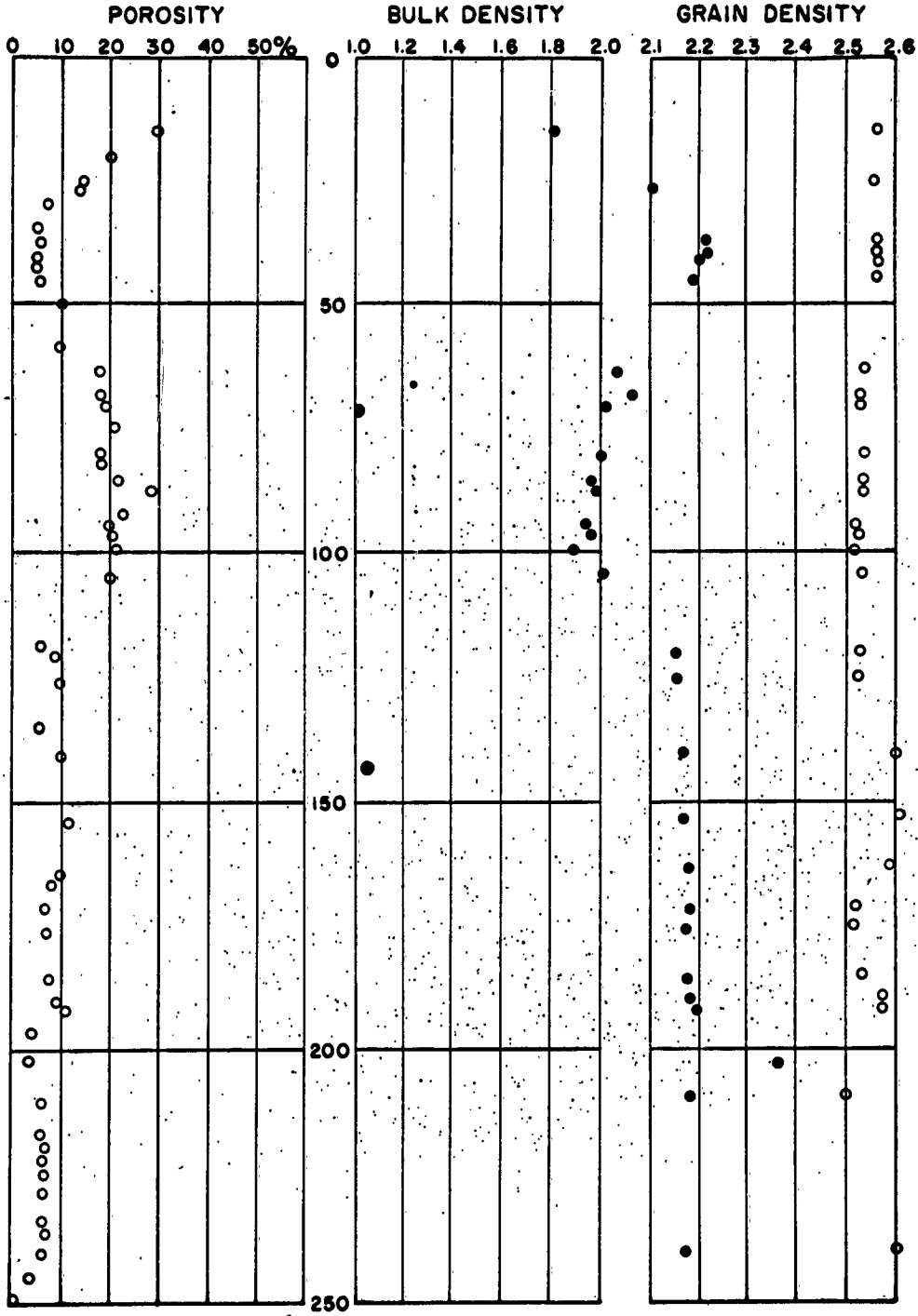

FIG. 4.5 POROSITY AND DENSITY MEASUREMENTS FOR SAMPLE FROM THE FIRST 250 FEET IN DRILL HOLE 3, UCRL SITE.

5.0 Post-Shot Physical Properties Oak Spring Formation and Subsurface Effects

The shape of the fracture zone surrounding the RAINIER Event is shown on Figure 5.1. The zones of varying degrees of disaggregation surrounding the shot chamber are shown on Figure 5.2.

Evaluation of changes in the physical properties were made by the U.S.G.S. by comparing the properties of post-shot samples near the explosion to the properties of post-shot samples of similar rocks distant from the explosion. The results are summarized in Figures 5.3. The summarized data, indicates explosion caused differences in certain physical properties, including permeability, porosity, water content, and strength properties.

The samples of breccia zone that were measured indicate that the porosity of both matrix and fragments is high.

The permeability of the brecciated rock could not be measured quantitatively, but was much greater than in the adjacent fractured rocks. The average water saturation of pore space of brecciated rocks was 73% as compared with over 100% in unbrecciated rocks.

The strength of the Breccia samples was low; the compressive strength of brecciated rocks is less than one-fourth the strength of unbrecciated rocks and much less than the strength of unaffected rocks. The dilitational velocity of some brecciated rocks was approximately half the velocity outside the zone of intense fracturing (greater than 110 feet from the explosion).

Outside the Breccia zone, but close to the source, the explosion-caused differences in strength, in permeability, and possibly in porosity were found to be small. Out to 110 feet, the strength of the rocks was low. The unconfined compressive strength increased three times near 110 feet and Young's Modulus increased ten times at this distance. The U.S.G.S. states that these are probably minimum values.

Permeability shows a general increase near 75 feet from ground zero. As in the case of the strength factors, while permeability

increases some four times it is also probably a minimum value. By inference the permeability should be relatively high for distances as much as 110 feet from ground zero.

Seismic Velocities

Prior to the RAINIER detonation, velocities were measured by the U.S.G.S. in a vertical drill hole approximately 100 feet west of RAINIER ground zero and in the U12b tunnel. Following the explosion, velocities were measured in the U12b tunnel, the exploratory tunnel, two underground drill holes and in the ground zero vertical drill hole (see Figure 5.4). In addition, the U.S.G.S. ran two reflection survey lines on the surface over the RAINIER chamber.

The (post-shot seismic) data from the tunnel and from surface shots observed in the ground zero hole indicate the presence of three distinct zones of about 70%, 40% and 10% velocity reduction surrounding the point of detonation. In zone 1 the velocity to a distance of roughly 50 feet is 2,300 ft/sec or about 6,000 ft/sec lower than the pre-shot value. This zone is probably the brecciated zone mapped in the exploratory tunnel. Considering the pre-shot and post-shot velocities of 8300 ft/sec and 2300 ft/sec, the reduction in elasticity is about 90%, indicating almost complete disaggregation.

In zone 2, the velocity from 50 to 100 feet from the detonation was reduced from 8300 ft/sec pre-shot to 4800 ft/sec post-shot indicating a 65% reduction in elasticity. From this it is evident that zone 2 was highly fractured but not disaggregated. In zone 3 from about 100 feet outward seismic data obtained in drill holes B and C and the tunnel indicate post-shot velocity is reduced by 10% from pre-shot velocity. Here the difference in velocity is largely attributed to fracturing.

It should be noted that the outer limits of zones 2 and 3 were indicated to be gradational rather than distinct.

Besides the velocity anomalies produced by BLANCA, LOGAN and RAINIER, there are those produced by the TAMALPAIS, NEPTUNE, EVANS and fifty ton high explosive tests carried out in the

immediate vicinity of the RAINIER explosion.

The U.S.G.S. reports that seismic measurements made by recording energy from shots on the surface in the ground zero hole indicated a small velocity variation between 300 and 400 feet (see Figure 5.4). Information obtained below 400 feet was questionable because of casing breaks.

Figure 5.5 shows the variation in velocity observed 325 feet west of EVANS ground zero using conventional uphole shooting procedure. Total logged section was 760 feet commencing at a depth of 50 feet and extending to a depth of 810 feet. Although no date is given for the survey it apparently was run following the RAINIER event and preceding the BLANCA event.

Average velocities measured at this location are given in Table 5.1.

Table 5.1 Average Velocities Observed 325 Feet West of EVANS Ground Zero by U.S.G.S. Following RAINIER Event

Depth (Feet) From	To	Velocity (Ft/s)
0	98	4500
98	237	10000
237	436	5000
436	810	6900

Figure 5.6 shows a sonic log recorded 25 feet from the EVANS ground zero hole sometime following the RAINIER event and preceding the BLANCA event. This location is 520 feet southwest of RAINIER and 300 feet northwest of U.E.D. uphole velocity survey R-1 (see enclosure 1). The survey logged a total of 630 feet commencing 110 feet from the surface.

The average velocities measured at this location are given in Table 5.2.

Table 5.2 Average Velocities Observed at EVANS Zero Location by U.S.G.S. Following RAINIER Event

Depth (Feet) From	To	Velocity (ft/s)
110	140	?
140	255	11,500
255	470	5,500
470	730	6,900

In the first thirty feet of logged section interval velocities vary from 4,300 to 12,800 feet per second.

LOGAN-BLANCA Sites

No post-shot evaluation of the change in physical properties at the LOGAN-BLANCA sites was made. The same is true for delineation of the zone of subsurface effect. However, damage in the tunnels indicates that the outer zone of fracturing extends to a distance of some 540 feet from the BLANCA explosion chamber and a lesser distance for LOGAN.

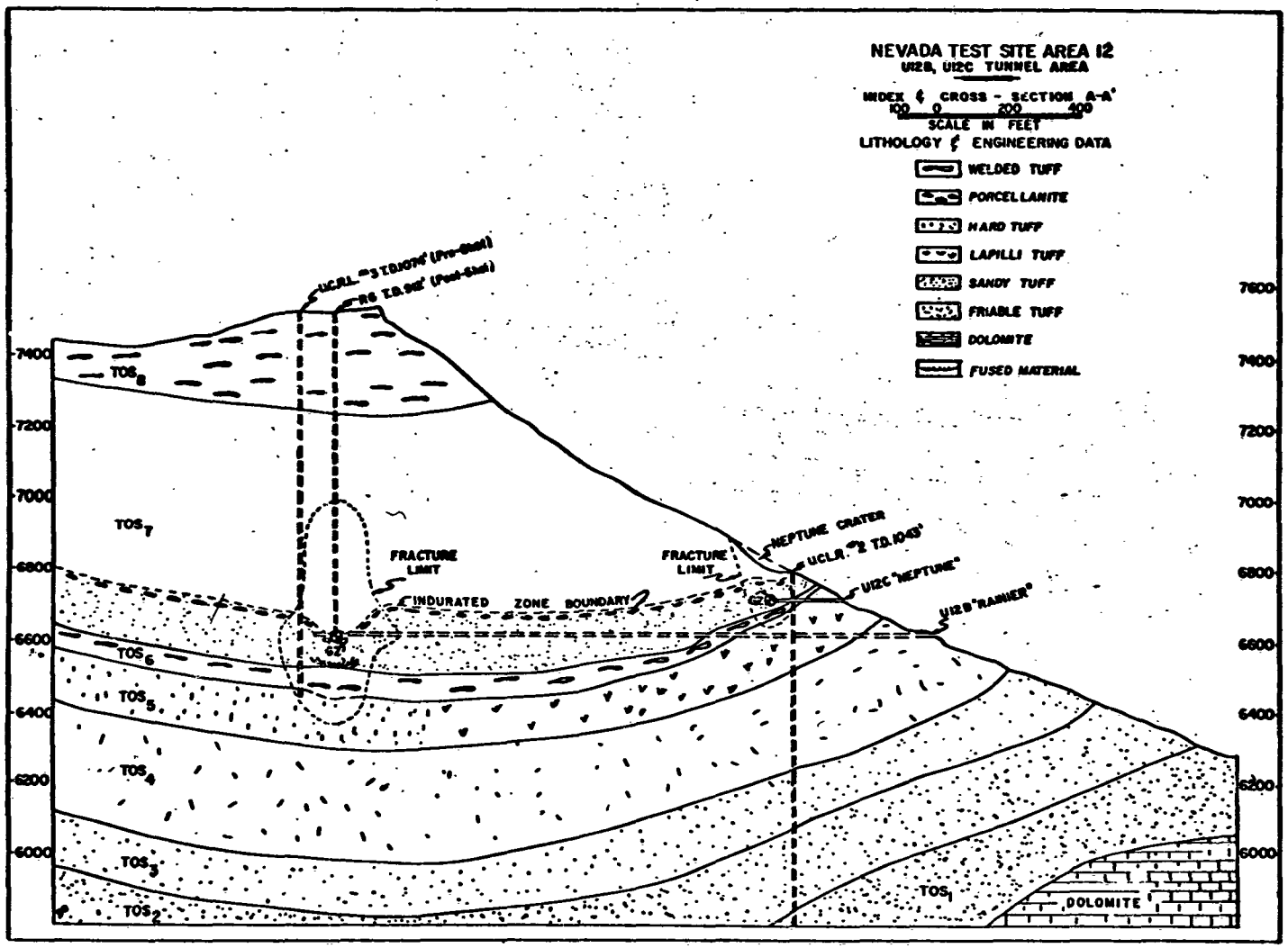

Fig. 5.1 Geologic cross section through Rainier and Neptune areas.

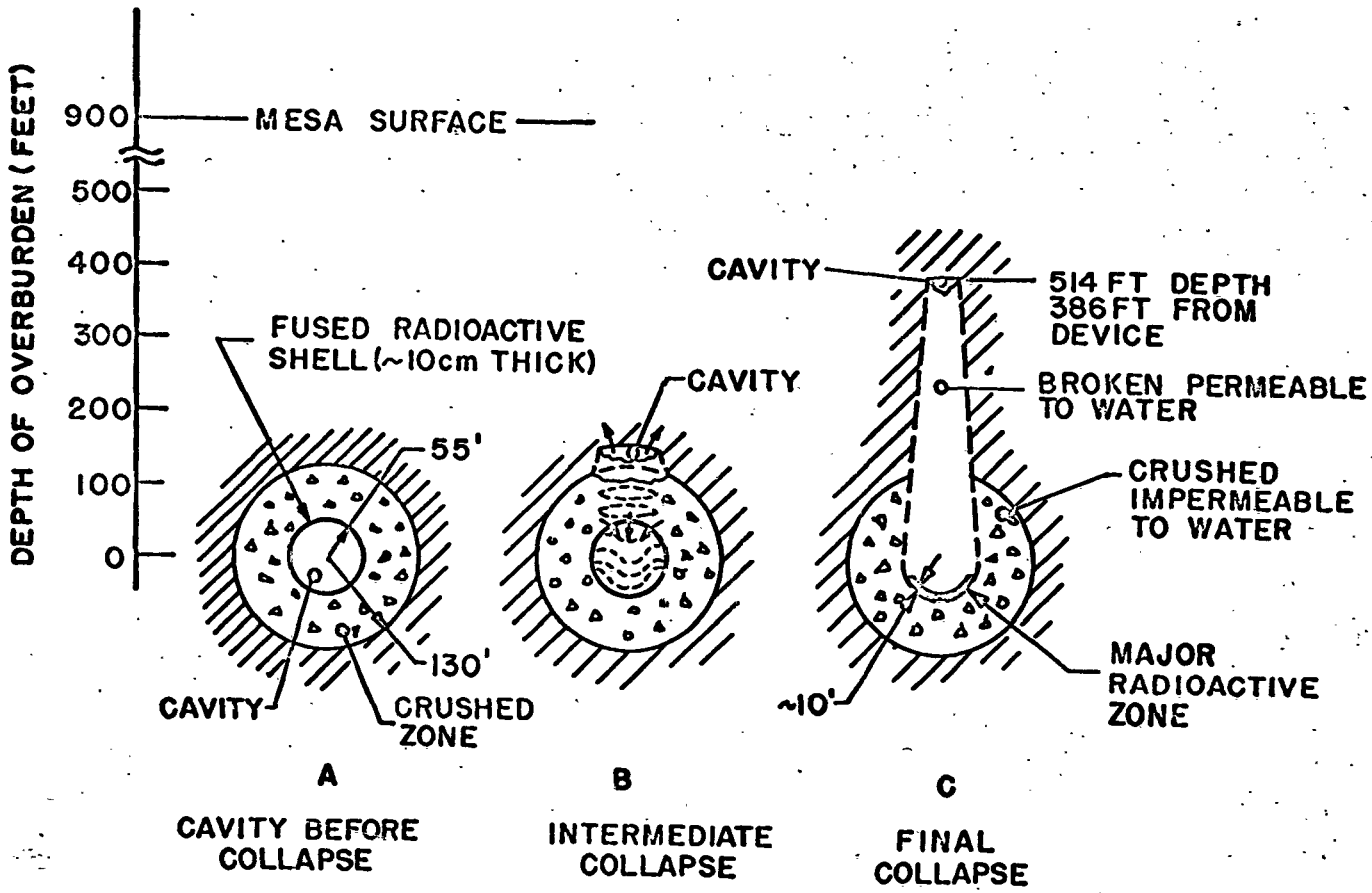

Fig.5.2 Reconstructed picture of strongly affected zones surrounding detonation point, Rainier Event.

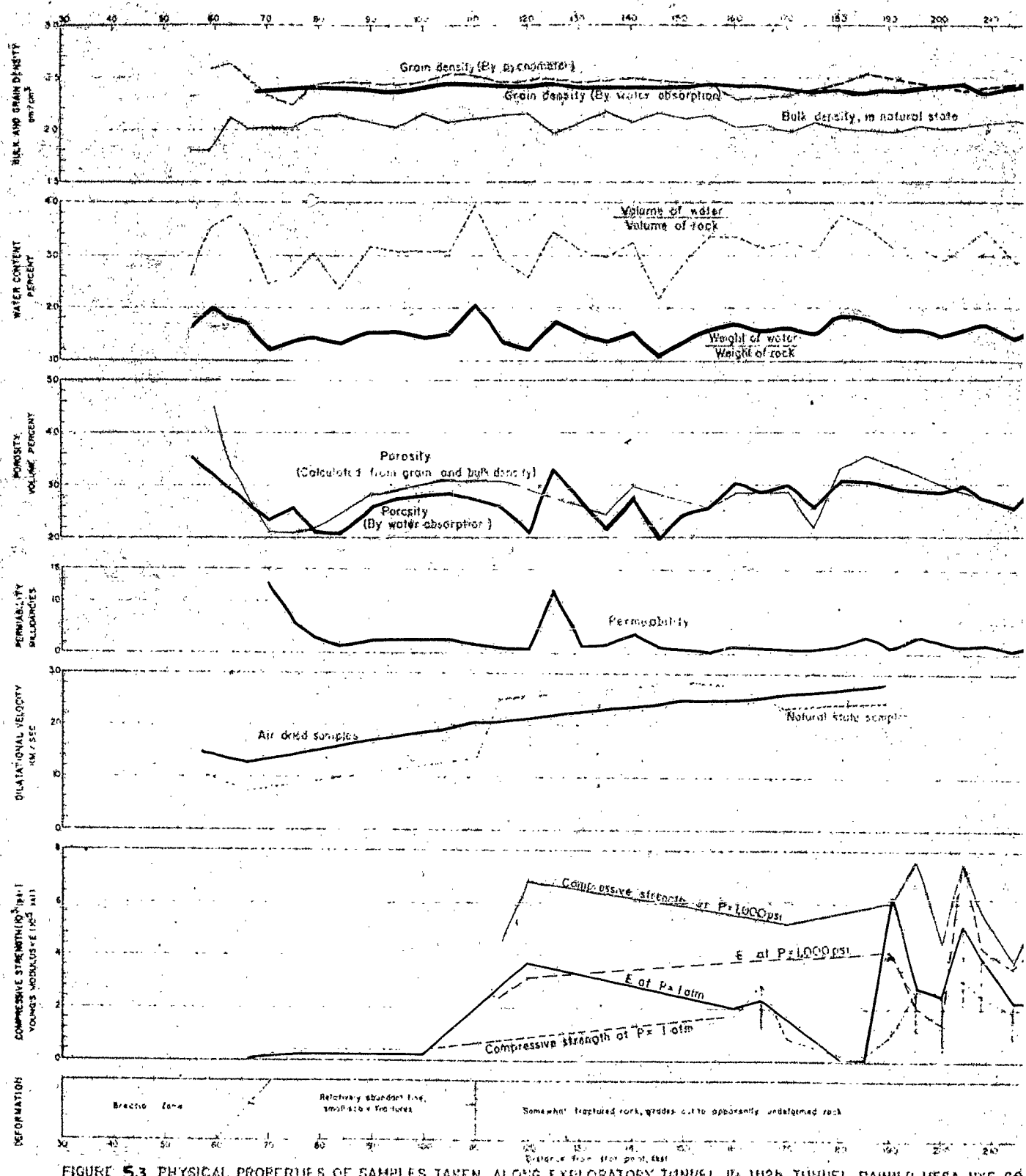

FIGURE 5.3 PHYSICAL PROPERTIES OF SAMPLES TAKEN ALONG EXPLORATORY TUNNEL IN U12b TUNNEL, RAINIER MESA, NYE CO

1

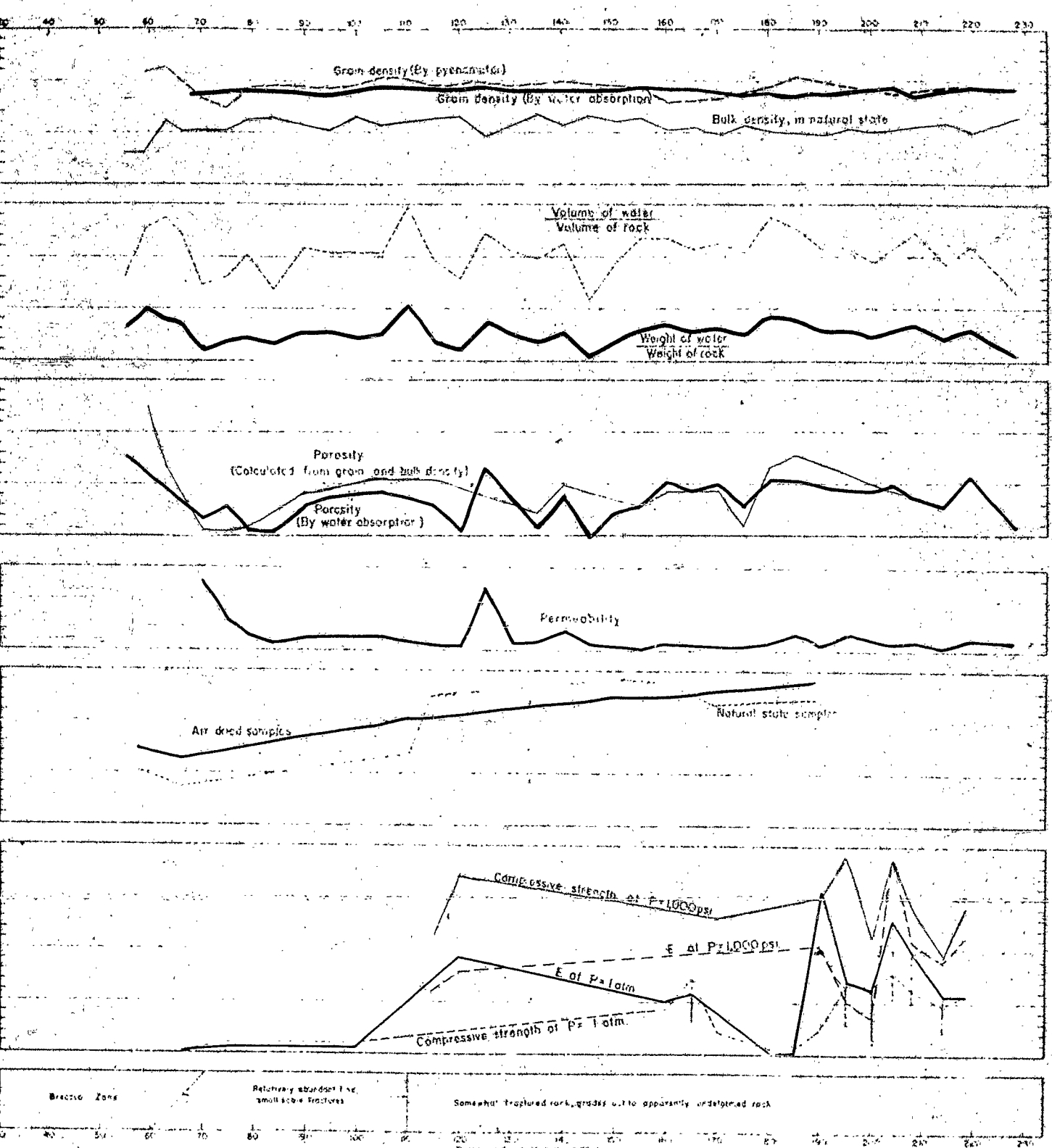

FIGURE 5.3 PHYSICAL PROPERTIES OF SAMPLES TAKEN ALONG EXPLORATORY TUNNEL IN U12b TUNNEL, RAINIER MESA, NYE COUNTY, NEVADA

2

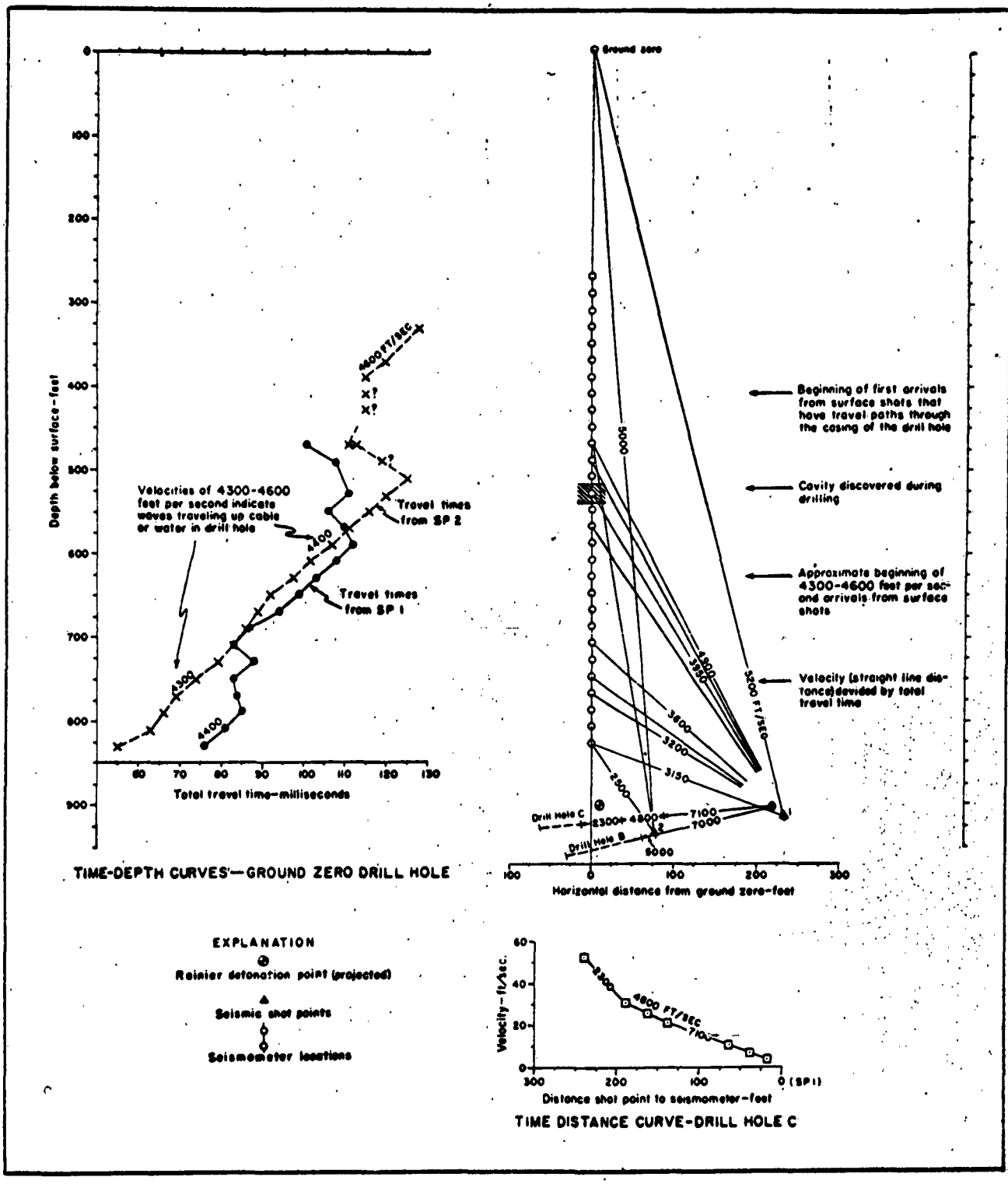

Fig. 5.4 Summary of post-shot seismic velocity data near Rainier explosion, Nevada Test Site

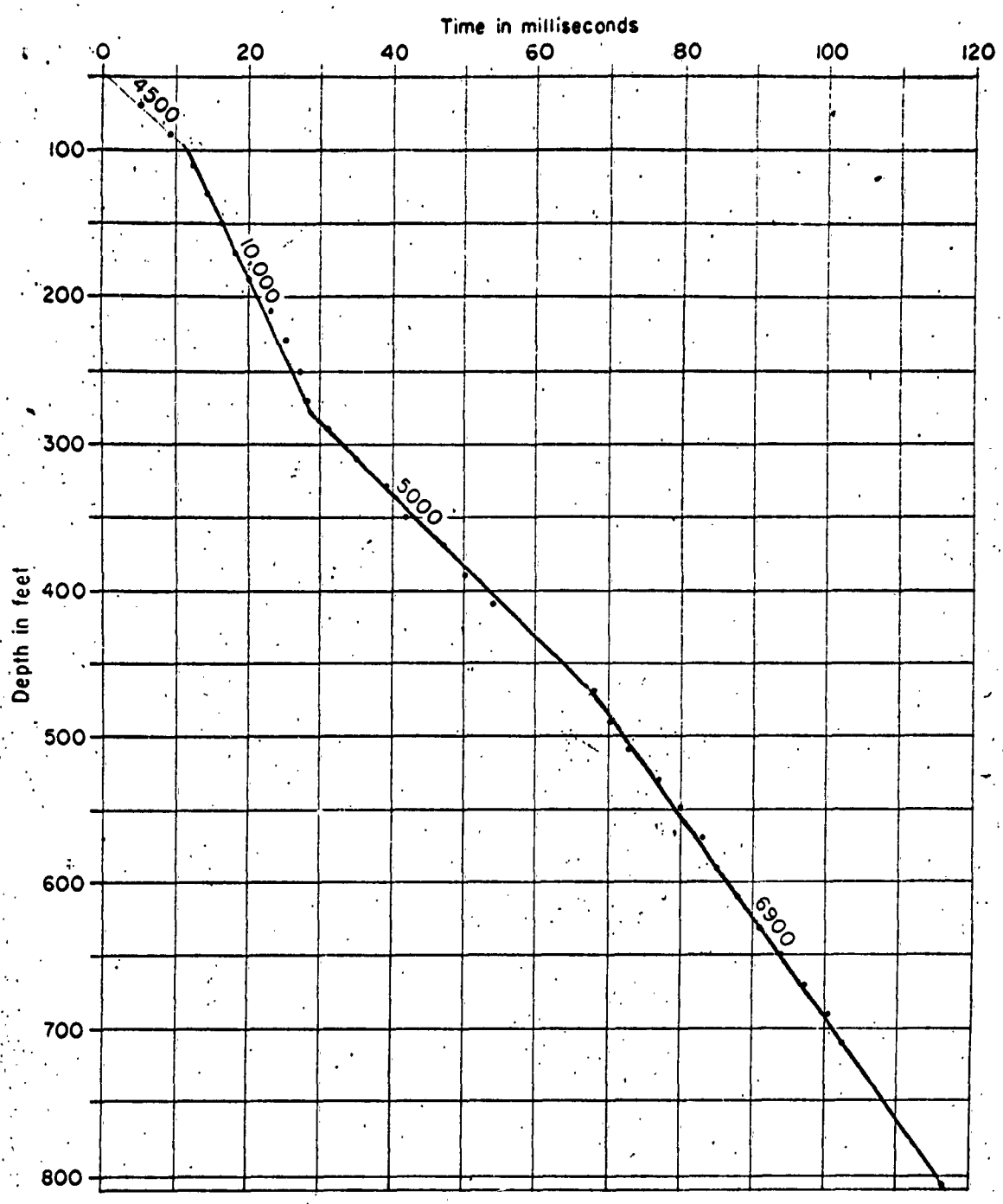

Figure 5.5—VERTICAL VELOCITY SURVEY IN HOLE NO. 5 LOCATED ABOUT 300 FEET WEST OF U12b.04 EXPLOSION CHAMBER

FIGURE 5.6 SONIC AND SPONTANEOUS POTENTIAL LOGS OF DRILL HOLE NO. 3 OVER U12b .04 SHOT CHAMBER, NEVADA TEST SITE, NYE COUNTY, NEVADA

Note: Log depth measured from ground level

Logs by Schlumberger Well Surveying Corp.

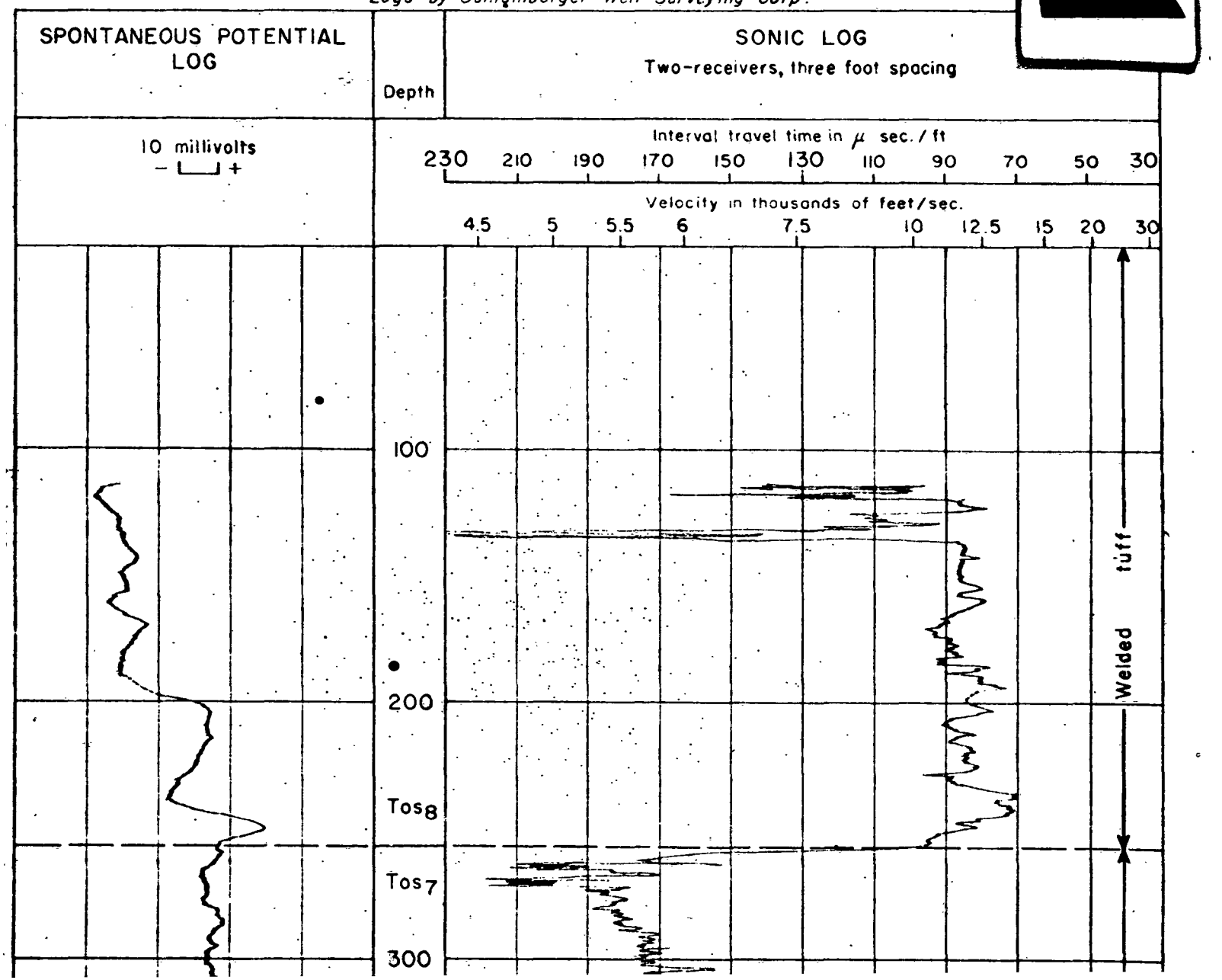

Nonwelded
Tuff
2
Tos8
Tos7
300
400
500
600

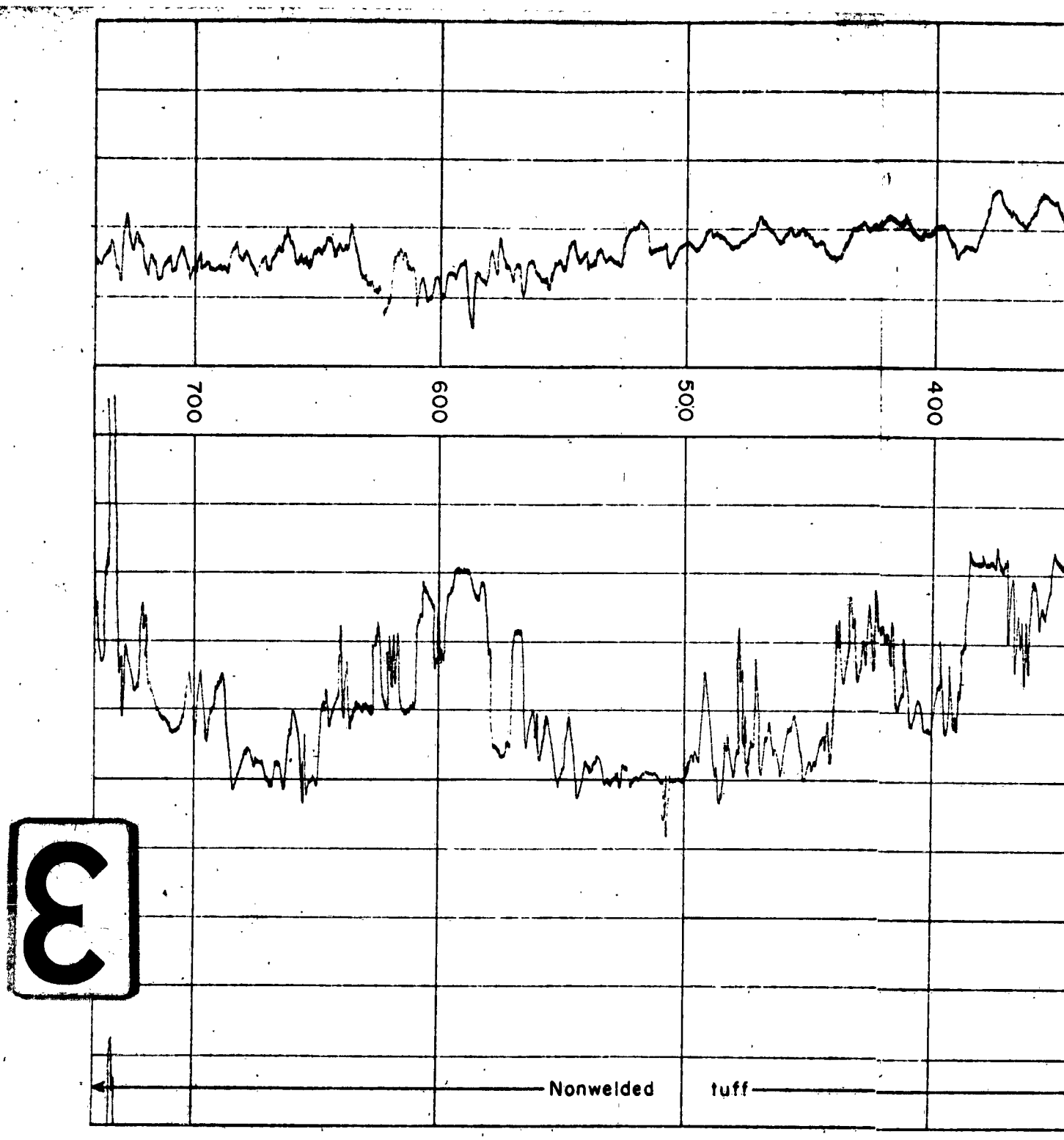
700
600
500
400
Nonwelded
tuff

6.0 Structural Changes

Surface Effects Due to RAINIER Test

The effects of the RAINIER explosion at the surface were observed on top of RAINIER Mesa and on the surrounding steep slopes. These effects consisted of rock falls, rock slides, fracturing of the welded and non-welded tuffs, and minor surface displacements. Approximately one linear mile of surface area along the mesa front was affected. Explosion-produced rock slides and rock falls occured along the rim of the mesa from ground zero. The largest explosion-produced slide occurred east of ground zero and extended down slope from the mesa rim 1,000 feet and was 200 to 300 feet wide.

The principal disturbance at the mesa surface above RAINIER was confined to a relatively small (less than 500 foot radius) region surrounding surface zero. Within this area, a large earth cap beginning approximately 180 feet below the surface, separated from the mesa due to spalling, rose one foot and settled back into place.

The explosion stresses produced numerous fractures in the welded tuff and soil on top of the mesa with widths of the order of 2 inches or less for distances of 300 feet. While fractures in the soil were more abundant, they were not as continuous as those in the welded tuff. It is believed that all of the post-explosion fractures formed along pre-existing fractures that strike north to north 15° E. and north 35° to 45° W. No surface displacements were measured along post-test fractures on top of the mesa.

Surface Effects Due to LOGAN Test

LOGAN was located some 4100 feet south and 700 feet east of the RAINIER test site. This separation is sufficiently great that the effects of the two explosions probably do not overlap. The location of the LOGAN event with respect to RAINIER Mesa is shown on Figure 6.1.

Most of the slope, from the nearest point on the surface to the explosion chamber, to the exposed base of the welded Tos$_B$

tuff some 600 feet away, was covered with colluvium and was involved in the slides produced by the explosion. The locations of these slides are shown on Figures 6.1a and 6.1b.

The explosion also produced extensive fracturing to radial distances of 3500 feet. The location and extent of these fractures is shown on Figure 6.1a. The largest concentration of post-explosion fractures was found in the welded Tos_8 tuff. However, a significant number of post-explosion fractures were also found in the indurated tuffs of Tos_1 to the lower portion of Tos_7. Most of these fractures are located within a 2,600 foot radial distance of the shot chamber.

Explosion-produced fractures vary from a few inches to 600 feet in length, and from a hairline to 1.5 feet in width. Many of these fractures are open to depths of 10 feet and several to depths of 20 feet below the surface.

In the welded tuffs of Tos_8, explosion-produced fractures are generally less than 120 feet long and are concentrated within 200 feet of the mesa rim. Most of these fractures closely parallel or coincide with the pre-explosion fractures. However, some of the fractures parallel the mesa rim.

Explosion-produced faults were mapped at radial distances of 2,300 feet from the shot. Displacements along these faults are generally less than .5 foot. The principal exception occurred at a radial distance of 1,000 feet and had a displacement of 2 feet.

The fracturing produced by the LOGAN explosion differs from that produced by the RAINIER explosion in that a significant number of the fractures do not parallel the pre-shot jointing.

Surface Effects Due to BLANCA Event

The principal difference between the surface effects of the BLANCA and LOGAN events is in the magnitude and range at which fracturing and slides were produced. The area and extent of the surface effects of BLANCA is shown on Figure 6.2a.

Examination of this figure shows that the most intense surface effects were concentrated within a distance of some 3,000 feet of ground zero. At this range fracturing produced by BLANCA overlapped fracturing produced by both LOGAN and RAINIER. Consequently, there was considerable superposition of the surface effects. However, comparison of figures 6.1a and 6.2a shows that the bulk of this superposition occurred in the vicinity of the LOGAN event. In the vicinity of the RAINIER event superposition of surface effects was probably insufficient to produce a significant concentration of fracturing.

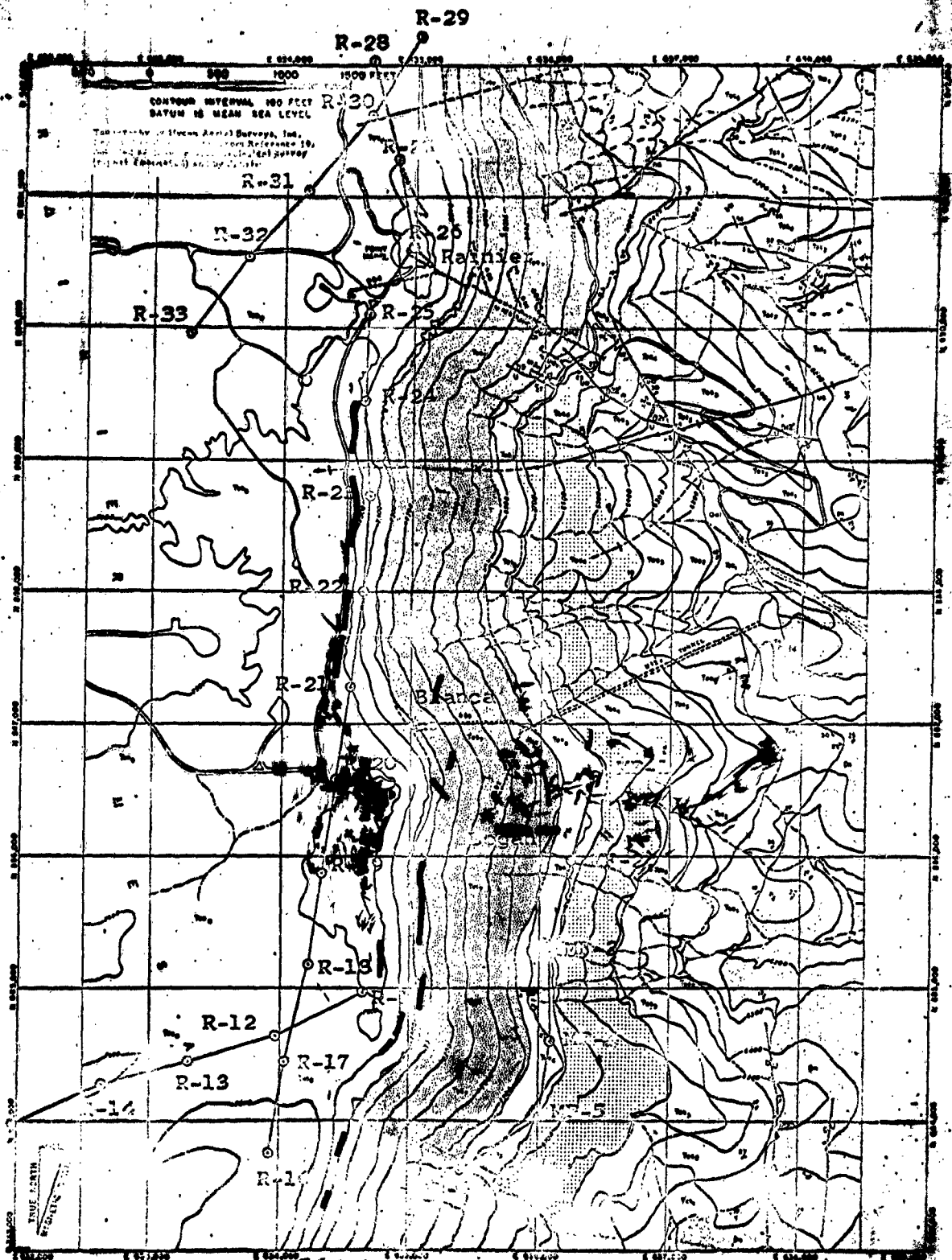

Figure 6.1a Showing effects of Logan event.

Fig. 6.1b

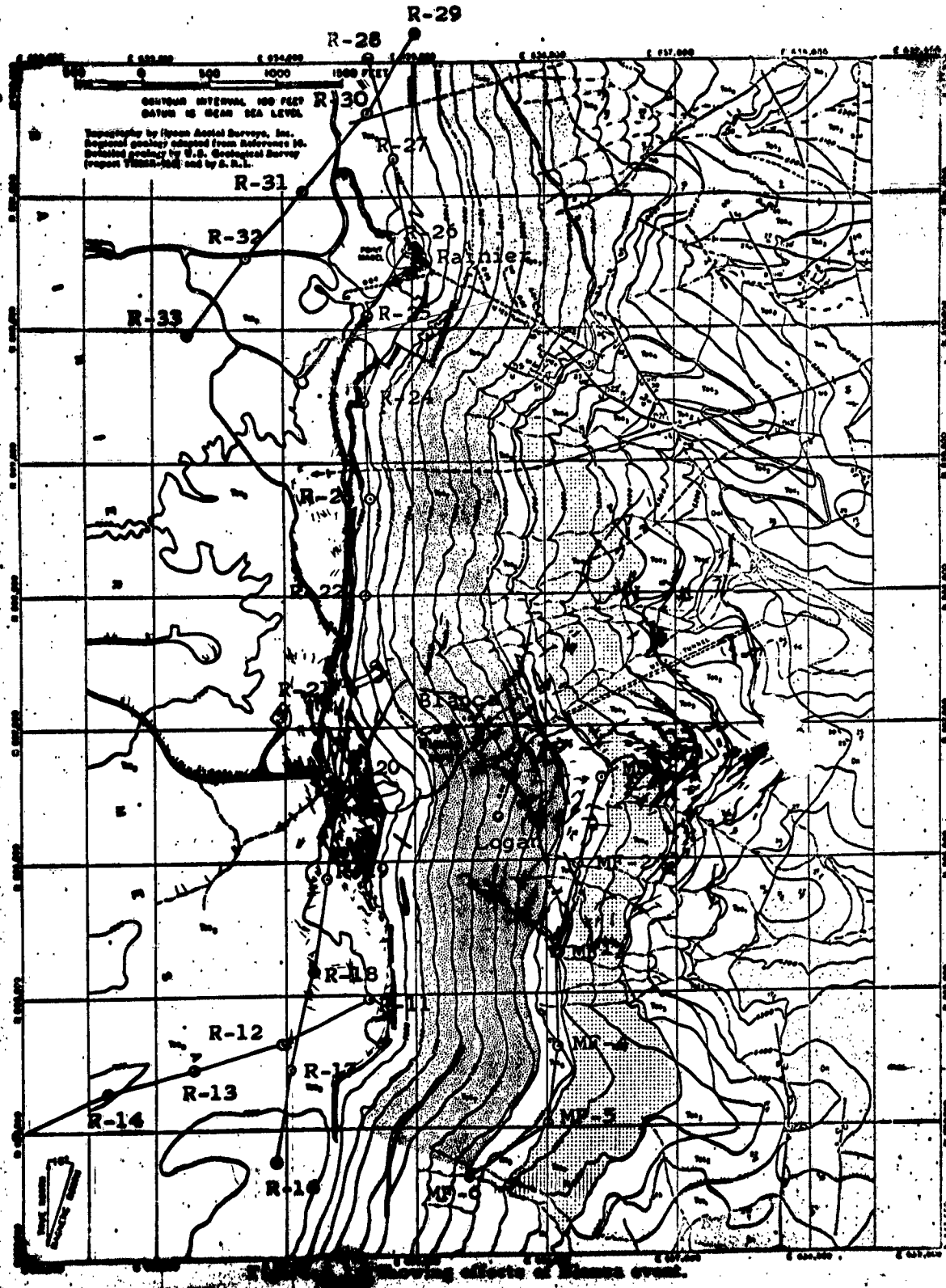
R-29
R-28
R-30
R-27
R-31
R-32
R-33
R-26
R-25
R-24
R-23
R-22
R-21
R-20
R-19
R-18
R-17
R-16
R-15
R-14
R-13
R-12
Rainier
Brace
Logan
MR-1
MR-2
MR-3
MR-4
MR-5
MR-6
20
26

Fig. 6.2b

7.0 Instrumentation

Seismic investigations in the RAINIER Mesa area consisted of uphole velocity surveys, near surface velocity profiling and horizontal seismic ranging. The same system of recording amplifiers was used throughout, but different detector components and spread geometries were employed to obtain the desired response characteristics and data. The response characteristics of individual components and systems together with spread geometries used for each type of seismic investigation are described below.

Uphole Velocity Survey

The recording layout for the uphole velocity survey consisted of three or four seismometer groups at three foot radii around the shot hole, and one group each at 10 feet, 20 feet and 30 feet. Each group consisted of two United Geophysical Corporation type 4-16 geophones with outputs in series. The geophones had a natural frequency of 21 cycles per second.

Near Surface Velocity Profiling

For the near surface velocity profiling two Electro-Technical Laboratories, type EV5-4, geophones with a natural frequency of 7.5 cycles per second, with outputs in parallel were used for each trace. Shotpoints were generally spaced 720 feet apart with geophone groups at 60 foot intervals. Total spread length for 24 traces was 1410 feet. An uphole geophone was always placed 10 feet from the hole. Shots were fired in the hole at one end of the spread and then at the other to obtain reverse coverage.

All observed data were recorded simultaneously on paper and magnetic tape using a United Geophysical Corporation, type 24-9 FM magnetic recording system. To provide a reference for evaluating the attenuation of seismic energy with distance on near surface velocity profiles, the recording system was calibrated for amplitude response. This consisted of balancing the amplifiers to give an amplitude of twenty millimeters, peak to peak displacement on all 24 recording traces for a given oscillator input signal. While this amplitude was used

as zero decibel reference, additional attenuation was generally needed to obtain measurable amplitudes on the records.

Horizontal Seismic Ranging

HSR arrays consisted of eight directional rays arranged at 45 degree intervals around a center point (see Figure 7.1). Each ray contained three seismometer groups, each of which contained sixteen geophones aligned in four rows of four geophones with alternate rows connected with reversed polarity. Hall-Sears type HS-J geophones with a natural frequency of 28 cycles per second were used. Maximum sensitivity could be directed either along (Program B) or broadside (Program A) to the ray. These arrays are illustrated on Figures 7.2 and 7.3. The electrical hookup of the cables to the recording system is shown on Figures 7.4 and 7.5. The directional response of the spread is shown on Figures 7.6 to 7.10. The frequency response of the array and amplifiers is shown on Figures 7.11 to 7.13.

Tatum Salt Dome

Recording spreads used in the seismic investigation of Tatum Salt Dome consisted of twelve geophone groups spaced 127.3 feet apart center to center. Each geophone group consisted of sixteen Hall-Sears, type HS-J, geophones with a natural frequency of 28 cycles per second connected in series - parallel as shown in Figure 7.14.

Shotpoints were also spaced 127.3 feet apart and each shotpoint was located at the midpoint of the spread.

Wide band pass (3-9) and narrow band pass (11-9) filters were used. Filter response curves are shown on Figure 7.15.

All recordings were made simultaneously on paper and magnetic tape. A United Geophysical Corporation recording unit consisting of a magnetic recording system, UGC 23-3A frequency modulated oscillator-demodulators, 19-4 magnetic tape transport, 1-32B amplifiers and a 5-30 camera was used.

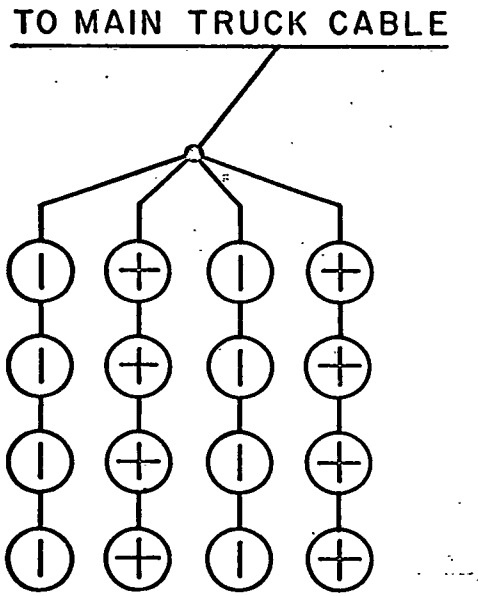

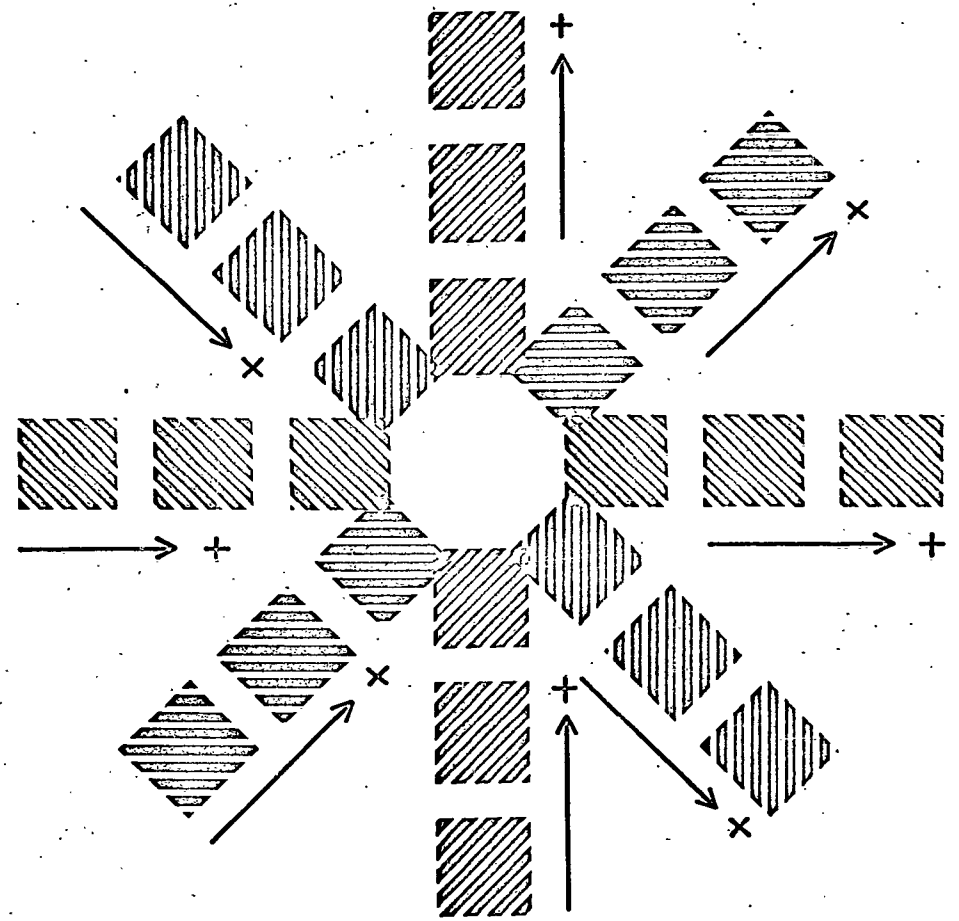

STATION LAYOUT OF DIRECTIONAL GEOPHONE
ARRAYS FOR HORIZONTAL SEISMIC RANGING

FIG. 7.1

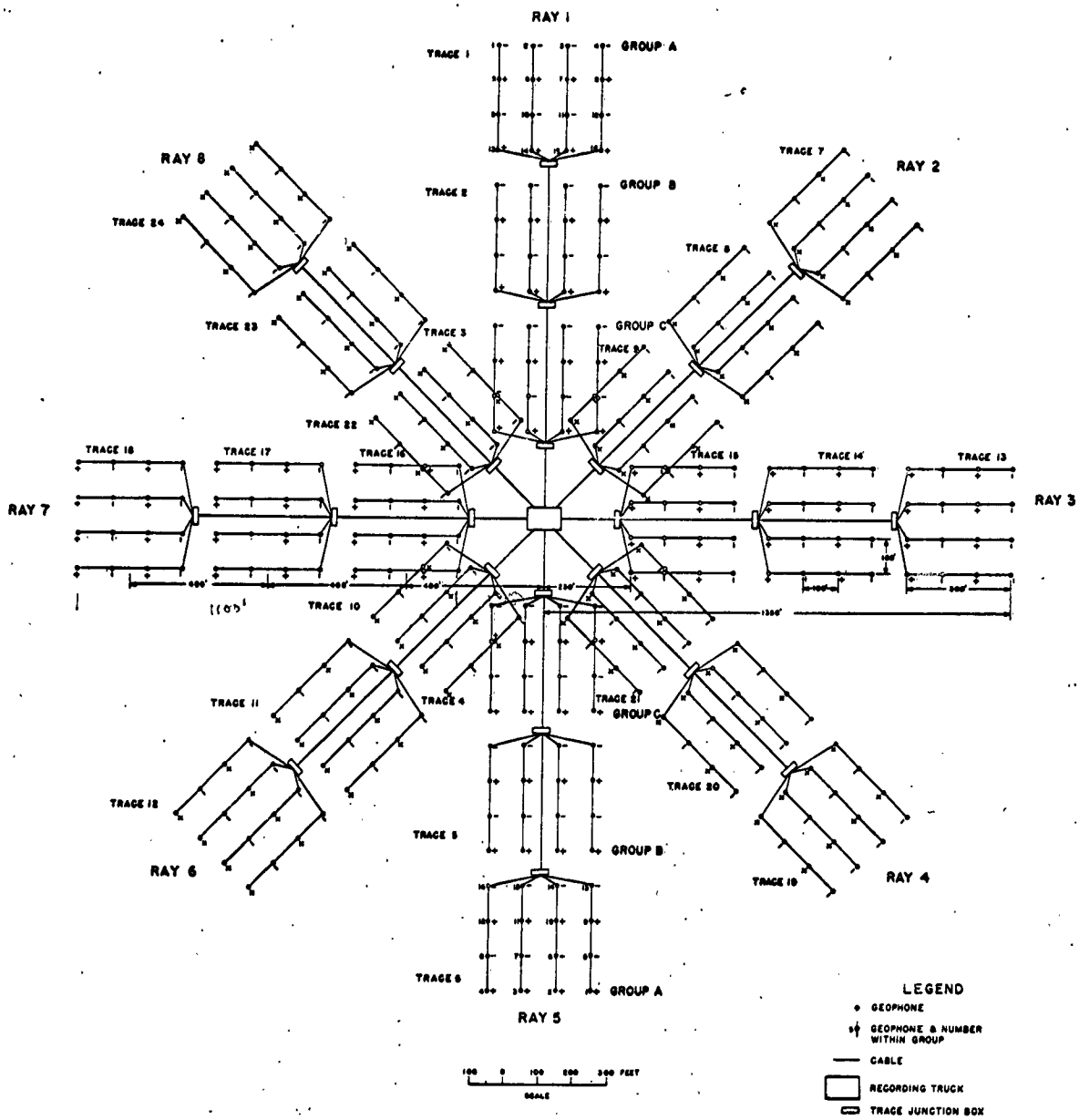

HORIZONTAL SEISMIC RANGING ARRAY

Fig. 7.2

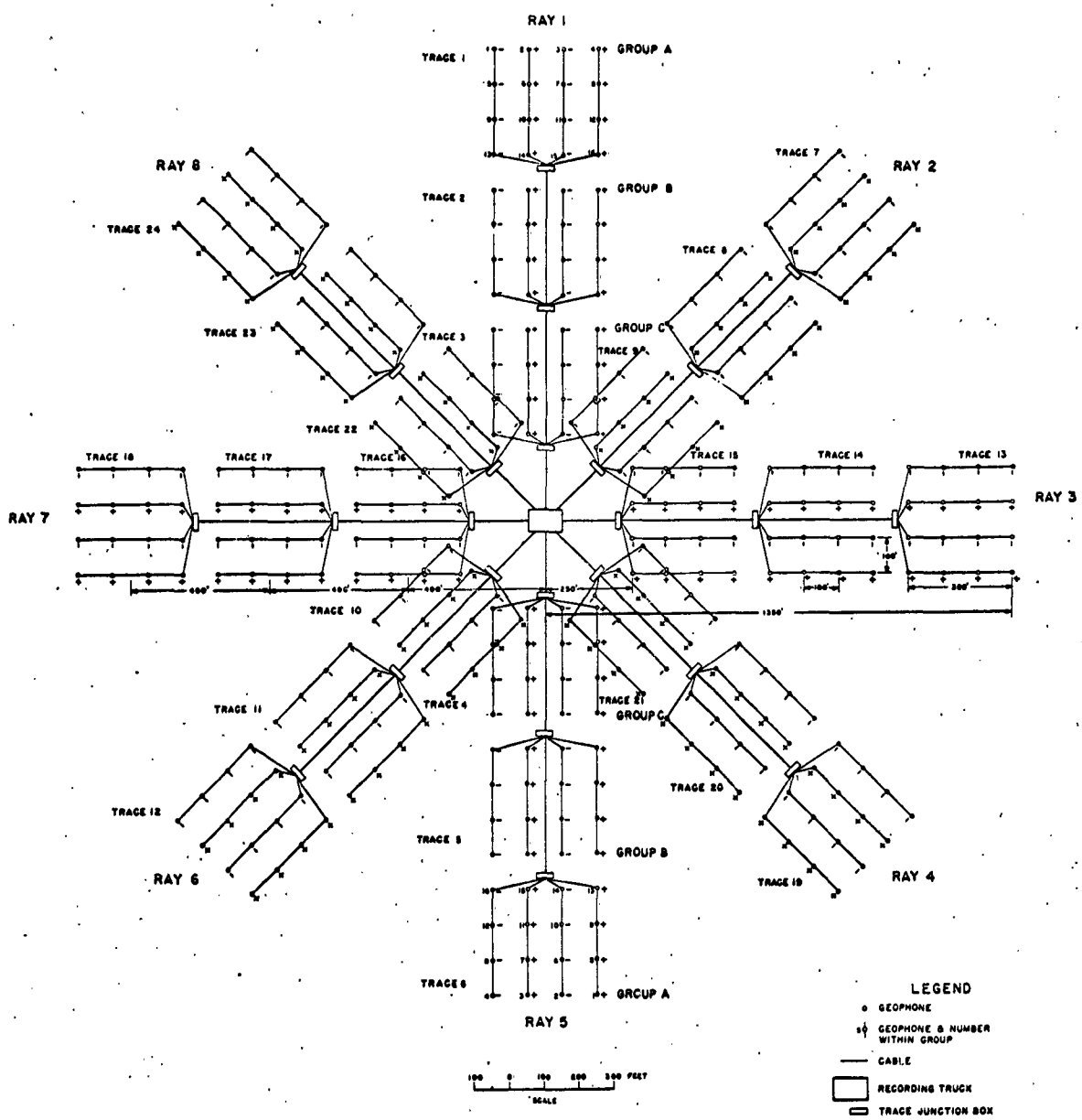

HORIZONTAL SEISMIC RANGING ARRAY

POLARITY ARRANGEMENT FOR

Program A

Fig. 7.3

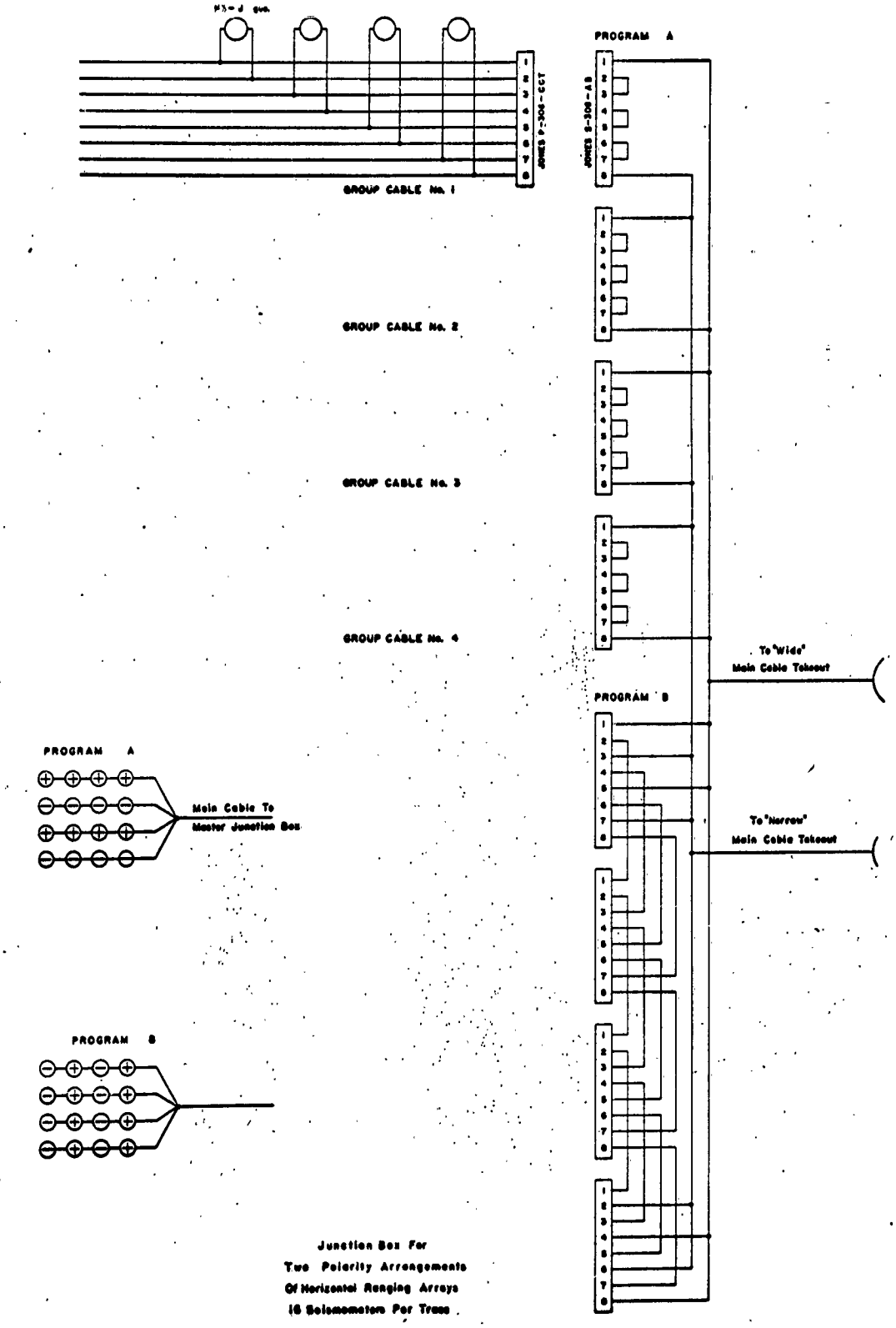

Junction Box Diagram.

Fig. 7.4

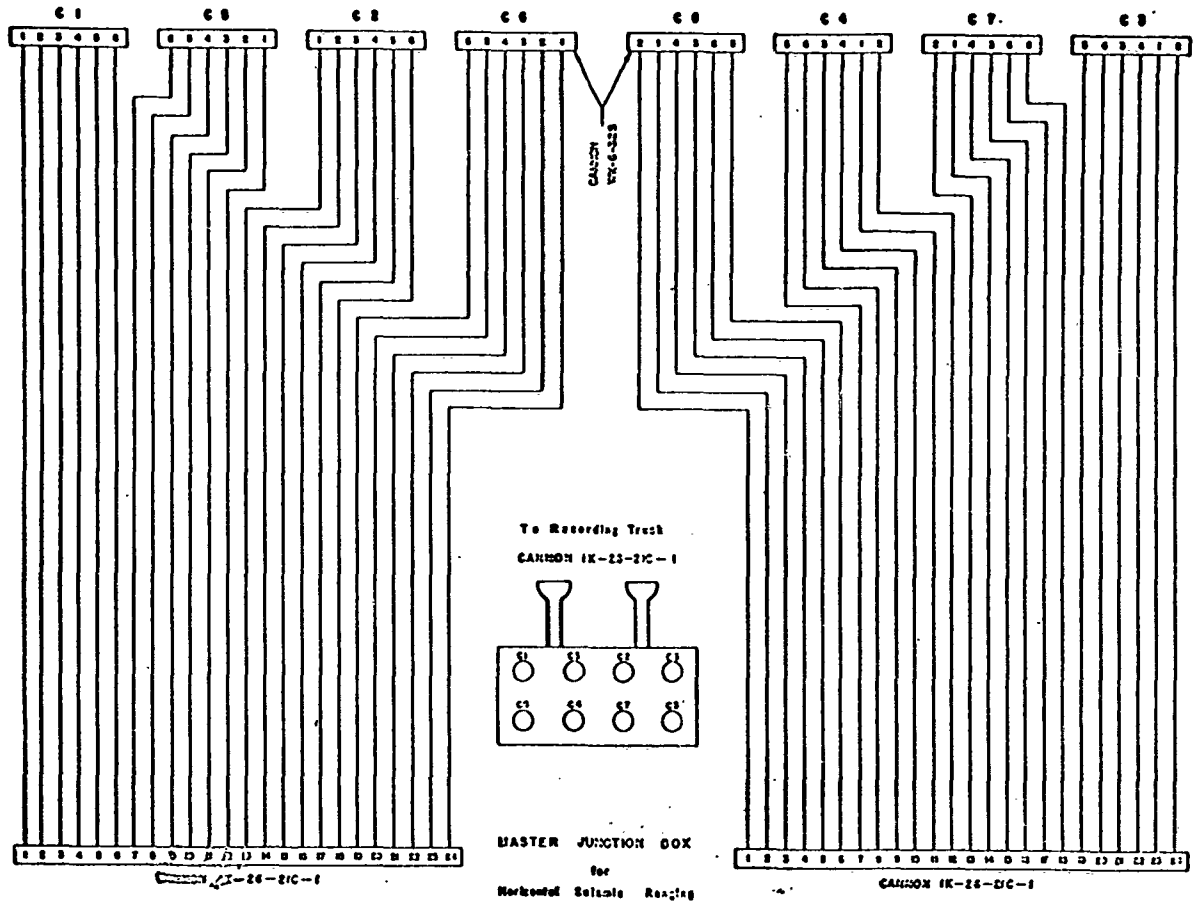

Fig. 7.5

Junction Box Diagram

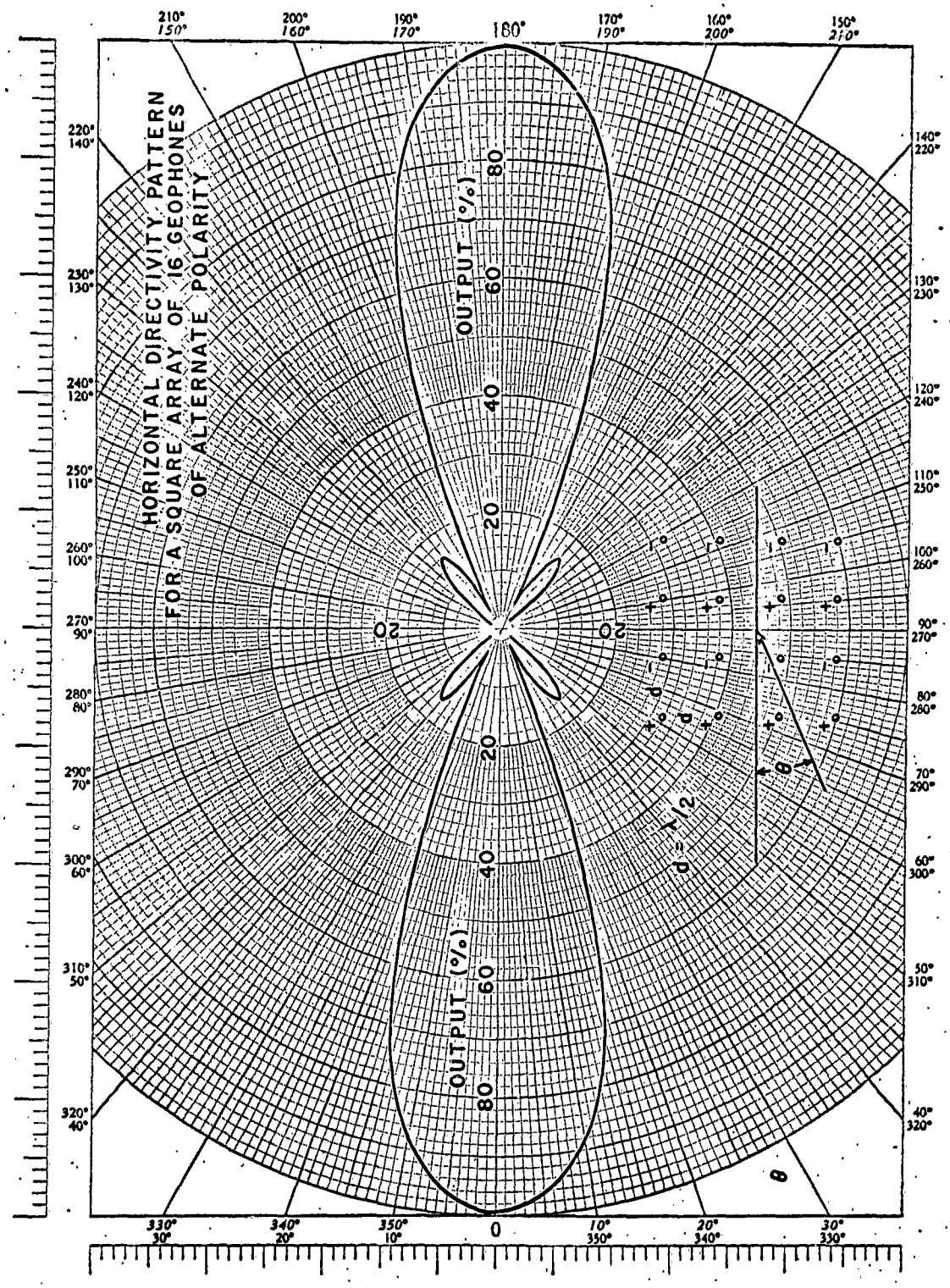
HORIZONTAL DIRECTIVITY PATTERN
FOR A SQUARE ARRAY OF 16 GEOPHONES
OF ALTERNATE POLARITY
OUTPUT (%)
OUTPUT (%)
d = λ/2
θ
θ
180°
0
20
40
60
80

Fig. 7.6

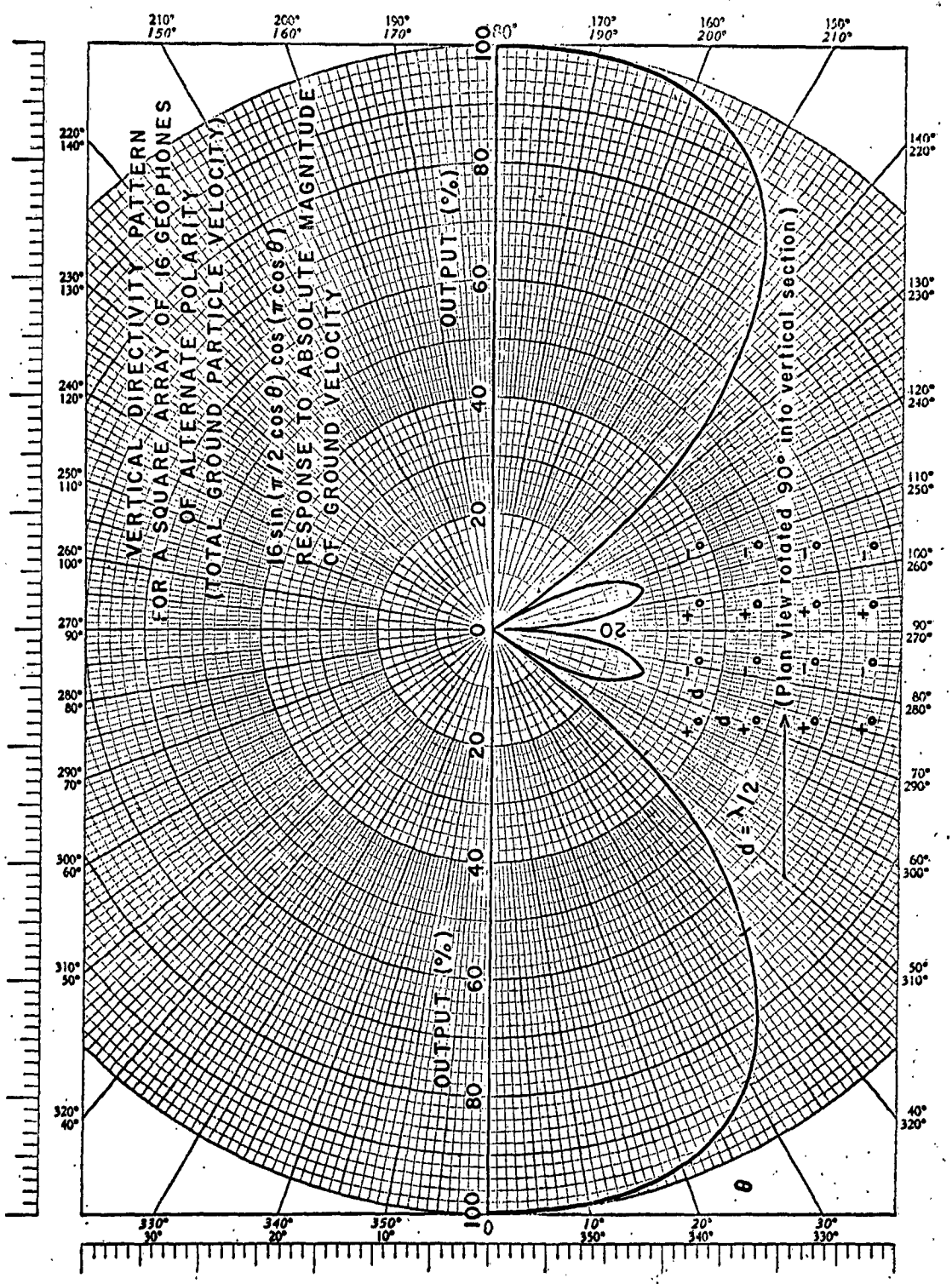
VERTICAL DIRECTIVITY PATTERN
FOR A SQUARE ARRAY OF 16 GEOPHONES
(TOTAL GROUND PARTICLE VELOCITY)
OF ALTERNATE POLARITY
16 sin (π/2 cos θ) cos (π cos θ)
RESPONSE TO ABSOLUTE MAGNITUDE
OF GROUND VELOCITY
OUTPUT (%)
OUTPUT (%)
(Plan view rotated 90° into vertical section)
d = λ/2
θ
210° 150°
200° 160°
190° 170°
180°
170° 190°
160° 200°
150° 210°
220° 140°
230° 130°
240° 120°
250° 110°
260° 100°
270° 90°
280° 80°
290° 70°
300° 60°
310° 50°
320° 40°
140° 220°
130° 230°
120° 240°
110° 250°
100° 260°
90° 270°
80° 280°
70° 290°
60° 300°
50° 310°
40° 320°
330° 30°
340° 20°
350° 10°
0
10° 350°
20° 340°
30° 330°
100
80
60
40
20
0
20
40
60
80
100

Fig. 7.7

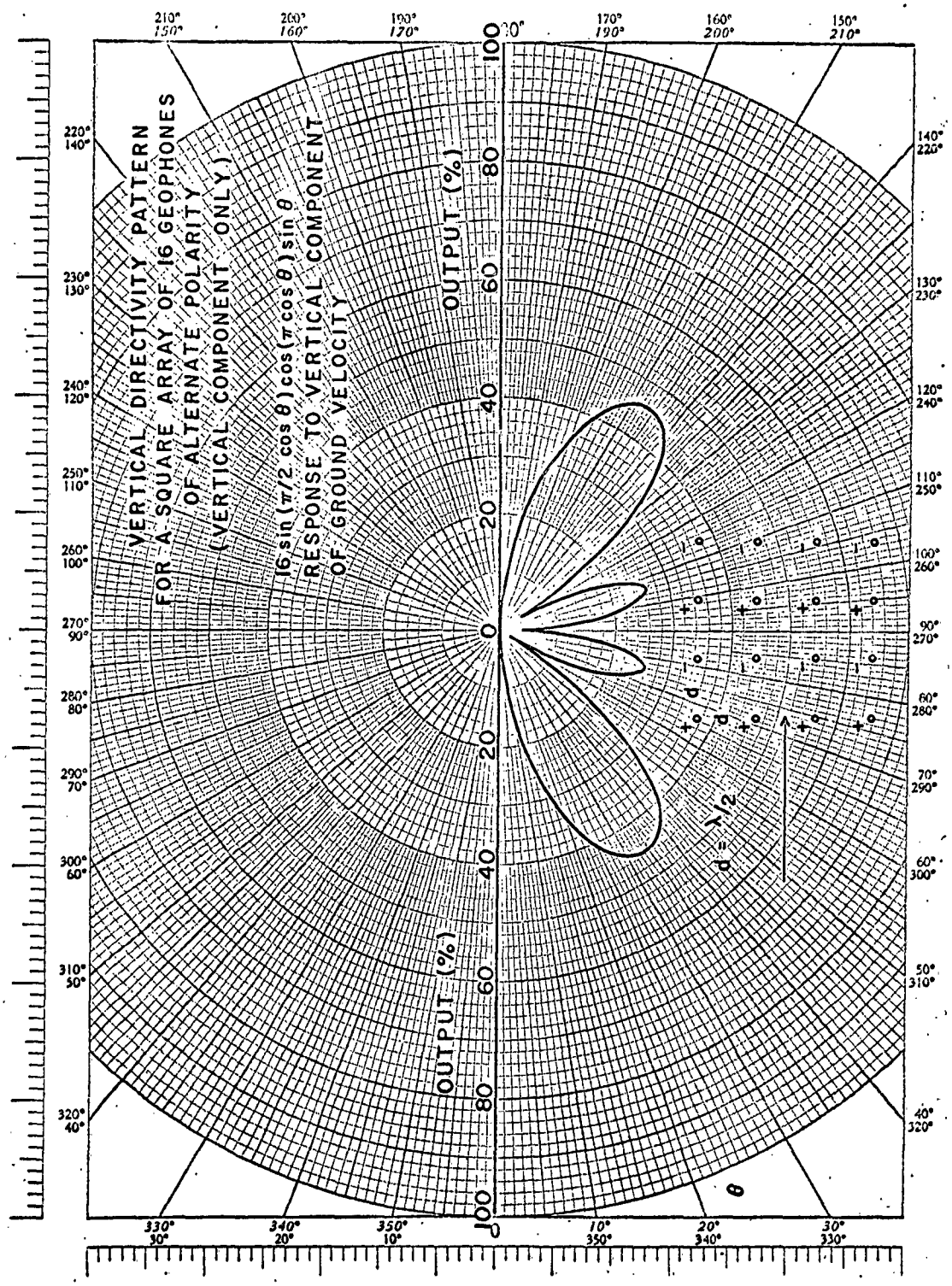
VERTICAL DIRECTIVITY PATTERN
FOR A SQUARE ARRAY OF 16 GEOPHONES
OF ALTERNATE POLARITY
(VERTICAL COMPONENT ONLY)
16 sin (π/2 cos θ) cos (π cos θ) sin θ
RESPONSE TO VERTICAL COMPONENT
OF GROUND VELOCITY
OUTPUT (%)
OUTPUT (%)
θ
210° 150°
200° 160°
190° 170°
180°
170° 190°
160° 200°
150° 210°
220° 140°
230° 130°
240° 120°
250° 110°
260° 100°
270° 90°
280° 80°
290° 70°
300° 60°
310° 50°
320° 40°
330° 30°
340° 20°
350° 10°
10° 350°
20° 340°
30° 330°
140° 220°
130° 230°
120° 240°
110° 250°
100° 260°
90° 270°
80° 280°
70° 290°
60° 300°
50° 310°
40° 320°
0
20
40
60
80
100

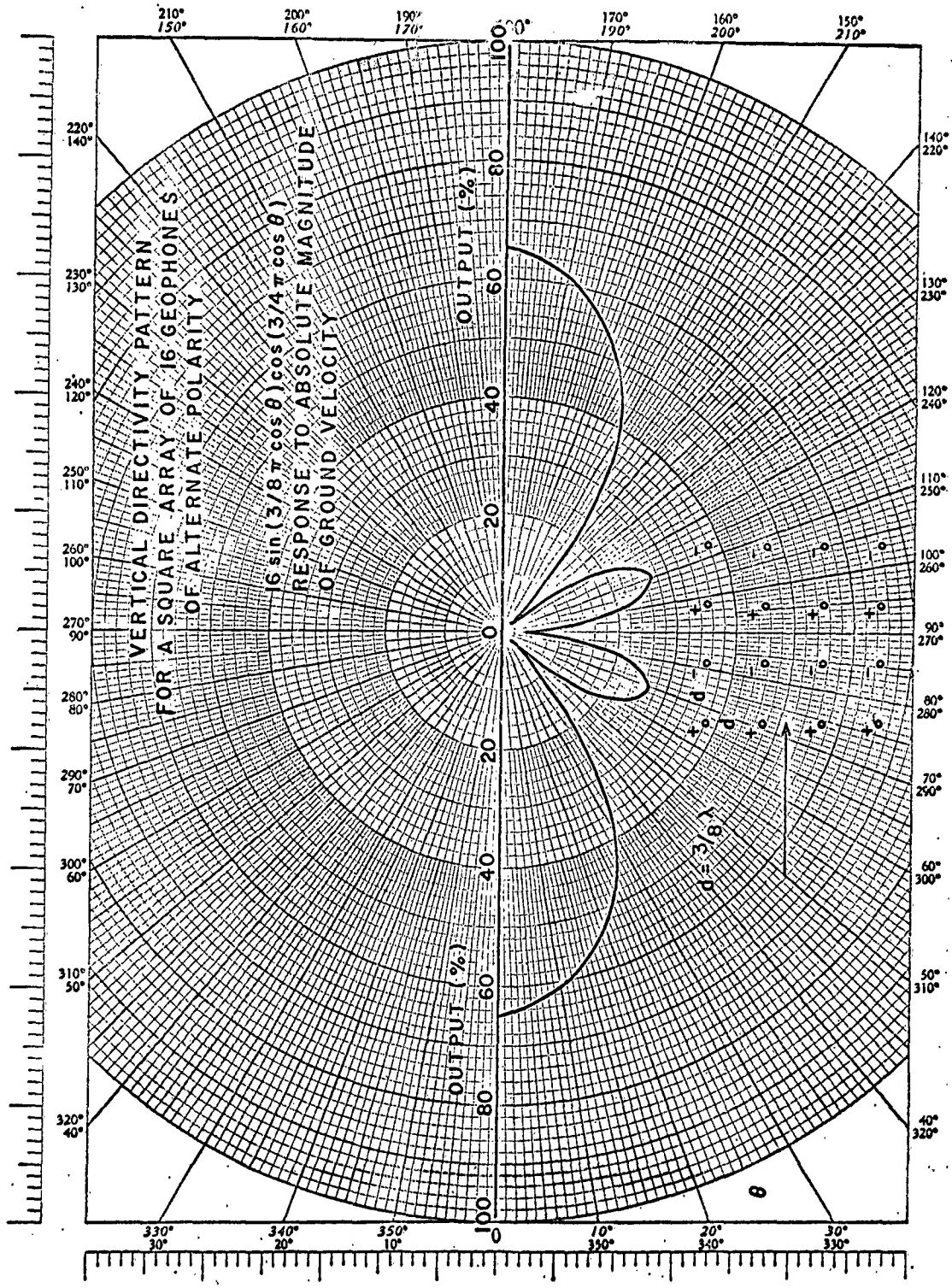
VERTICAL DIRECTIVITY PATTERN
FOR A SQUARE ARRAY OF 16 GEOPHONES
OF ALTERNATE POLARITY
16 sin (3/8 π cos θ) cos (3/4 π cos θ)
RESPONSE TO ABSOLUTE MAGNITUDE
OF GROUND VELOCITY
OUTPUT (%)
OUTPUT (%)
d = 3/8 λ
θ

Fig. 7.9

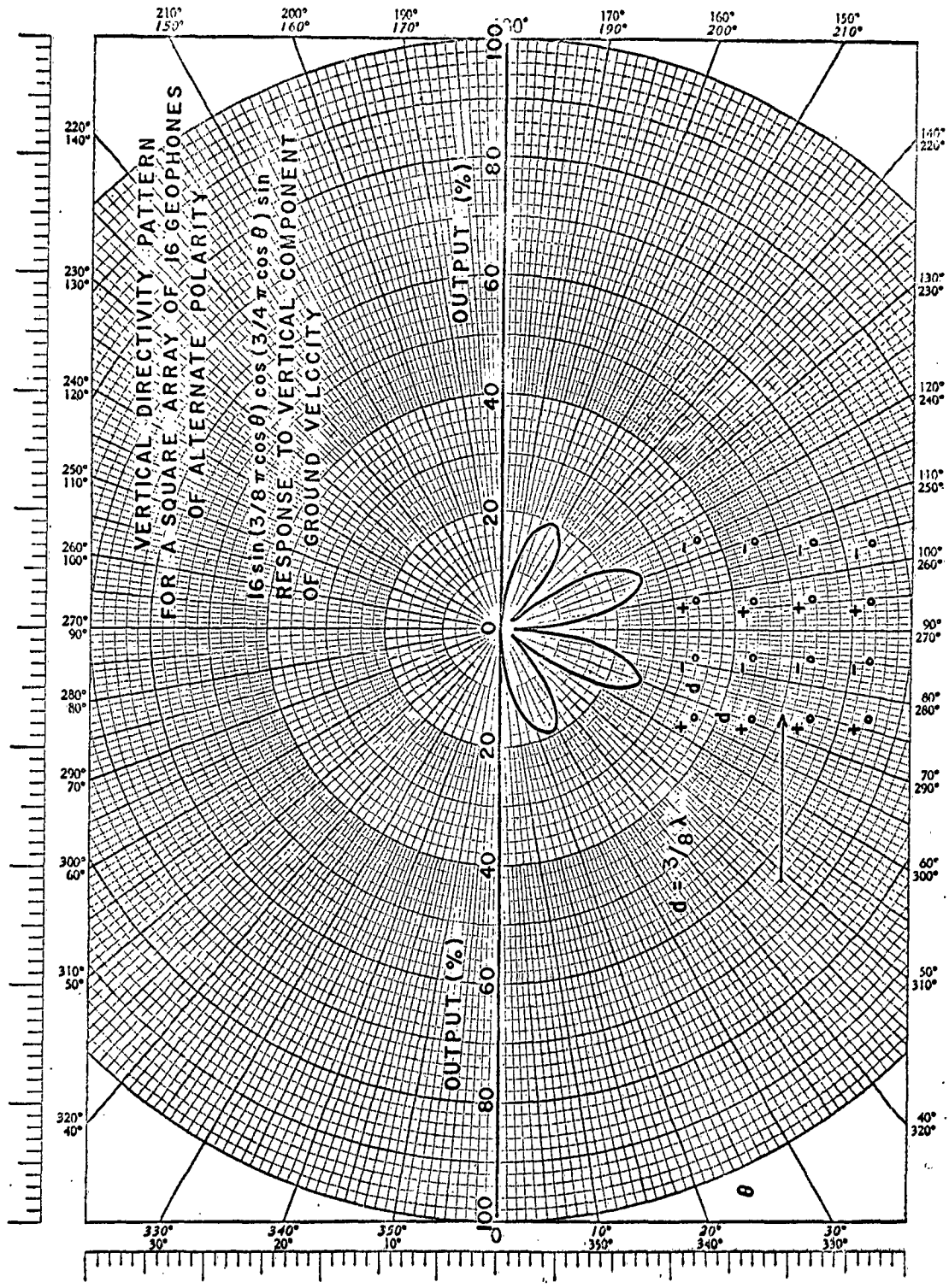
VERTICAL DIRECTIVITY PATTERN
FOR A SQUARE ARRAY OF 16 GEOPHONES
OF ALTERNATE POLARITY
16 sin (3/8 π cos θ) cos (3/4 π cos θ) sin
RESPONSE TO VERTICAL COMPONENT
OF GROUND VELOCITY
OUTPUT (%)
OUTPUT (%)
d = 3/8 λ
θ

Fig. 7.10

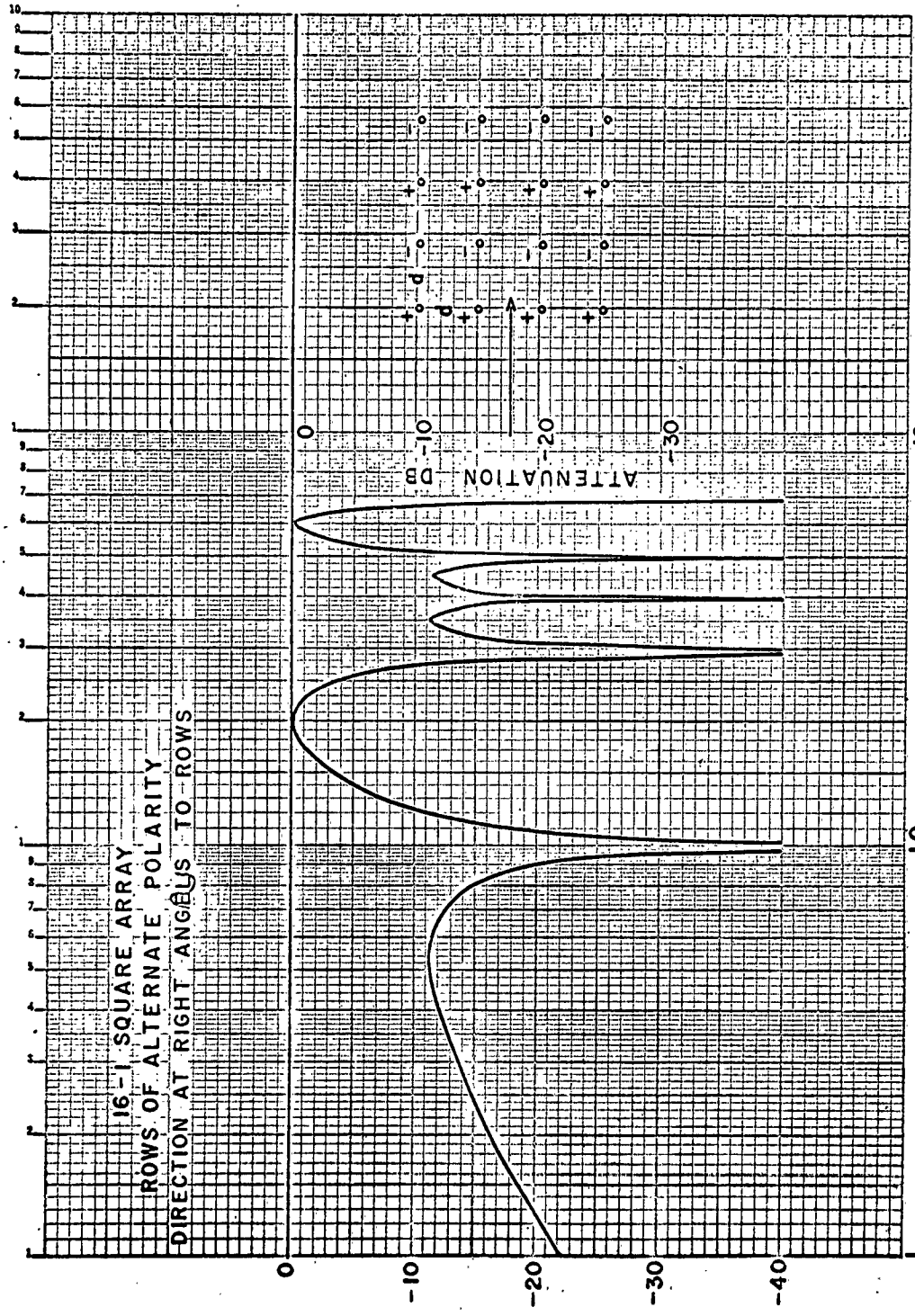
16-1 SQUARE ARRAY
ROWS OF ALTERNATE POLARITY
DIRECTION AT RIGHT ANGLES TO ROWS
ATTENUATION DB
0
-10
-20
-30
-40
1.0
10
F = 4 d/λ = 4 d/v f

Fig. 7.11

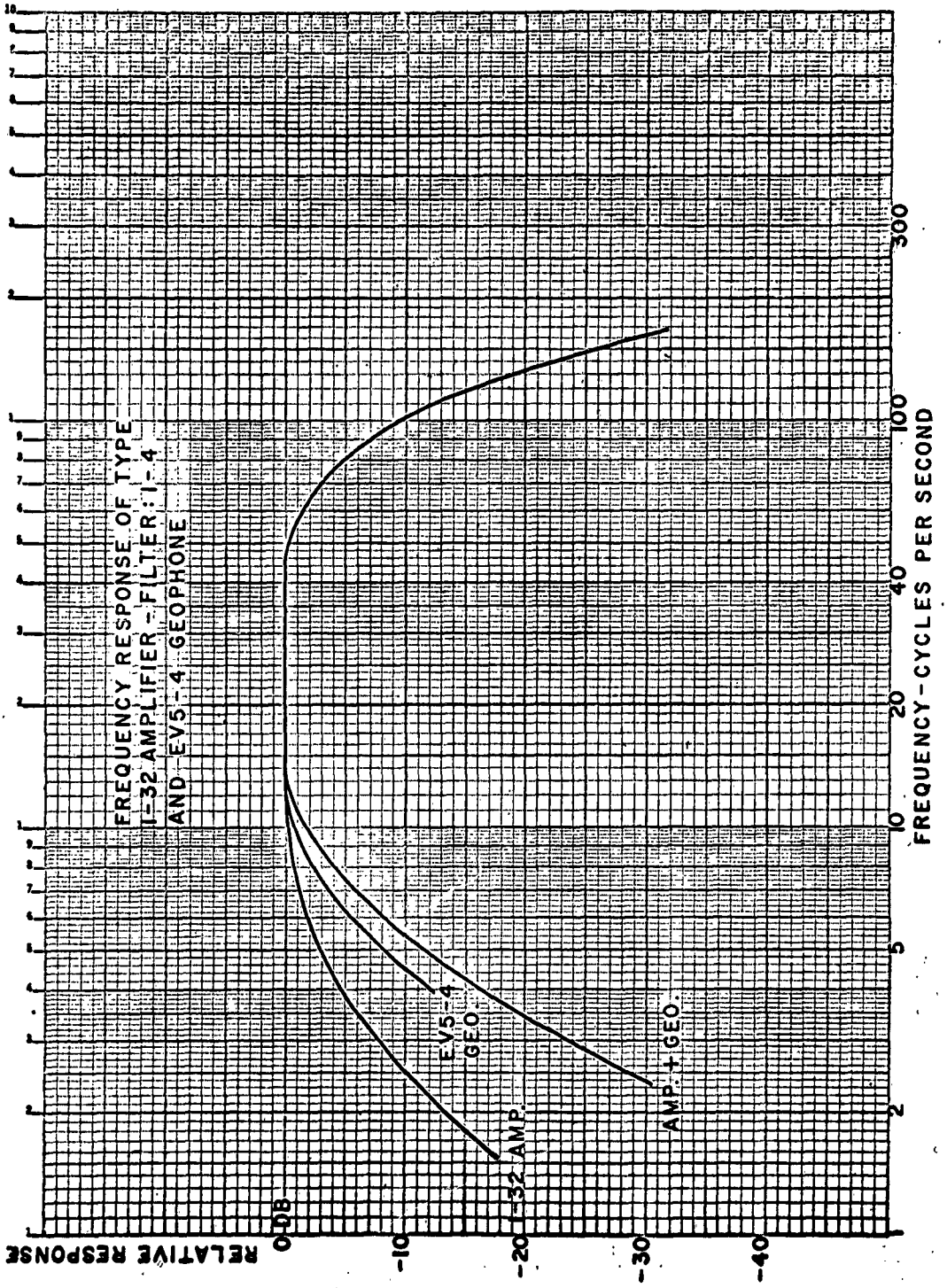
FREQUENCY RESPONSE OF TYPE
I-32 AMPLIFIER - FILTER: I-4
AND EV5-4 GEOPHONE
RELATIVE RESPONSE
0 DB
-10
-20
-30
-40
1
2
5
10
20
40
100
300
FREQUENCY - CYCLES PER SECOND
EV5-4
GEO.
I-32 AMP.
AMP. + GEO.

Fig. 7.12

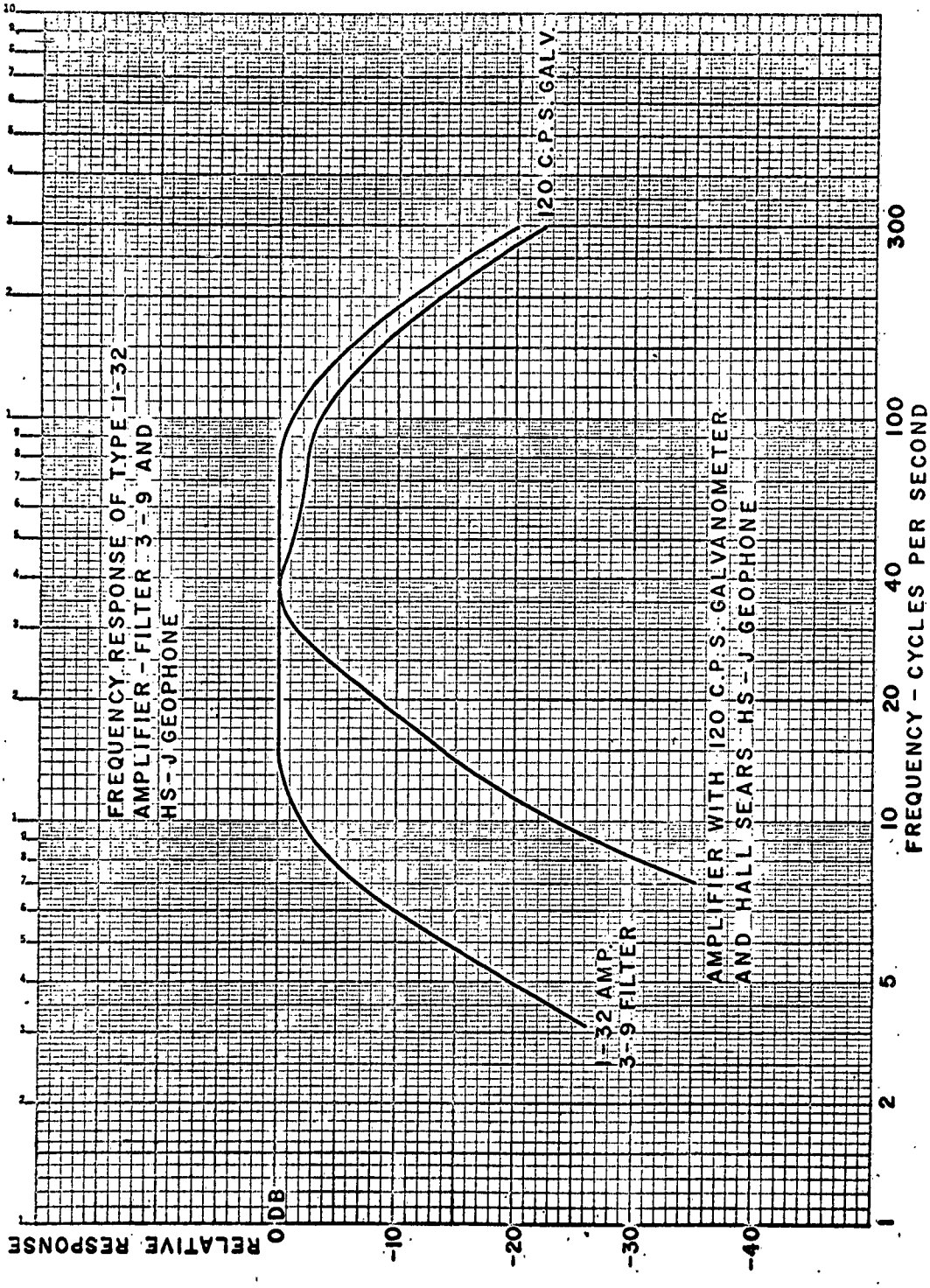
FREQUENCY RESPONSE OF TYPE 1-32 AMPLIFIER-FILTER 3-9 AND HS-J GEOPHONE
120 C.P.S. GALV.
AMPLIFIER WITH 120 C.P.S. GALVANOMETER AND HALL SEARS HS-J GEOPHONE
1-32 AMP. 3-9 FILTER
RELATIVE RESPONSE
0 DB
-10
-20
-30
-40
1
2
5
10
20
40
100
300
FREQUENCY - CYCLES PER SECOND

Fig. 7.13

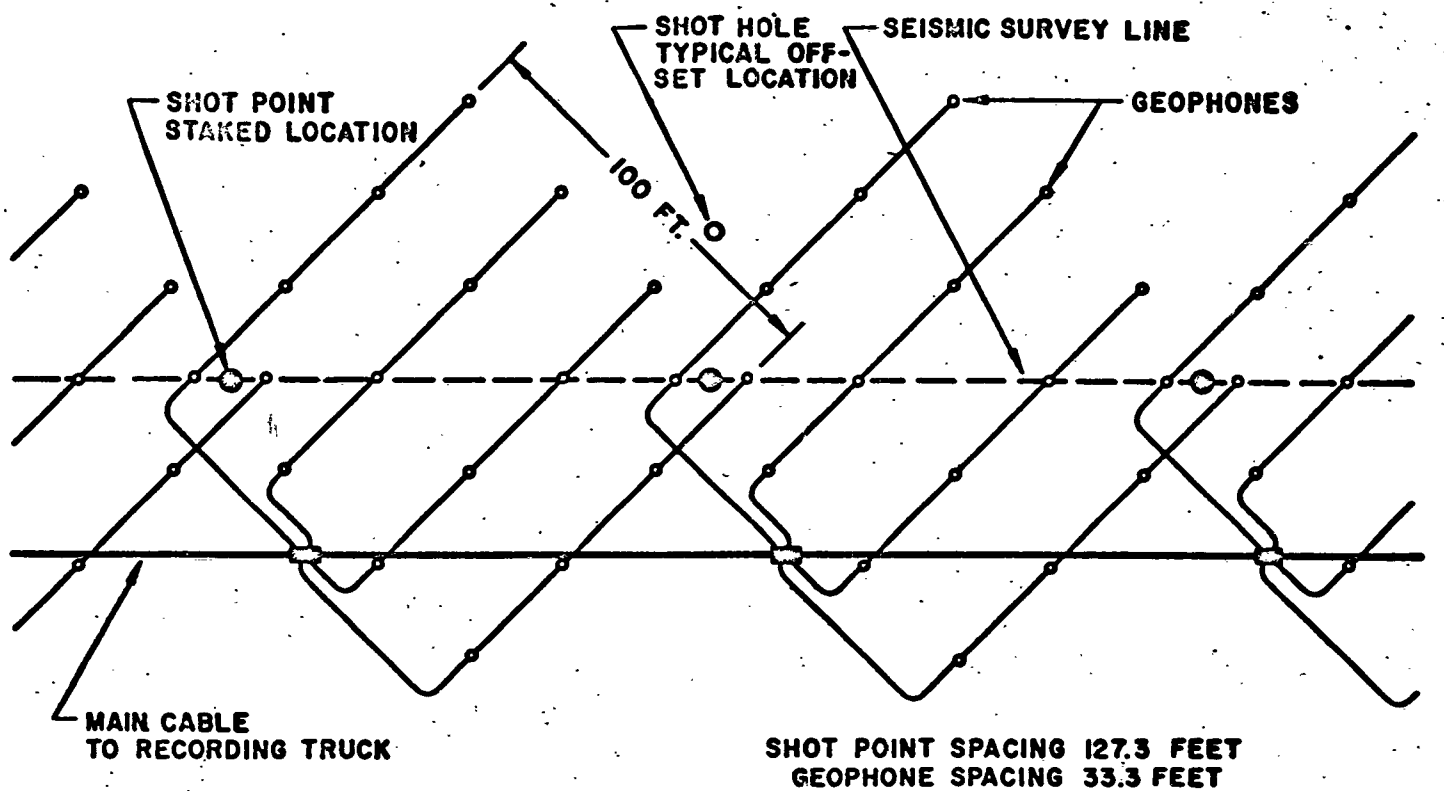

PROJECT DRIBBLE
GEOPHONE ARRAY FOR
SEISMIC FOCUSING PROFILING

Fig. 7.14

K&E SEMI-LOGARITHMIC 359-71
KEUFFEL & ESSER CO. MADE IN U.S.A.
3 CYCLES X 70 DIVISIONS

TATUM

TATUM

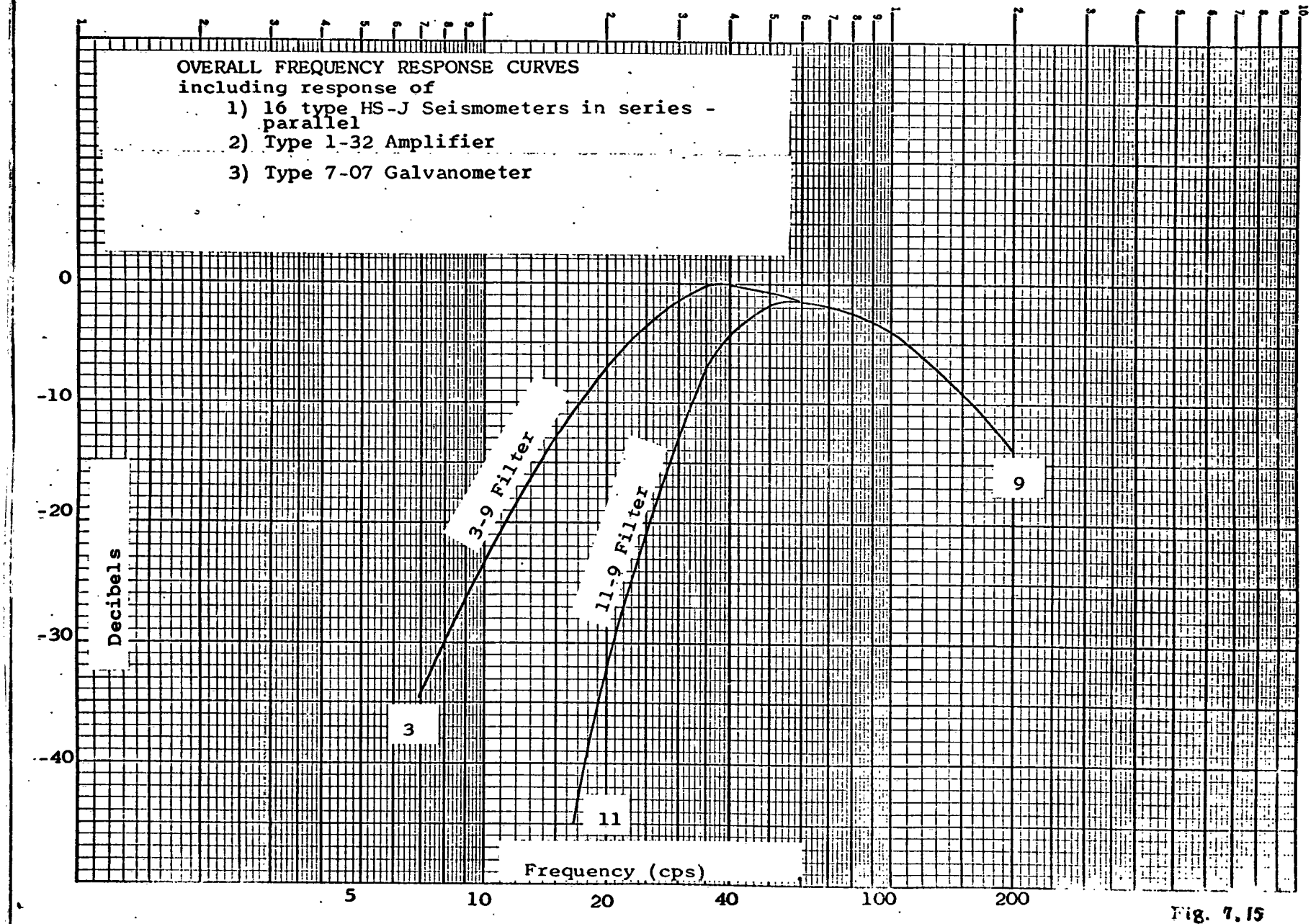

Fig. 7.15

8.0 Uphole Velocity Surveys

Figures 8.1 to 8.5 show the variation in interval and average velocity with depth observed at U.E.D. uphole velocity surveys R-1, R-7, R-8, R-9, and R-10 on top of RAINIER Mesa. With the exception of R-1, all of the uphole velocity surveys are located a considerable distance from the east face of RAINIER Mesa (see enclosure 1).

The depth of the U.E.D. vertical velocity investigations on top of RAINIER Mesa varied from 120 to 195 feet. According to the interval velocities delineated, the uphole surveys penetrated essentially the same velocity section at all locations.

All holes were drilled without water and uphole shots were not tamped.

The average charge size ($1\frac{1}{4}$ pounds), shot interval (10 feet) and recording spread geometry employed for the uphole velocity surveys was conventional. While this procedure yielded satisfactory results, examination of the recorded interval times suggests that there was appreciable variation in hole conditions from shot to shot up the hole. This is particularly true of the uphole data recorded at velocity survey location R-1.

The source of the erratic variation in interval times was not ascertainable. Some of the variation derives from secondary effects associated with uphole shooting, some from errors in determining the time of arrival on the records and some from cavities and fracturing of the section. However, it is notable that the interval times recorded at uphole location R-1 show a much greater degree of scatter than at the other locations. The greater degree of scattering in interval times may be a reflection of the fracturing produced by the nuclear detonations or local variation in the lithology and degree of welding.

A general description of the velocity stratification of the welded Oak Spring Tos_8 tuff follows. With the exception of uphole location R-7, which lies farthest to the north, all of

the surveys indicate a velocity of 4800 to 5600 feet per second in the upper 60 to 80 feet of section. From depths of 80 to 125 feet, all of the surveys indicate a velocity inversion with velocities ranging from 1900 to 4900 feet per second preceded by a high velocity layer with velocities of 8,000 to 10,000 feet per second. Below the velocity inversion all of the velocity surveys show a second high velocity layer with a velocity ranging from 8,000 to 13,000 feet per second.

Figure 8.6 shows the apparent correlation of velocity horizons delineated at uphole locations in the western part of RAINIER Mesa with velocity horizons delineated at uphole location R-1 near the eastern rim of the mesa. In making these correlations regional dip and correspondence in velocities were used as a guide.

Figure 8.7 shows the apparent correlation of the velocity horizons from hole to hole in the north-south direction on the west side of RAINIER Mesa. The correlations are consistent except at the north end of the profile between uphole locations R-8 and R-7.

While uphole location R-7 apparently lies farther updip from the axis of the indicated syncline than R-8, it may lie farther down dip regionally. If such were the case and the beds were truncated by erosion, the upper portion of the R-7 hole might be expected to have penetrated younger section, particularly as it is located at a higher elevation. Under these conditions, observed velocity horizons at locations R-7 and R-8 should correlate as shown. If the structural situation were other than described, correlation of the velocity horizons would require appreciable lateral change in velocity indicative of faulting or an abrupt and anomalous variation in the physical character of the lithology to account for the difference in velocity stratification.

The field operations report supplied by United Electro Dynamics, Inc. states that a fracture zone was frequently encountered, in drilling shot holes, at depths of 80 to 100 feet on RAINIER Mesa. Further reference to a fracture zone is made in U.S.G.S. Technical Letter 762 in the discussion of a variable velocity

interval delineated at a depth of 110 to 140 feet by the sonic log recorded at EVANS ground zero (see Figure 5.6). Observed velocities in this interval on the sonic log vary from 4300 to 12,800 feet per second. The correspondence in the depth of the fracture zone and the depth of the velocity inversion suggests they are interrelated, particularly as the velocity stratification shows a tendency to parallel surface topography. However, horizontal fracture zones are so numerous at depths of 80 to 100 feet in the welded Tos_8 tuff that an equivalent effect may result without regional continuity of any one zone.

The thickness of the low velocity layer or zone responsible for the velocity inversion is not well defined regionally, particularly in the eastern part of RAINIER Mesa. In the western part of the "Mesa" three velocity surveys indicate a thickness of some 15 feet for a distance approaching one mile in the north-south direction. Along the eastern edge of the "Mesa" two surveys show indication of the layer but only one of these uphole velocity surveys, R-1, logged sufficient shallow section to delineate its probable total thickness of 60 feet. The second velocity survey indicating the layer was recorded at EVANS ground zero as part of the nuclear test program, but due to commencement of logging at a depth of 110 feet below the surface delineated only 30 feet of the layer (see Figure 5.6). Since both velocity surveys in the east indicate a thicker layer than was delineated in the west, there is either appreciable areal variation in the effective total thickness of fracturing responsible for the velocity reduction or a difference in lithology.

It should be noted that thickening from west to east is not confined to the zone of velocity inversion but is also indicated in the shallower velocity layers. Also notable is the smaller north-south variation in the thicknesses of the velocity layers in the west and the thickness of the high velocity layer denoting the bottom of the Oak Spring Tos_8 tuff between uphole surveys UCRL-3 and EVANS ground zero along the east edge of RAINIER Mesa. However, thickening of the high velocity layer from east to west between the EVANS

ground zero velocity survey and the uphole survey 300 feet to the west (see Figure 5.5) suggests that the thicknesses of the horizons may vary abruptly, and to a greater degree in the east-west direction than in the north-south direction.

Below the 5000 foot per second surface velocity layer, interval velocities delineated by the uphole surveys are lower in the west than in the east part of RAINIER Mesa (see Figure 8.6). Reference to Figure 8.7 showing uphole velocities observed in the western part of RAINIER Mesa discloses that lateral variation in velocity, excluding location R-7, is not as great in the north-south direction essentially parallel to strike as in the east-west direction. Along the east edge of RAINIER Mesa, between locations R-1, EVANS ground zero and UCRL-3 the velocity of the base of the welded Tos_8 tuff also varies less in the north-south direction than in the east-west direction. The correlation between the direction of lateral velocity change, and direction of thickening of the velocity horizons suggests a connection with the amount of overburden. However, a lower degree of welding, more extensive fracturing, compaction due to overburden, or a combination of all three would produce the same effect.

The high velocity layer denoting the base of the welded Oak Spring Tos_8 tuff shows no recognizable pattern of velocity variation which can be attributed to the effects of the nuclear tests. Before the RAINIER event and eighty feet from ground zero the base of the welded Tos8 tuff had a velocity of 12,000 feet per second. At the two EVANS uphole surveys 520 and 800 feet southwest of RAINIER ground zero, the velocity of the base of the welded Tos_8 tuff following the RAINIER event and preceding the BLANCA event was observed to be respectively 11,500 and 10,000 feet per second. At U.E.D. uphole location R-1, 830 feet south of RAINIER ground zero, the velocity of the base of the welded tuff measured following the BLANCA event is indicated to be 12,800 feet per second. Comparison of the velocities of the base of the welded Tos_8 tuff at the R-1 and EVANS locations, at respective distances of 830 and 800 feet from RAINIER ground zero, discloses a velocity difference of 2800 feet per second. Approaching RAINIER ground zero from U.E.D. location R-1, the velocity of

the base of the welded Tos_8 tuff decreases from 12,800 to 11,500 feet per second. Approaching the RAINIER site from the more distant EVANS uphole survey location the velocity of the base of welded Tos_8 tuff increases from 10,000 to 11,500 feet per second. Unless there was considerable asymmetry in the radial distribution of structural effects surrounding the RAINIER event, the velocity of the base of the welded Tos_8 tuff should be lower at 520 feet than at 800 feet from RAINIER ground zero.

Although the velocity of the base of the Tos_8 tuff does not show the pattern of variation one should expect near RAINIER ground zero, there is insufficient basis for concluding that the effect of the shot on the tuff at these distances cannot be detected. Uncertainties connected with the effect of EVANS, BLANCA and LOGAN on the velocity measurements, lateral velocity variation, and the lack of post-RAINIER velocity data for the tuff at RAINIER ground zero and pre-RAINIER velocity data for the tuff in the vicinity of the EVANS site materially affect the evaluation.

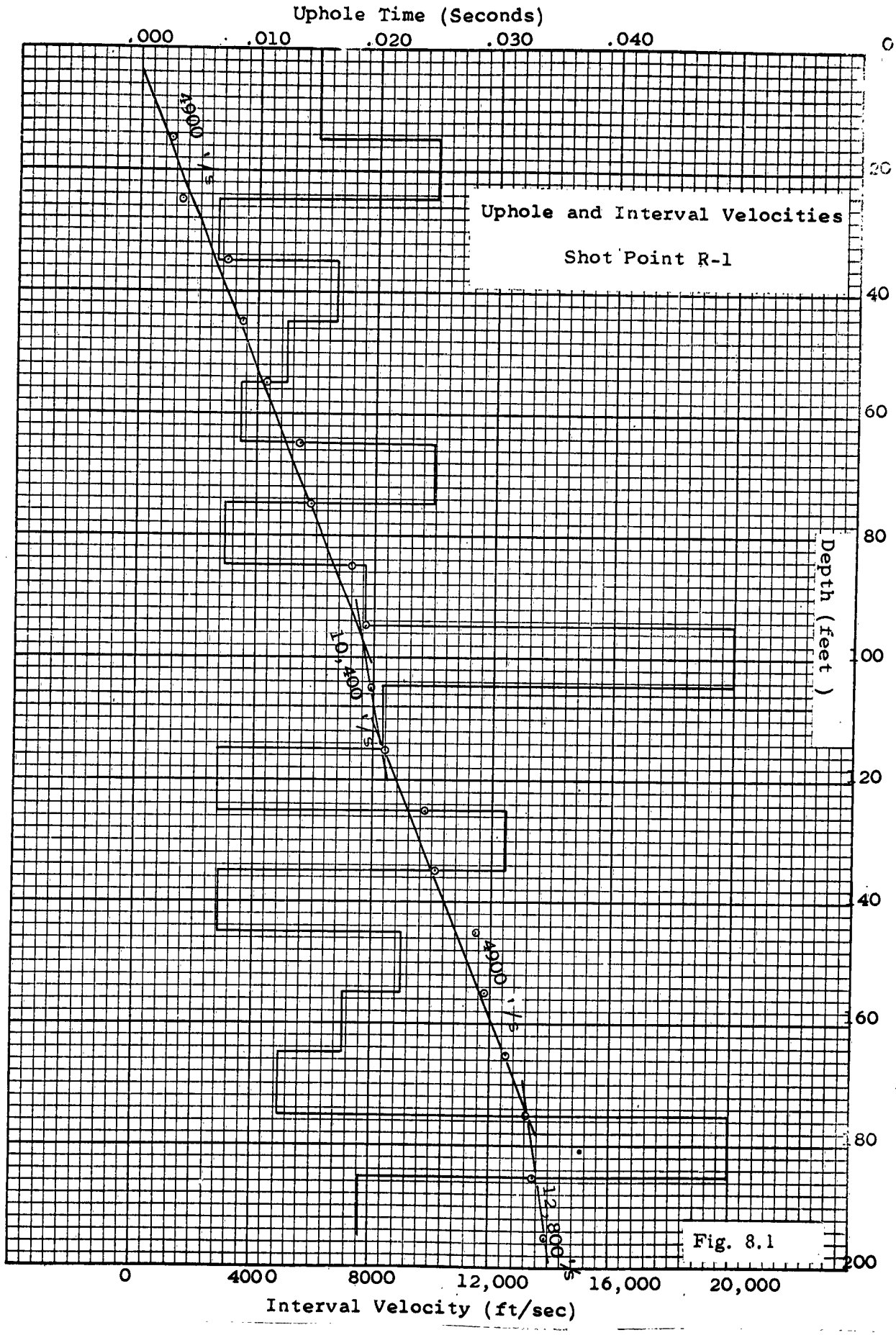

Fig. 8.1

K&E 10 X 10 TO THE INCH KEUFFEL & ESSER CO. 359-5 MADE IN U.S.A.

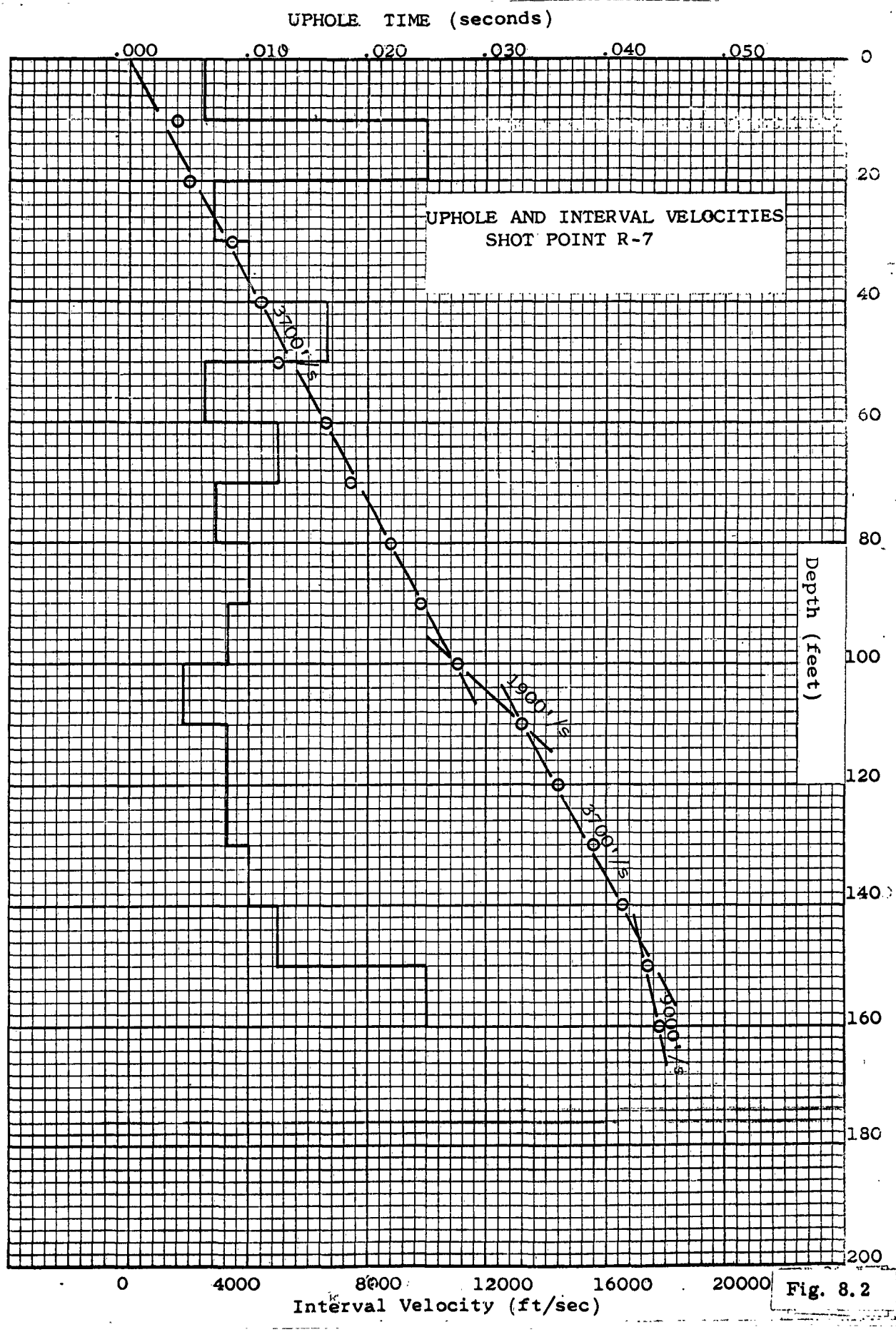
UPHOLE TIME (seconds)
.000
.010
.020
.030
.040
.050
0
20
40
60
80
100
120
140
160
180
200
UPHOLE AND INTERVAL VELOCITIES
SHOT POINT R-7
3700 ft/s
1900 ft/s
3700 ft/s
3000 ft/s
Depth (feet)
0
4000
8000
12000
16000
20000
Interval Velocity (ft/sec)
10 X 10 TO THE INCH 359-5
KEUFFEL & ESSER CO. MADE IN U.S.A.

Fig. 8.2

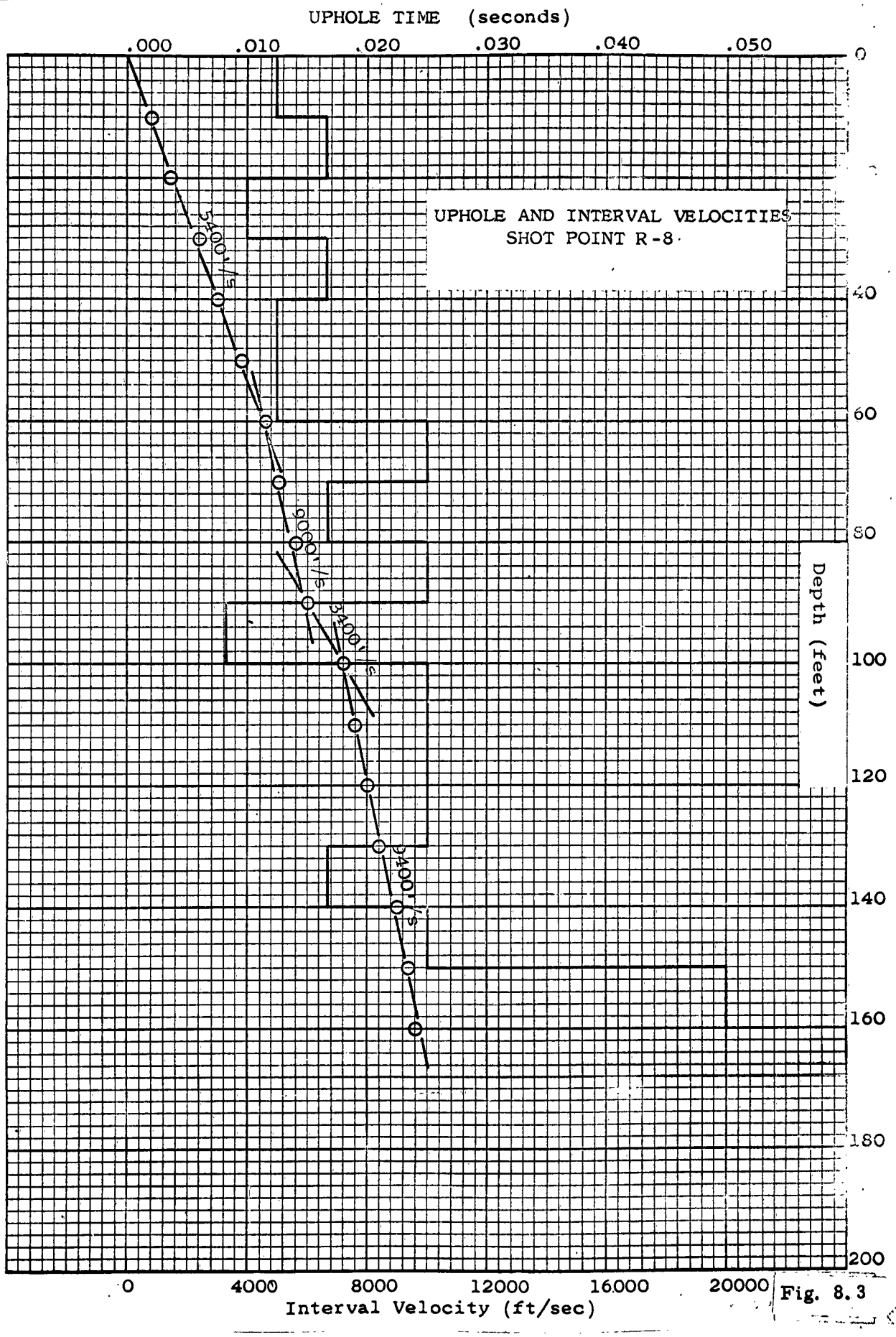

Fig. 8.3

K&E 10 X 10 TO THE INCH 359-5 KEUFFEL & ESSER CO. MADE IN U.S.A.

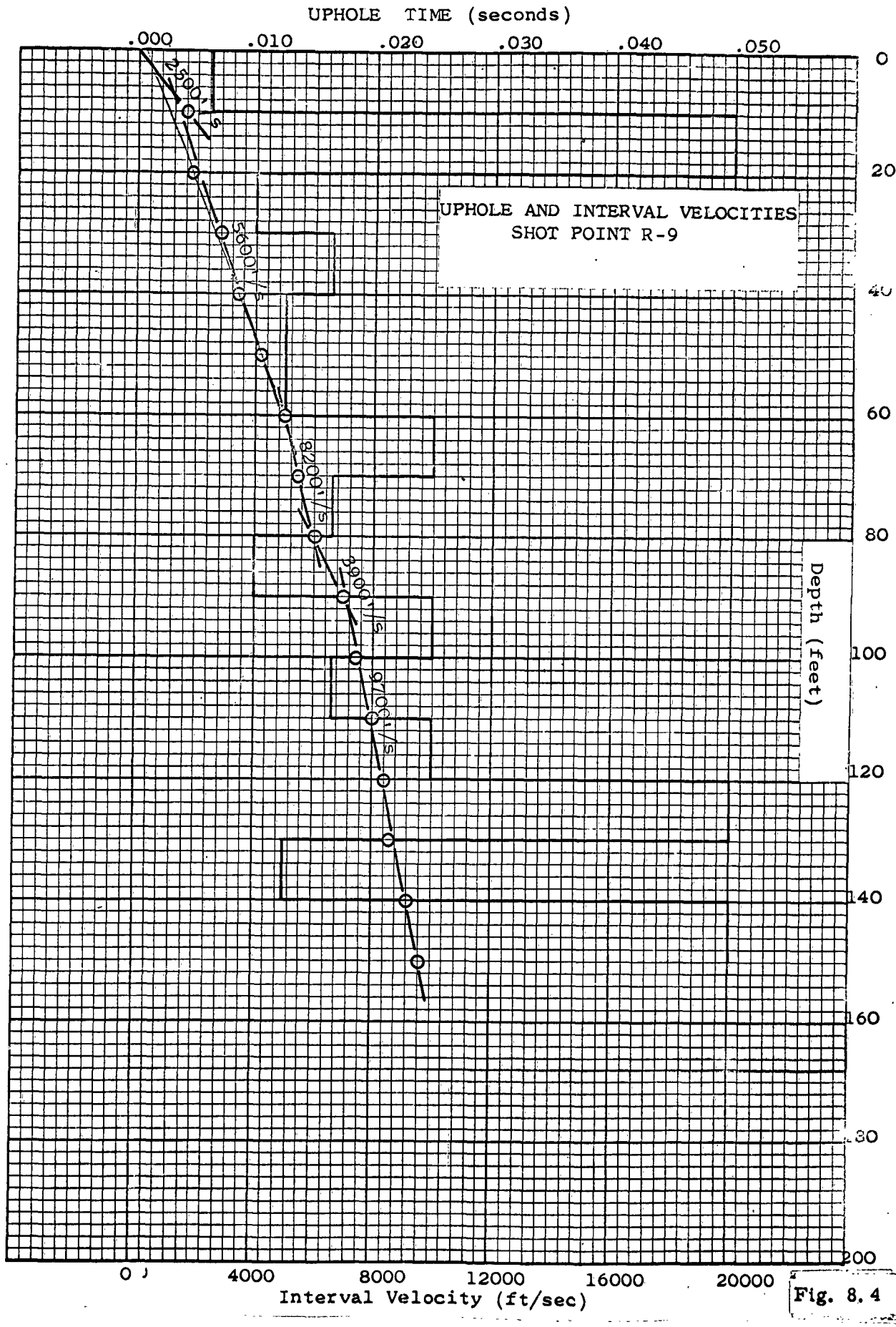

Fig. 8.4

K&E 10 X 10 TO THE INCH 359-5 KEUFFEL & ESSER CO. MADE IN U.S.A.

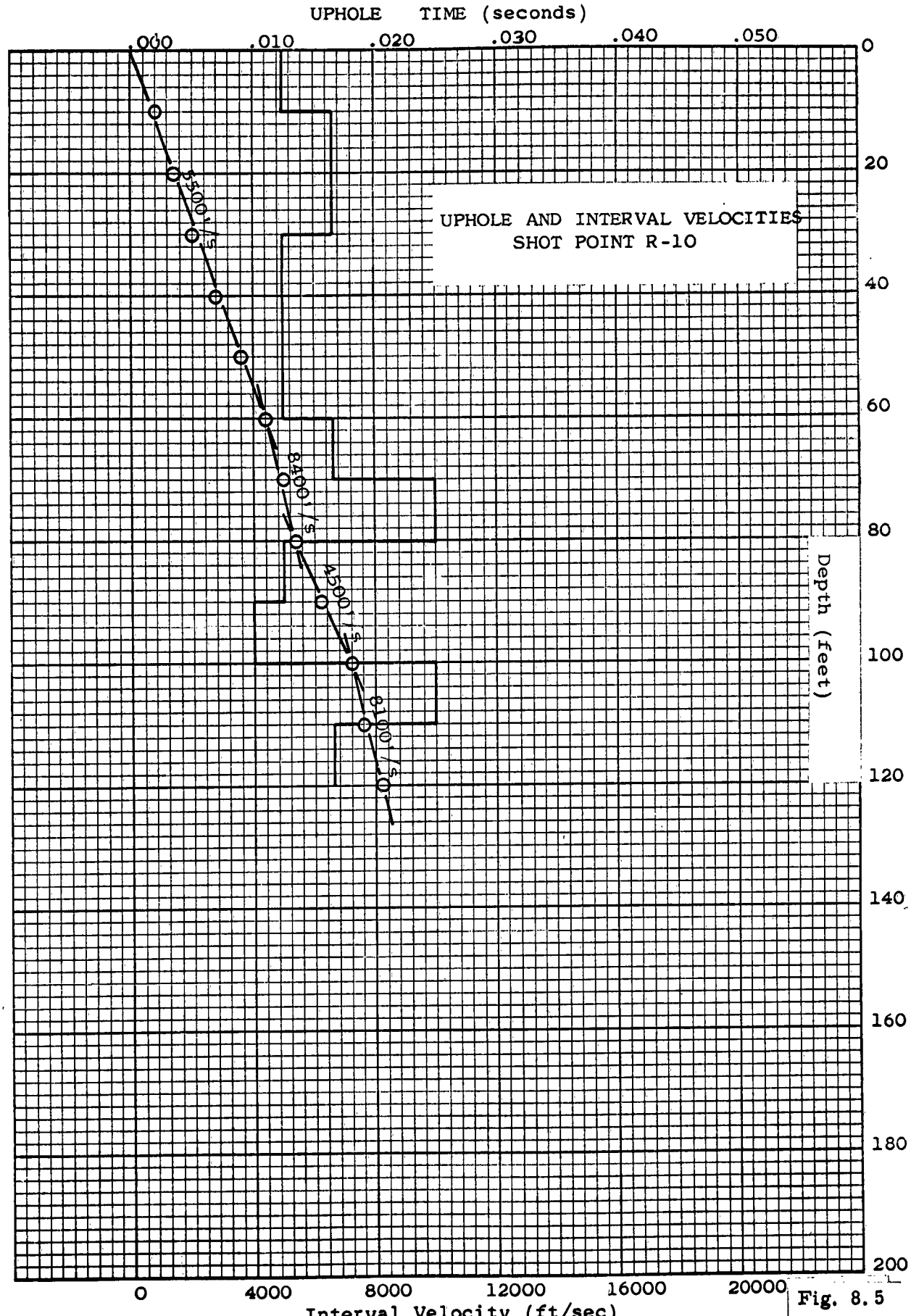

10 X 10 TO THE INCH 359-5
KEUFFEL & ESSER CO. MADE IN U.S.A.

Fig. 8.5

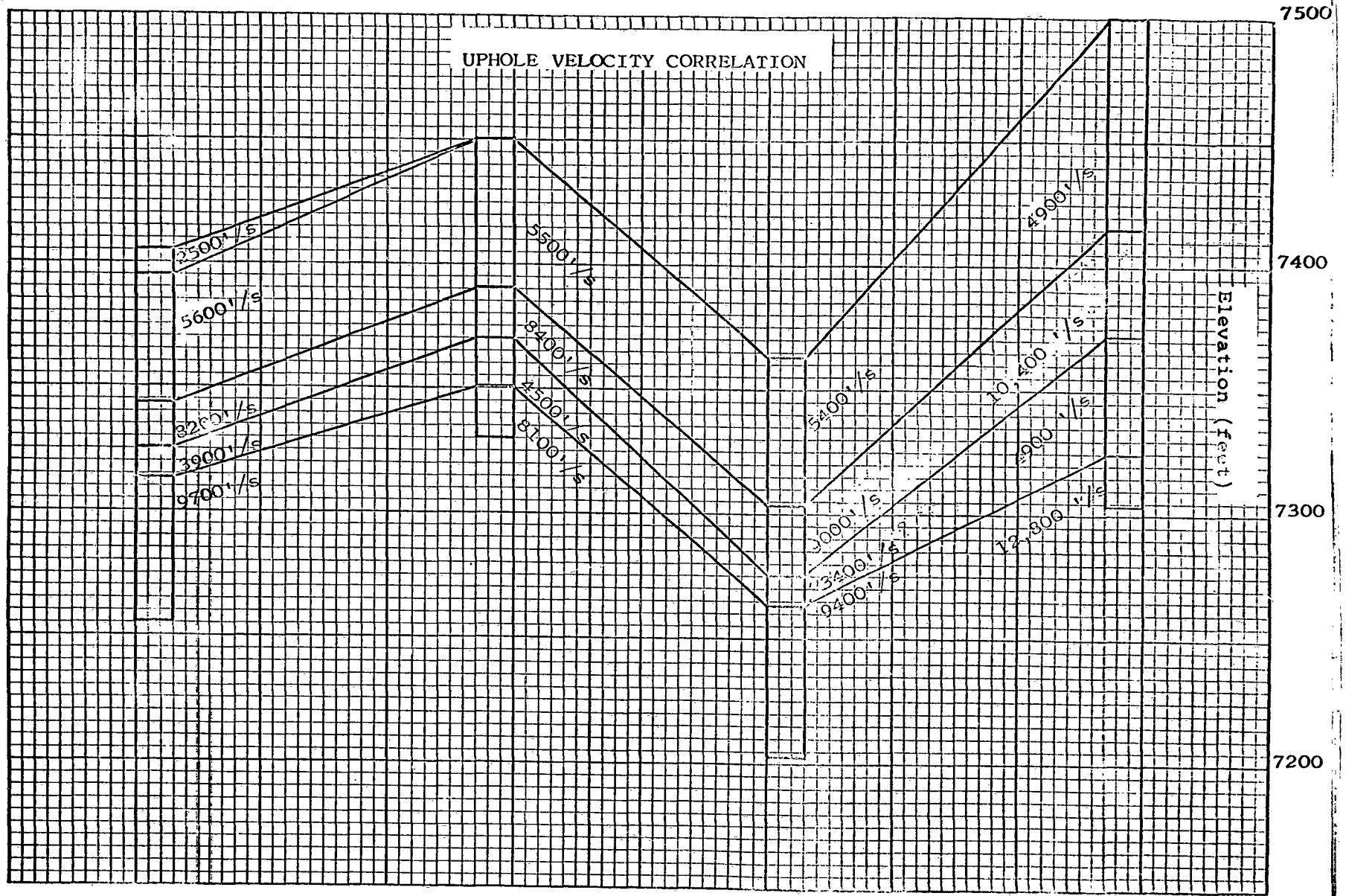

Not to scale

Fig. 8.6

South

K+E 10 X 10 TO THE INCH 359-5
KEUFFEL & ESSER CO. MADE IN U.S.A.

North

R-10 R-9 R-8 R-7

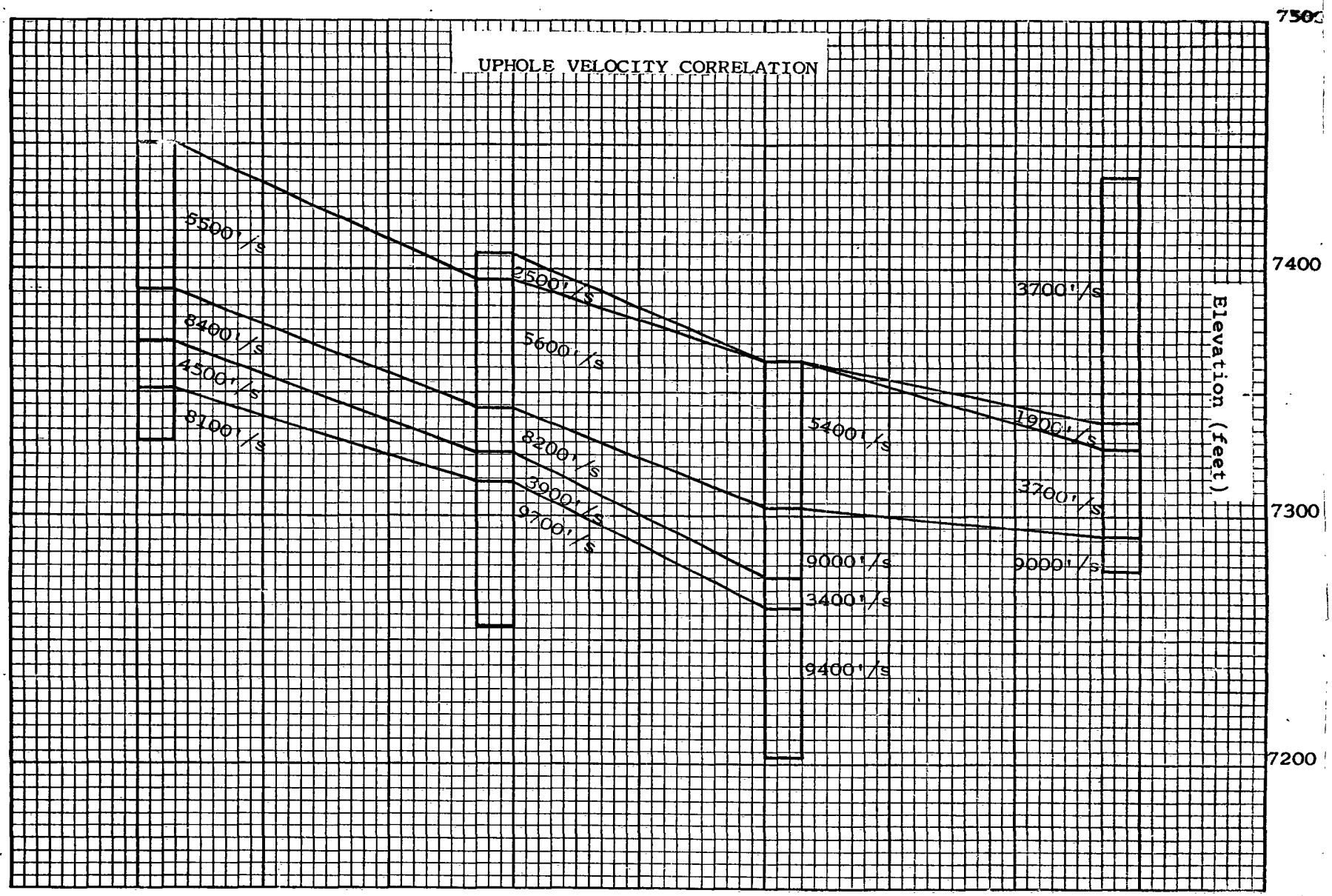

Not to scale

Fig. 8.7

9.0 Near Surface Velocity Profiling

The objective of the near surface velocity survey on RAINIER Mesa was to delineate anomalous horizontal velocity variation in the shallow Oak Spring tuff due to the effects of the underground explosions. At the horizontal range of the survey from the LOGAN and BLANCA events, horizontal velocity probably should be affected only by fracturing and/or faulting. At the RAINIER site interlayer spalling as well as fracturing should have an effect on horizontal velocity.

Four lines of near surface velocity profiles were shot on RAINIER Mesa. Three of these lines, 1, 2, and 3, were located on top of the "Mesa" and one line, MF, was located below the rim on the east face of the "Mesa" (see Figure 9.1).

Lines 1 and MF were located to pass as close to the sites of the nuclear events as feasible. The distances to the NSV profiles on these lines nearest to each event are as follows:

Line Number	Profile Number	BLANCA Event Horizontal Distance (Ft)	Slant Distance (Ft)
1	R20-NSV21	870 W	1700 W
MF1	MF1	1500 SE	1325 SE
		LOGAN Event	
MF1	MF1	710 E	845 E
		RAINIER Event	
1	R26-NSV25	0	900

Charge sizes on NSVP lines 1, 2, and 3 on top of RAINIER Mesa ranged from 20 to 70 pounds. The predominant charge size was from 50 to 70 pounds.

All shot holes were drilled with air to an estimated 30 feet below any fracture zone or a maximum depth of 165 feet. All shots were tamped without use of water using dry material.

Figures 9.2, and 9.3 show the average velocity to the surface from the deep shot of each near surface velocity profile along lines 1, 2 and 3 on top of RAINIER Mesa. At five of the near surface velocity profiles, R-21, R-23, R-29, R-31, and R-32, the deep shot was between 75 to 100 feet deep.. Of the remaining 18 profiles, R-11, R-12, R-13, R-16, R-17 and R-27 had deep shots at depths of 125 to 145 feet. The balance of the profiles had shots at depths between 100 and 125 feet.

Figure 9.4 shows the average velocities obtained from the near surface velocity profiles and uphole velocity surveys. The resulting map discloses that the areal variation in the average velocity of the upper most 75 to 150 feet of the Oak Spring tuff to be oriented roughly parallel to the structural axis of RAINIER Mesa. However, the significance of the velocity map depends upon the extent to which the variation in average velocity depends upon the relationship of the sampled section to the thicknesses, velocities and depths of the velocity horizons and of the velocity horizons to surface elevation. Along the east rim of RAINIER Mesa, average uphole velocities show a marked increase from south to north with decreasing elevation. This is probably attributable to the fact that the bulk of the deep shots were at depths of 100 to 120 feet and, allowing for erosion of the low velocity surface layer, sampled increasingly greater amounts of high velocity section with decreasing elevation. Since there is a decrease in elevation from east to west and the shot depth is essentially consistent we must assume that the increase in velocity derives from the same source as in the north-south direction. The question which could not be answered was whether the variation in velocity was commensurate with the ratio of sampled high and low velocity material. While variations in shot depth of 20 to 30 feet in any one hole produced little variation in the average uphole velocity, the same variation in shot depth due to a change in elevation often produced considerable variation in the uphole velocity.

Comparison of Figures 6.1, 6.2, and 9.4 shows that the location of the velocity low near Egg Point, coincides with the area of most intense fracturing on RAINIER Mesa due to the LOGAN and BLANCA events. However, since the average velocity variation is

greatly influenced by the depth of the shot and surface elevation, the extent of the velocity variation attributable to fracturing is unknown. However, it should be noted that the two faults shown on the map of RAINIER Mesa, if extended, would also traverse the area of the average velocity low north of Egg Point.

The first time of arrival data recorded on the near surface velocity profiles is shown plotted against distance on Figures 9.5 to 9.44.

The quality of the first breaks varies widely. Regionally, the first breaks are of better quality on the southern half of line 1 and on line 2 than on the northern half of line 1 or on line 3. Beyond 900 feet the onset of the first arrival energy is generally indeterminate. Consequently, most of the first times of arrival were determined from first troughs. Since there is some variation in the periods of the troughs the procedure has introduced some scatter. However, the scatter shown on the graphs does not all derive from the use of first troughs. An equal, if not greater amount of scatter accrues from variation in the lithology and transmission properties along the spread. As a consequence of this scatter, there is believed to be a potential error of 10 to 15 percent in the apparent velocities derived from the first arrival time data.

The degree of uncertainty in deriving horizontal velocity from first arrival times recorded on near surface velocity profiles is sufficiently high that delineation of variation in velocity attributable to the effects of the explosion may not be feasible. Post-shot evaluation of the effect of the RAINIER event on the physical properties of the tuff by the U.S.G.S. (see Section 5.0) disclosed a velocity reduction of 10 percent 100 feet from the weapon point. At the distance at which the near surface velocity survey on RAINIER Mesa is located from the LOGAN and BLANCA events fracturing and, therefore velocity should have suffered a lesser reduction than was observed 100 feet from RAINIER event. Thus, the potential error of 10 to 15 percent in the velocities delineated by near surface profiling may mask the velocity reduction produced by the explosions which one wishes to delineate.

The rapid attenuation of first arrival energy with distance observed on the near surface velocity profiles is characteristic of velocity reversal. Since such velocity reversal was delineated by the uphole velocity surveys at depths ranging from 80 to 100 feet on RAINIER Mesa, velocity reversal seems reasonably certain in both the north-south and east-west directions. It is not certain that the zone of velocity reversal is continuous or parallel to the velocity stratification although it has been considered to be such in correlating the velocity horizons defined by the uphole velocity surveys. Neither is it known with certainty what the relationship is between the velocity stratification and surface topography. Additional uncertainty in interpreting the first time of arrival data recorded on the near surface velocity profiles derives from the placement of the shot with respect to the velocity reversal. Some effects of shot placement and lateral variation in thickness and interval velocity are outlined in succeeding paragraphs.

The possible transmission paths for a shot above a velocity reversal and pattern of velocity stratification such as delineated by the uphole velocity surveys on RAINIER Mesa are illustrated in the accompanying figures.

In Figure 9.45A, the transmission paths are shown for a velocity stratification of the form

$$V_{oo} < V_1 < V_2$$

If the Voo layer were not present, the time-distance graph would be indicated by lines 1 and 2 in Figure 9.45B. Some results of variation in the velocity ratios are as follows:

A. When V_2 equals or is less than V_1, energy which has traveled through V_2 cannot reach any geophone as a first arrival because energy which traveled through V_1 will arrive first.

B. The character of the time-distance curve, as defined by lines 1 and 3, will be the same regardless of the location of the Voo layer within the V_1 layer, so long as V_1 has sufficient thickness to act as a refractor.

Figures 9.46 to 9.49 illustrate the variations which may be encountered when the velocities and thicknesses of Voo, V_1 and V_2 vary laterally with the shot still located at the upper interface of the V_1 layer. If the shot were fired in the Voo layer the energy could travel up to V_1, along V_1 and then up through Vo to the surface; or it could travel down to V_2, along V_2 and then up through Voo, V_1 and Vo to the surface. The actual path taken by the first arrival energy depends upon the velocities and thicknesses of V_1, Voo and V_2 and the position of the shot. In the accompanying illustrations and discussion the velocity V_2 is identified with the high velocity layer constituting the base of the welded Tos_8 tuff, velocity V_1 is identified with the upper high velocity layer, and Voo is identified with the low velocity layer between V_1 and V_2.

Figure 9.50 shows the first time of arrival data recorded on the near surface velocity profiles along line 1 graphed against distance. The refraction velocities resulting from averaging reversed segments of the time-distance graphs are shown on Figure 9.2 plotted adjacent to the average uphole velocities obtained from the deep shot of the near surface velocity profiles. The salient features of the refraction velocity profiles are the reduction in velocity from north to south commensurate with the reduction in average uphole velocity, the generally low refraction velocities and the abrupt transition from low to higher refraction velocities at NSVP-21.

To evaluate the significance of the reduction in refraction velocities from north to south, commencing at NSVP-21, it is first required to know the position of the shot with respect to velocity reversal and the paths taken by the first arrival energy to the surface on each profile. Neither of the above can be defined from the existing refraction data alone since one assumption made in all refraction methods is that there is no decrease in velocity with depth. Velocity reversals lead to calculations of depth that are too deep, and if the amount of decrease varies laterally, as indicated by the uphole velocity surveys, it will also have a substantial effect on the dip calculations. The presence of velocity inversion plus lateral velocity variation, therefore prevents valid determination of the correlation and depths of the velocity horizons penetrated

by the first arrival energy from profile to profile and, therefore evaluation of the different features of the refraction velocity profile.

It should be noted that when it can be positively determined that the shot has been fired below the velocity reversal, the uphole method of computation provides a reasonably accurate near surface correction. Thus, by employing uphole shooting in conjunction with the refraction method it should have been possible to evaluate the refraction data. However, in order to use the combined uphole-refraction method, the following conditions must be satisfied:

1. At least every fifth or sixth shot hole, more, depending upon the rate of lateral velocity variation, must penetrate through the Voo or low velocity layer.

2. The critical distance on the time distance plots must be less than $x/2$ where x is a half spread length.

Another feature of the first time of arrival data recorded on the different near surface velocity profiles is the indication of faulting. Specific profiles on which the time of arrival data indicate faults are R20-NSV 21, R21-NSV 20, and R25-NSV 26, R27-NSV 26. Location of these faults is of dubious value since it is not known whether they occurred along old fractures or were newly created.

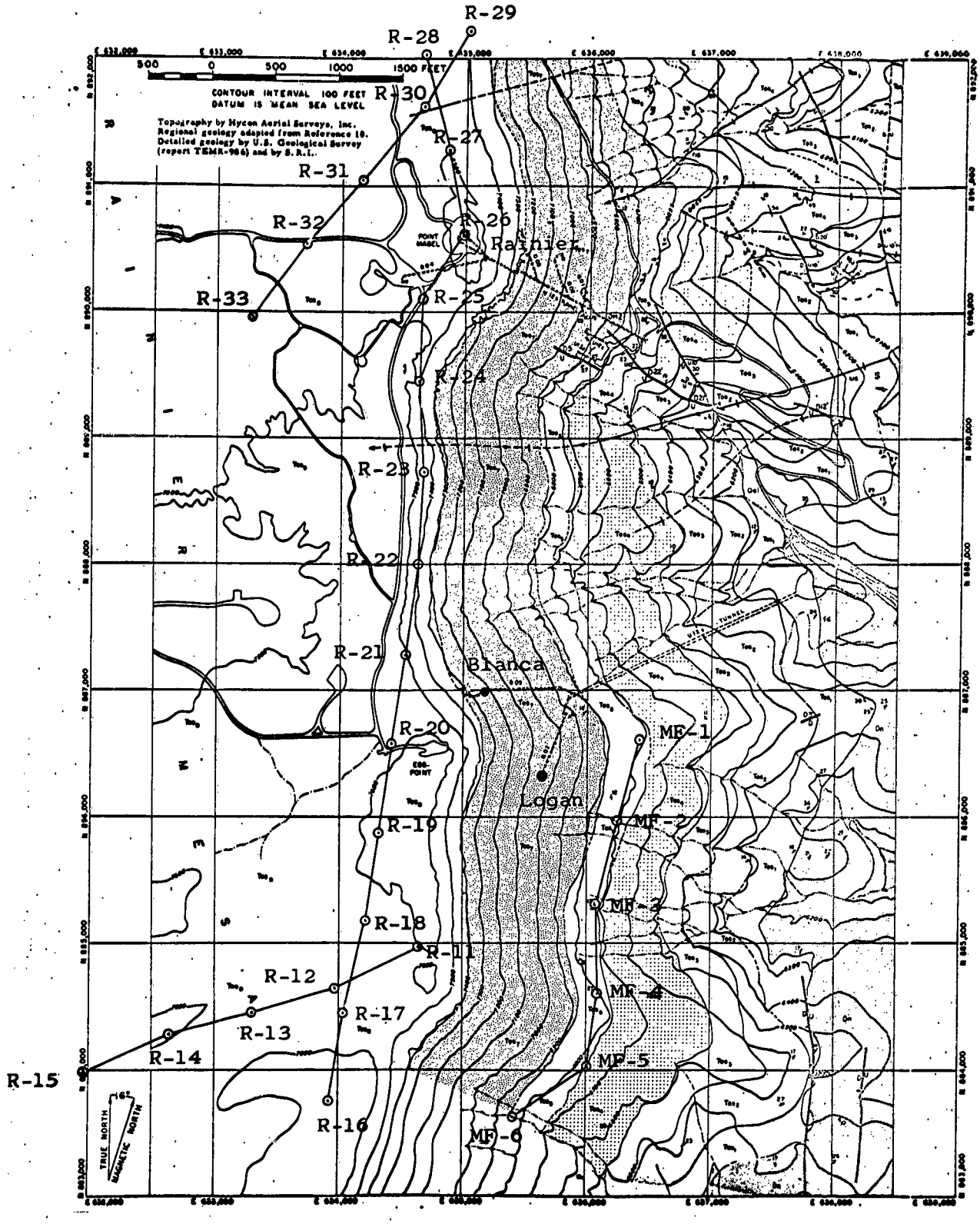
R-29
R-28
R-30
R-27
R-31
R-32
R-26
Rainier
R-33
R-25
R-24
R-23
R-22
R-21
Blanca
R-20
MF-1
Logan
MF-2
R-19
MF-3
R-18
R-11
R-12
MF-4
R-17
R-13
R-14
MF-5
R-15
R-16
MF-6
CONTOUR INTERVAL 100 FEET
DATUM IS MEAN SEA LEVEL
Topography by Hycon Aerial Surveys, Inc.
Regional geology adapted from Reference 10.
Detailed geology by U.S. Geological Survey
(report TEMR-966) and by S.R.I..
TRUE NORTH
MAGNETIC NORTH

Fig. 9.1

K•E 10 X 10 TO THE CM. 359-14
KEUFFEL & ESSER CO. MADE IN U.S.A.

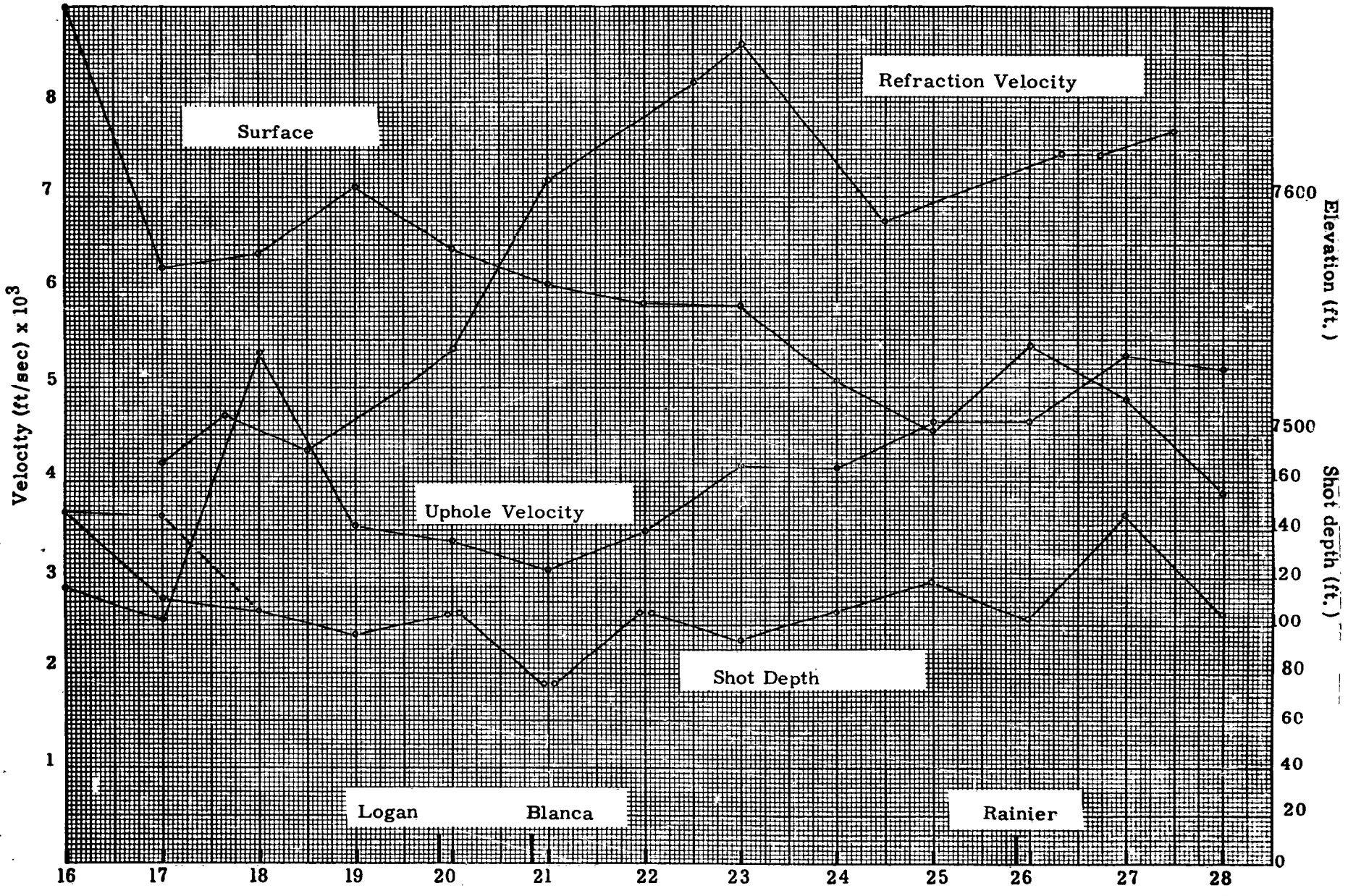

Fig. 9.2

K+E 10 X 10 TO THE CM. 358-14
KEUFFEL & ESSER CO. MADE IN U.S.A.

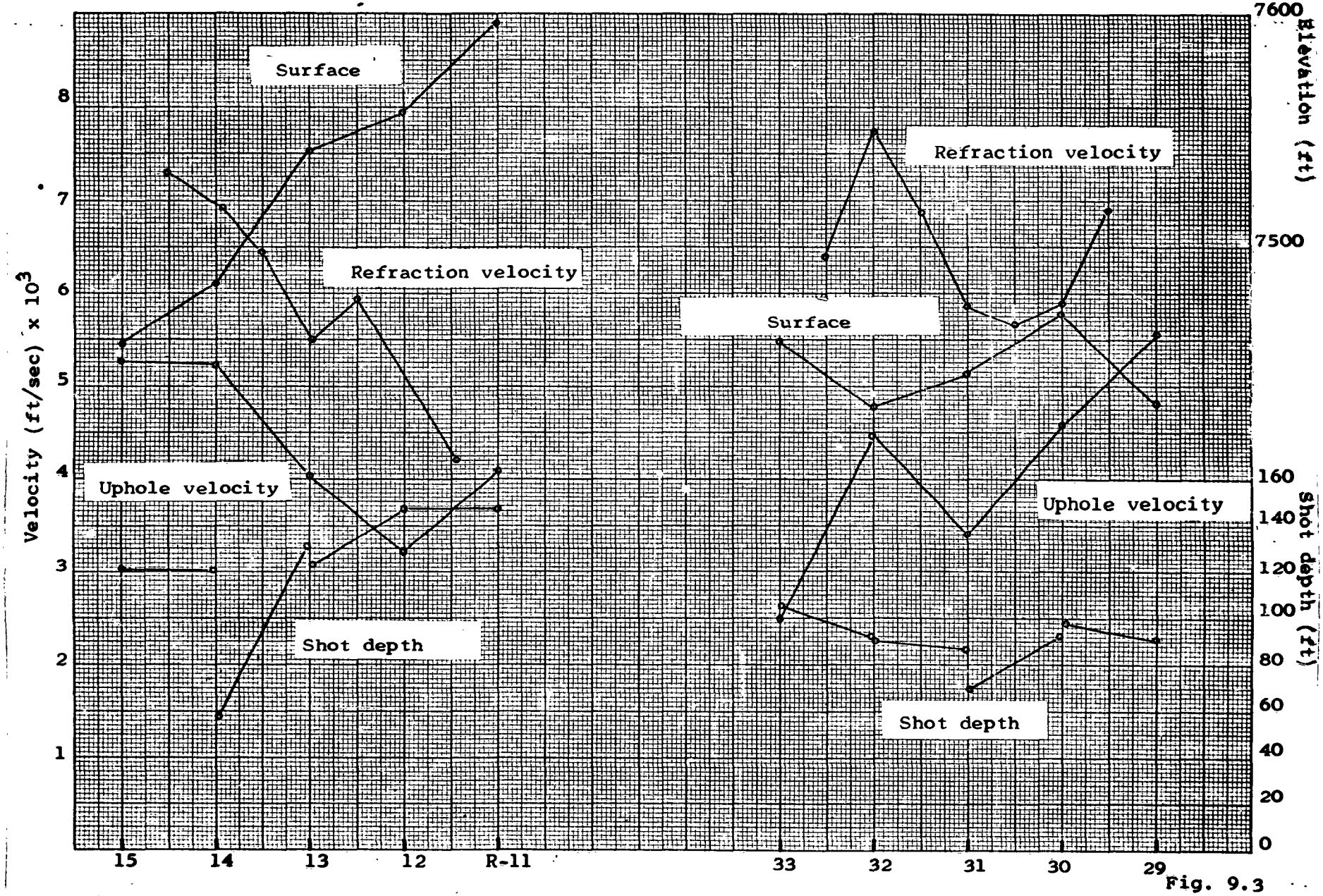

Fig. 9.3

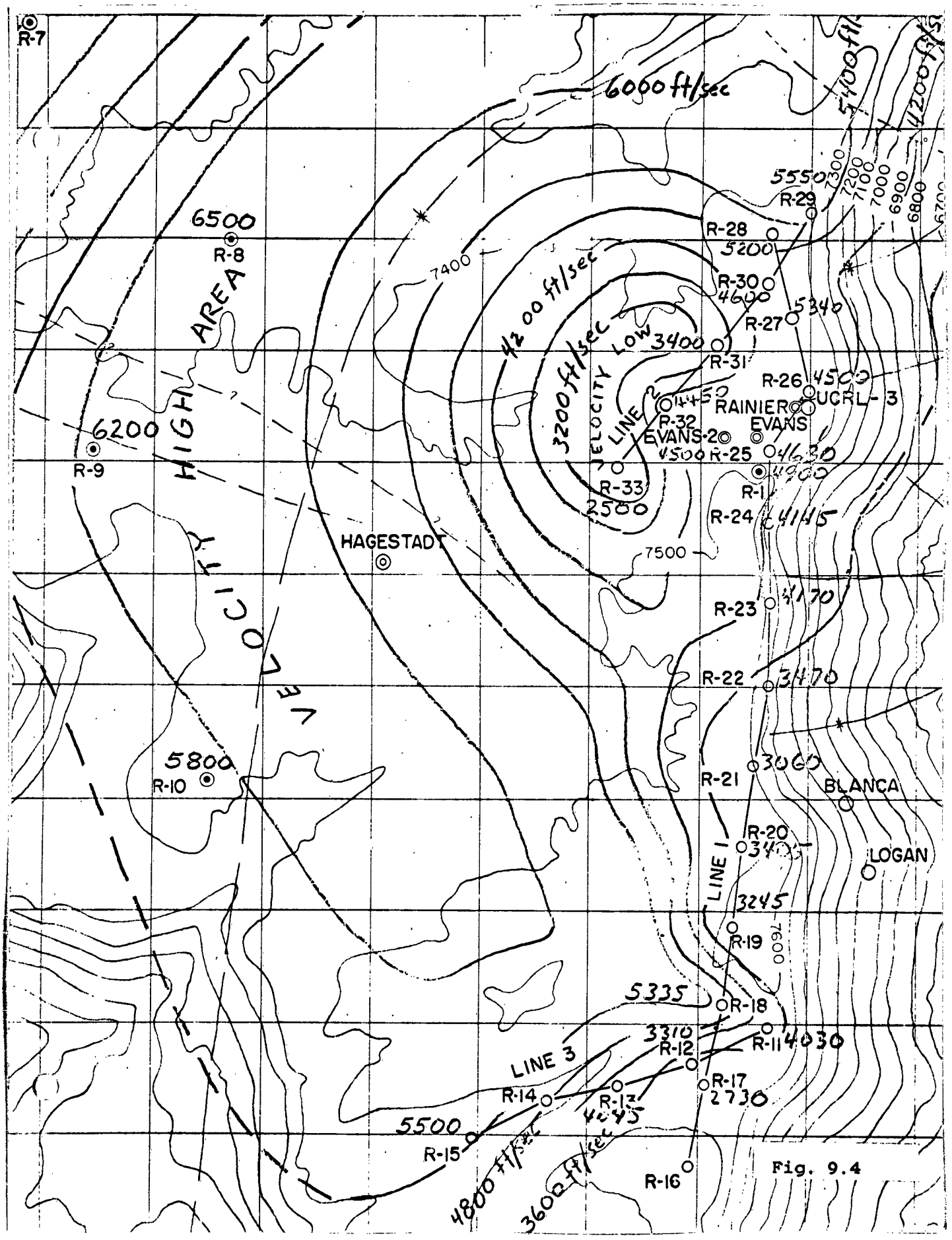
R-7
6000 ft/sec
5400 ft/sec
4200 ft/sec
5550
R-29
7300
7200
7100
7000
6900
6800
6500
R-8
HIGH VELOCITY AREA
R-28
5200
7400
4200 ft/sec
R-30
4600
5340
R-27
3200 ft/sec
LOW VELOCITY
3400
R-31
R-26
4500
UCRL-3
LINE 2
4450
RAINIER
6200
R-32
EVANS
EVANS-2
4500
R-25
4630
R-9
R-33
2500
R-1
4145
R-24
HAGESTADT
7500
R-23
4170
R-22
3470
5800
R-10
R-21
3060
BLANCA
R-20
LOGAN
LINE 1
3245
R-19
7600
5335
R-18
3310
R-12
R-11
4030
LINE 3
R-14
R-13
R-17
2730
5500
R-15
4800 ft/sec
3600 ft/sec
R-16

Fig. 9.4

K&E 10 X 10 TO THE CM. 359-14
KEUFFEL & ESSER CO. MADE IN U.S.A.

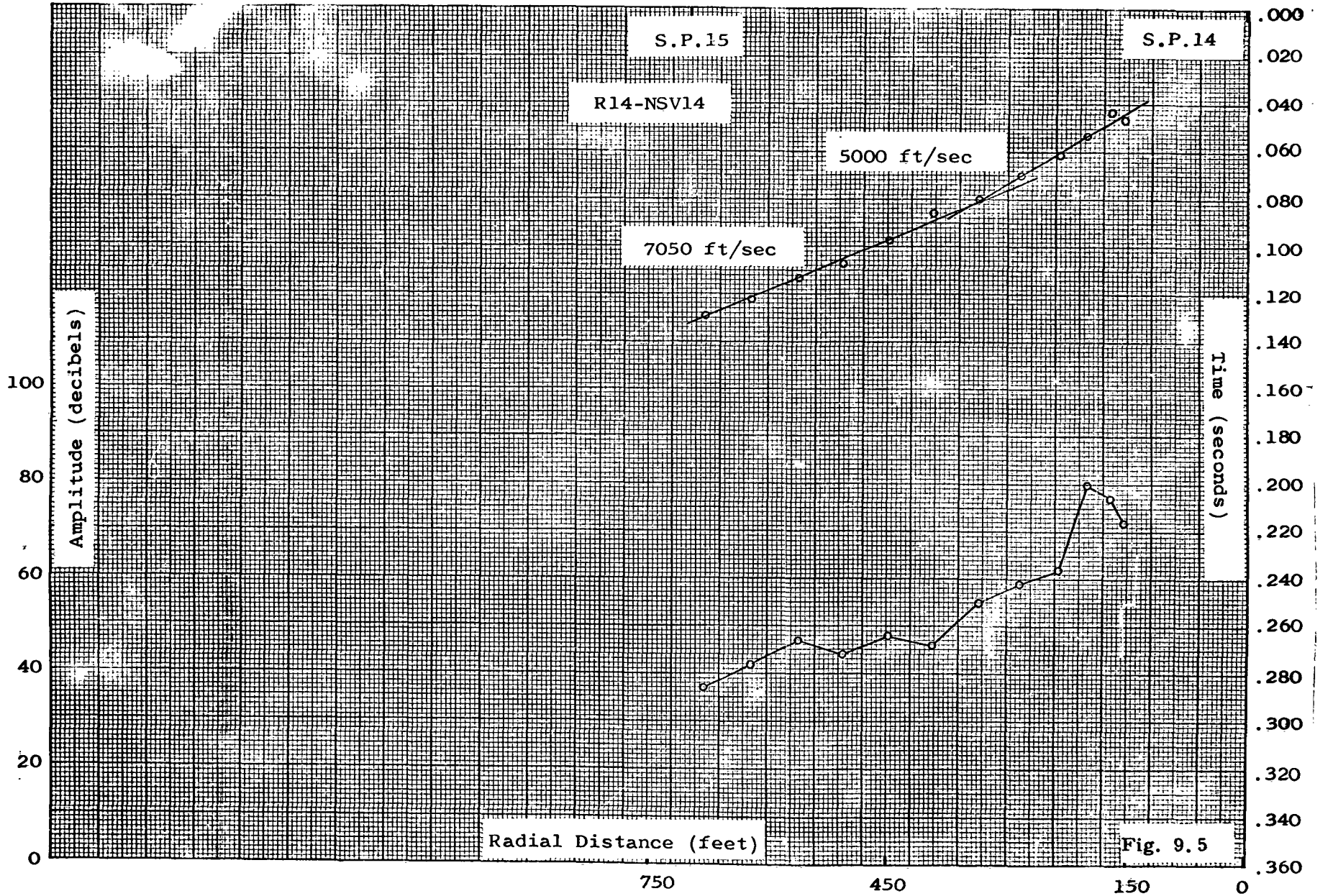

Fig. 9.5

K&E 10 X 10 TO THE CM. 358-14
KEUFFEL & ESSER CO. MADE IN U.S.A.

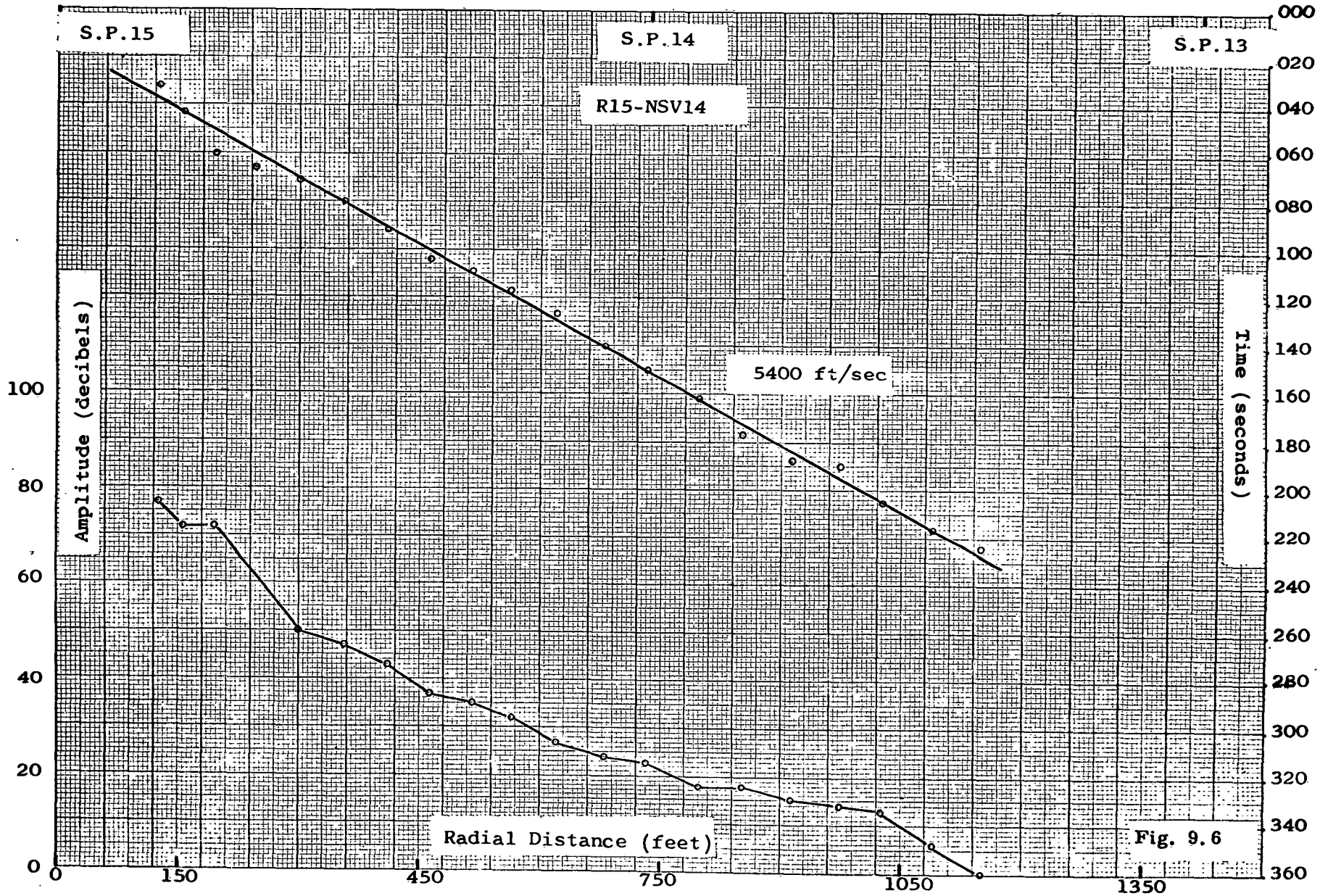

Fig. 9.6

K+E 10 X 10 TO THE CM. 359-14
KEUFFEL & ESSER CO. MADE IN U.S.A

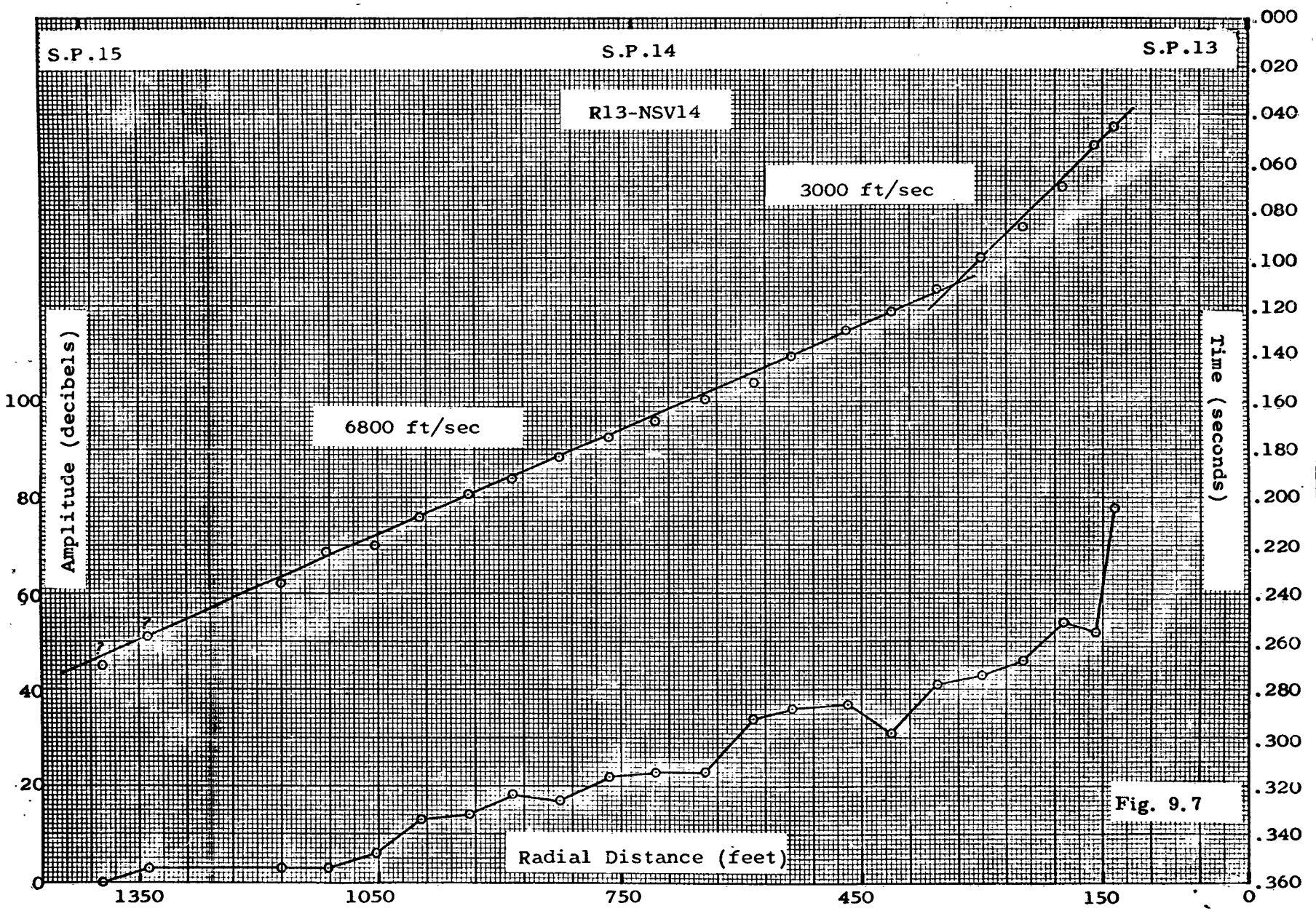

Fig. 9.7

K&E 10 X 10 TO THE CM. 359-14
KEUFFEL & ESSER CO. MADE IN U.S.A.

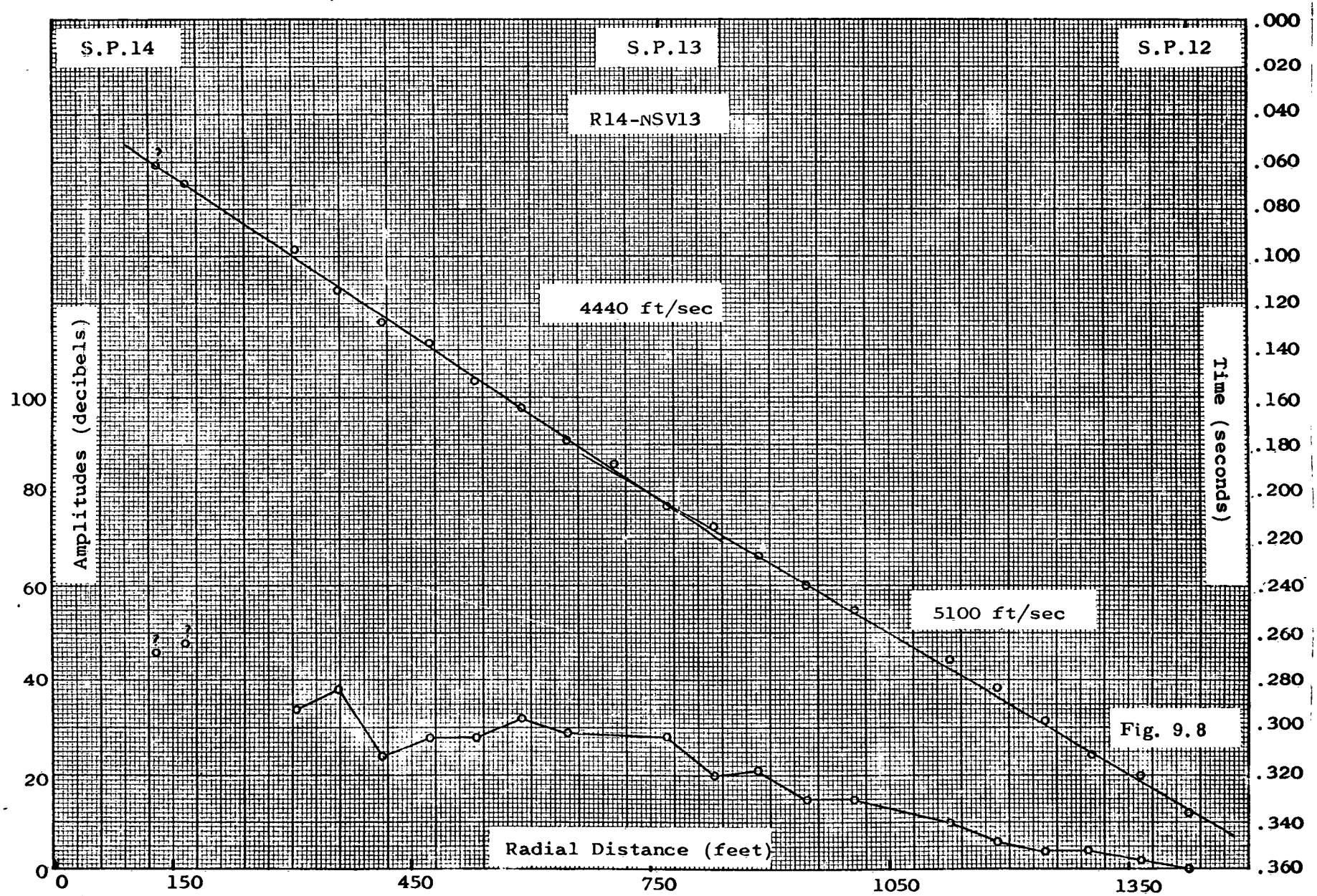

Fig. 9.8

K&E 10 X 10 TO THE CM. 359-14
KEUFFEL & ESSER CO. MADE IN U.S.A.

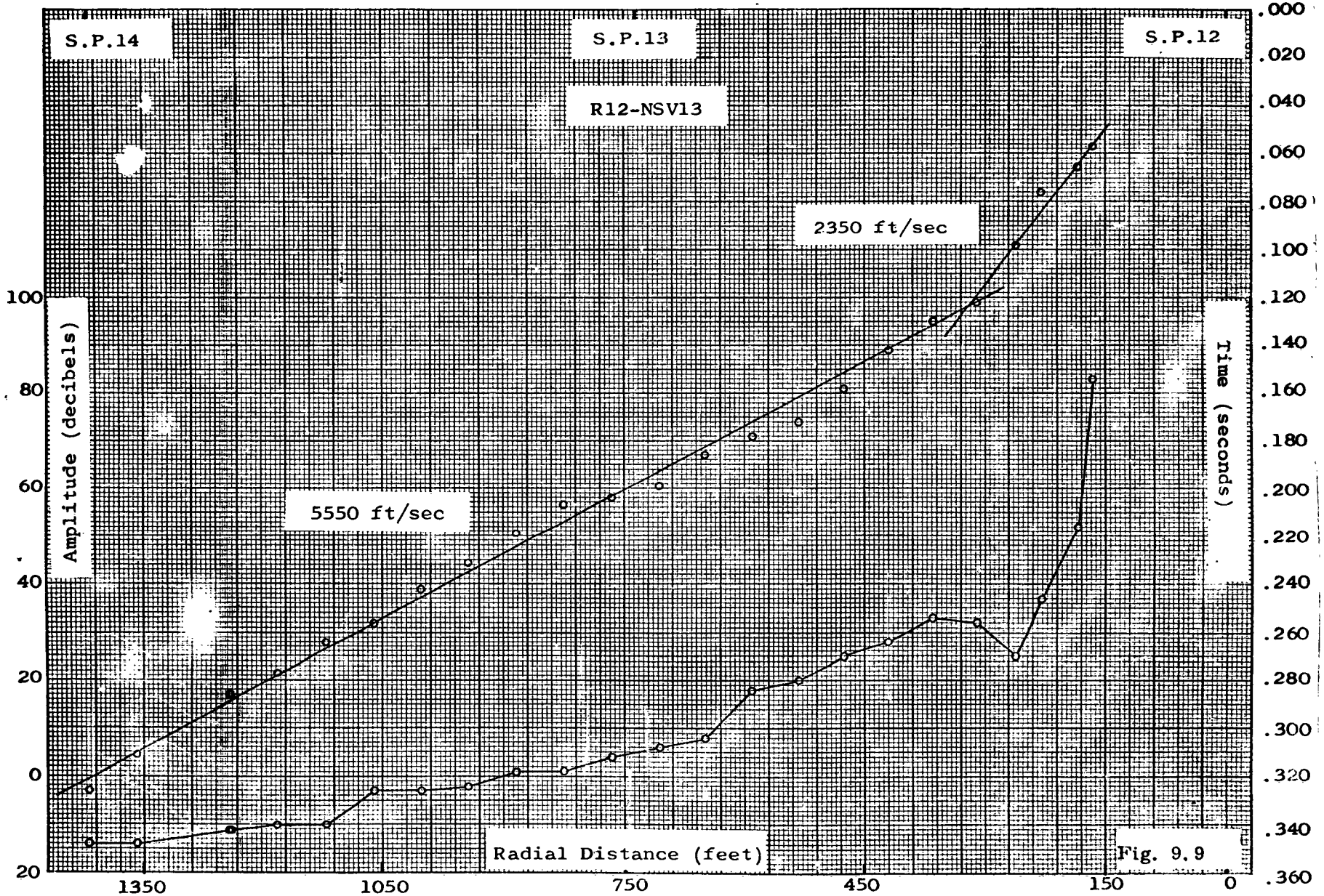

Fig. 9.9

K+E 10 X 10 TO THE CM. 359-14
KEUFFEL & ESSER CO. MADE IN U.S.A.

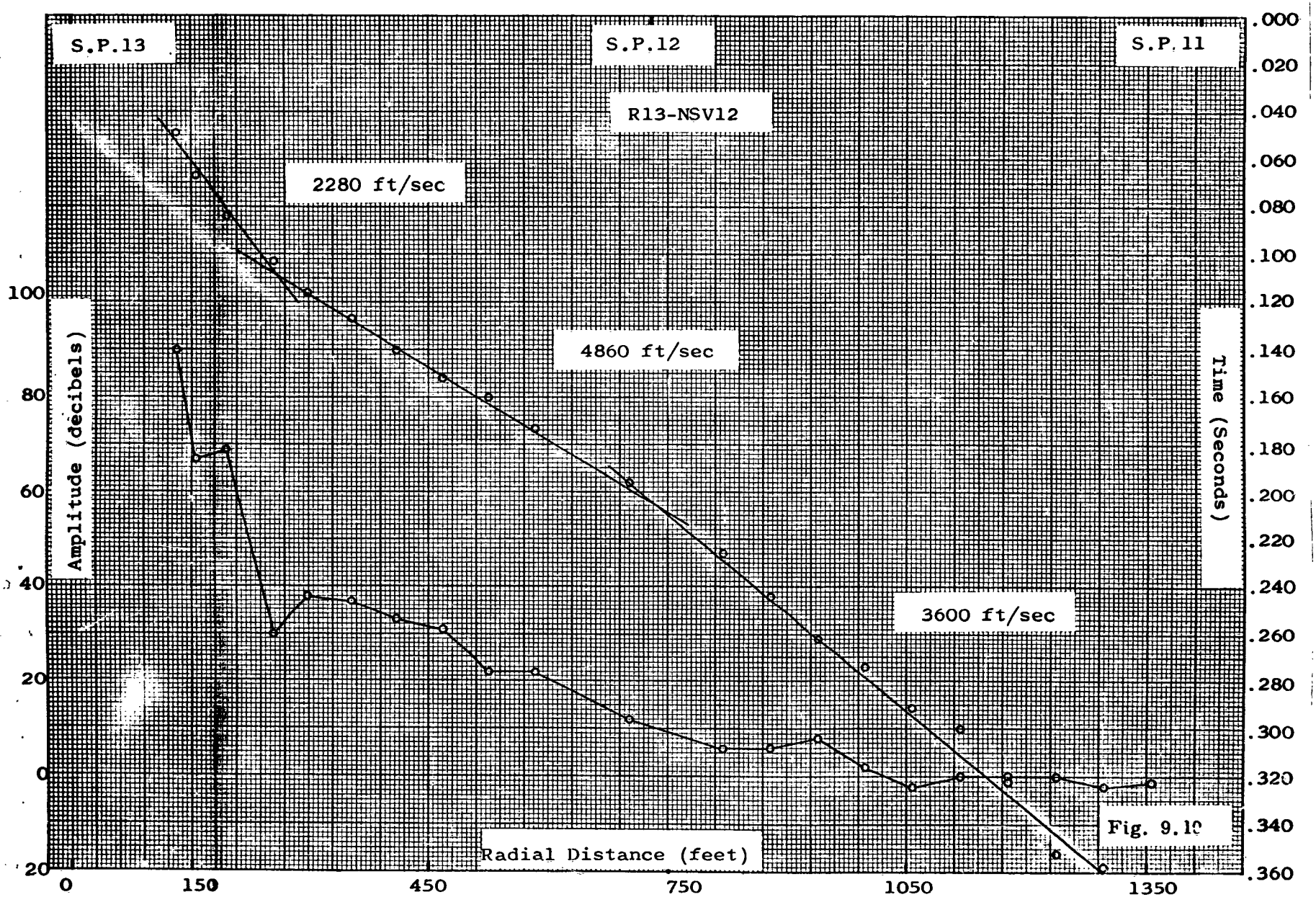

Fig. 9.10

K+E 10 X 10 TO THE CM. 359-14 KEUFFEL & ESSER CO. MADE IN U.S.A.

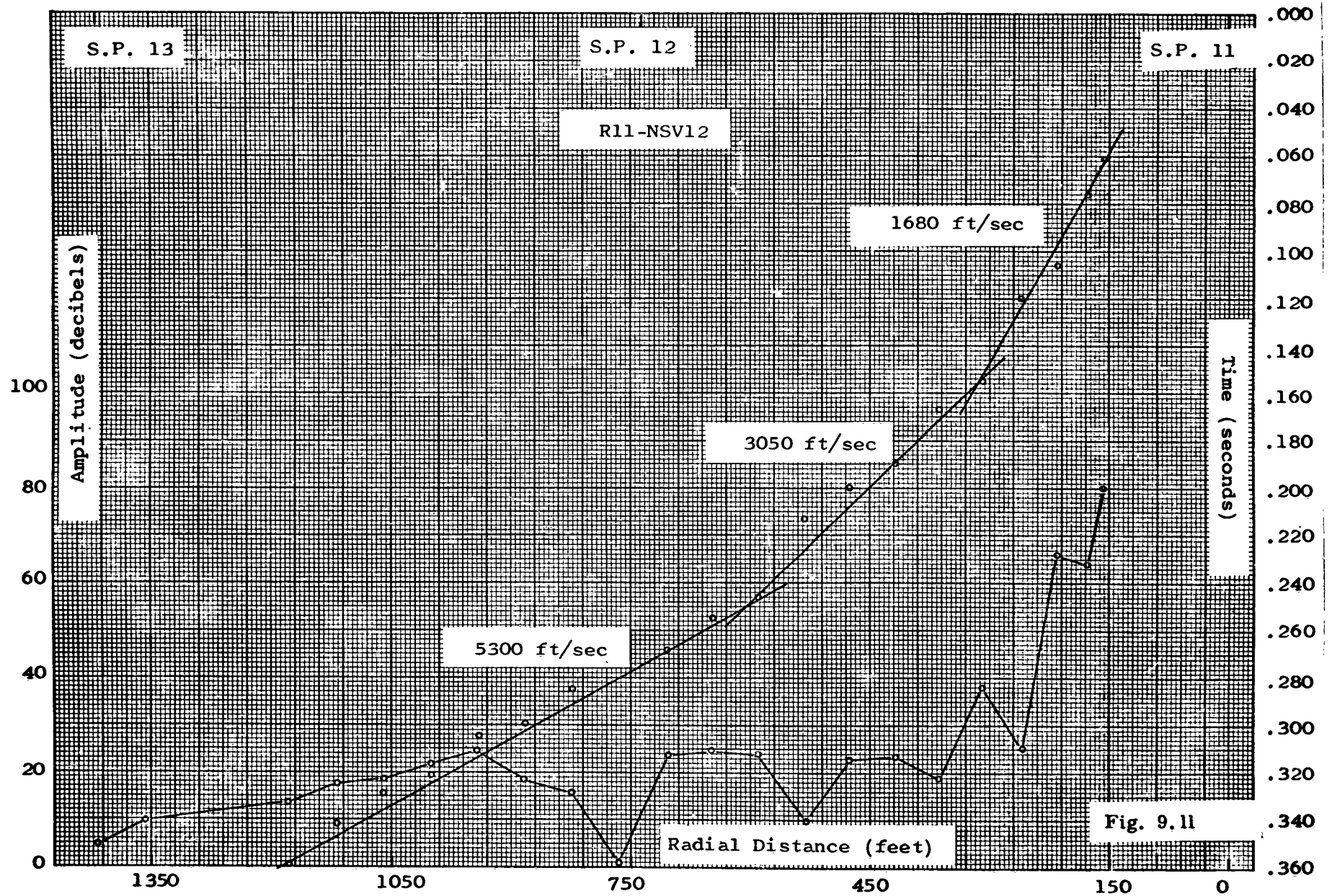

Fig. 9.11

K&E 10 X 10 TO THE CM. 359-14
KEUFFEL & ESSER CO. MADE IN U.S.A.

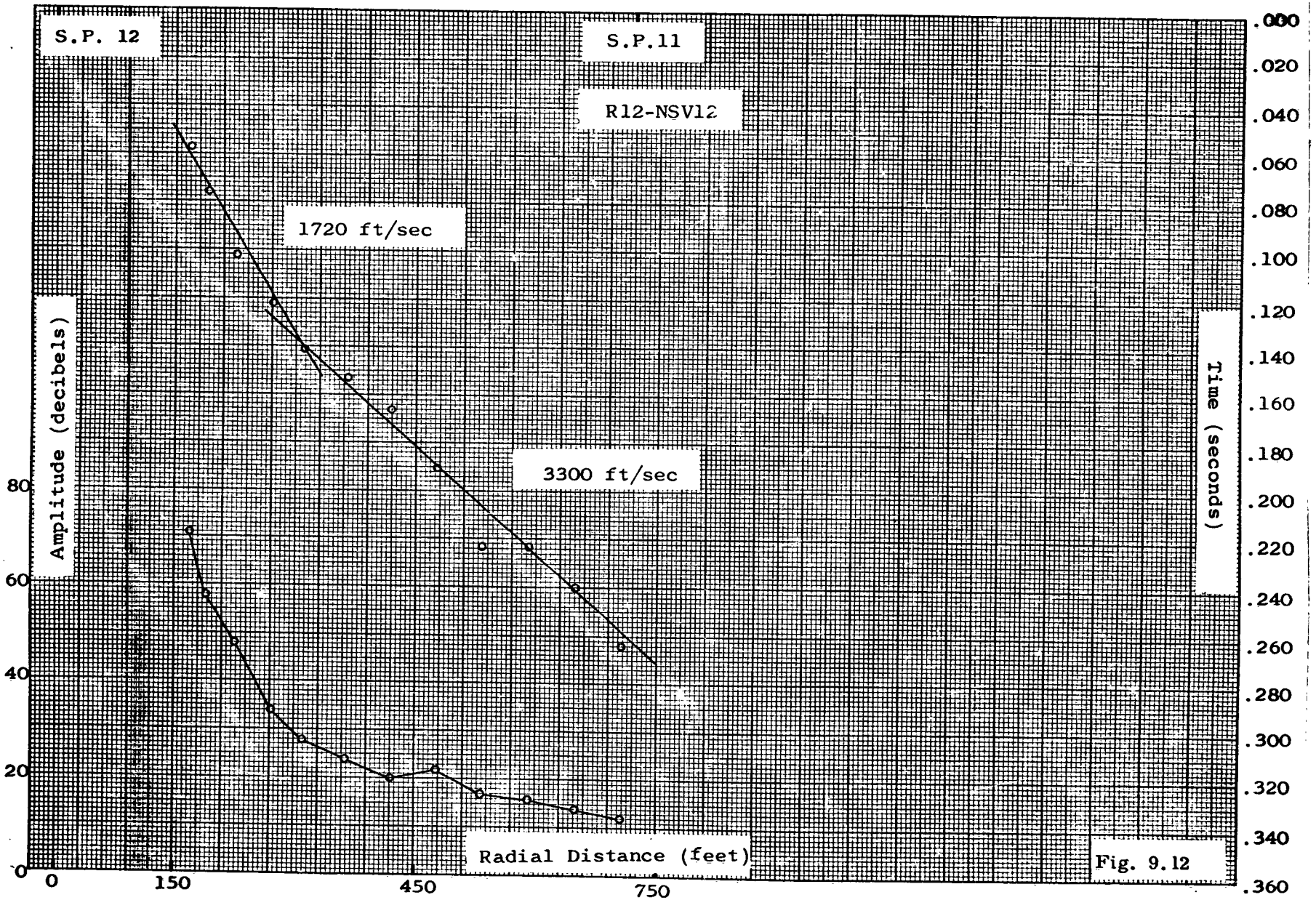

Fig. 9.12

K&E 10 X 10 TO THE CM. 359-14
KEUFFEL & ESSER CO. MADE IN U.S.A.

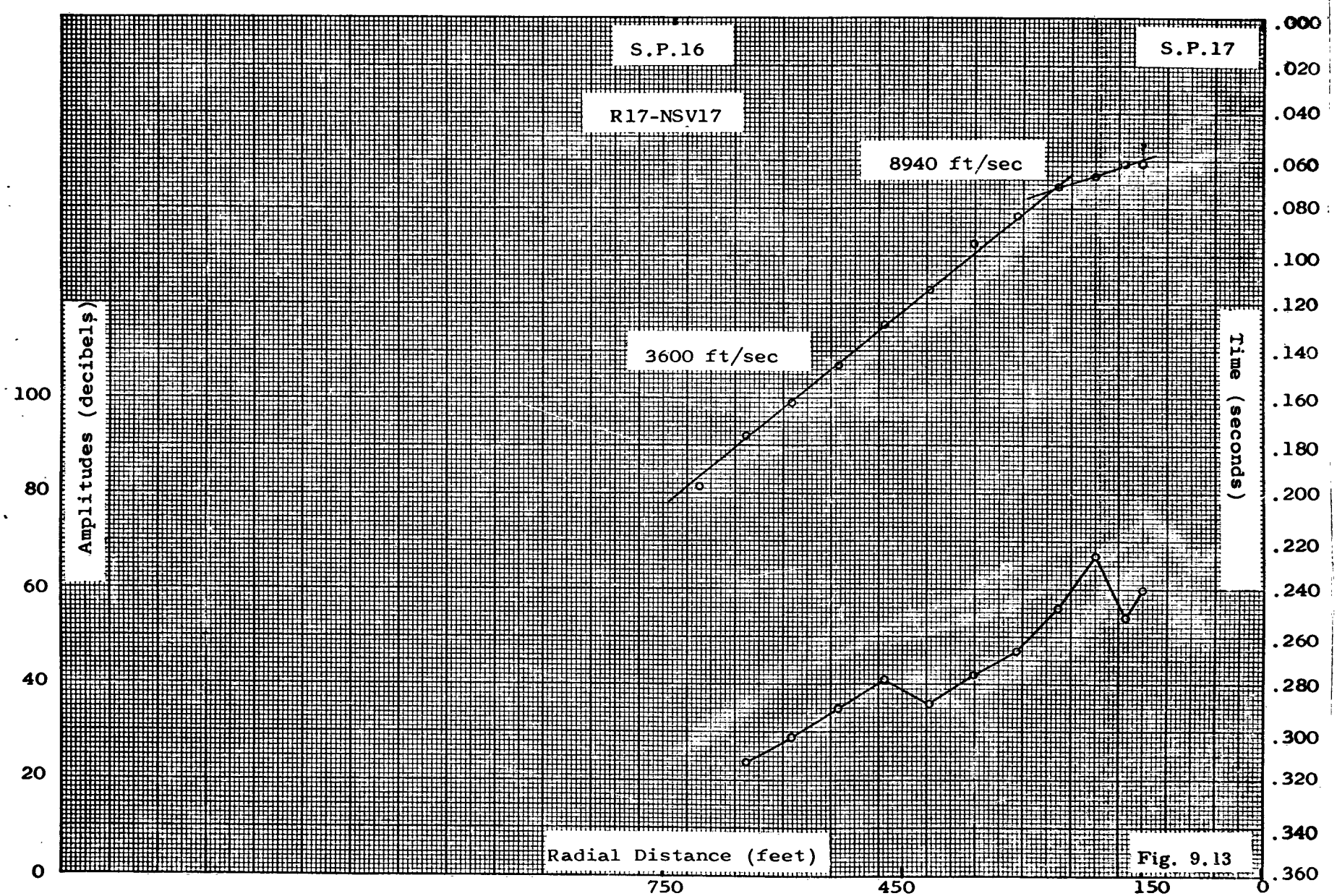

Fig. 9.13

K&E 10 X 10 TO THE CM. 359-14
KEUFFEL & ESSER CO. MADE IN U.S.A.

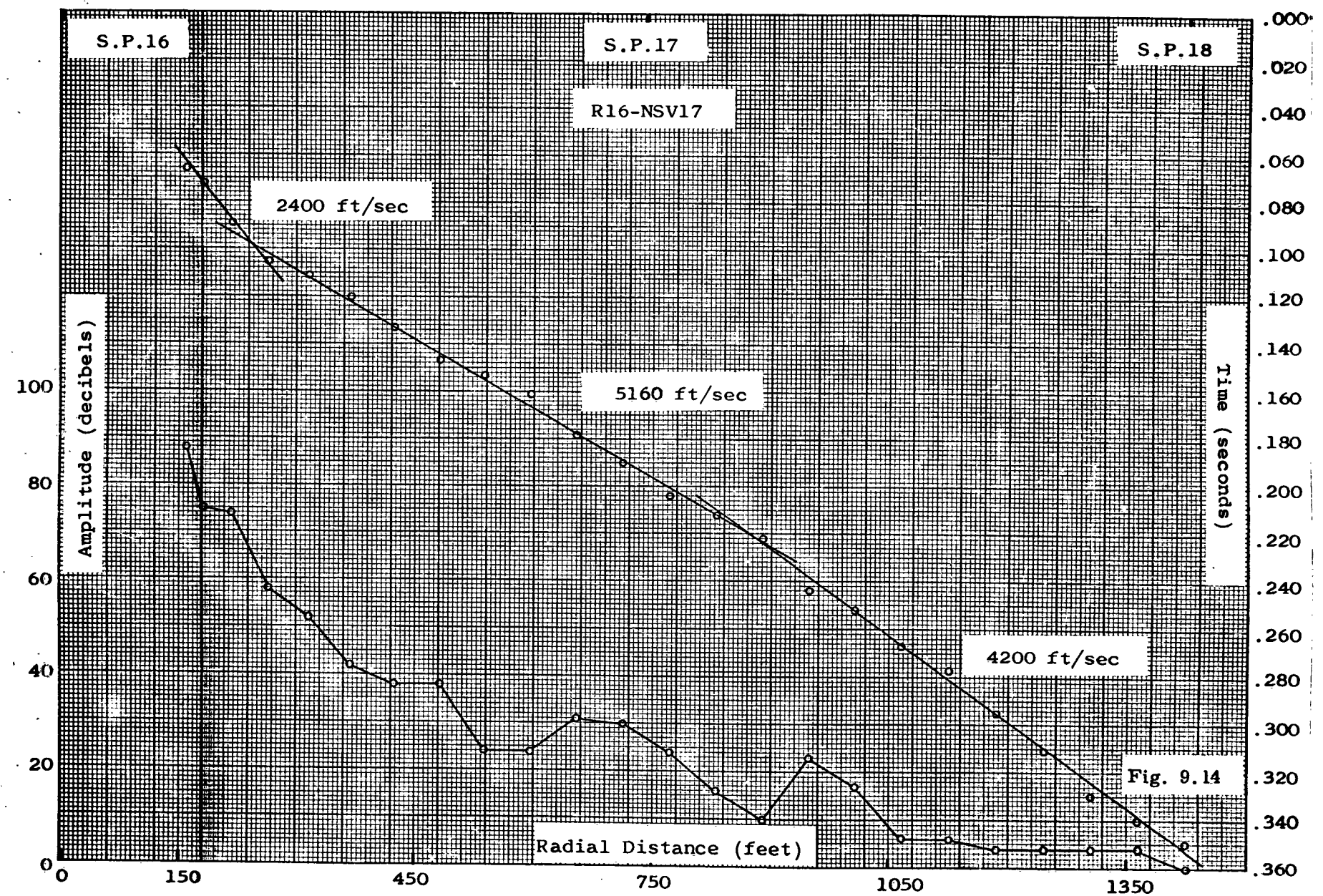

Fig. 9.14

K&E 10 X 10 TO THE CM. 359-14
KEUFFEL & ESSER CO. MADE IN U.S.A.

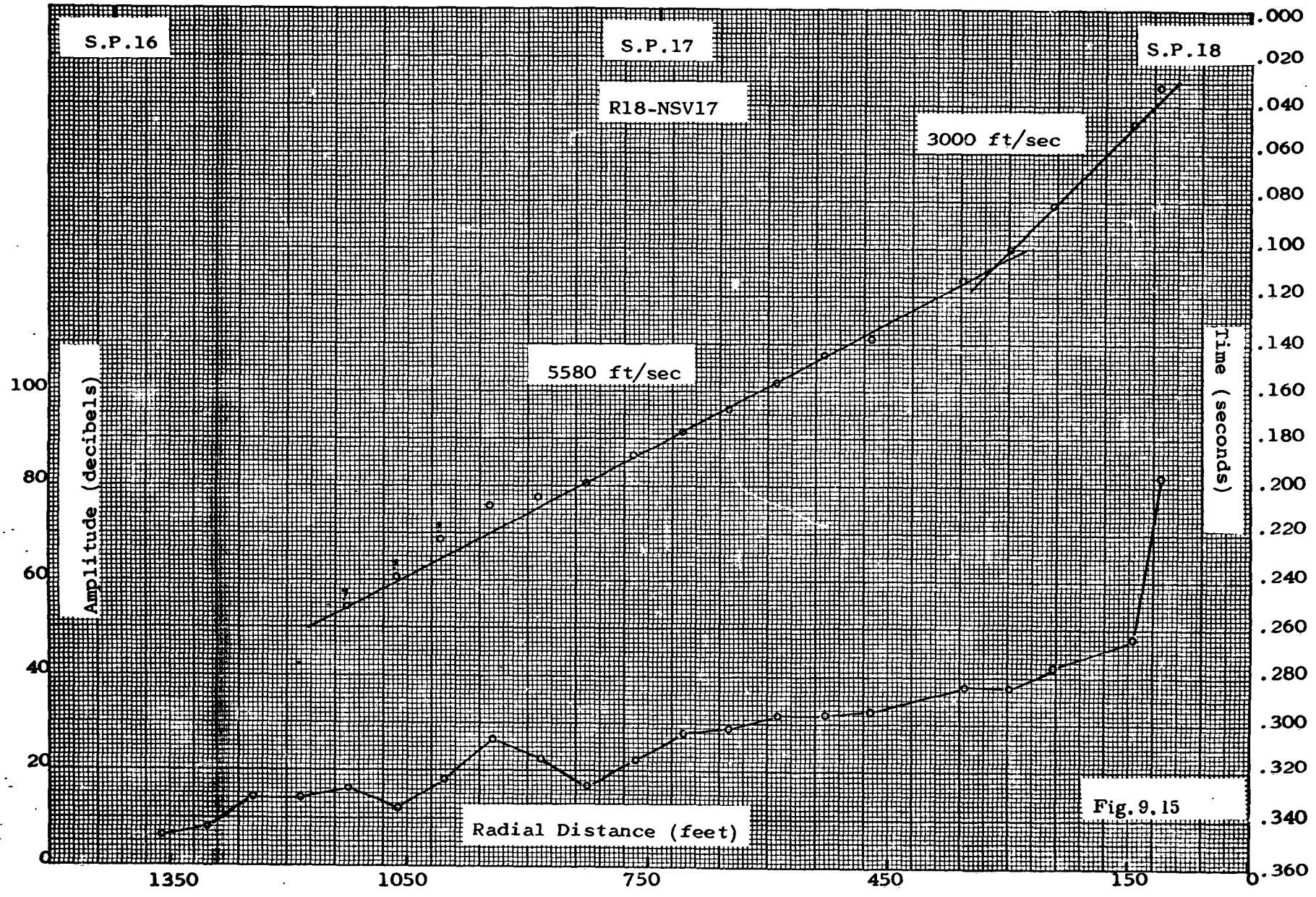

Fig. 9.15

K+E 10 X 10 TO THE CM. 358-14
KEUFFEL & ESSER CO. MADE IN U.S.A.

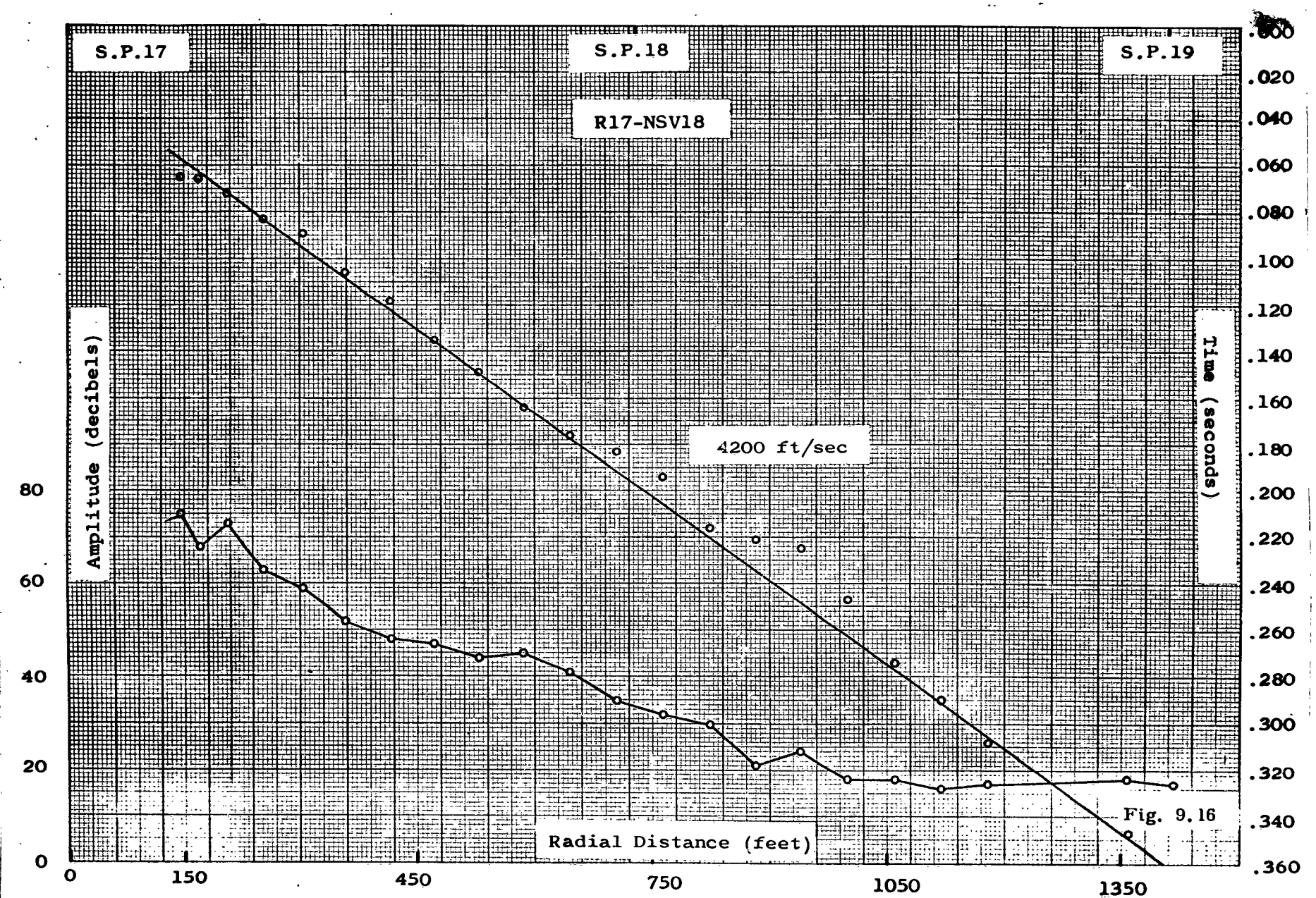

Fig. 9.16

K·E 10 X 10 TO THE CM. 359-14
KEUFFEL & ESSER CO. MADE IN U.S.A.

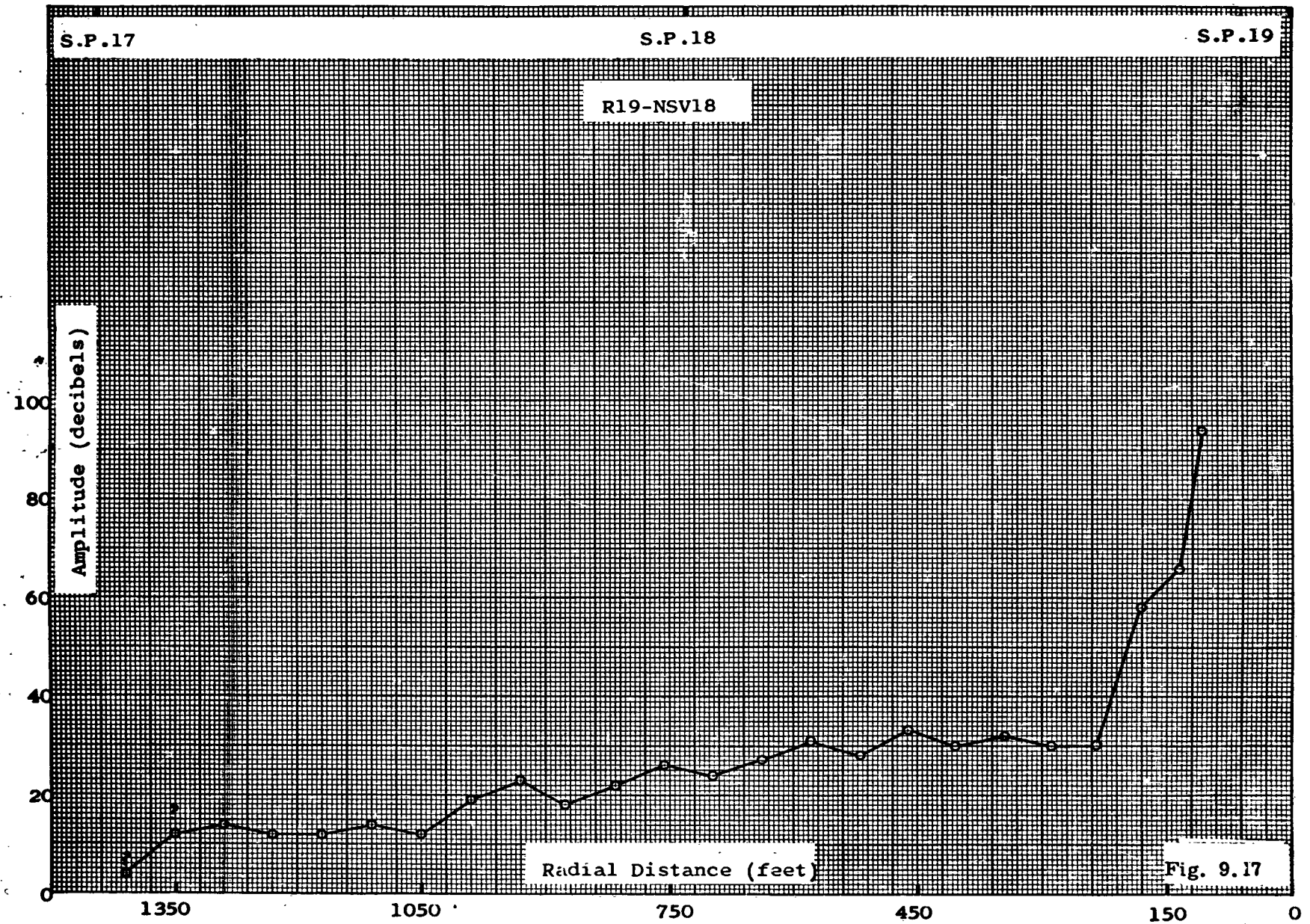

Fig. 9.17

K·E 10 X 10 TO THE CM. 359-14
KEUFFEL & ESSER CO. MADE IN U.S.A.

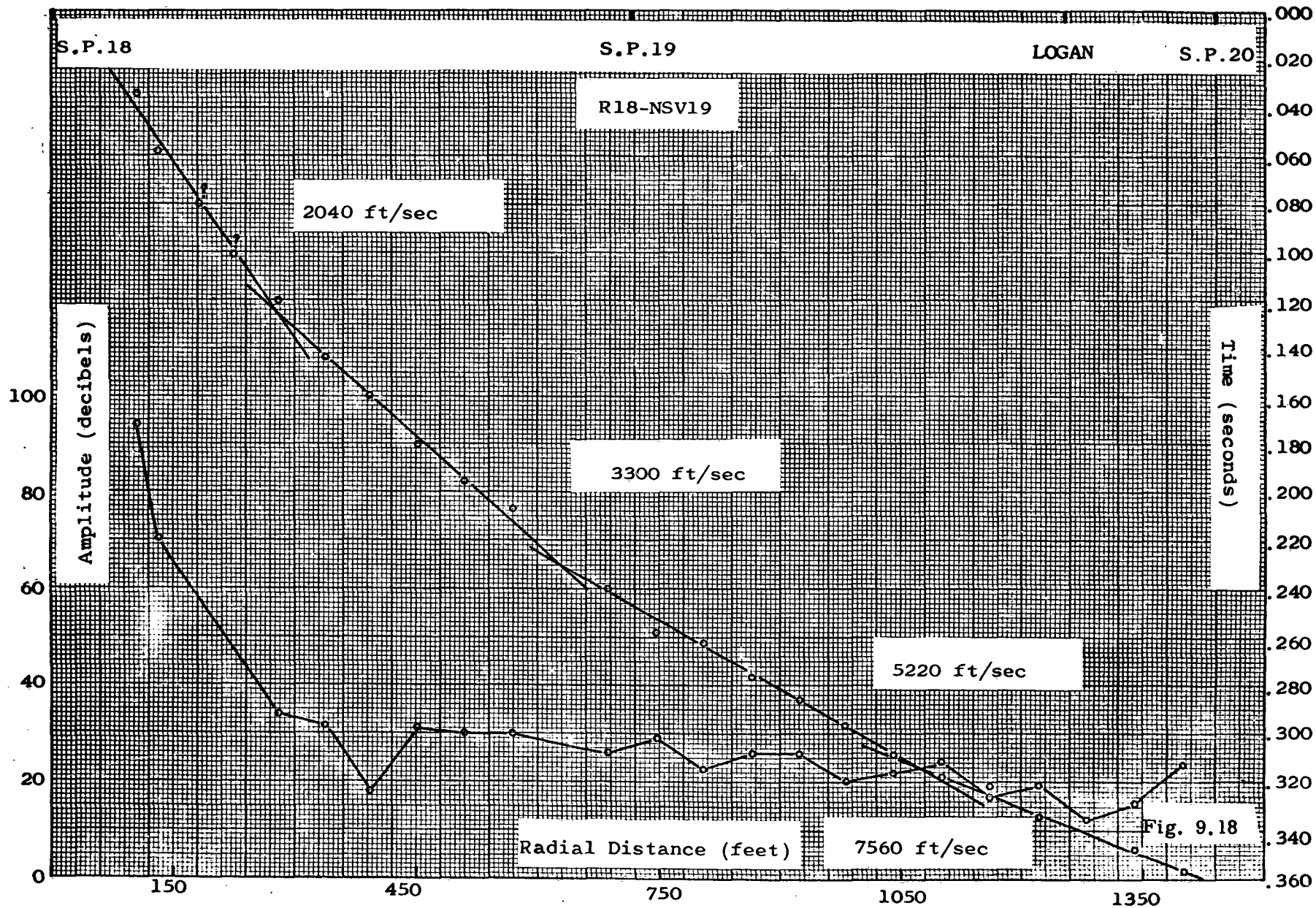

Fig. 9.18

K+E 10 X 10 TO THE CM. 359-14
KEUFFEL & ESSER CO. MADE IN U.S.A.

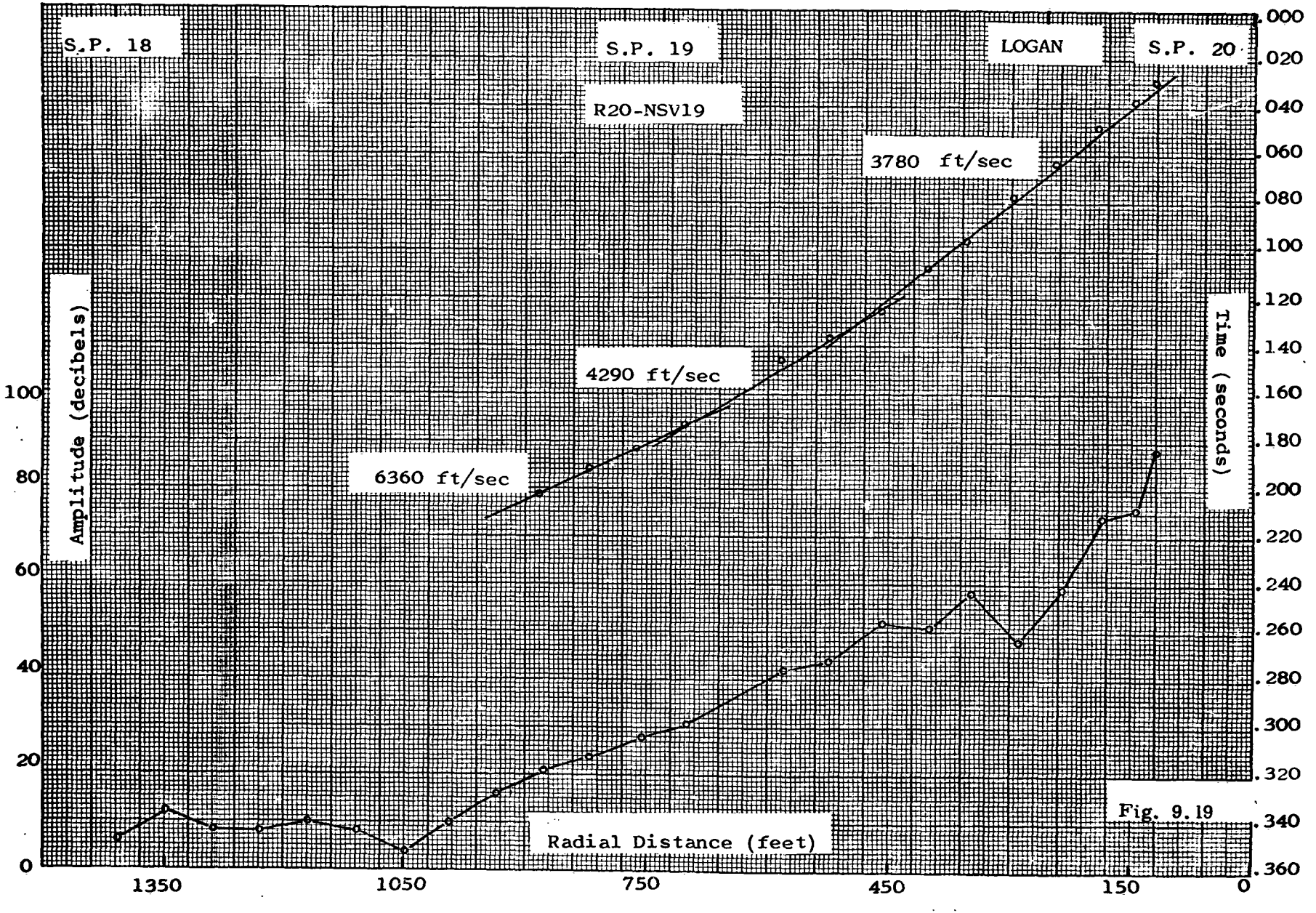

Fig. 9.19

K&E 10 X 10 TO THE CM. 359-14
KEUFFEL & ESSER CO. MADE IN U.S.A.

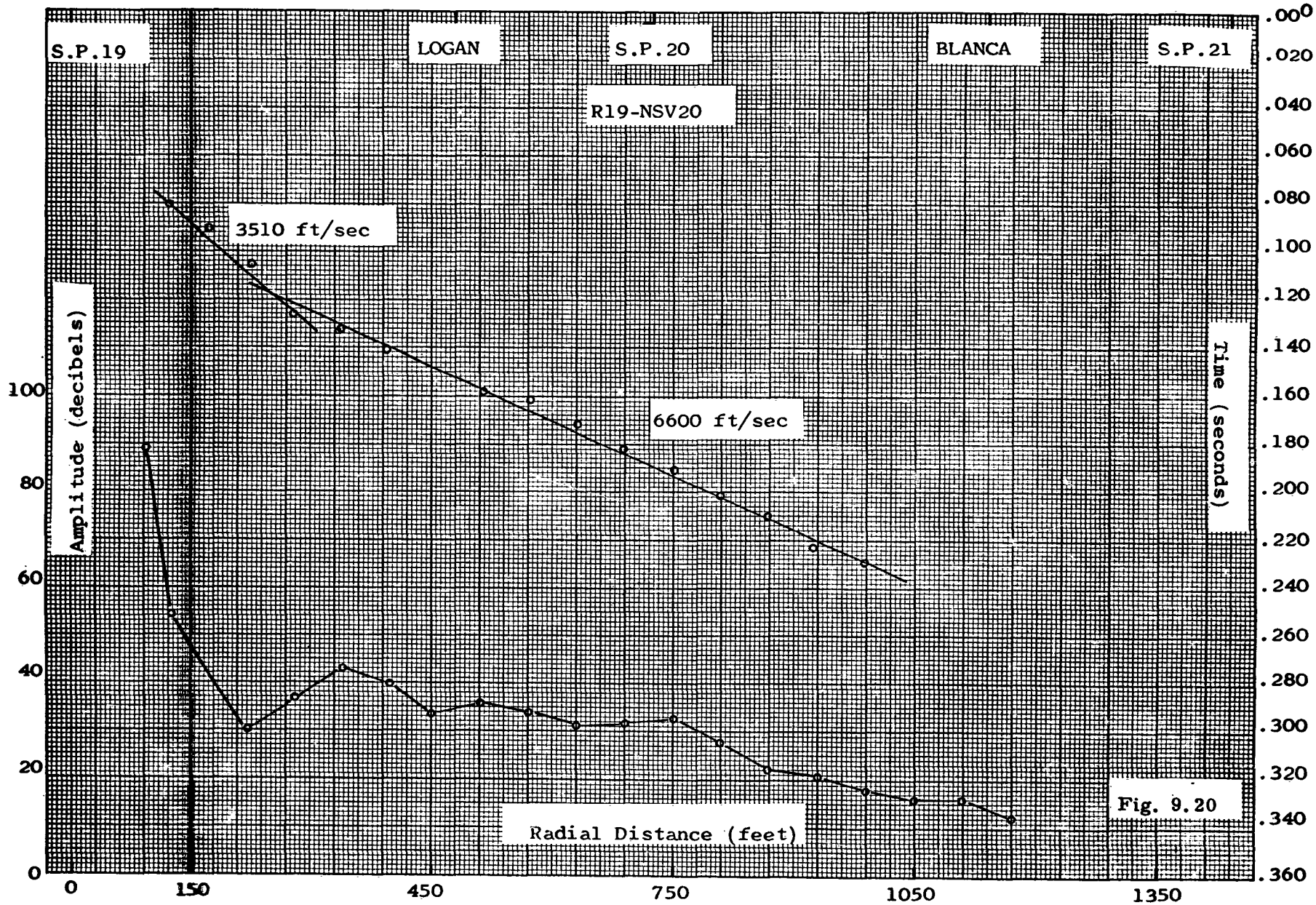

Fig. 9.20

K+E 10 X 10 TO THE CM. 359-14
KEUFFEL & ESSER CO. MADE IN U.S.A.

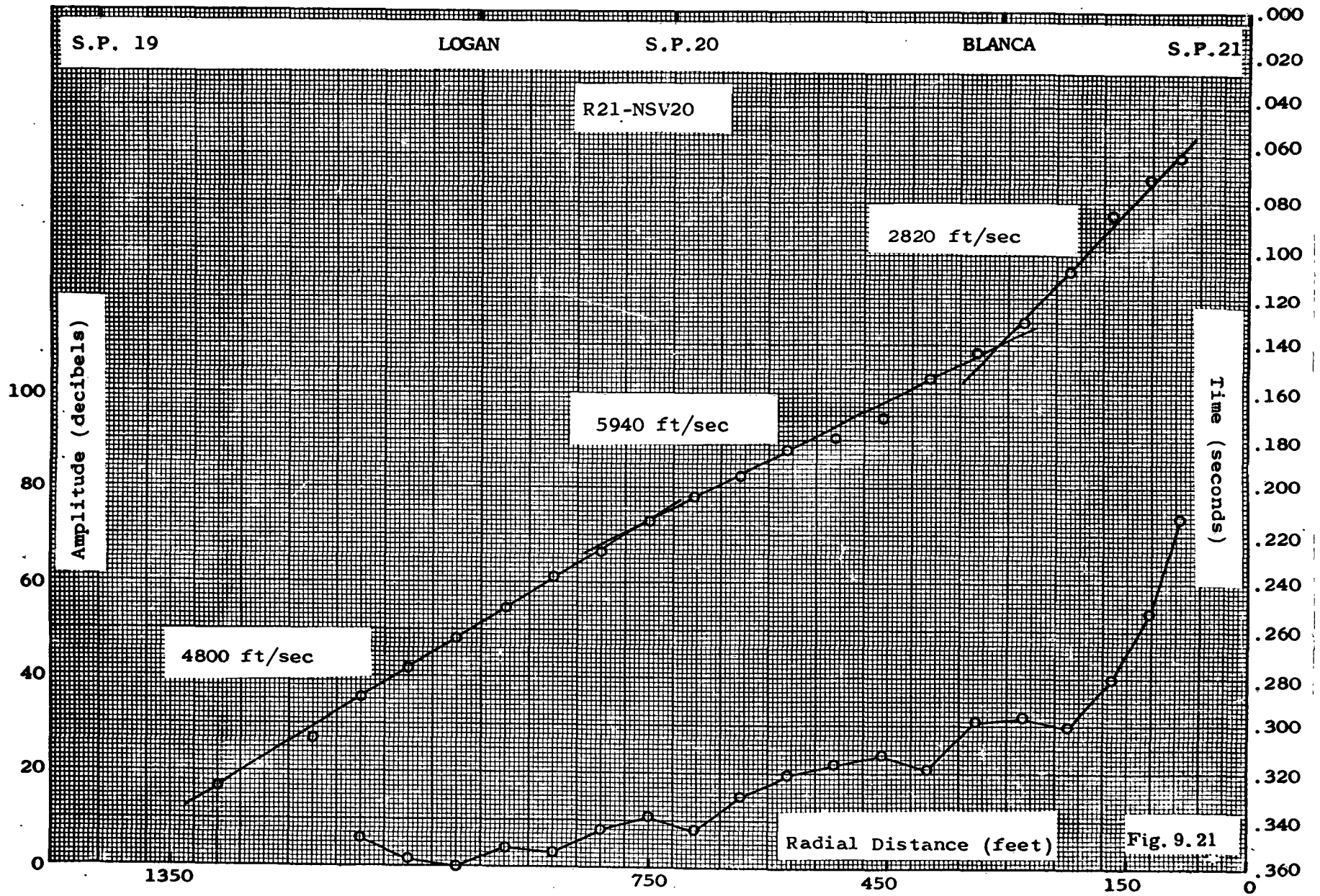

Fig. 9.21

K+E 10 X 10 TO THE CM. 359-14
KEUFFEL & ESSER CO. MADE IN U.S.A.

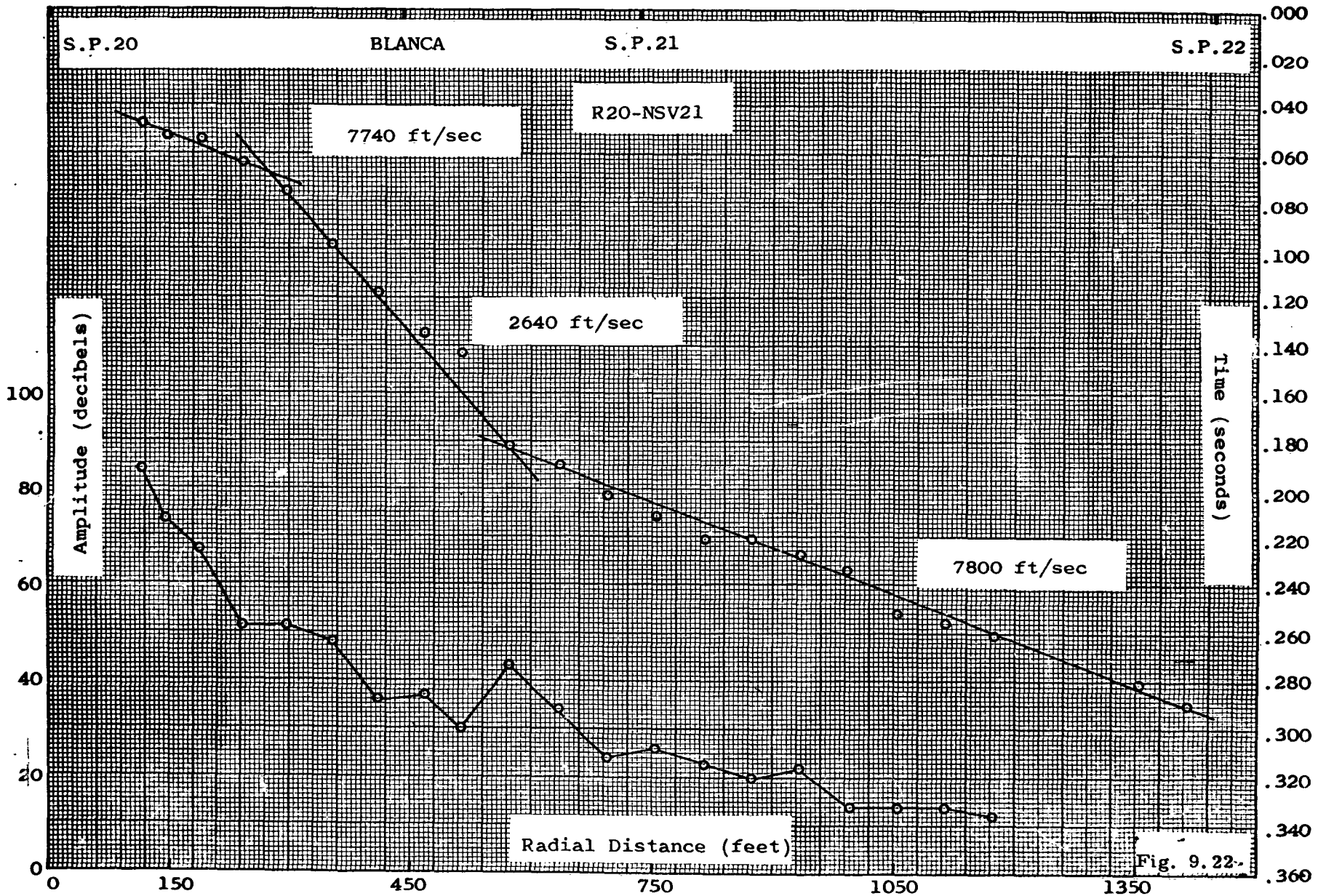

Fig. 9.22.

K+E 10 X 10 TO THE CM. 359-14
KEUFFEL & ESSER CO. MADE IN U.S.A.

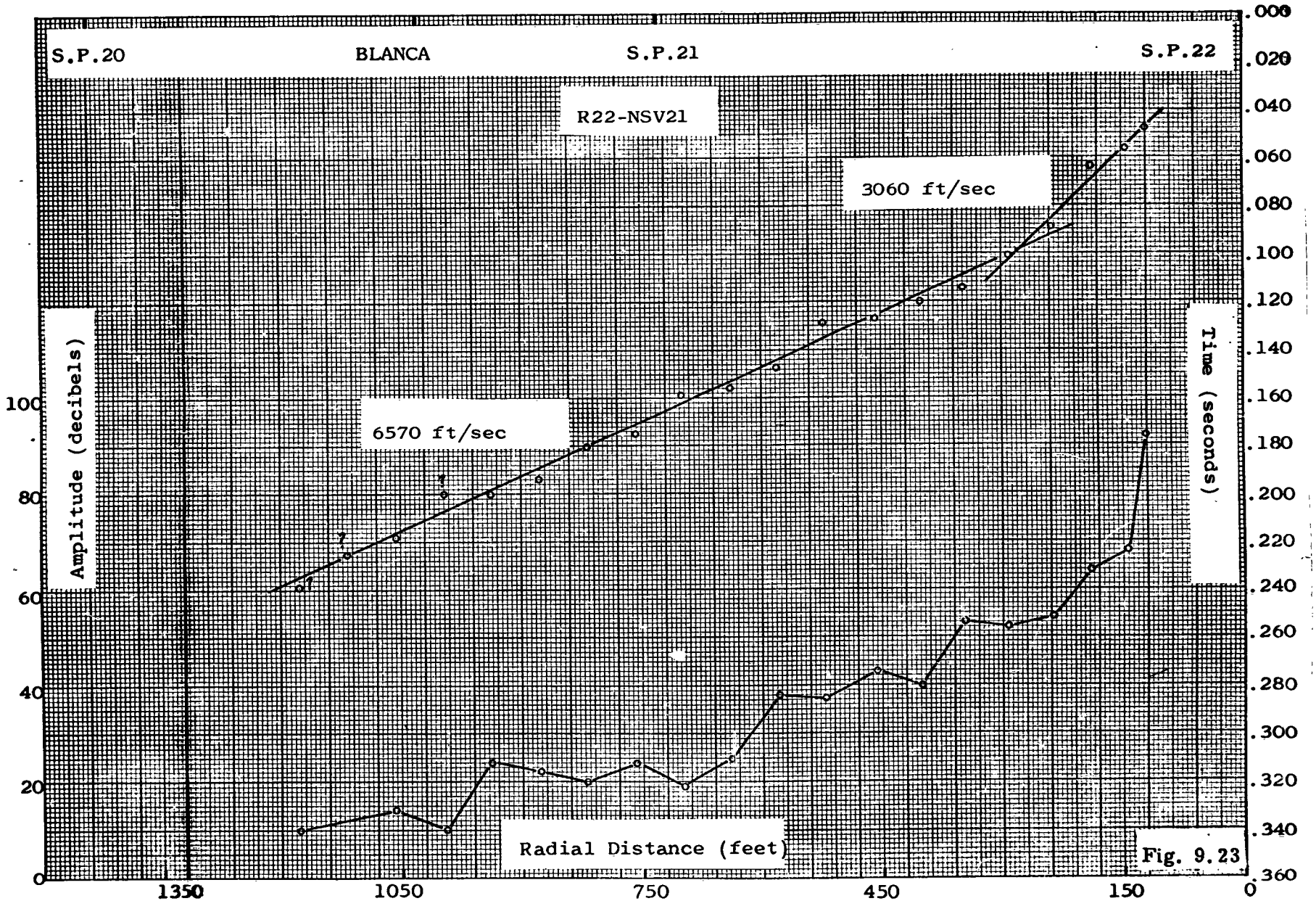

Fig. 9.23

K+E 10 X 10 TO THE CM. 359-14
KEUFFEL & ESSER CO. MADE IN U.S.A.

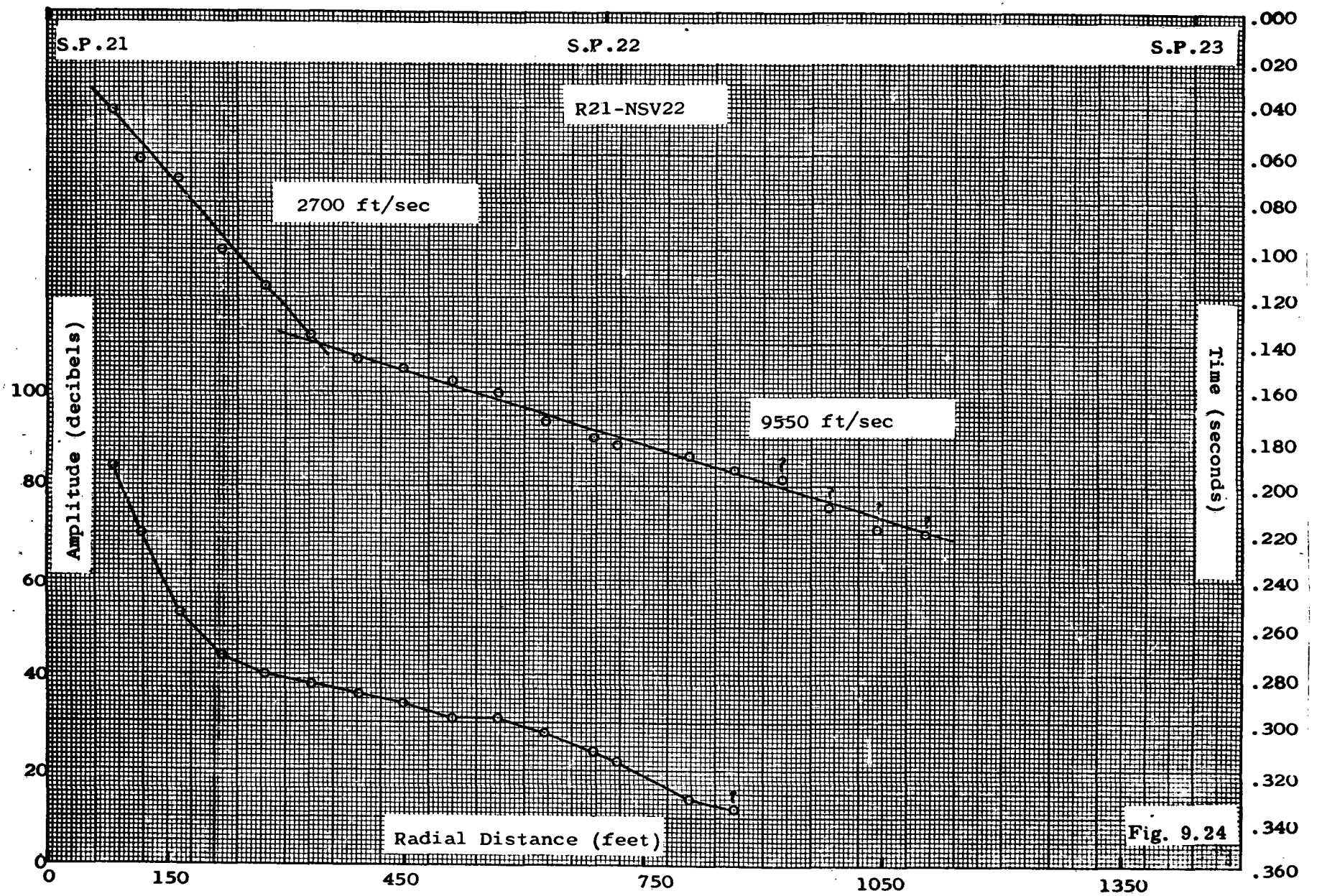

Fig. 9.24

K·E 10 X 10 TO THE CM. 359-14
KEUFFEL & ESSER CO. MADE IN U.S.A.

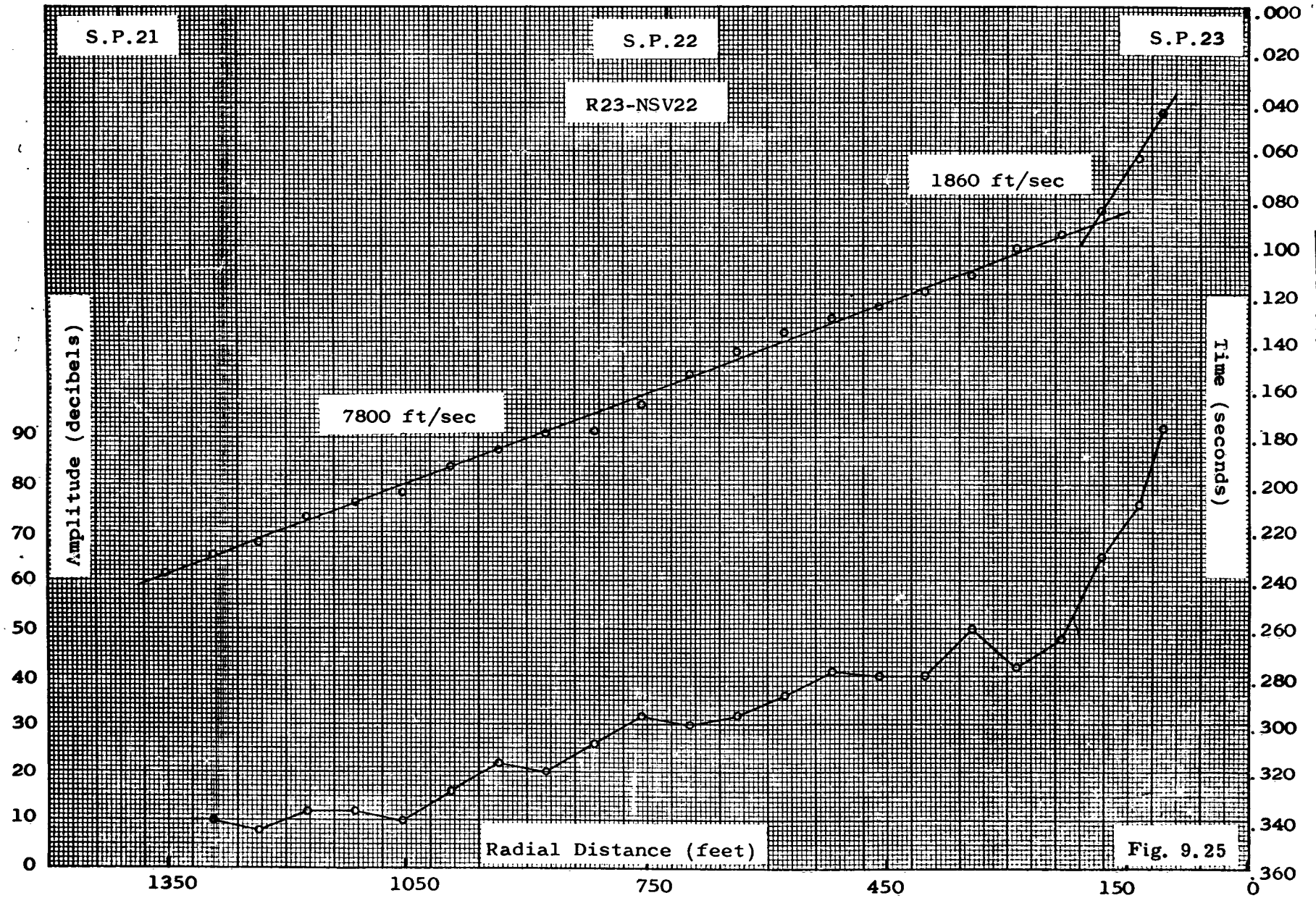

Fig. 9.25

K+E 10 X 10 TO THE CM. 359-14
KEUFFEL & ESSER CO. MADE IN U.S.A.

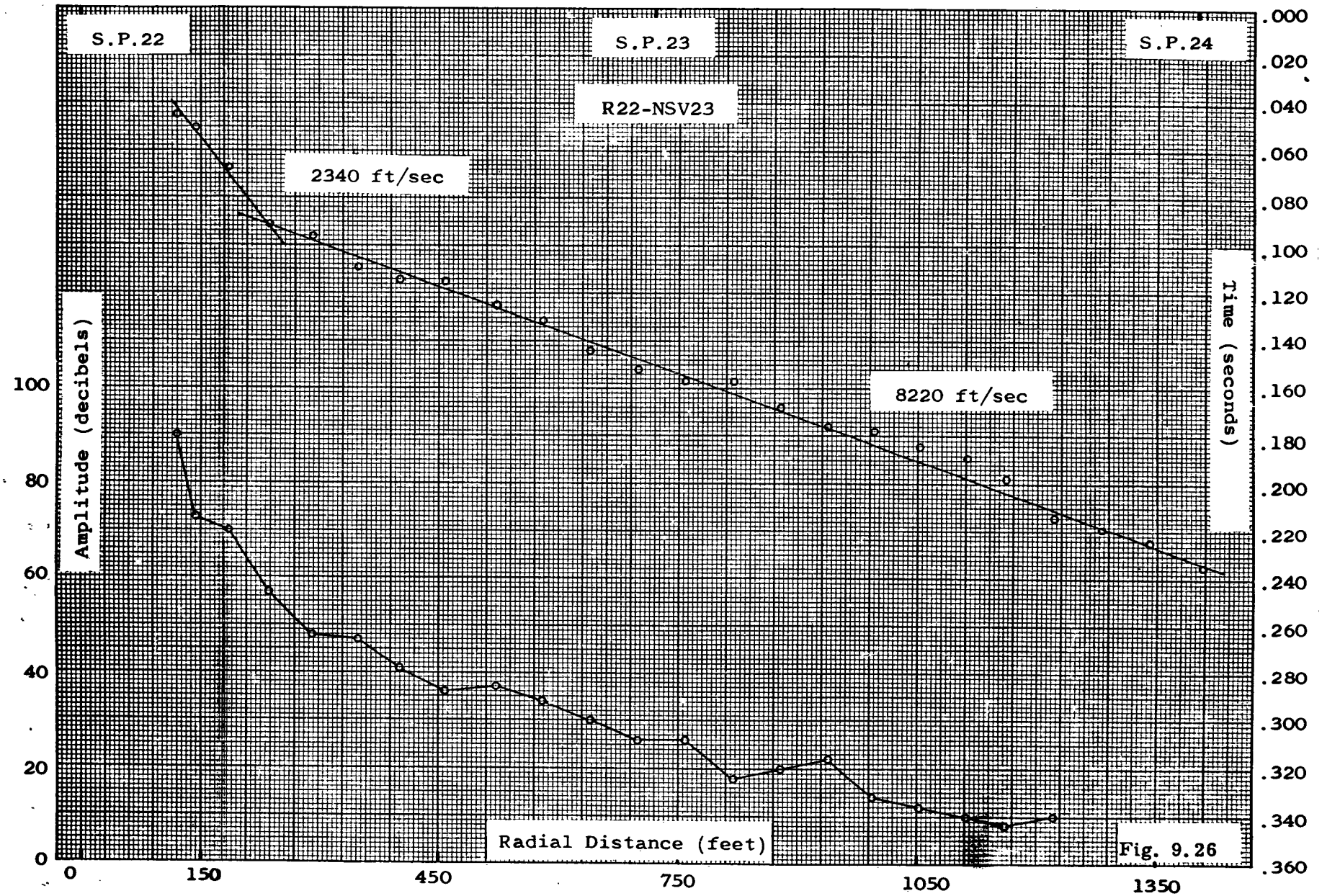

Fig. 9.26

K&E 10 X 10 TO THE CM. 359-14
KEUFFEL & ESSER CO. MADE IN U.S.A.

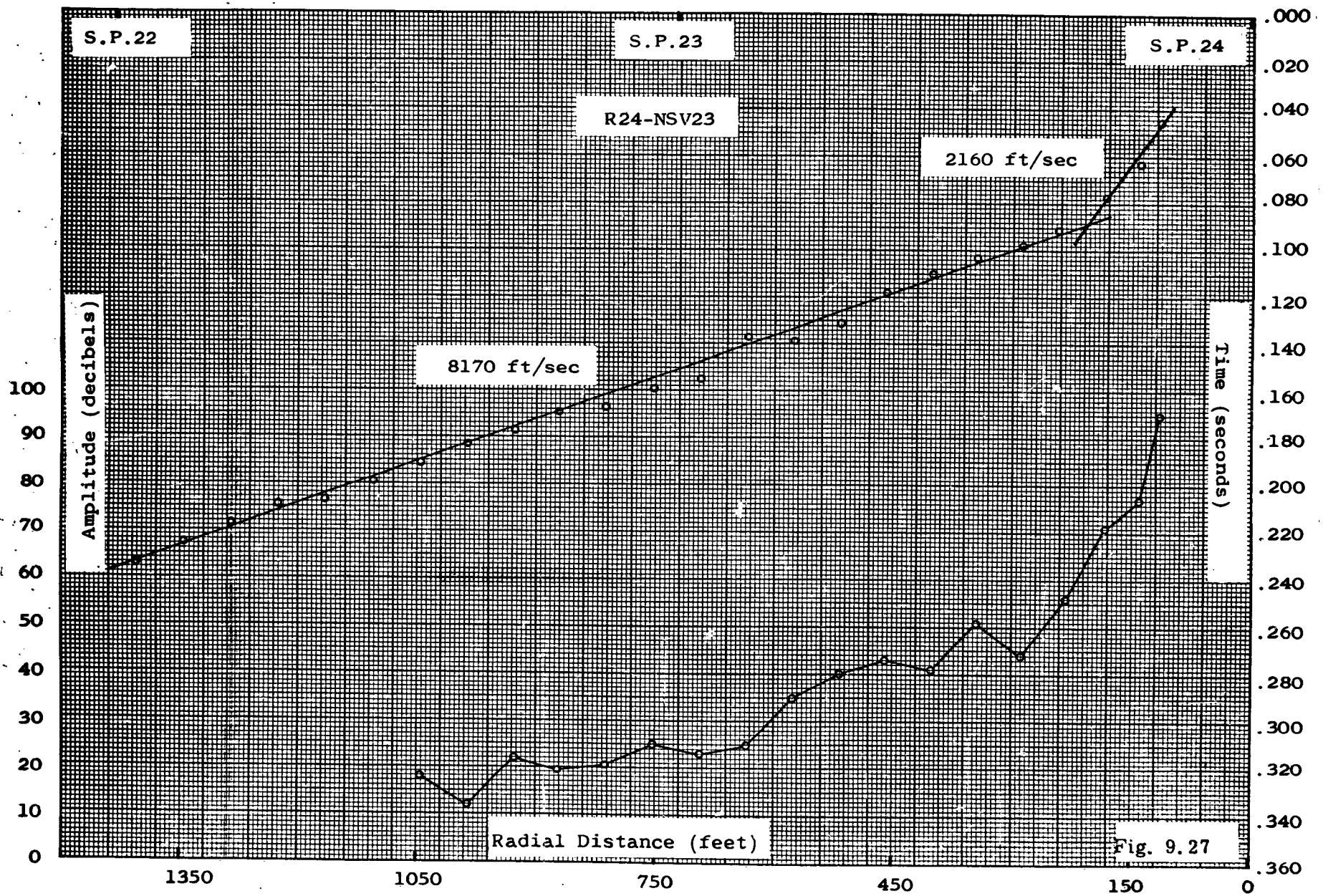

Fig. 9.27

K+E 10 X 10 TO THE CM. 359-14
KEUFFEL & ESSER CO. MADE IN U.S.A.

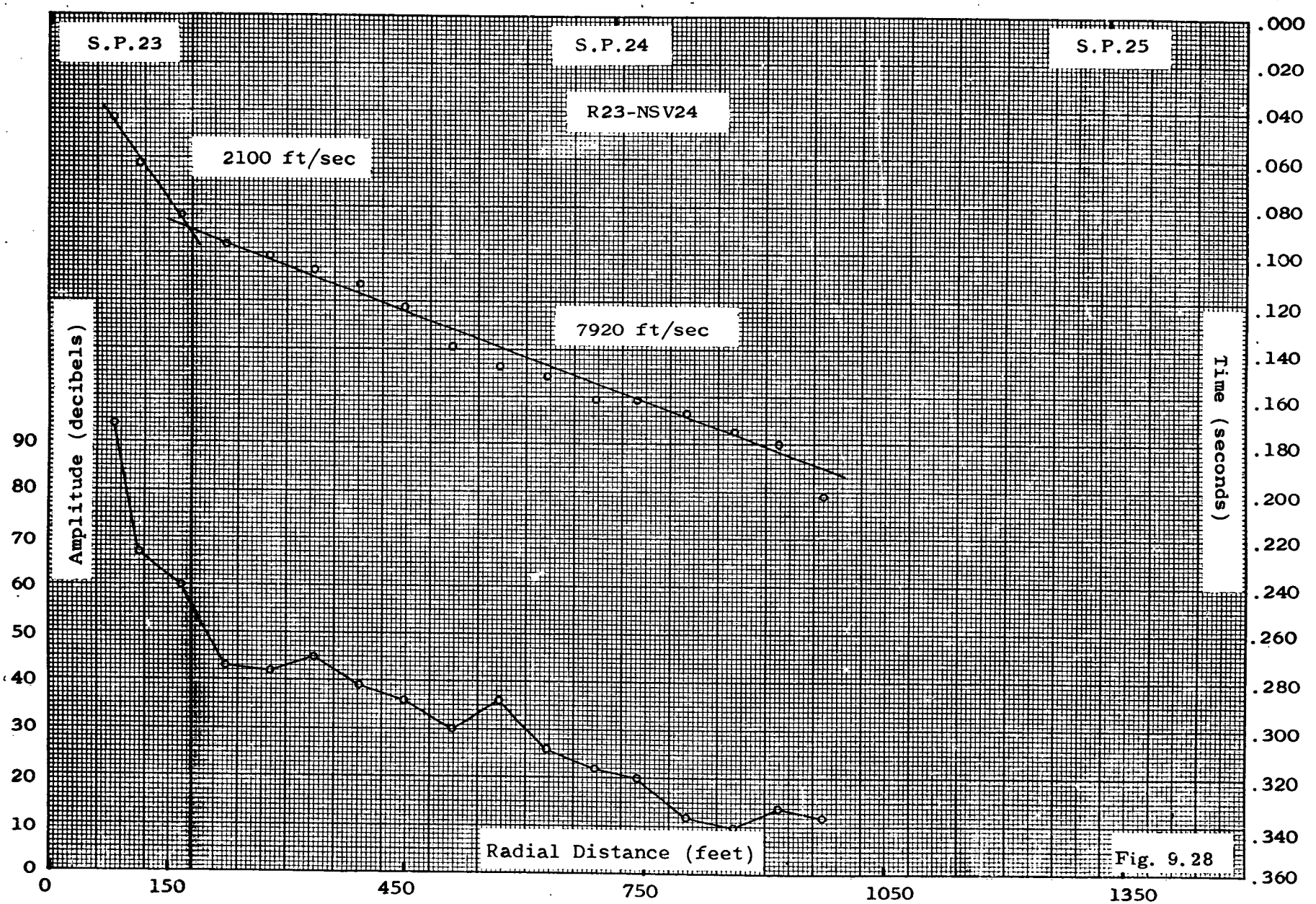

Fig. 9.28

K+E 10 X 10 TO THE CM. 359-14
KEUFFEL & ESSER CO. MADE IN U.S.A.

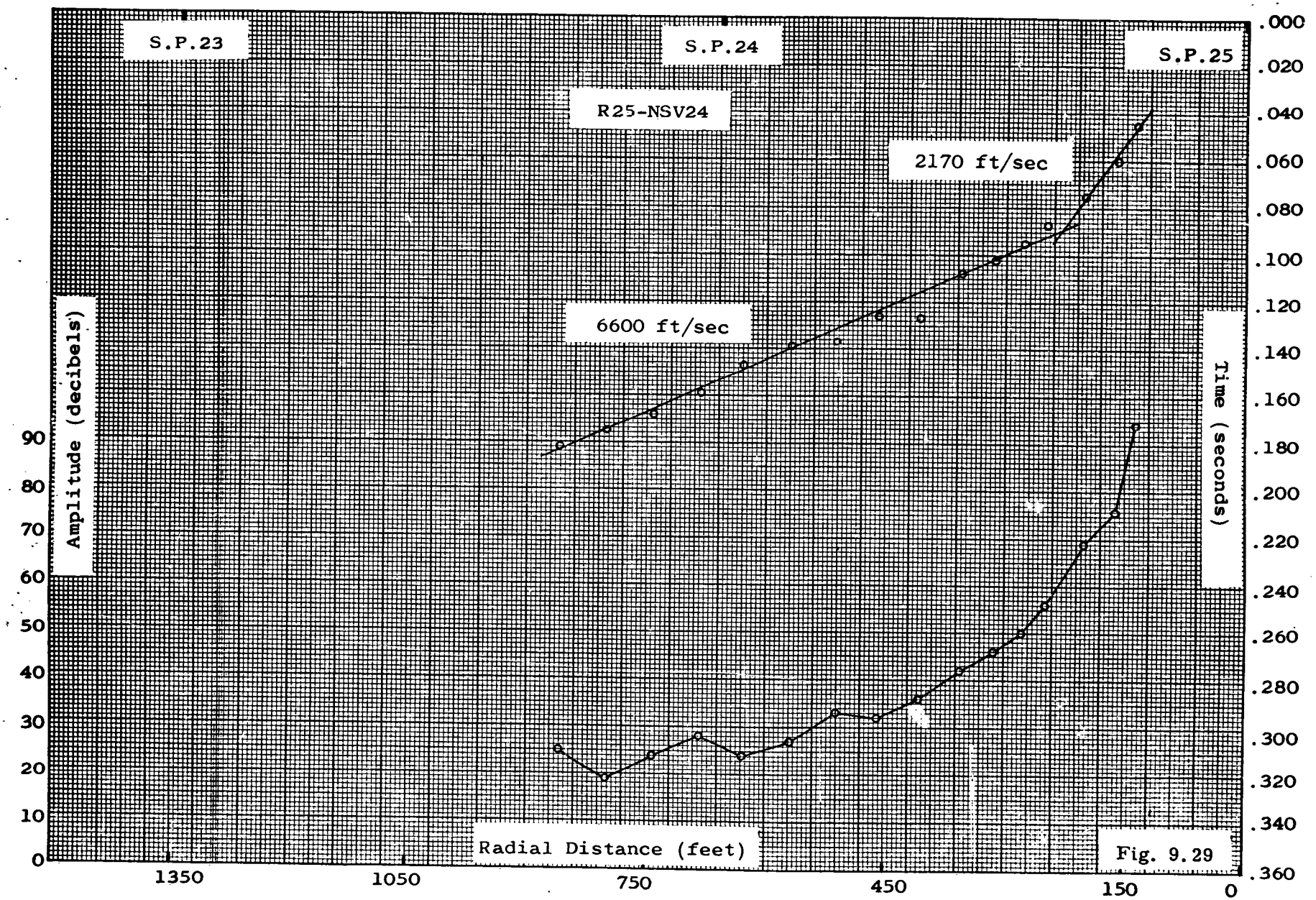

Fig. 9.29

K+E 10 X 10 TO THE CM. 359-14
KEUFFEL & ESSER CO. MADE IN U.S.A.

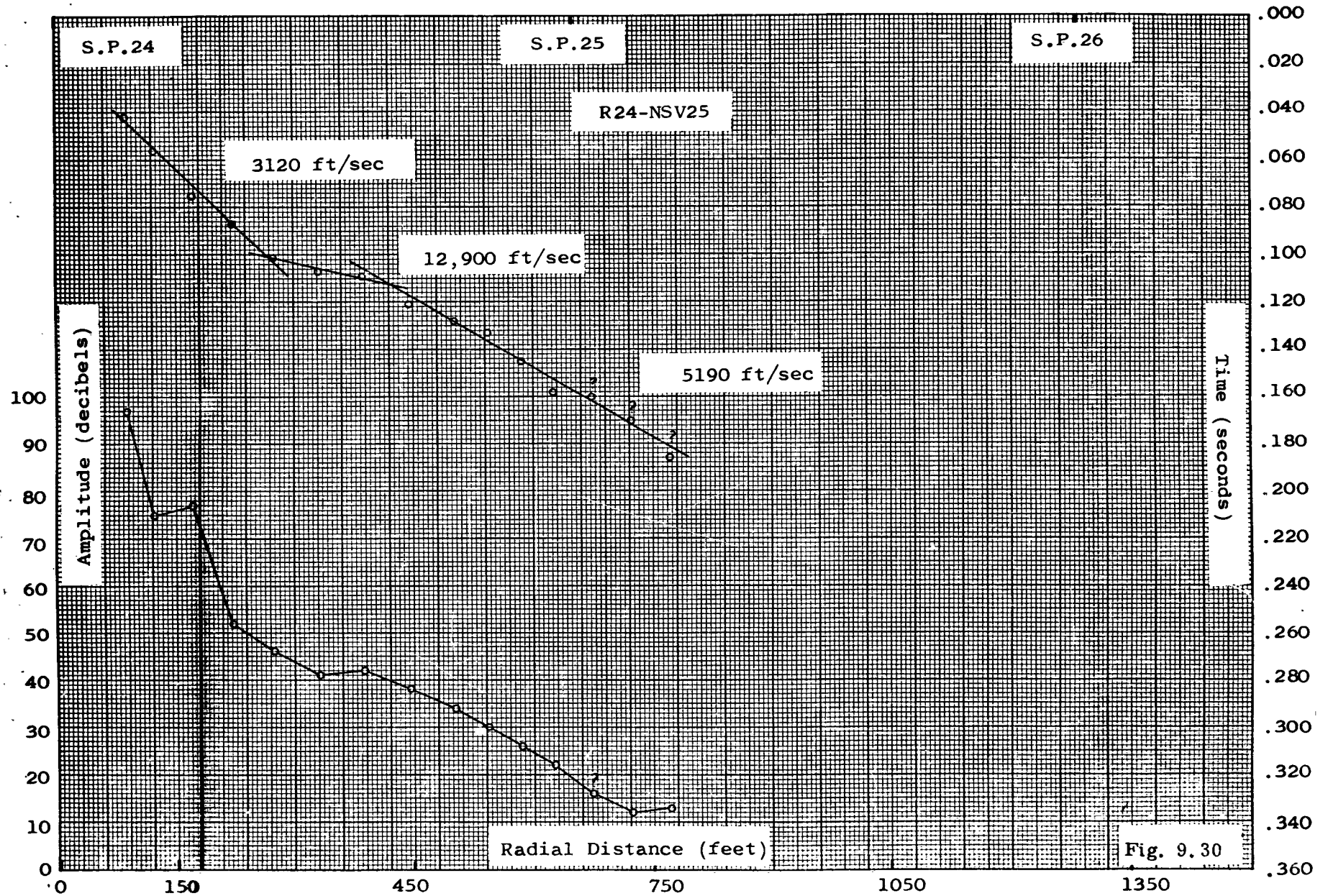

Fig. 9.30

K•E 10 X 10 TO THE CM. 359-14
KEUFFEL & ESSER CO. MADE IN U.S.A.

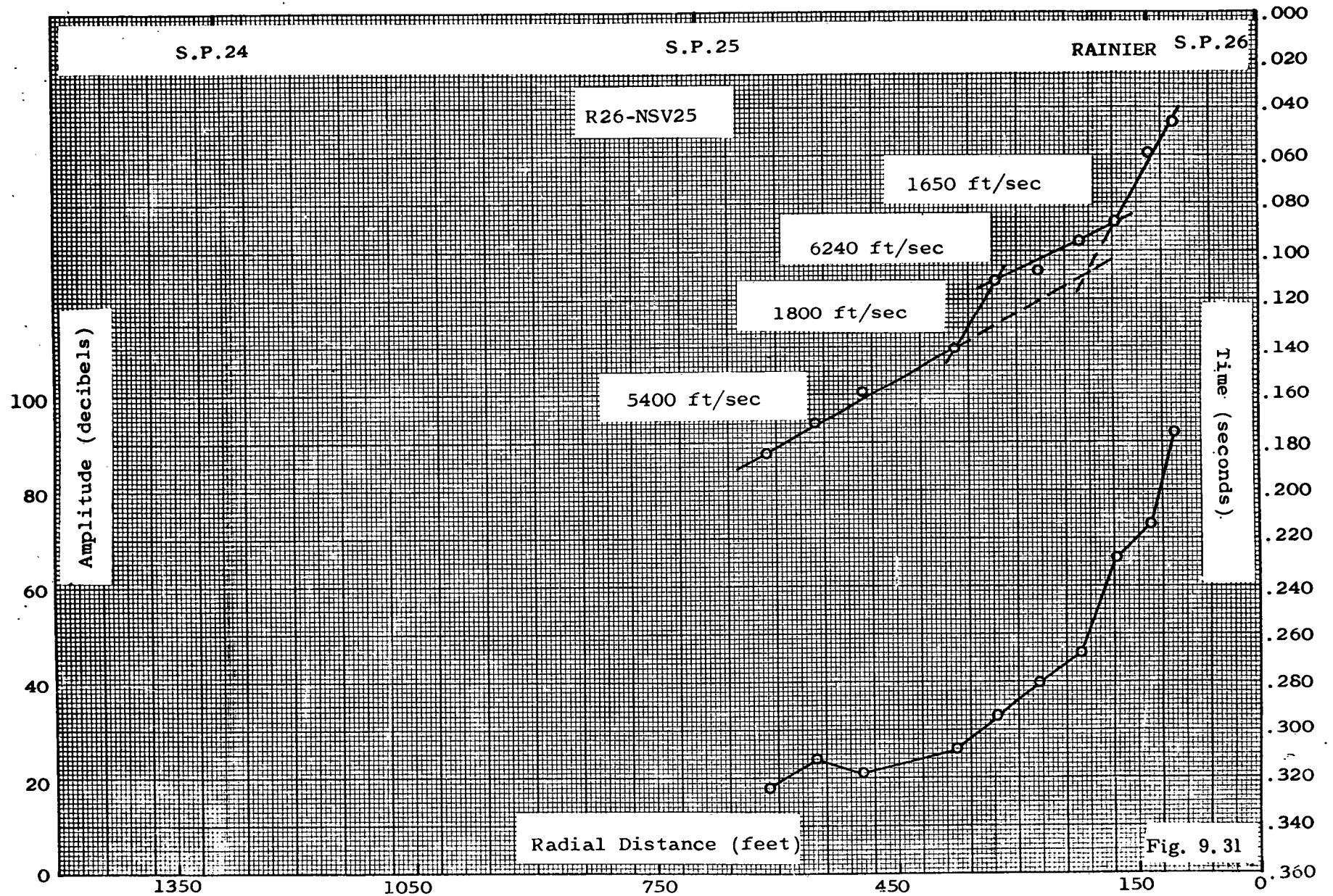

Fig. 9.31

K&E 10 X 10 TO THE CM. 359-14 KEUFFEL & ESSER CO. MADE IN U.S.A

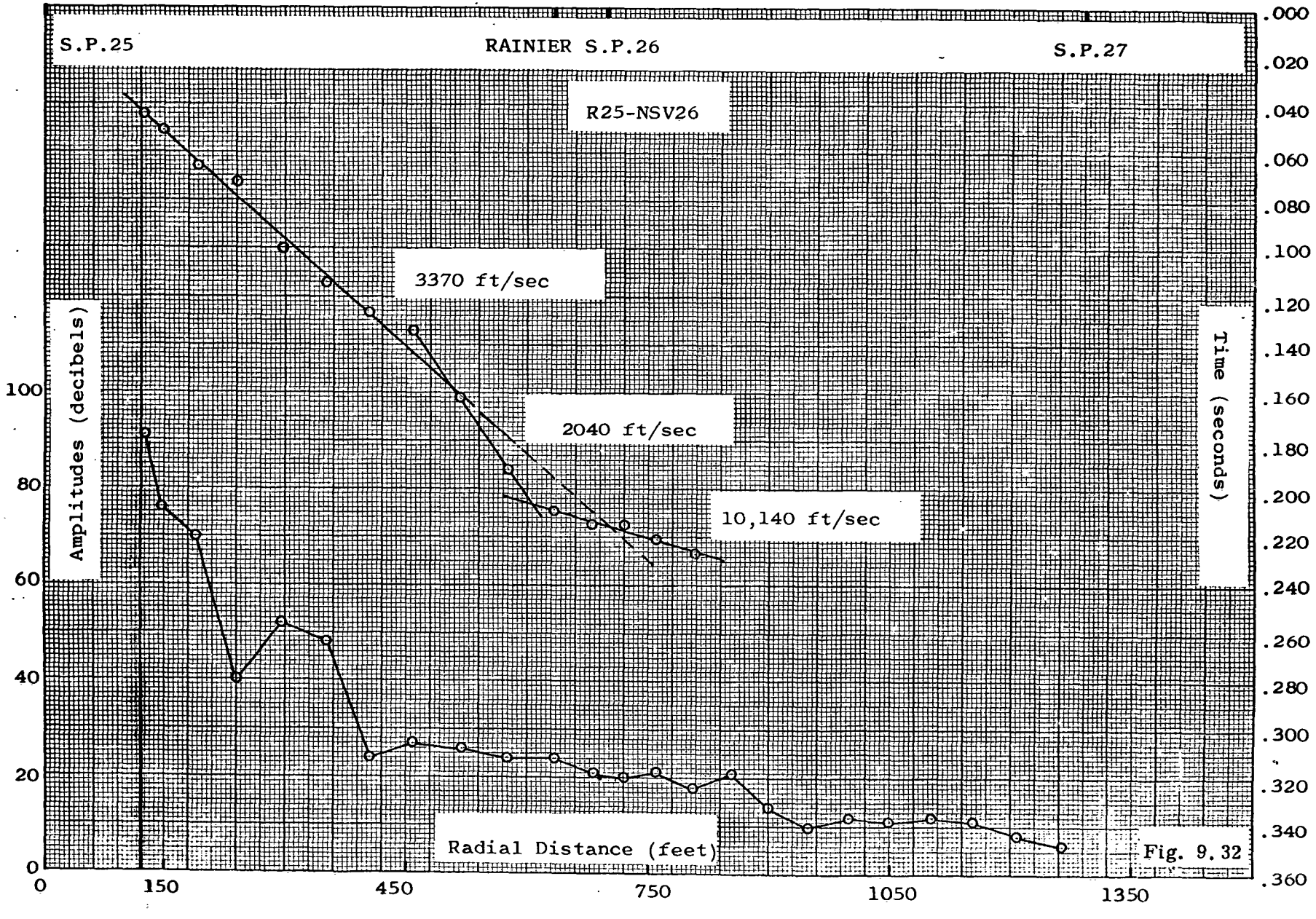

Fig. 9.32

K+E 10 X 10 TO THE CM. 359-14
KEUFFEL & ESSER CO. MADE IN U.S.A.

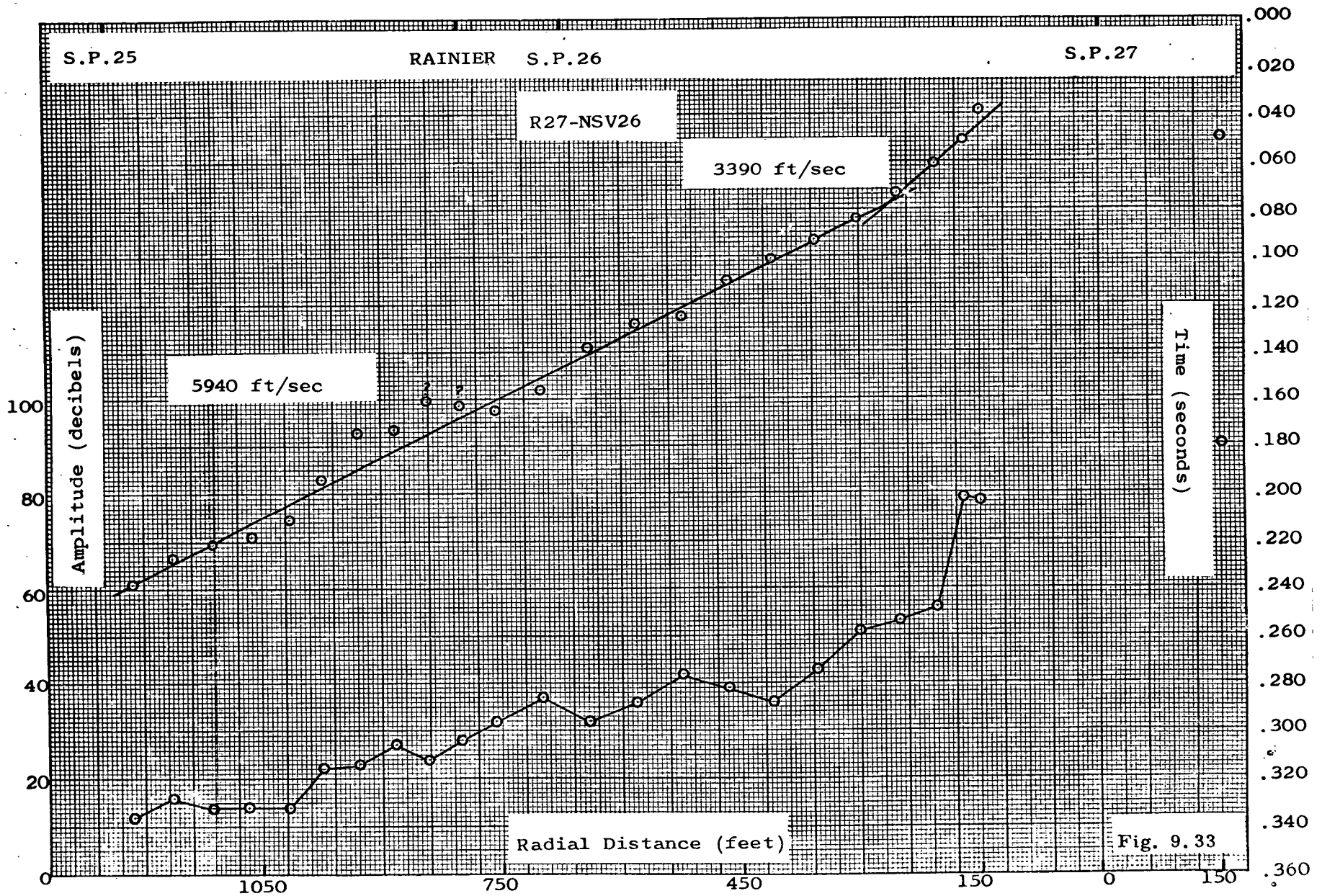

Fig. 9.33

K+E 10 X 10 TO THE CM. 359-14
KEUFFEL & ESSER CO. MADE IN U.S.A

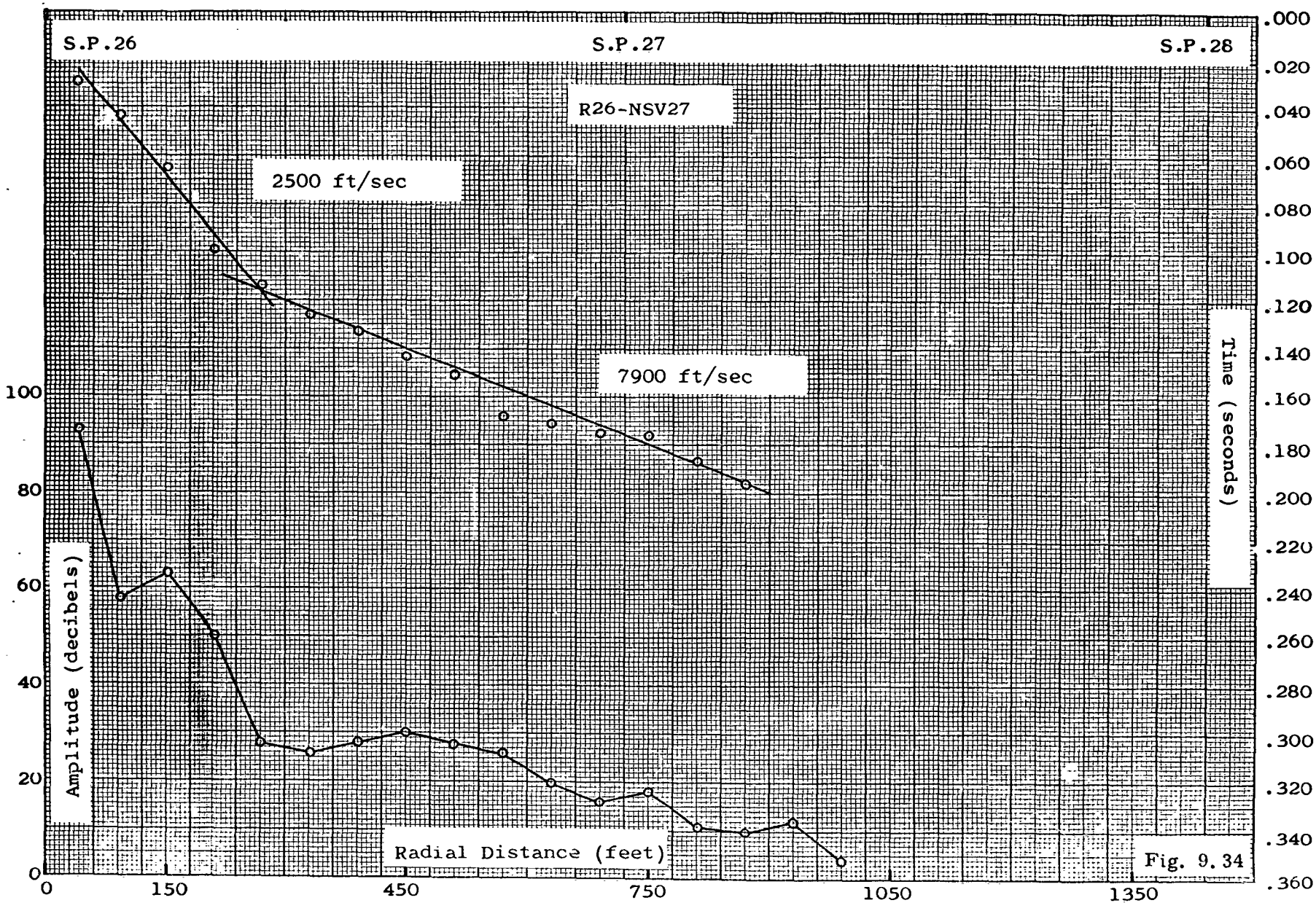

Fig. 9.34

K&E 10 X 10 TO THE CM. 359-14
KEUFFEL & ESSER CO. MADE IN U.S.A.

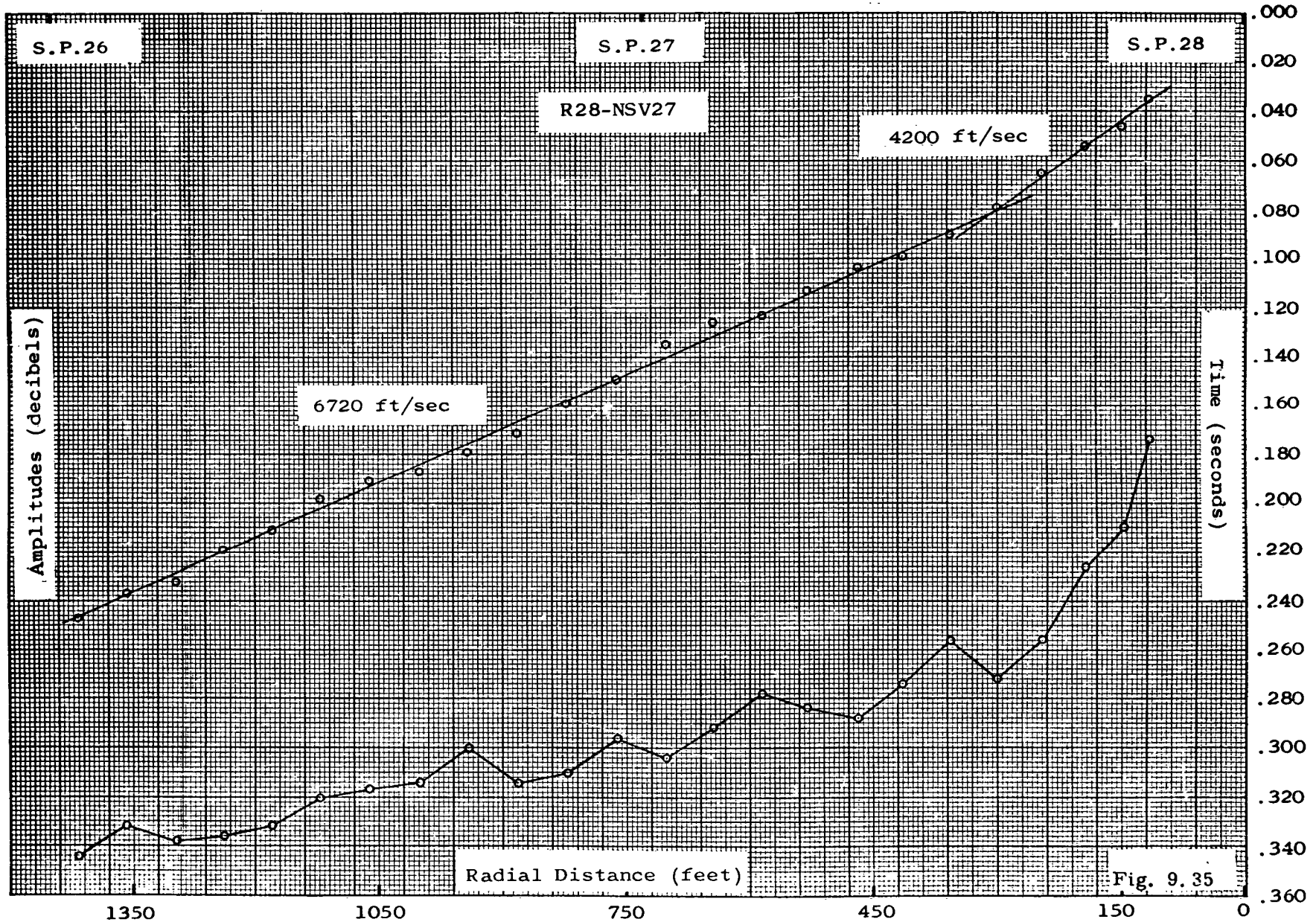

Fig. 9.35

K&E 10 X 10 TO THE CM. 359-14
KEUFFEL & ESSER CO. MADE IN U.S.A.

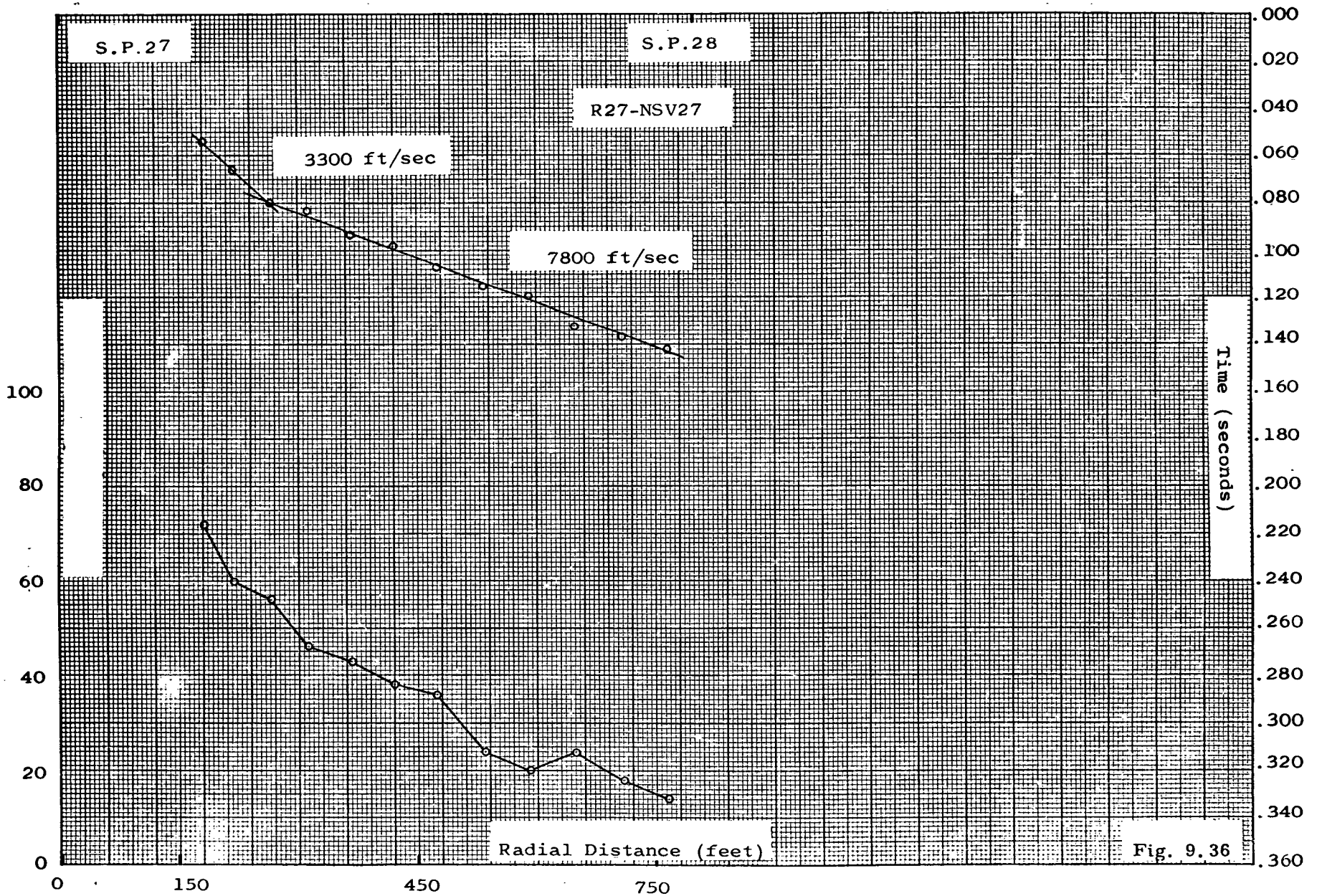

Fig. 9.36

K&E 10 X 10 TO THE CM. 359-14
KEUFFEL & ESSER CO. MADE IN U.S.A.

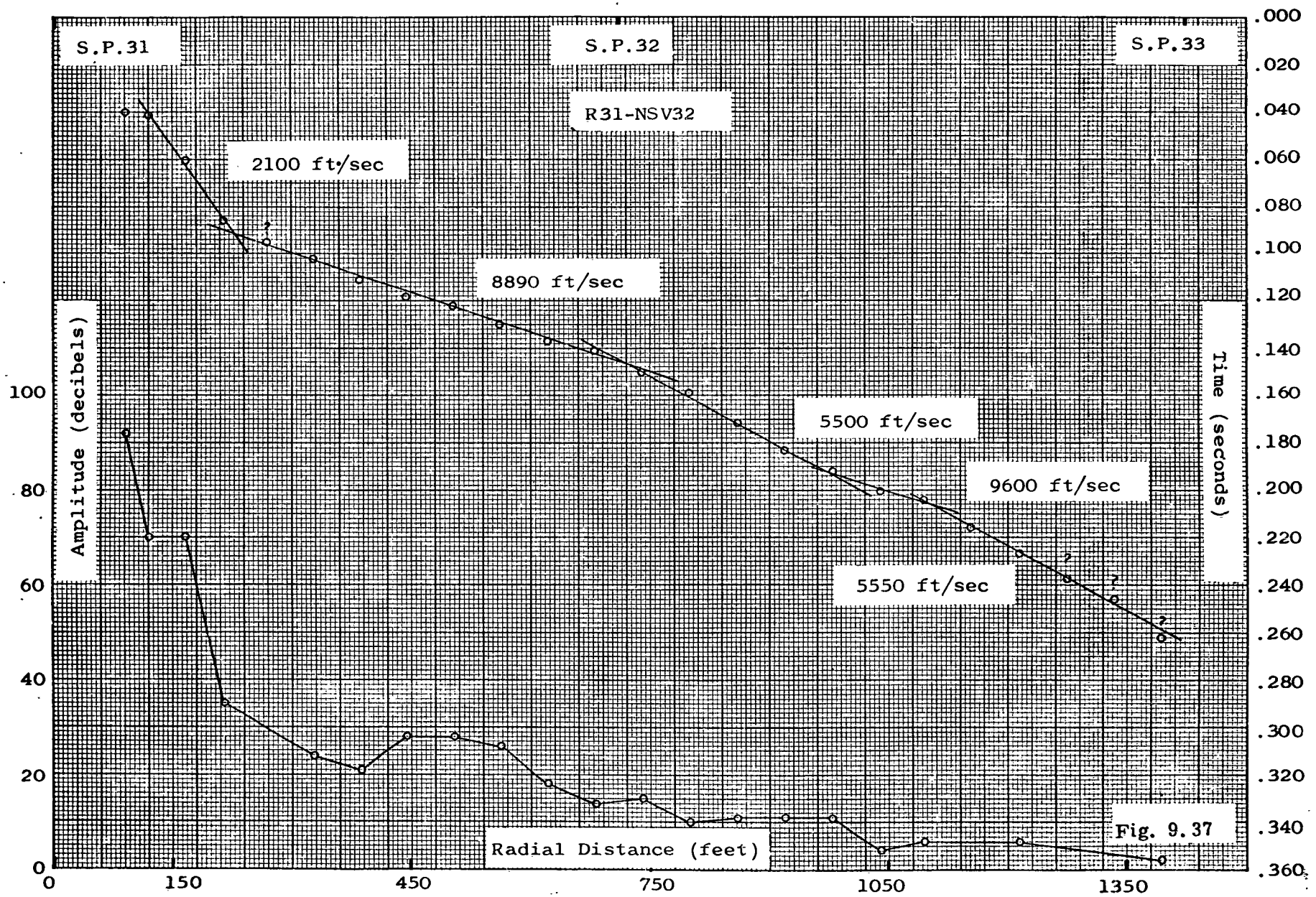

Fig. 9.37

K•Σ 10 X 10 TO THE CM. 359-14
KEUFFEL & ESSER CO. MADE IN U.S.A.

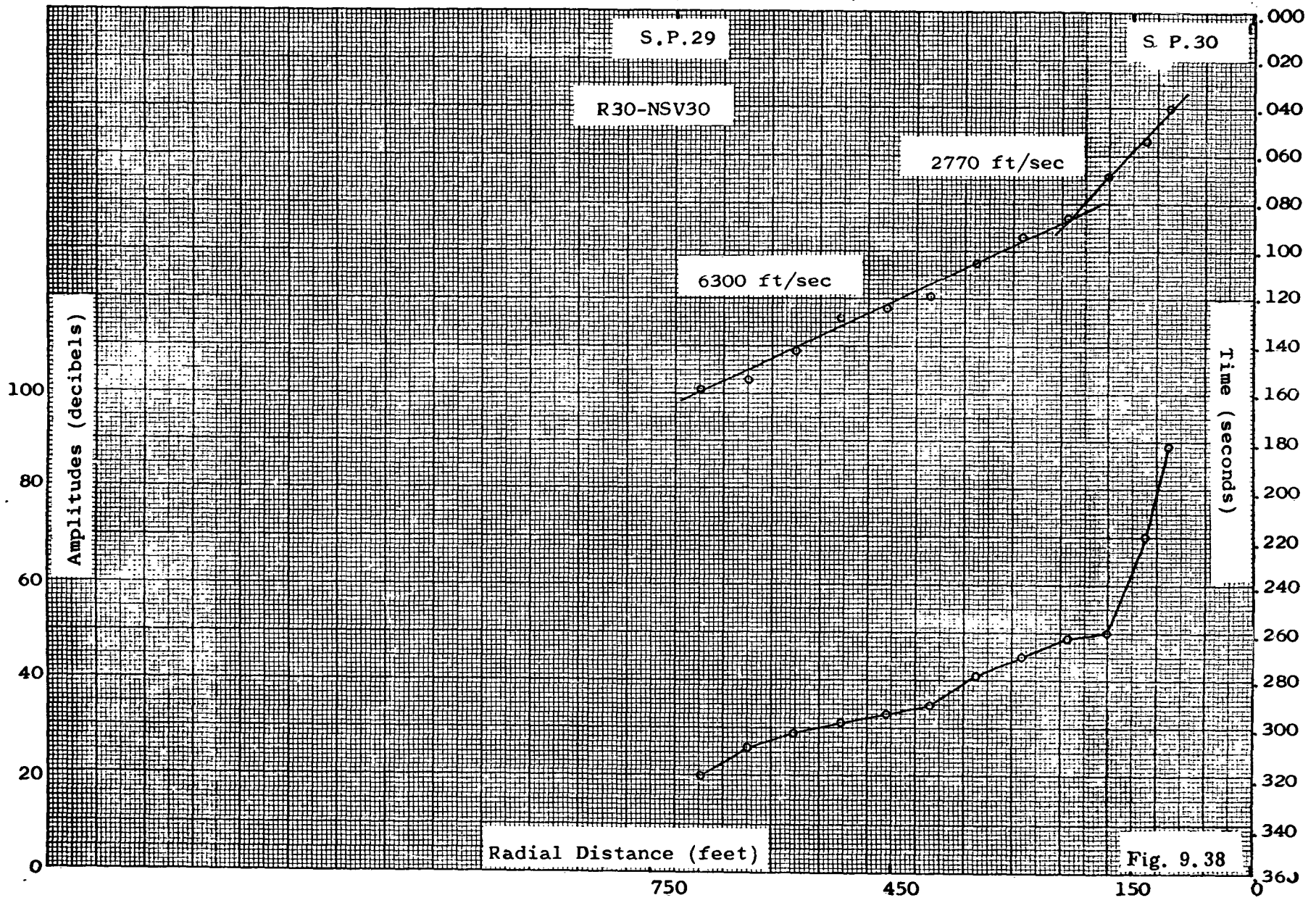

Fig. 9.38

K·E 10 X 10 TO THE CM. 359-14
KEUFFEL & ESSER CO. MADE IN U.S.A.

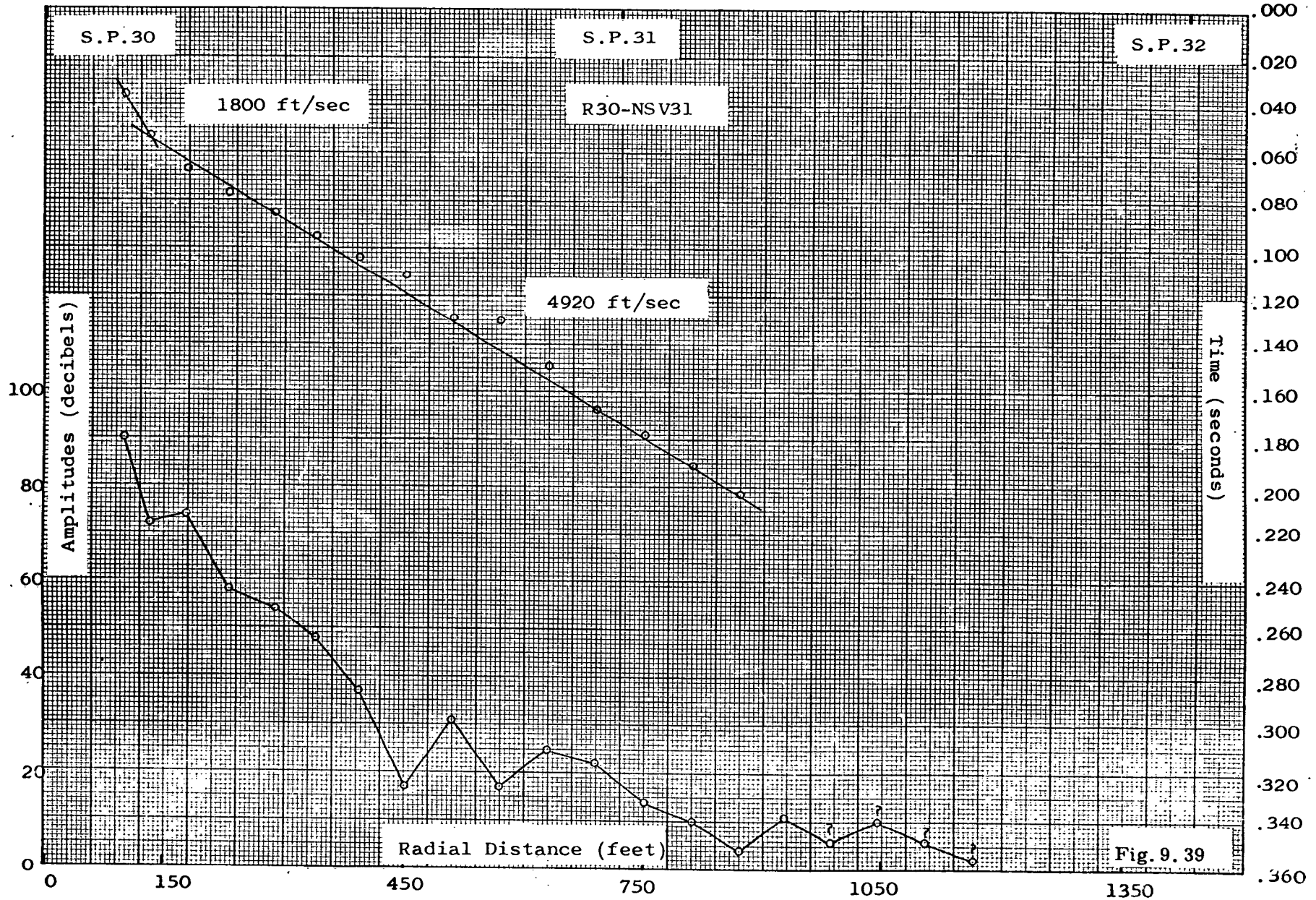

Fig. 9.39

K&E 10 X 10 TO THE CM. 359-14
KEUFFEL & ESSER CO. MADE IN U.S.A.

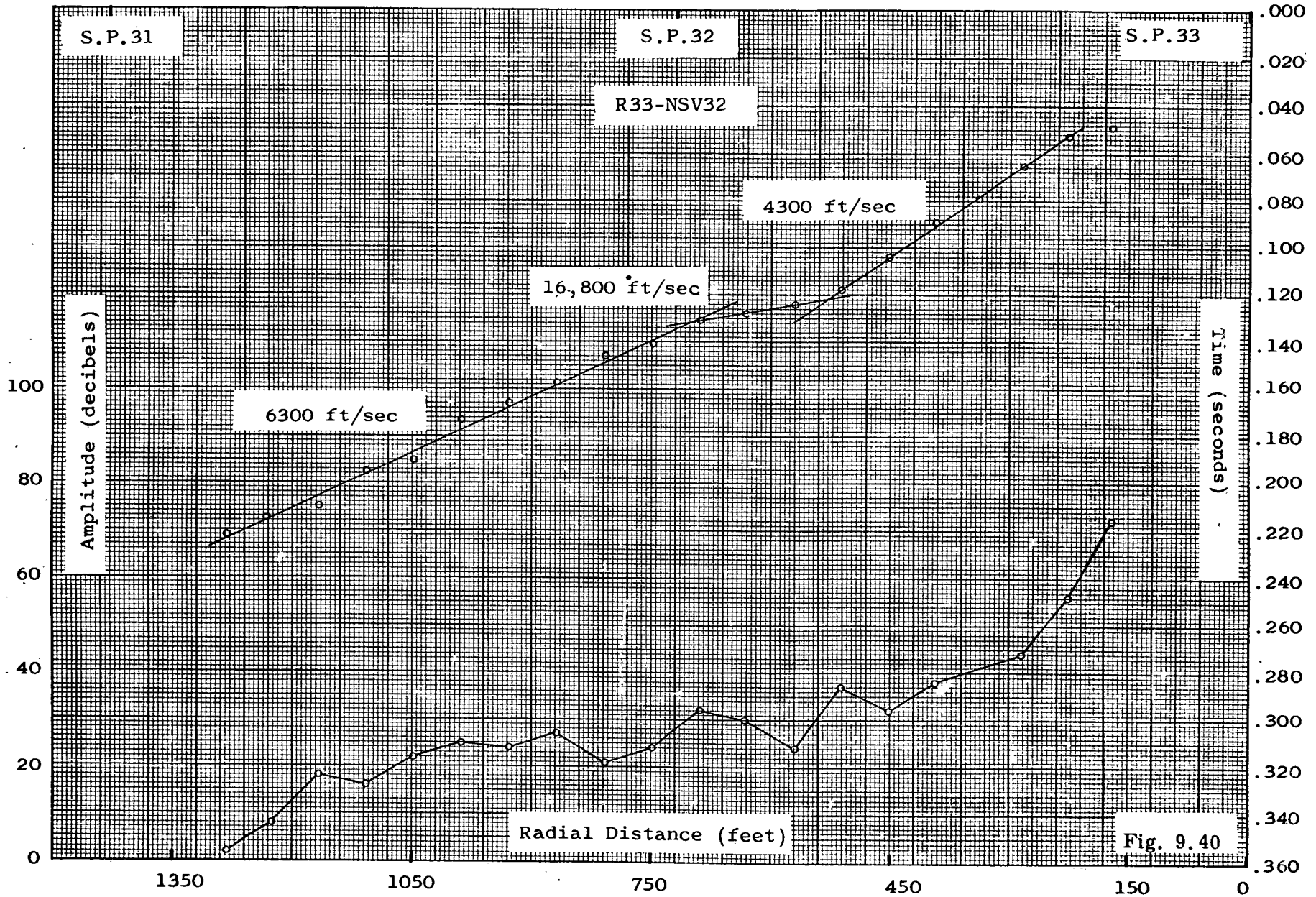

Fig. 9.40

K&E 10 X 10 TO THE CM. 359-14
KEUFFEL & ESSER CO. MADE IN U.S.A.

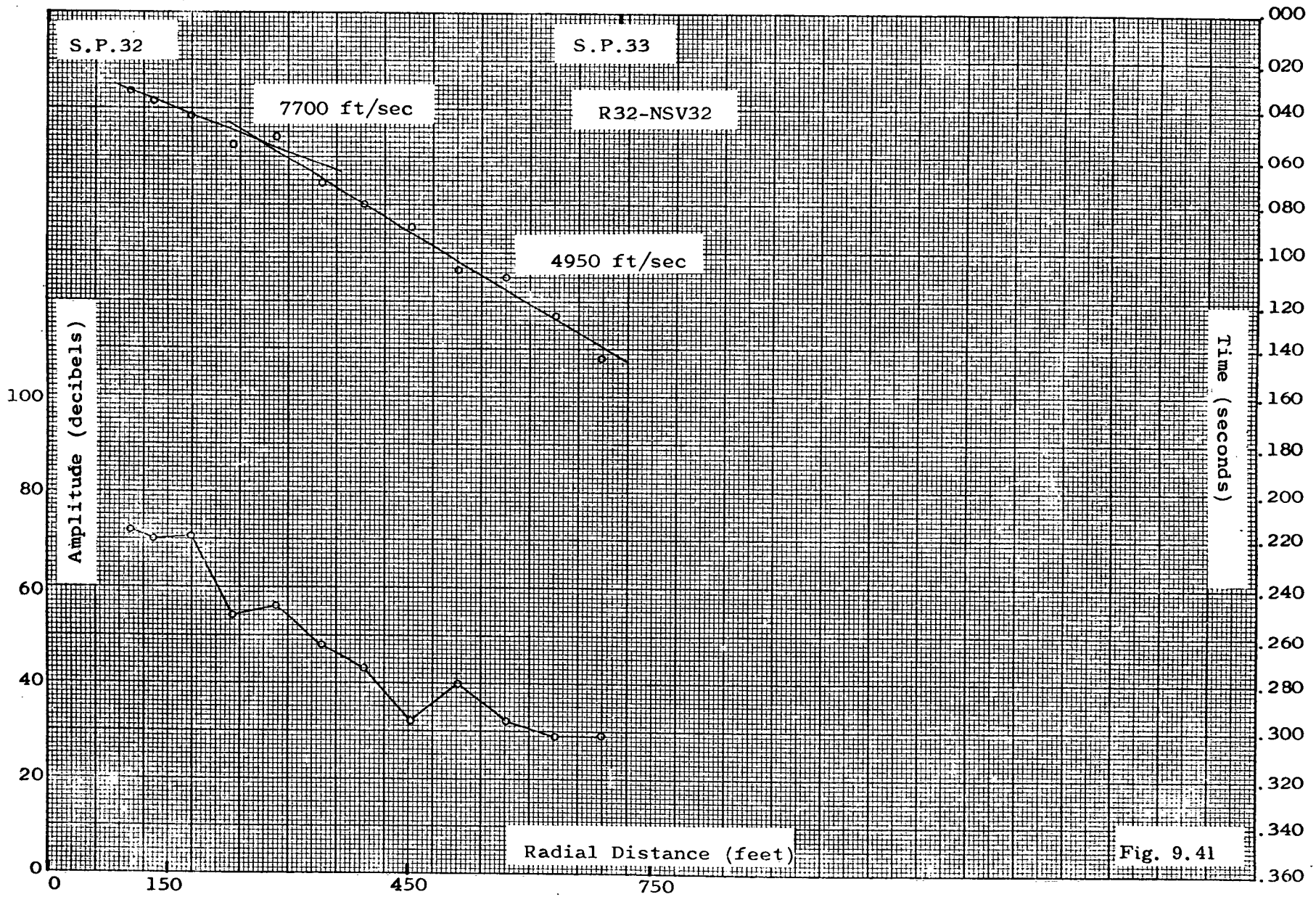

Fig. 9.41

K&E 10 X 10 TO THE CM. 359-14
KEUFFEL & ESSER CO. MADE IN U.S.A.

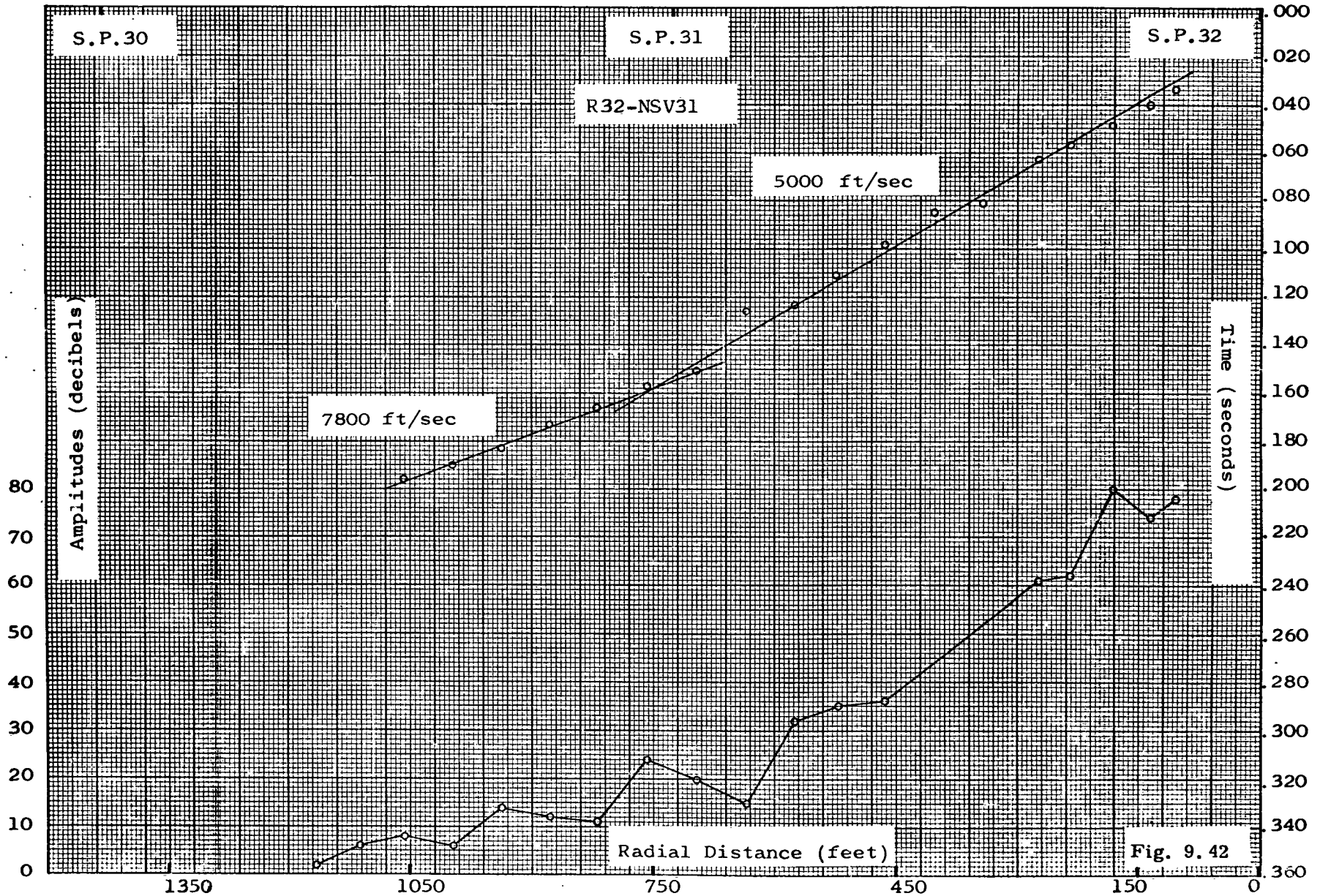

Fig. 9.42

K&E 10 X 10 TO THE CM. 359-14
KEUFFEL & ESSER CO. MADE IN U.S.A.

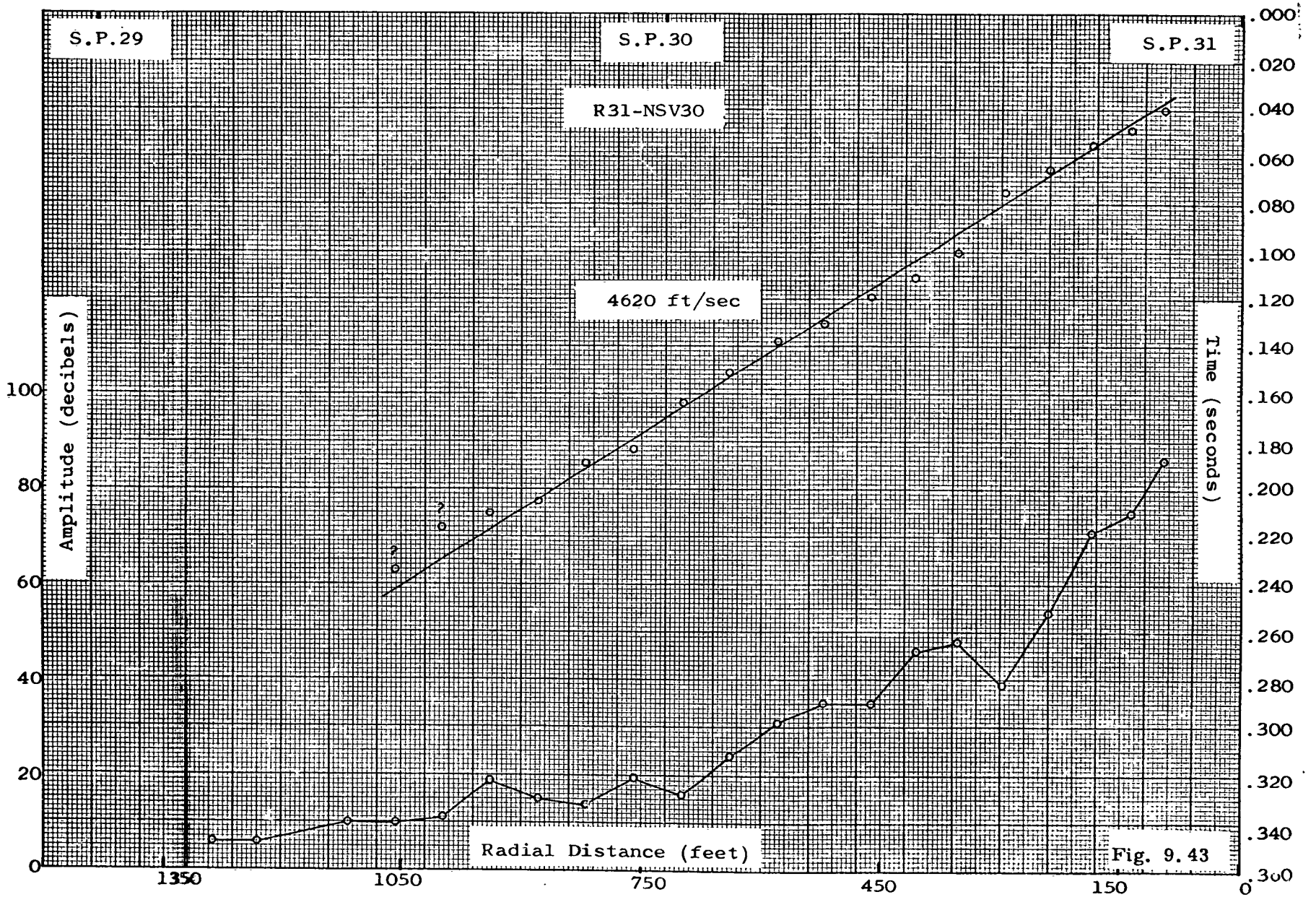

Fig. 9.43

K&E 10 X 10 TO THE CM. 359-14
KEUFFEL & ESSER CO. MADE IN U.S.A.

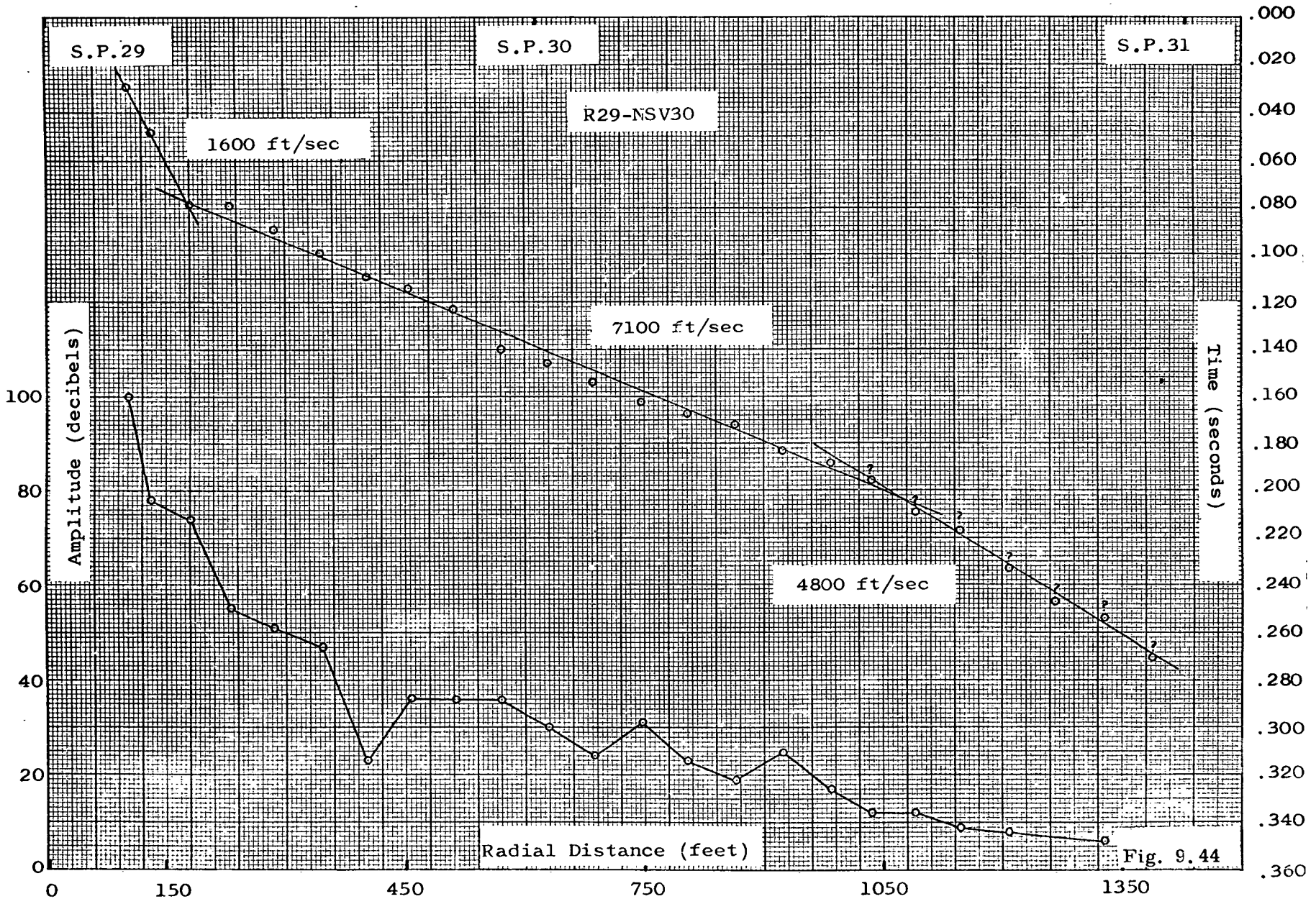

Fig. 9.44

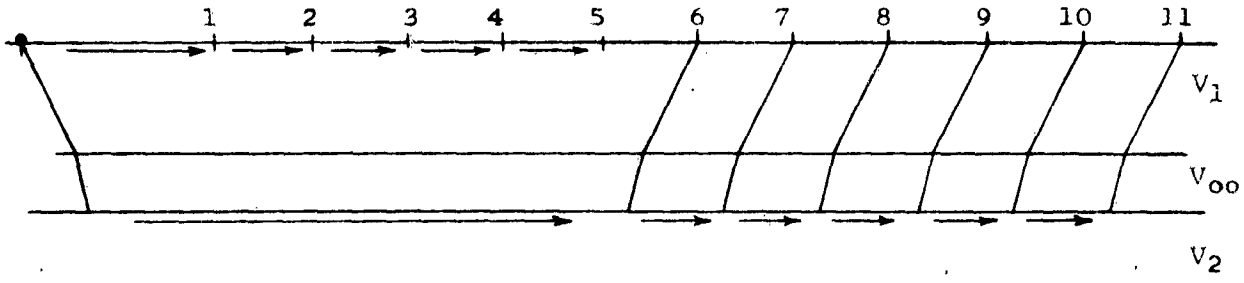

A

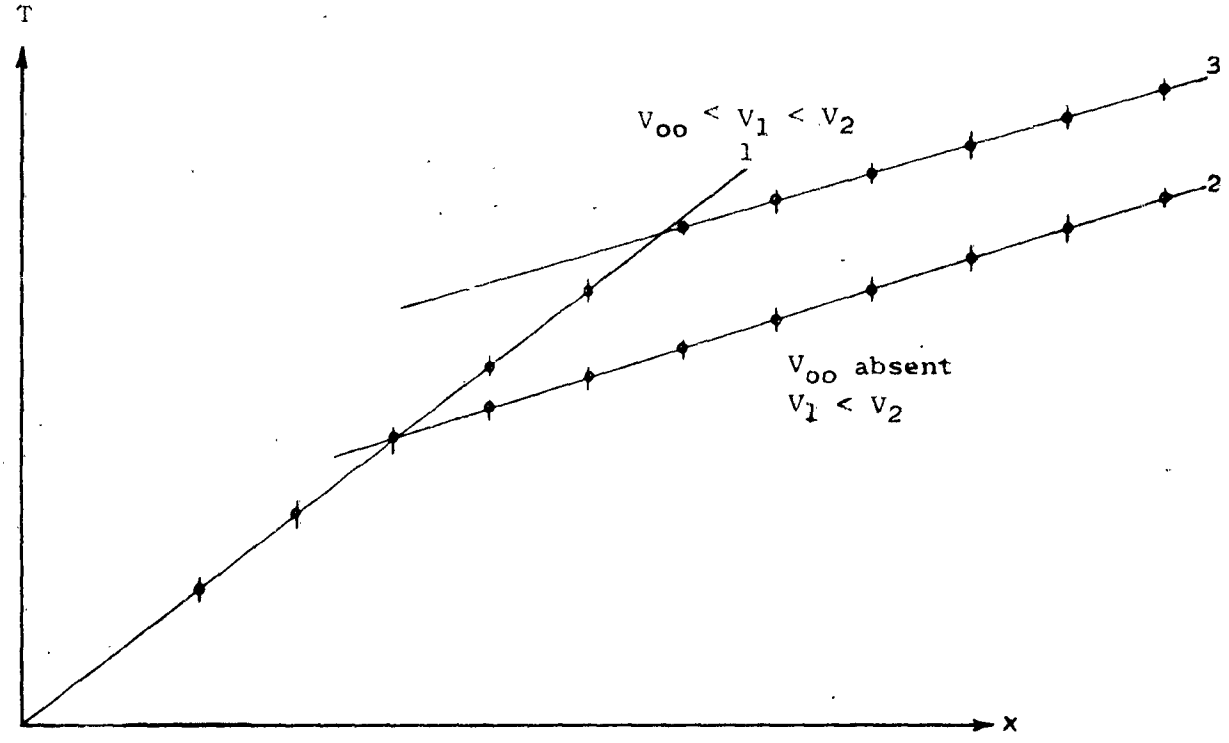

B

FIGURE - - 9.45

Lines 1 and 2 - Time Distance Graph for V_1 and V_2

Lines 1 and 3 - Time Distance Graph for V_1, V_{oo} and V_2

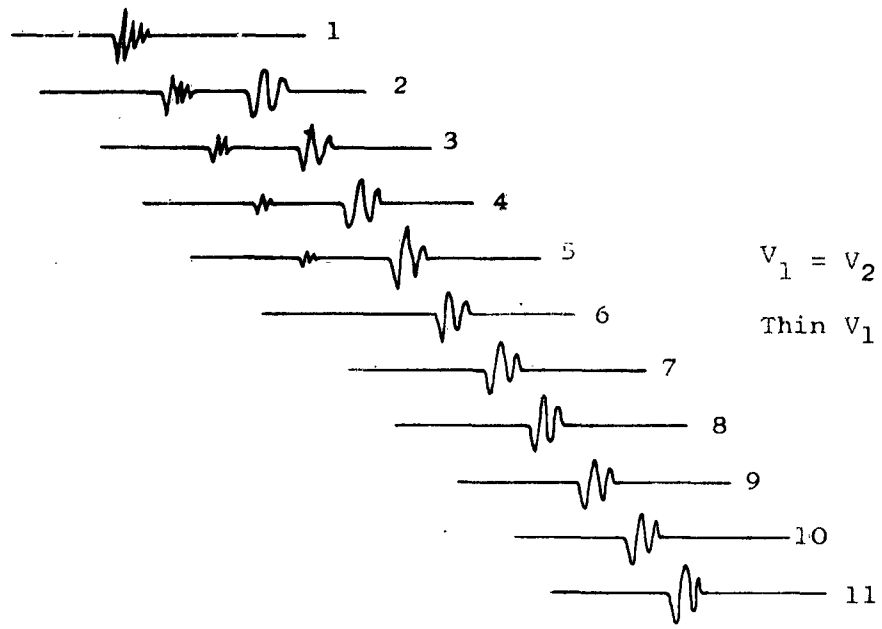

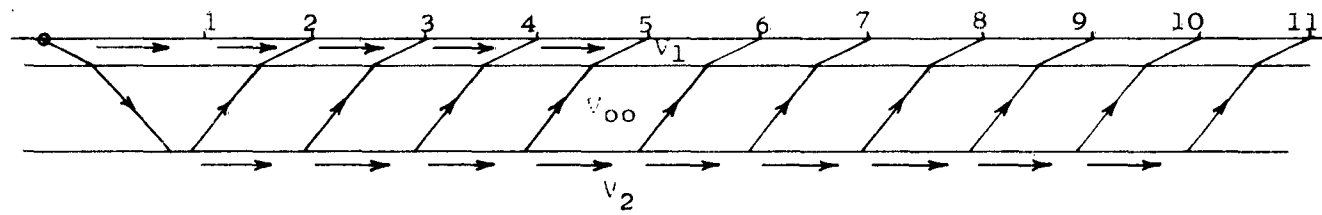

FIGURE - - 9.46

1st Arrivals (1-11) Travel Through V_1

-- Very High Frequency

-- Rapid Attenuation With Distance: (6-11) Not Visible

2nd Arrivals (2-11) Travel Through V_L

No Second Arrival on 1 since

$X_1 \cdot 2d_1 \tan 12 + 2doo \tan OOL$

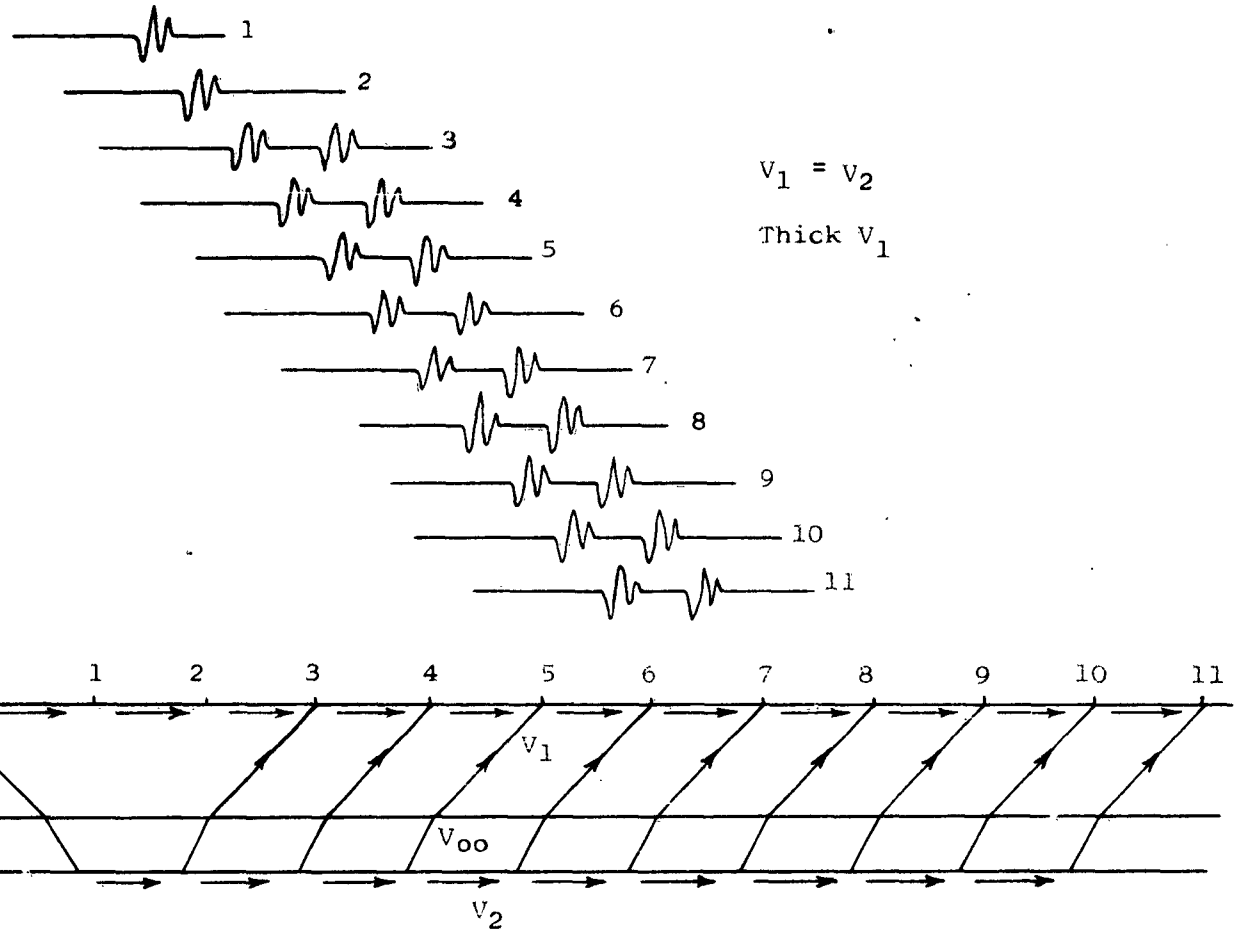

FIGURE - -9.47

1st Arrivals (1-11) Travel Through V_1

2nd Arrivals (3-11) Travel Through V_2

No Second Arrivals on 1 or 2 since

$X_2 < 2d_1 \tan 12 + 2d_{oo} \tan 002$

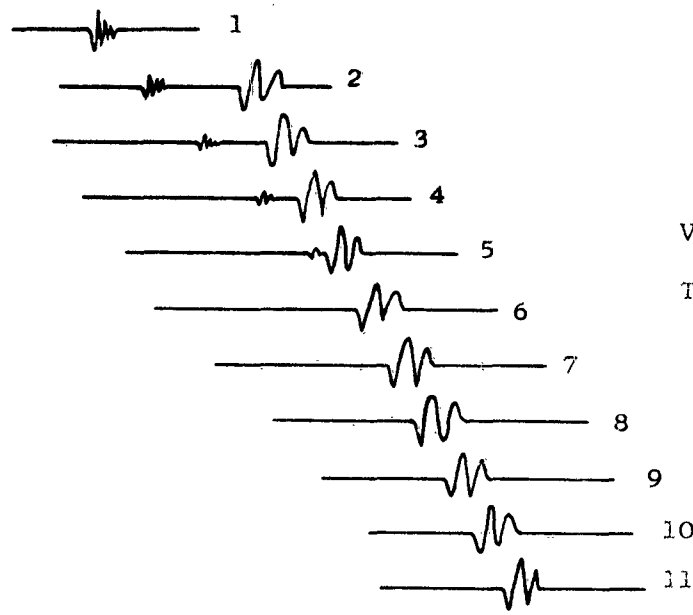

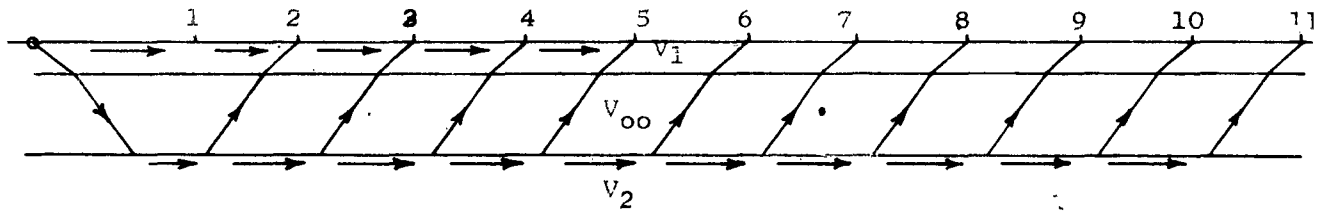

FIGURE - - 9.48

1st Arrivals (1-5) Travel Through V_1

-- Very High Frequency

-- Rapid Attenuation With Distance

1st Arrivals (6-11) Travel Through V_2

2nd Arrivals (6-11) Travel Through V_1 But Not Visible Due to Attenuation

2nd Arrivals (2-5) Travel Through V_2

No Second Arrivals on 1 since

$$X_1 < 2d_1 \tan 12 + 2doo \tan OOL$$

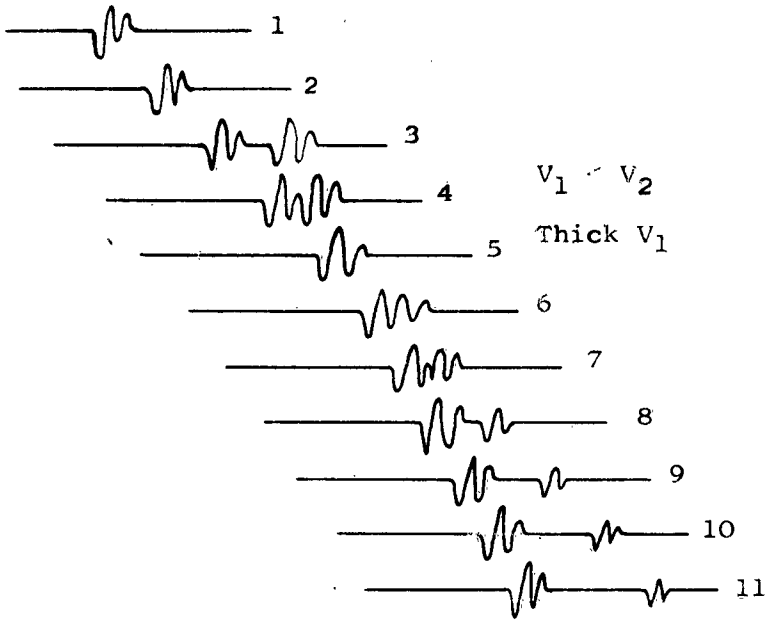

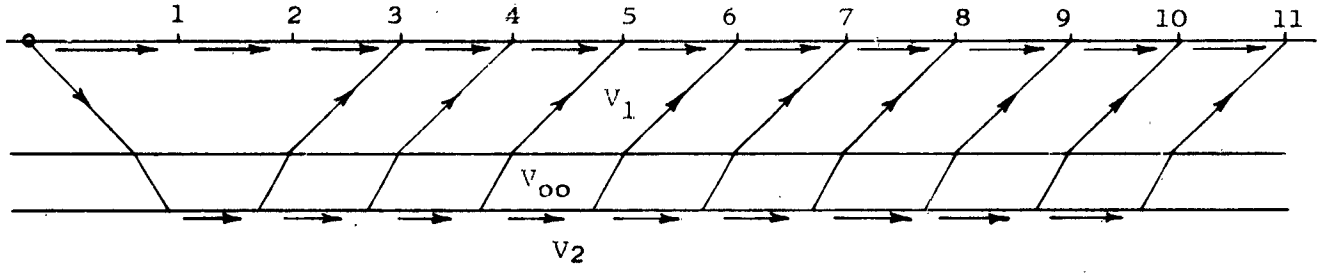

FIGURE - -9.49

1st Arrivals (1-5) Travel Through V_1

1st Arrivals (6-11) Travel Through V_2

2nd Arrivals (6-11) Travel Through V_1

2nd Arrivals (3-5) Travel Through V_2

No Second Arrivals on 1 or 2 since

$$X_2 < 2d_1 \tan 12 = 2doo \tan 002$$

No Excessive High Frequency Breaks or Rapid Attenuation With Distance.

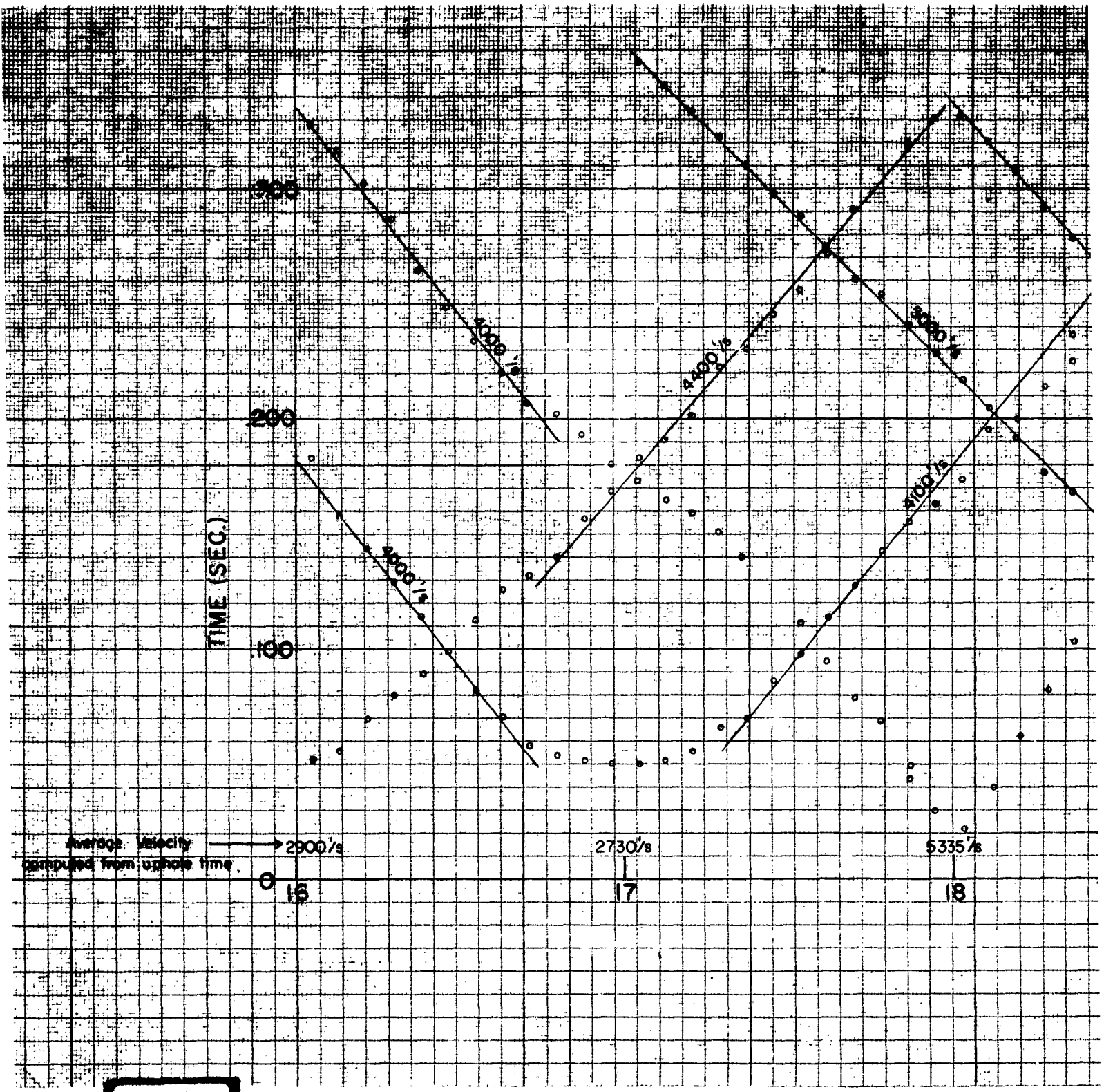
300
200
100
TIME (SEC.)
4000 ft/s
4400 ft/s
5100 ft/s
Average Velocity computed from uphole time
2900 ft/s
2730 ft/s
5335 ft/s
0
15
17
18

1

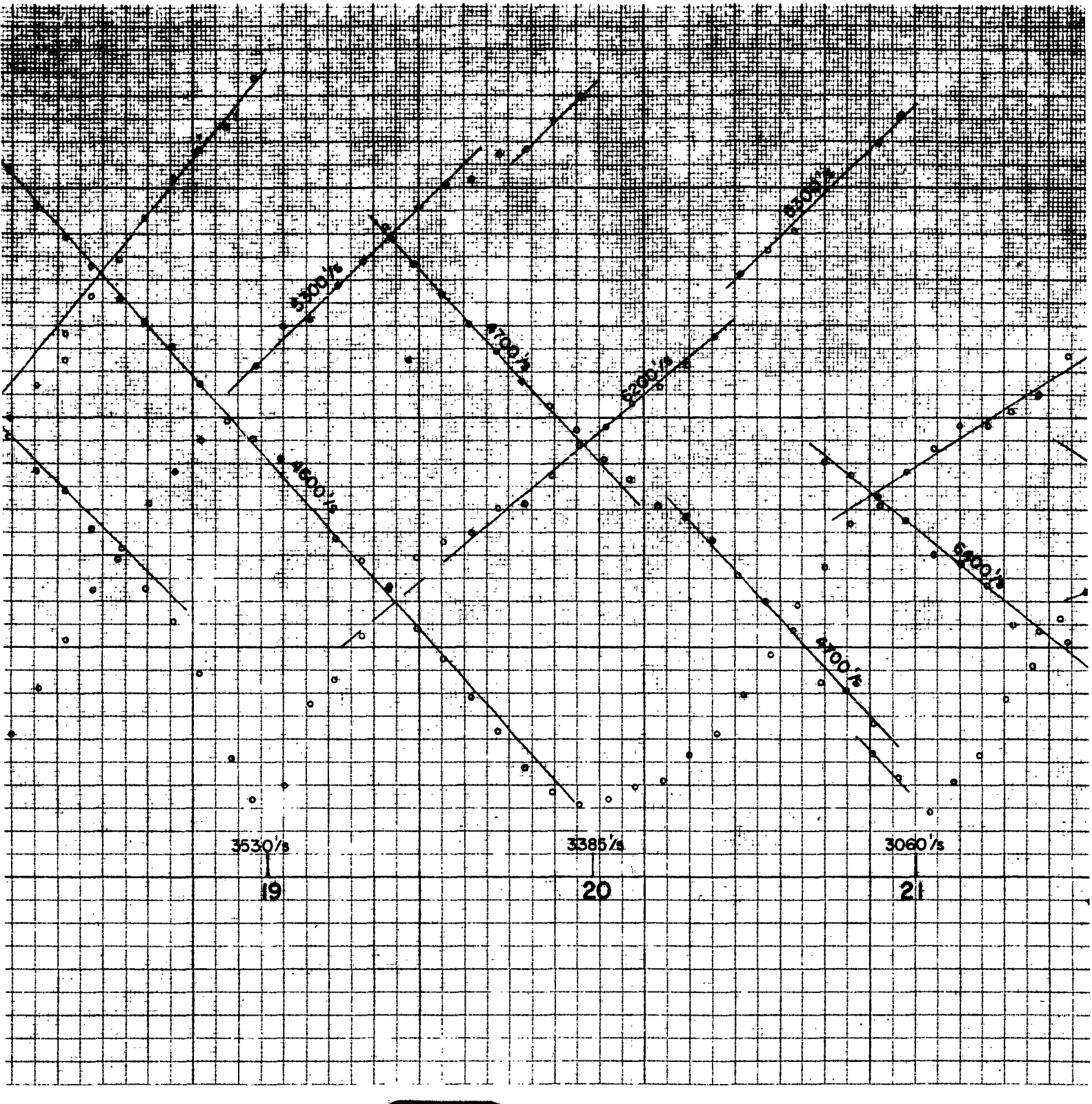
5300'/s
4700'/s
5200'/s
5300'/s
4600'/s
5400'/s
4700'/s
3530'/s
19
3385'/s
20
3060'/s
21

2

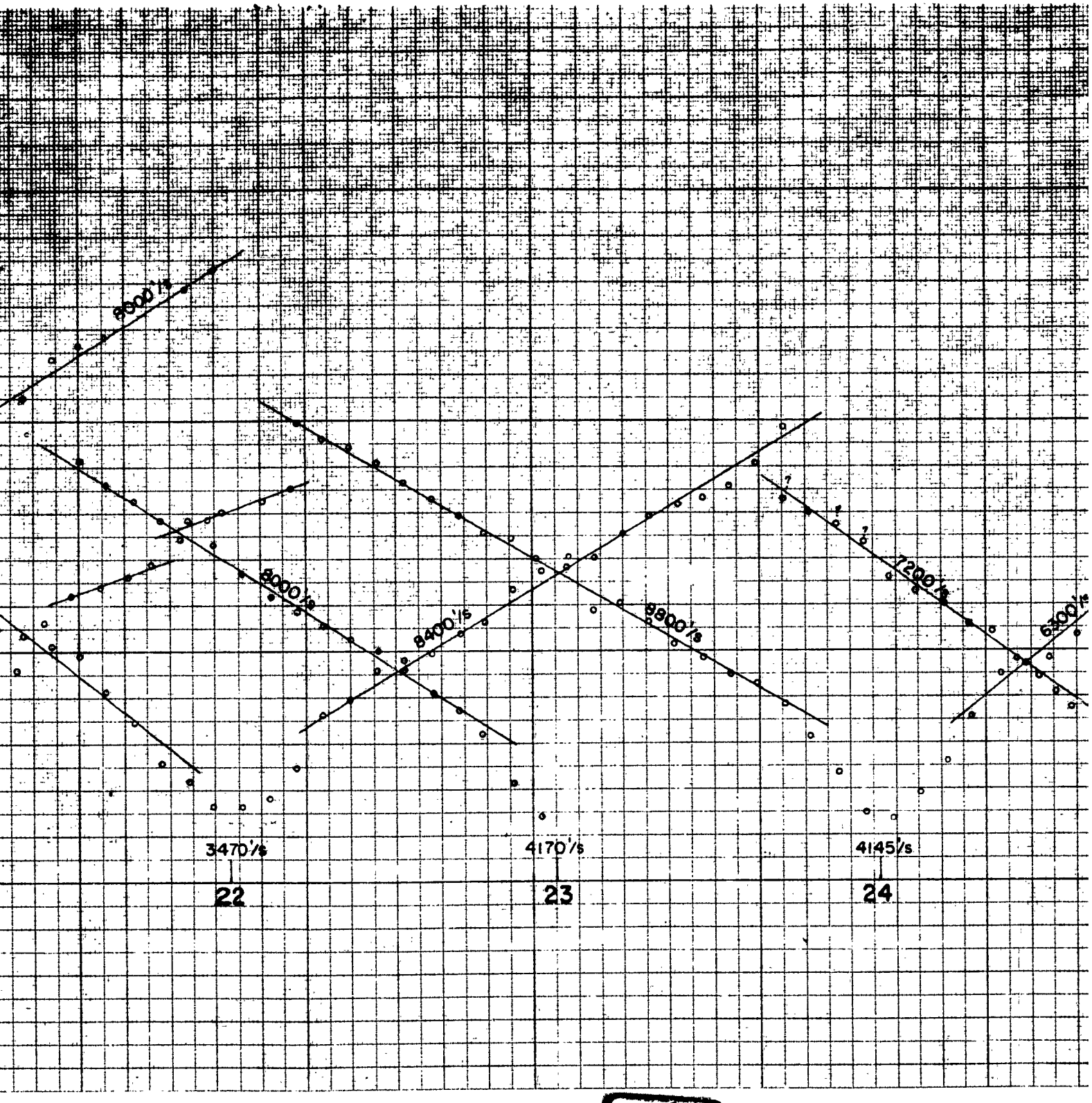
9600'/s
8000'/s
8400'/s
9900'/s
7200'/s
6300'/s
3470'/s
22
4170'/s
23
4145'/s
24

3

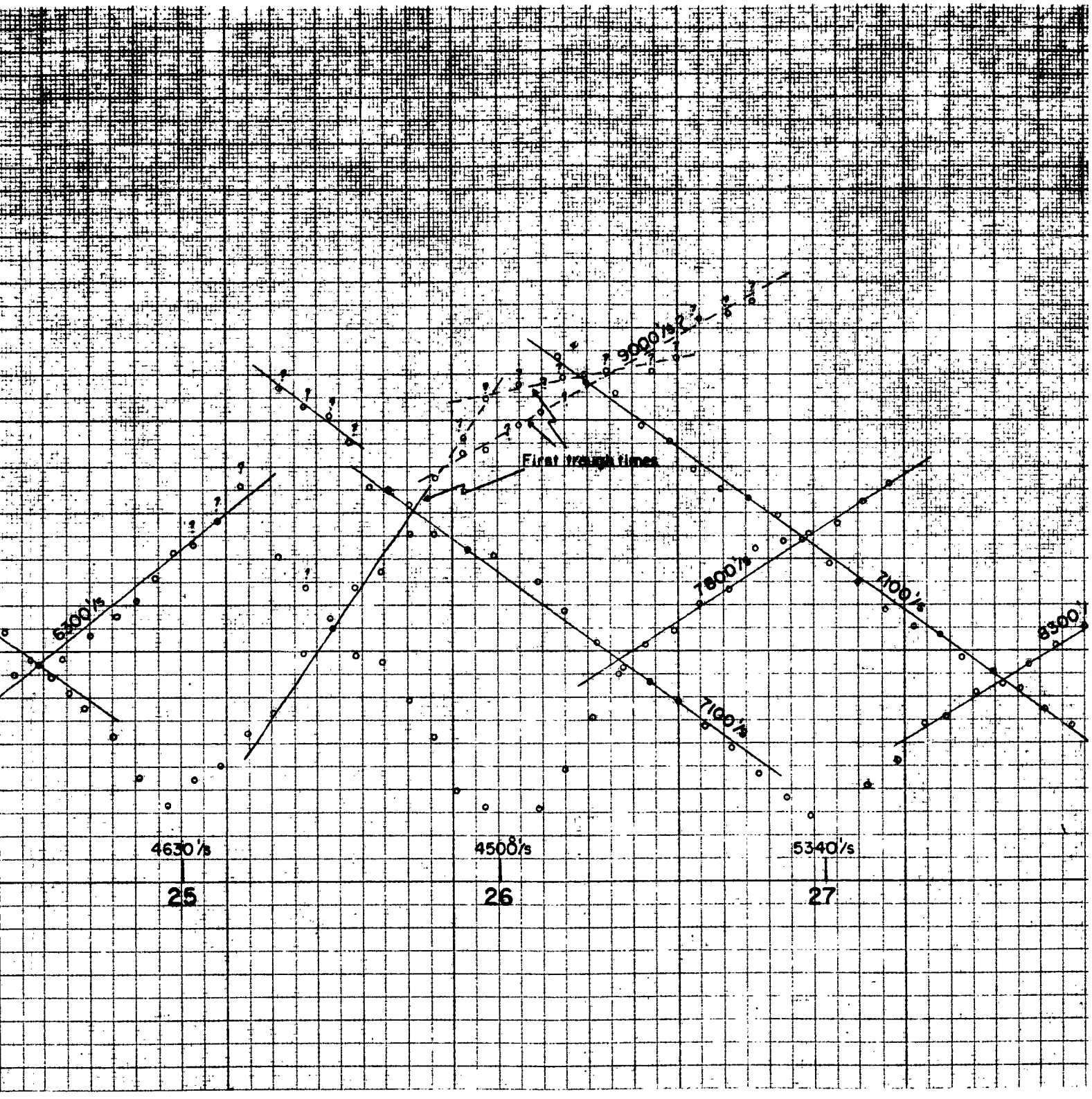
9000'/s
First trough times
6300'/s
7800'/s
7100'/s
7100'/s
8300'
4630'/s
4500'/s
5340'/s
25
26
27

4

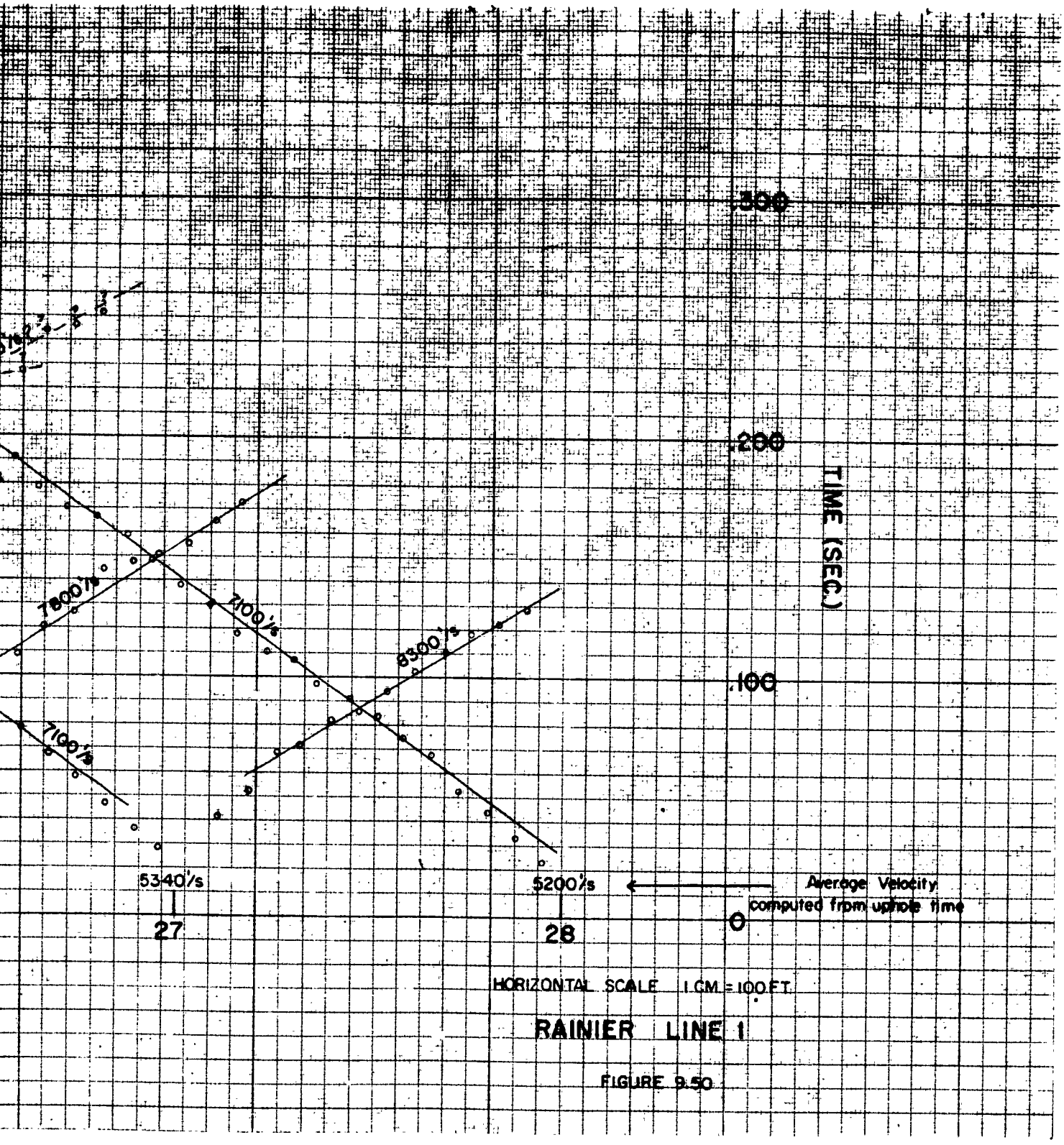

HORIZONTAL SCALE 1 CM = 100 FT.

RAINIER LINE 1

FIGURE 9.50

5

10.0 First Arrival Amplitudes

Also of interest in detecting the location of underground explosions are changes in the amplitude of first arrival energy attributable to alteration of the medium. Apart from the effect of the explosions on the mechanical and physical properties of the tuff, there is the effect on the structural geometry. It is probable that only the cumulative attenuation of amplitude due to fracturing of the tuff will be of sufficient magnitude to be recognizable at the distances at which the near surface velocity survey on top of RAINIER Mesa was conducted from the LOGAN, BLANCA and RAINIER events. Alteration of the physical properties and structural displacements are probably too small at these distances to produce an effect on the amplitudes of first arrival energy distinguishable from those deriving from other sources.

Changes in the amplitude of the recorded first arrival energy may be ascribed to changes in the source and source conditions, changes in the medium and the effects of geophone plant. To make a definitive evaluation of the attenuation of first arrival amplitudes with respect to the medium it is required that variations in amplitude deriving from changes in the charge size, shot depth and geophone plant be kept to a minimum, otherwise there is so much scatter in the data from record to record that reliance can be placed only on general trends.

Figures 10.1 and 10.2 show the variation in amplitude of the direct first arrival energy recorded at the near geophone location to the shot point and the variation in scaled depth of the deep shot of each profile recorded along NSVP Line 1. Comparison of the recorded amplitudes with the scaled depths of the shots indicates that there was substantial variation in the different parameters which affect amplitude from shot to shot in the same hole and from shot point to shot point along the line. Since no calibration shots were made, the variation in recorded amplitude deriving from changes in coupling and transmission impedance and geophone plant is unknown. However, it is evident that much of the variation derives from changes in the scaled depth of the shots. As a result, comparison of the peak recorded amplitudes of the direct and refraction arrivals

along the line and with proximity to the sites of the LOGAN, BLANCA and RAINIER events is unfeasible.

Excluding variations in the source, source conditions, and geophone plant, the amplitude of the recorded first arrival energy is markedly affected by the geometry of the refracting surface and the purely mechanical properties of the rocks. Before any information on the medium can be obtained from amplitude variations, they must first be corrected for the geometrical attenuation due to the spreading out of the wave front. For the refracted arrivals dealt with here, the amplitude of the refracted wave should vary approximately as $d^{-1/2} L^{-3/2}$ where $\underline{d}$ is the orthogonal projection on the interface of the distance between the source and detector, and L is the distance the wave traveled in the lower medium. However, since there is a velocity inversion at depth, and the depth and configuration of the refractors is indeterminate, there was no way of evaluating the geometrical spreading correction to be applied. As a consequence, it was necessary to confine the analysis to evaluating the gross attenuation of the amplitude of the refraction arrivals from profile to profile. If the thicknesses of the refractors differ, as indicated by the uphole surveys, there should be an accompanying difference in the rates at which the amplitude of the first arrival energy attenuates with distance in each of the refractors. The weakness in this method of approach is that no allowance is made for random lateral changes in the thicknesses, velocities and depths of the refractors and the accompanying variation in the geometrical spreading correction. Thus, the apparent rates of attenuation may differ in a random manner.

The amplitudes of the first refraction arrivals recorded on the near surface velocity profiles (see Figures 9.5 to 9.44) along Lines 1 and 2 were converted from decibels to an estimated millimeter scale using an assumed amplification factor of 10^{-4} and the equation

$$db = 20 \log \frac{A2}{A1}$$

where A_1 = 10 millimeters is zero decibel reference and A_2 = observed amplitude in millimeters. The resulting values of

amplitude are shown plotted on log-log paper (see Figures 10.3 to 10.30) together with the curves fitted by least squares procedure to an equation of the form

$$A = k/d^m$$

where A = amplitude
d = distance between source and detector
k,m = constants.

This formula was used because it appears unlikely that the first arrival energy penetrated below the welded Tos_8 tuff or a depth of something less than 275 feet in which case the geometrical spreading correction $d^{-1/2} L^{-3/2}$ should approach d^{-2} for the velocities and range of horizontal distances involved.

Had it been possible to determine the depths of the refractors indicated by the time-distance graphs and correct for geometrical spreading one should be able to observe the same discontinuities in the amplitude-distance graphs as are apparent in the time-distance graphs. Since this was not possible, the equation $A = k/d^m$ was fitted to the apparent visual alignments of the log-log plots of the amplitude data. Since there is considerable scatter in the plotted amplitudes, alternate choices of alignment may be made. Without additional information there is no way of making a definitive evaluation of which alignment denotes the correct apparent rate of attenuation.

Comparison of the rates of attenuation of amplitude with distance (see Figures 10.3 to 10.30) on the profiles along NSVP Lines 1 and 3 discloses no recognizable pattern of variation. The rates of attenuation of late refraction arrivals having low velocities are comparable with the rates of attenuation of late refraction arrivals having the highest observed velocities. In addition, very few of the reversed profiles exhibit comparable rates of attenuation. Since the rates of attenuation of the late refraction arrivals range from a low of $R^{-2.76}$ to a high of something in excess of $R^{-6.0}$, there is also appreciable scatter. It is evident that there is sufficient variation in the structural geometry and lithology, that an interpretation cannot be made without delineation of the depth of the refractors and a correction for geometrical spreading.

K&E 10 X 10 TO THE INCH 359-5
KEUFFEL & ESSER CO. MADE IN U.S.A.

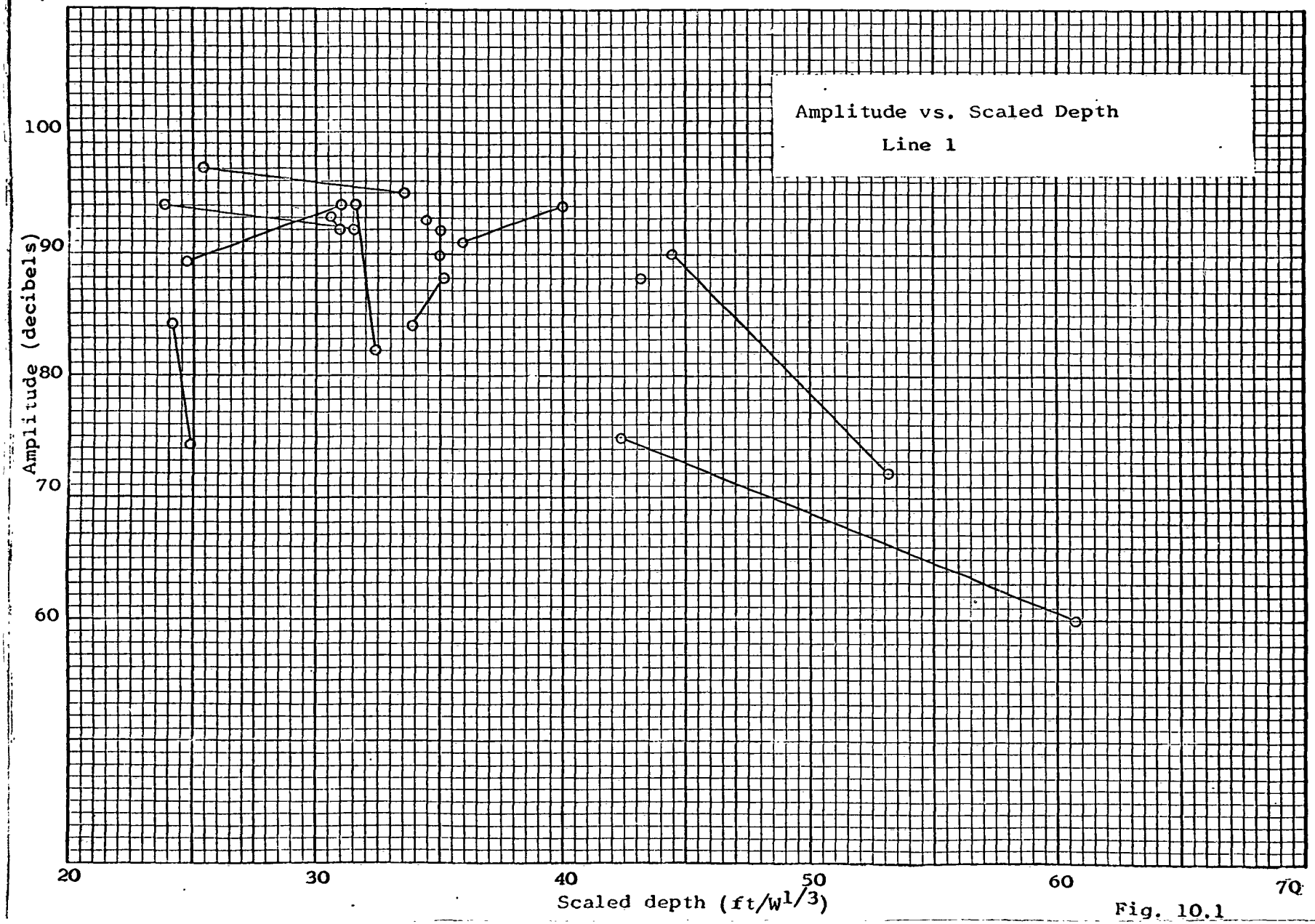

Fig. 10.1

K&E 10 X 10 TO THE CM. 359-14
KEUFFEL & ESSER CO. MADE IN U.S.A.

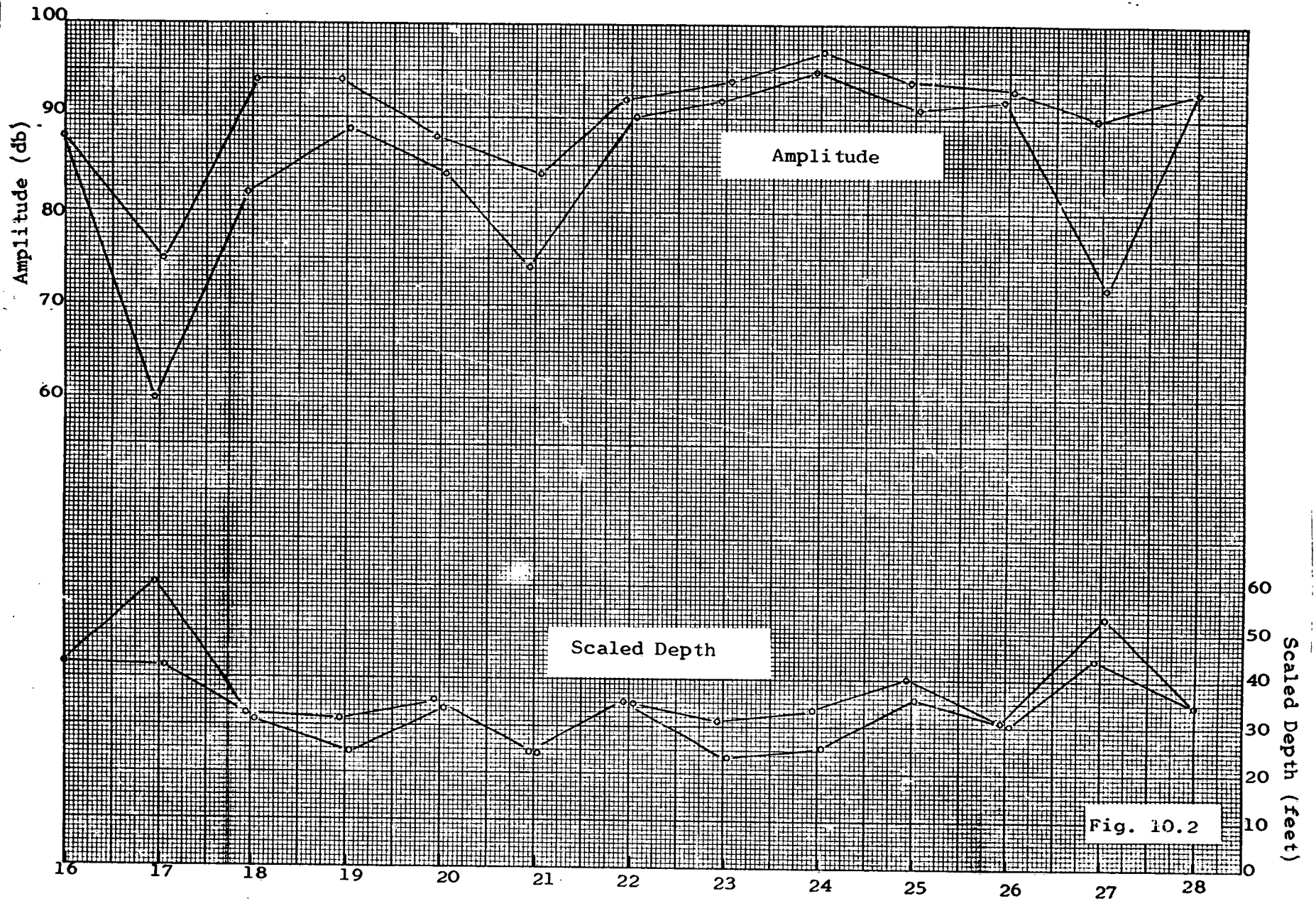

Fig. 10.2

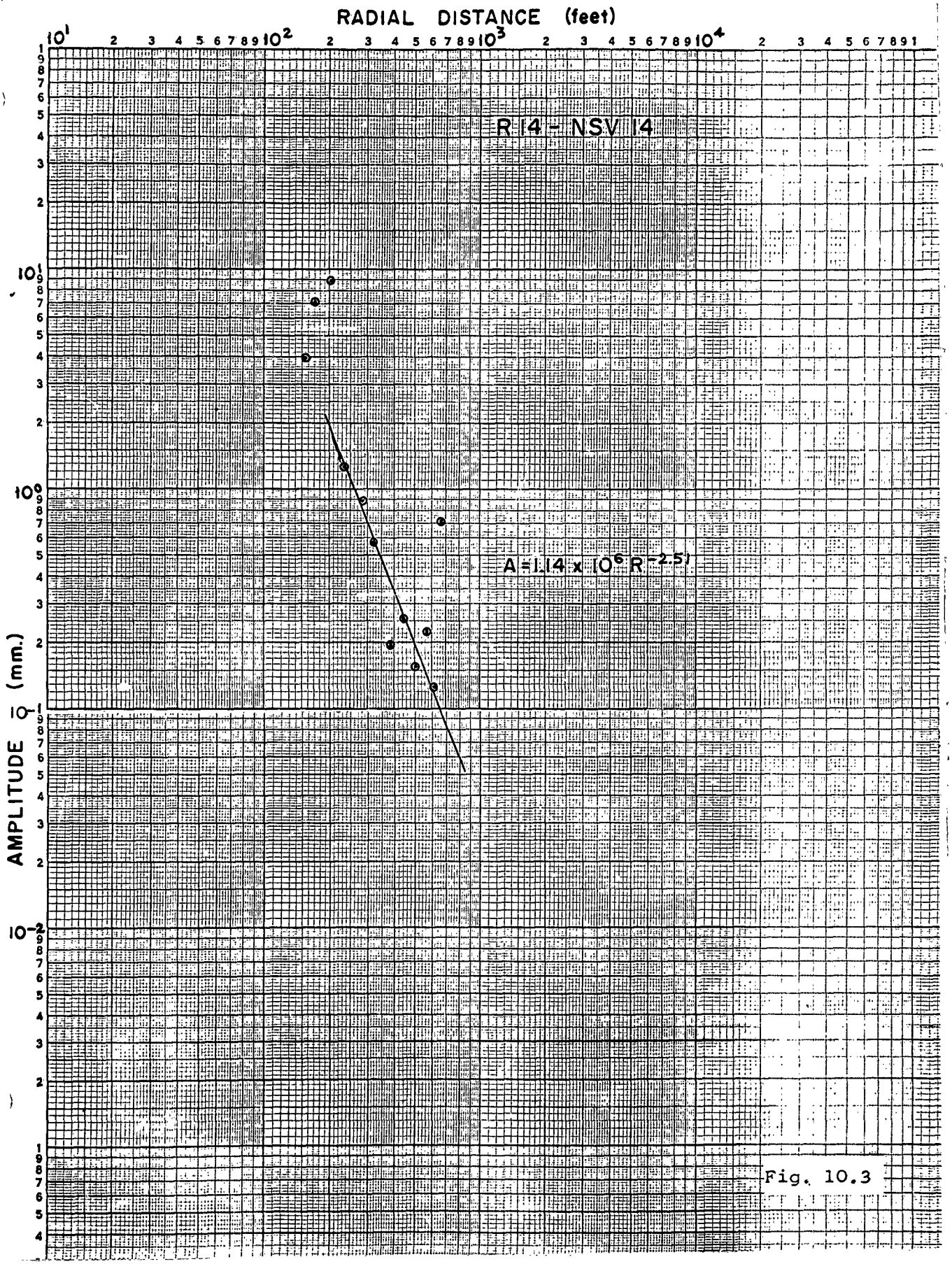

Fig. 10.3

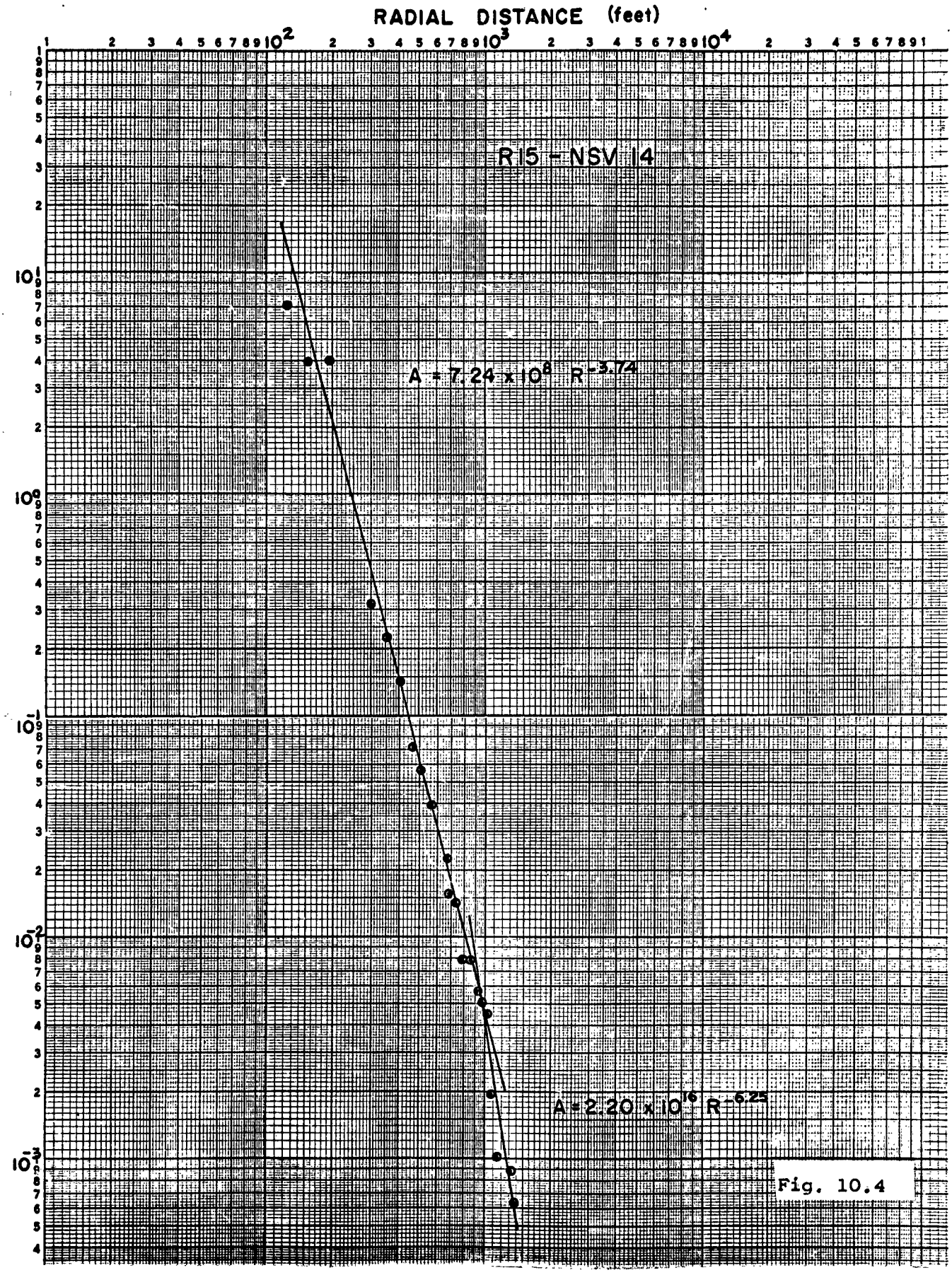
RADIAL DISTANCE (feet)
R15 - NSV 14
A = 7.24 x 10^8 R^-3.74
A = 2.20 x 10^16 R^-6.25

Fig. 10.4

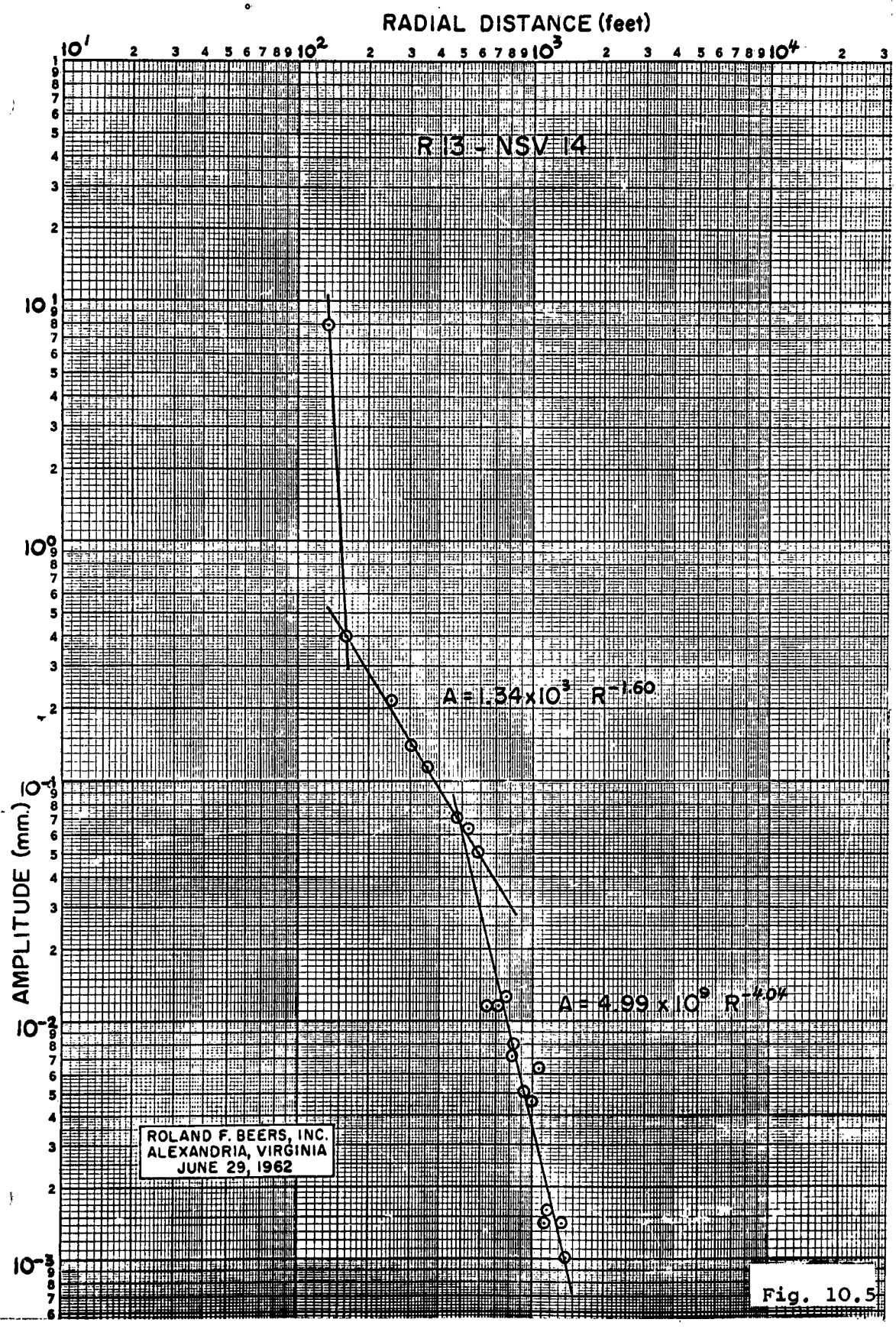
RADIAL DISTANCE (feet)
R 13 - NSV 14
A = 1.34 x 10^3 R^-1.60
A = 4.99 x 10^9 R^-4.04
AMPLITUDE (mm.)
ROLAND F. BEERS, INC.
ALEXANDRIA, VIRGINIA
JUNE 29, 1962

Fig. 10.5

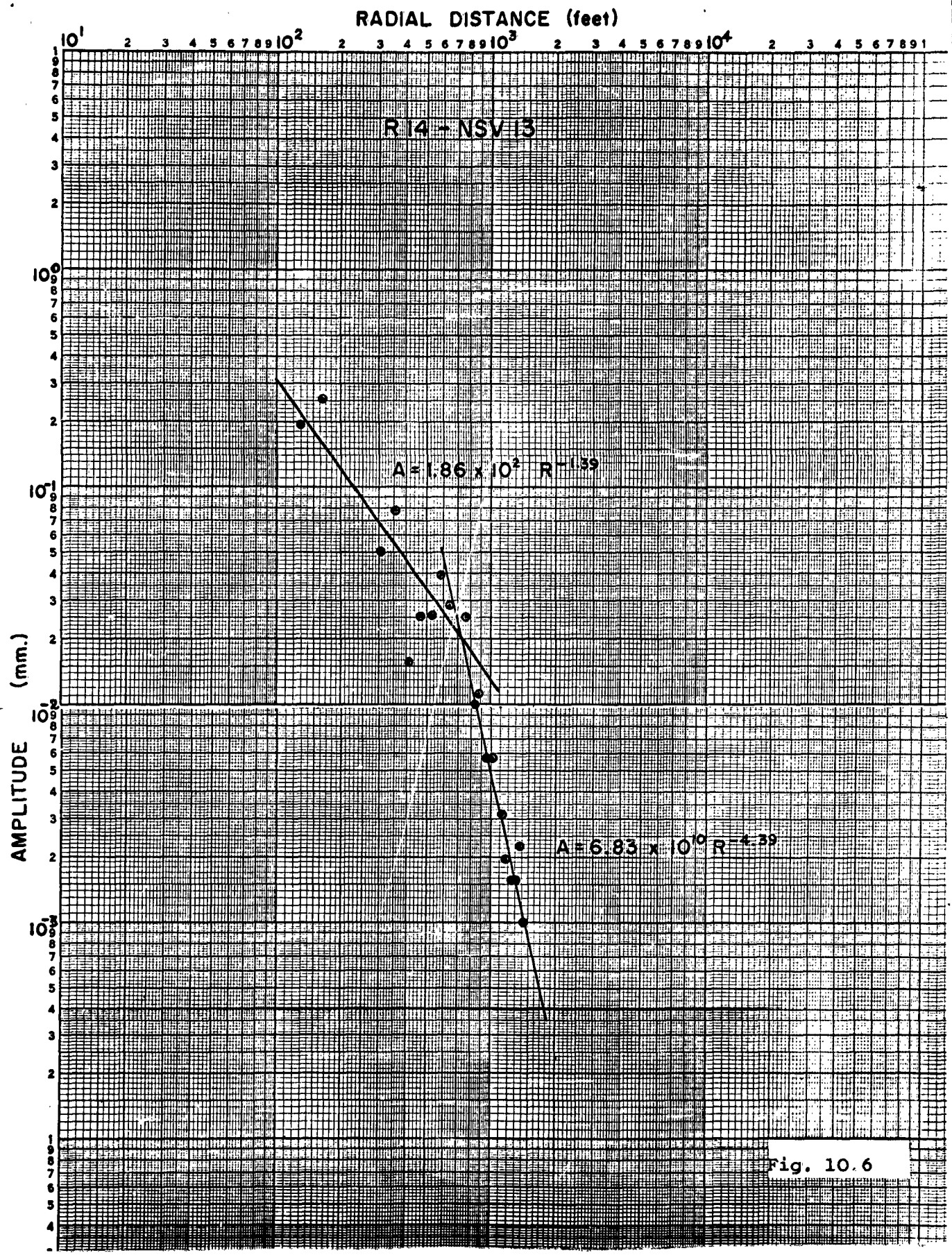
RADIAL DISTANCE (feet)
R 14 - NSV 13
A = 1.86 x 10² R^-1.39
A = 6.83 x 10¹⁰ R^-4.39
AMPLITUDE (mm.)

Fig. 10.6

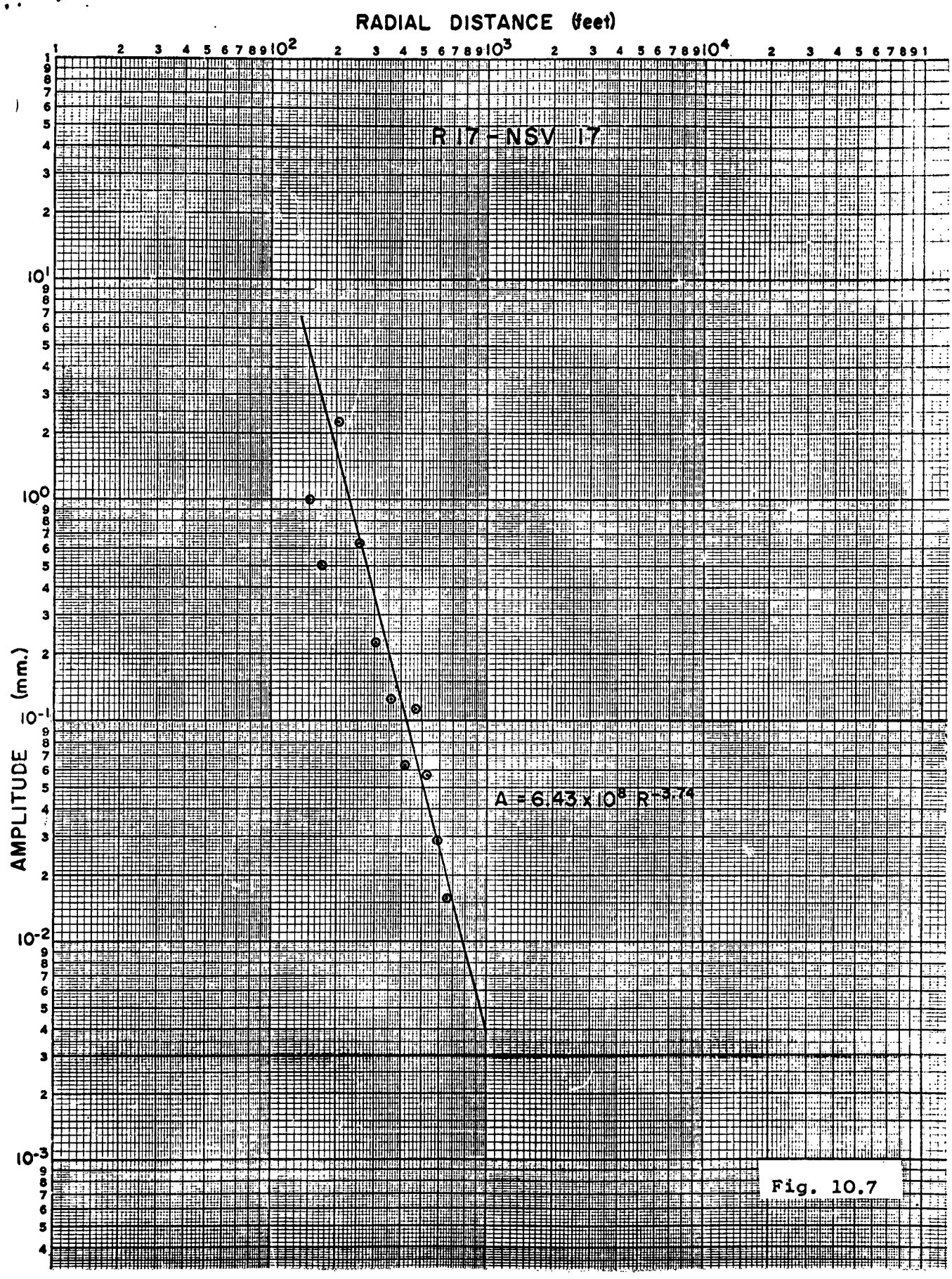

Fig. 10.7

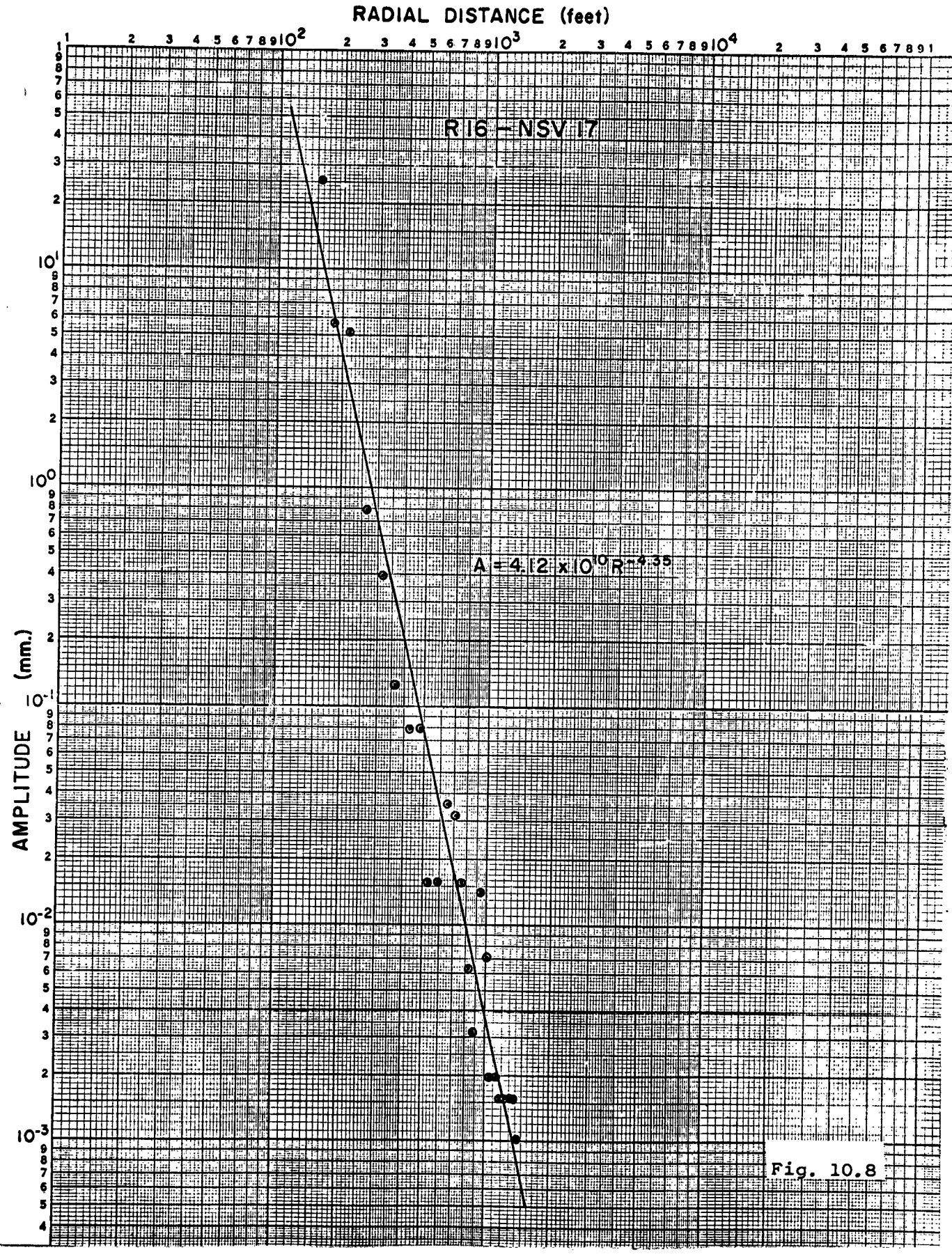
RADIAL DISTANCE (feet)
R16 - NSV 17
A = 4.12 x 10^10 R^-4.35
AMPLITUDE (mm.)

Fig. 10.8

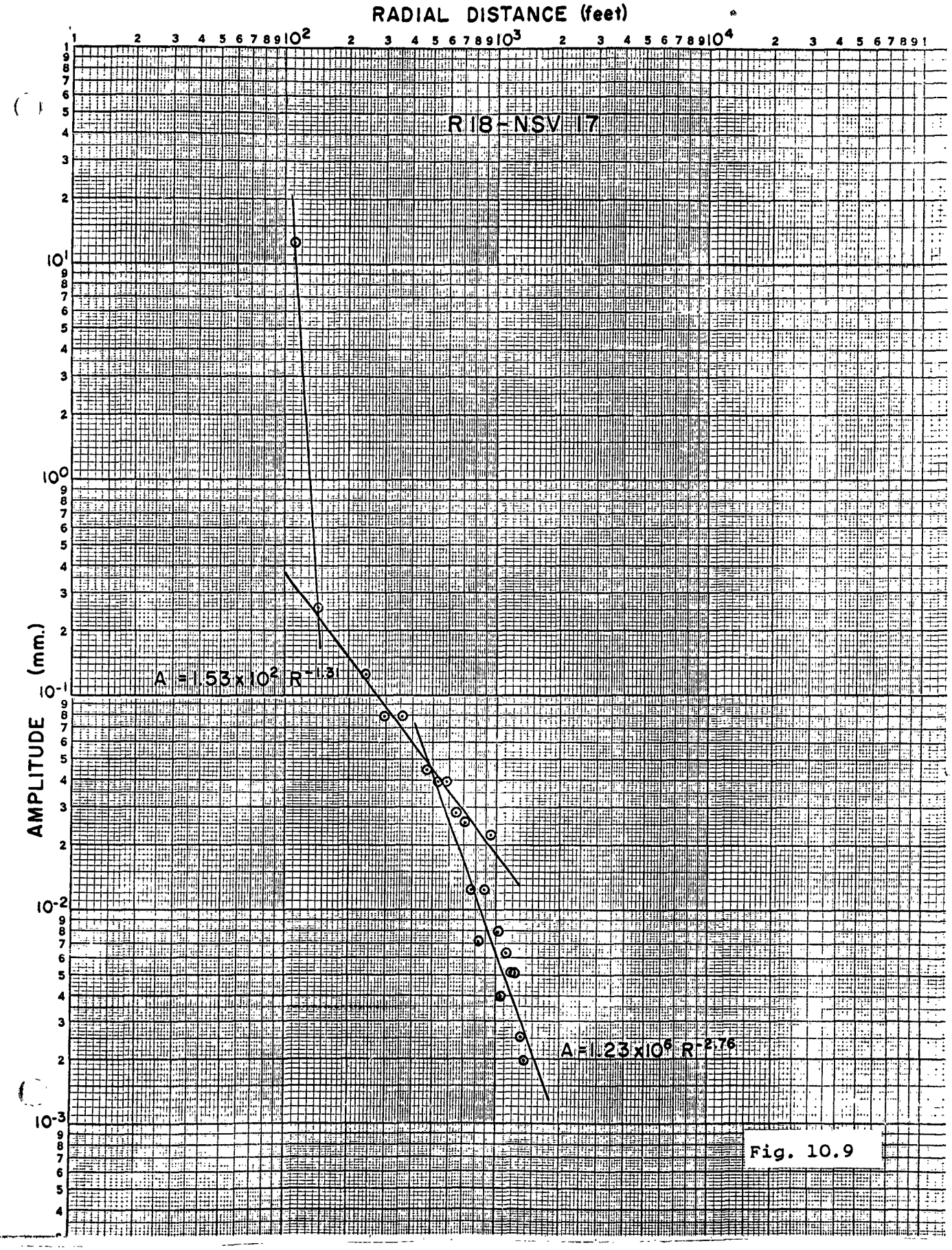
RADIAL DISTANCE (feet)
R18-NSV 17
AMPLITUDE (mm.)
A = 1.53 x 10² R^-1.31
A = 1.23 x 10⁶ R^-2.76

Fig. 10.9

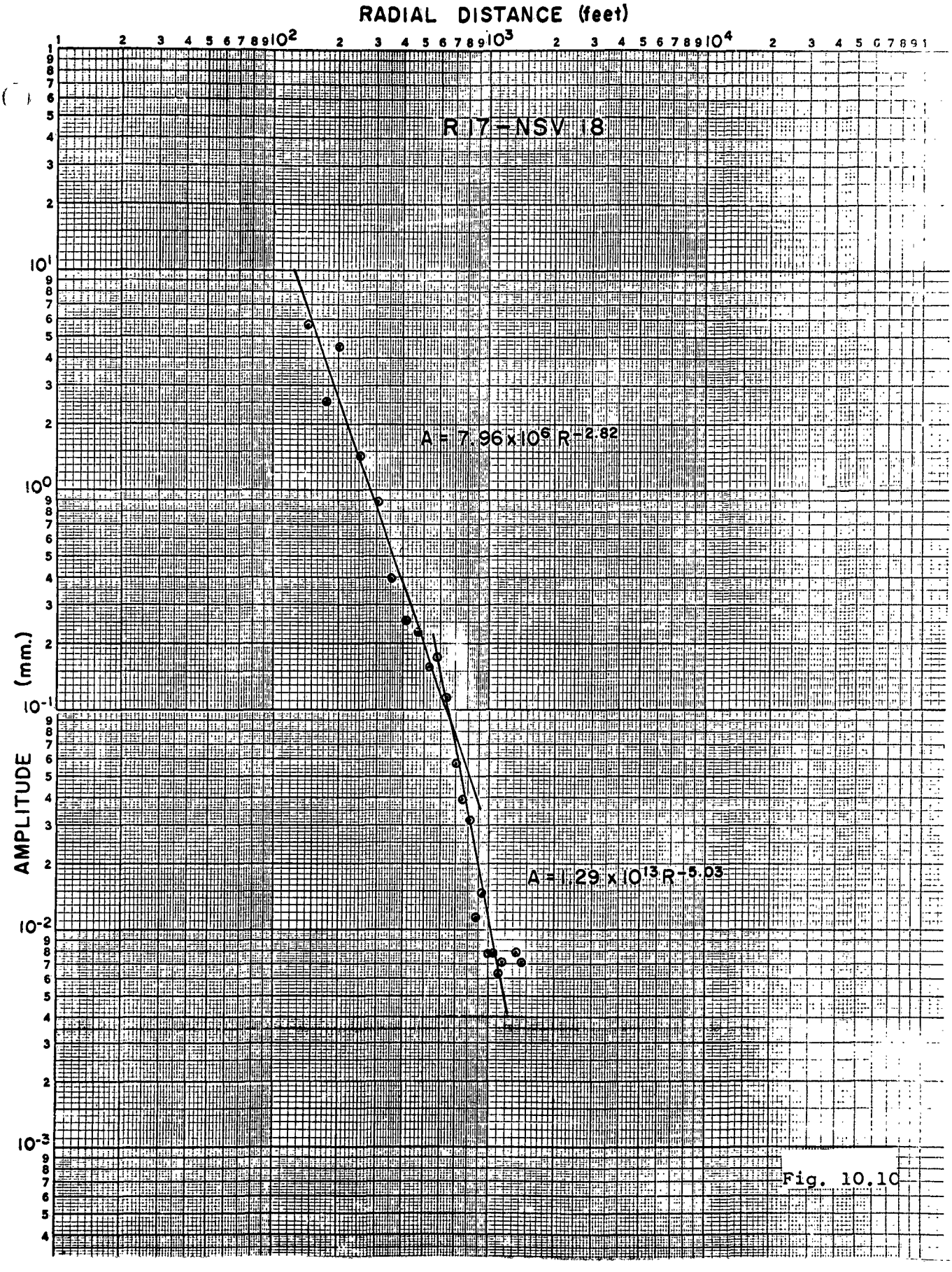
RADIAL DISTANCE (feet)
R17-NSV 18
A = 7.96 x 10^6 R^-2.82
A = 1.29 x 10^13 R^-5.03
AMPLITUDE (mm.)

Fig. 10.1C

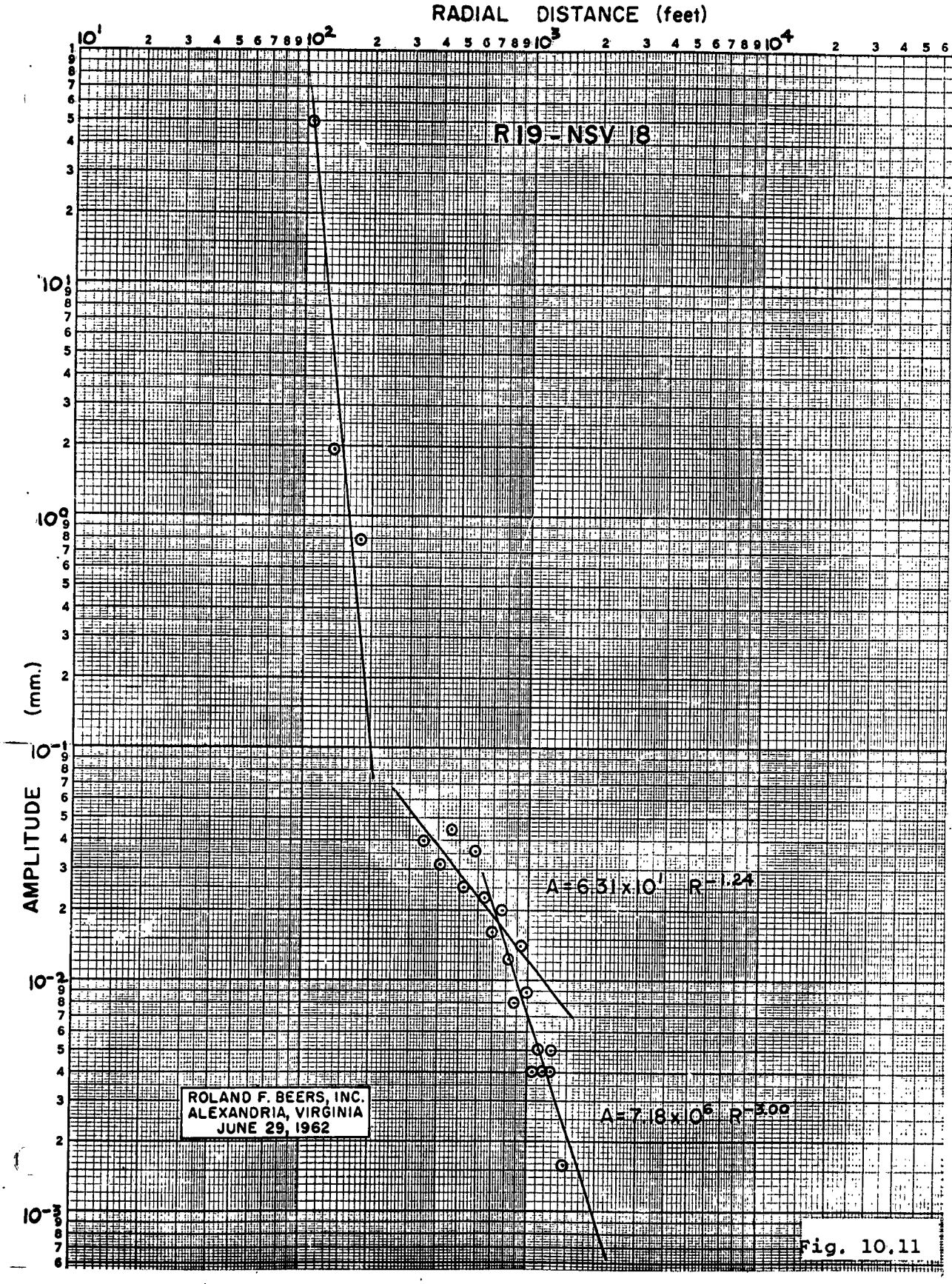
RADIAL DISTANCE (feet)
R19-NSV 18
AMPLITUDE (mm.)
A=6.31x10^1 R^-1.24
A=7.18x10^6 R^-3.00
ROLAND F. BEERS, INC.
ALEXANDRIA, VIRGINIA
JUNE 29, 1962

Fig. 10.11

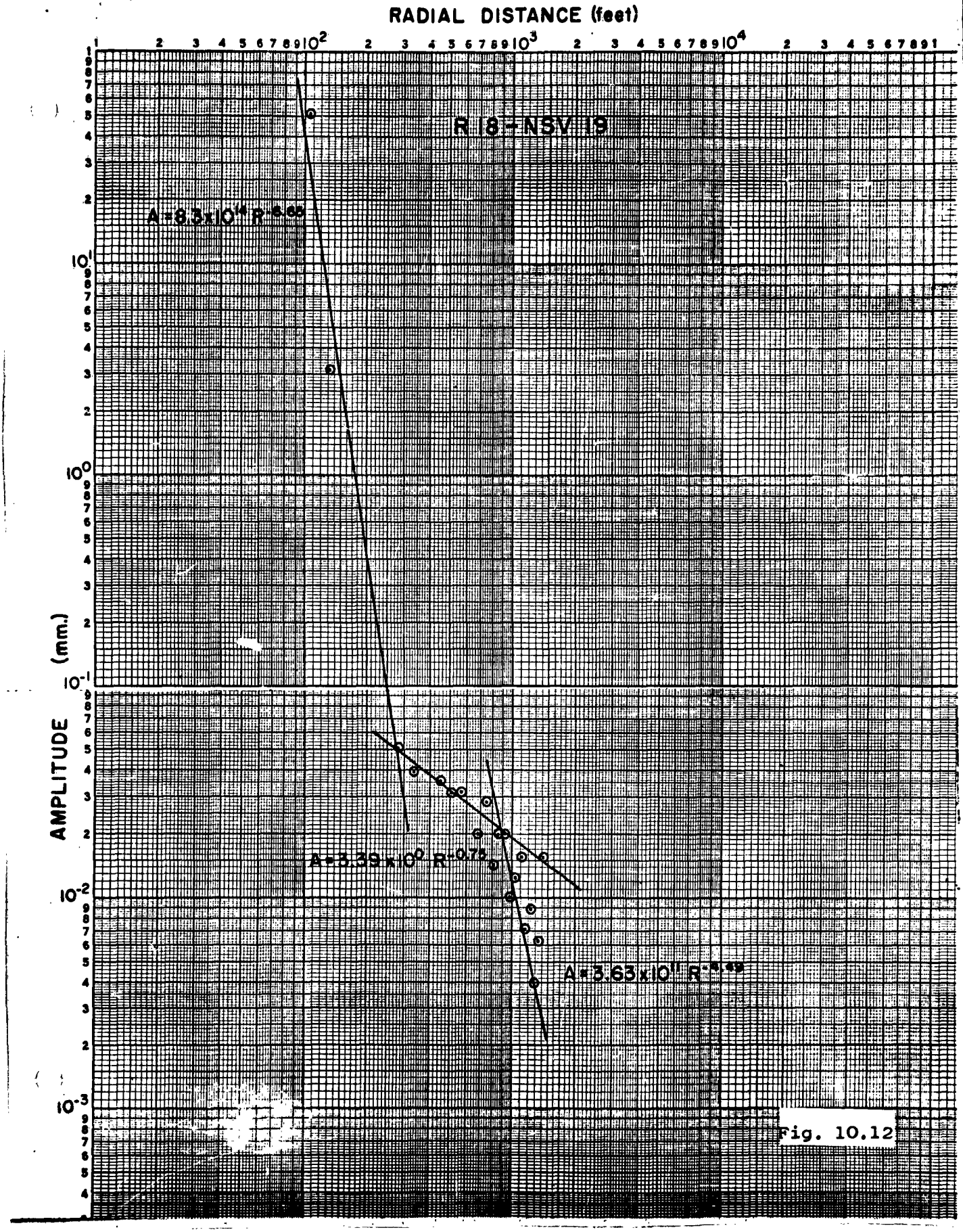
RADIAL DISTANCE (feet)
R 18-NSV 19
A=8.3x10^14 R^-6.69
A=3.39x10^0 R^-0.75
A=3.63x10^11 R^-5.49
AMPLITUDE (mm.)

Fig. 10.12

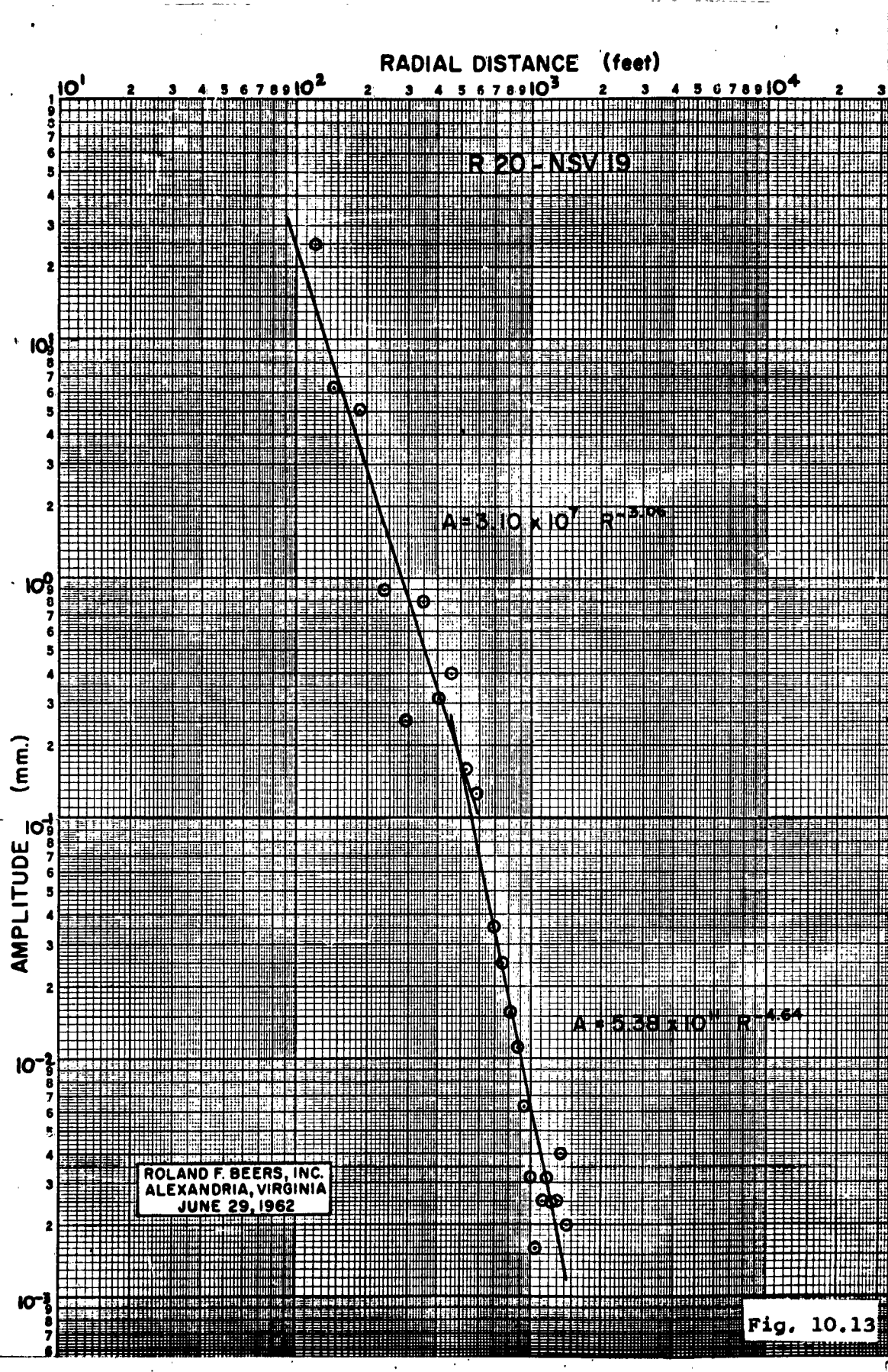
RADIAL DISTANCE (feet)
R 20 - NSV 19
A = 3.10 x 10^7 R^-3.06
A = 5.38 x 10^11 R^-4.64
AMPLITUDE (mm.)
ROLAND F. BEERS, INC.
ALEXANDRIA, VIRGINIA
JUNE 29, 1962

Fig. 10.13

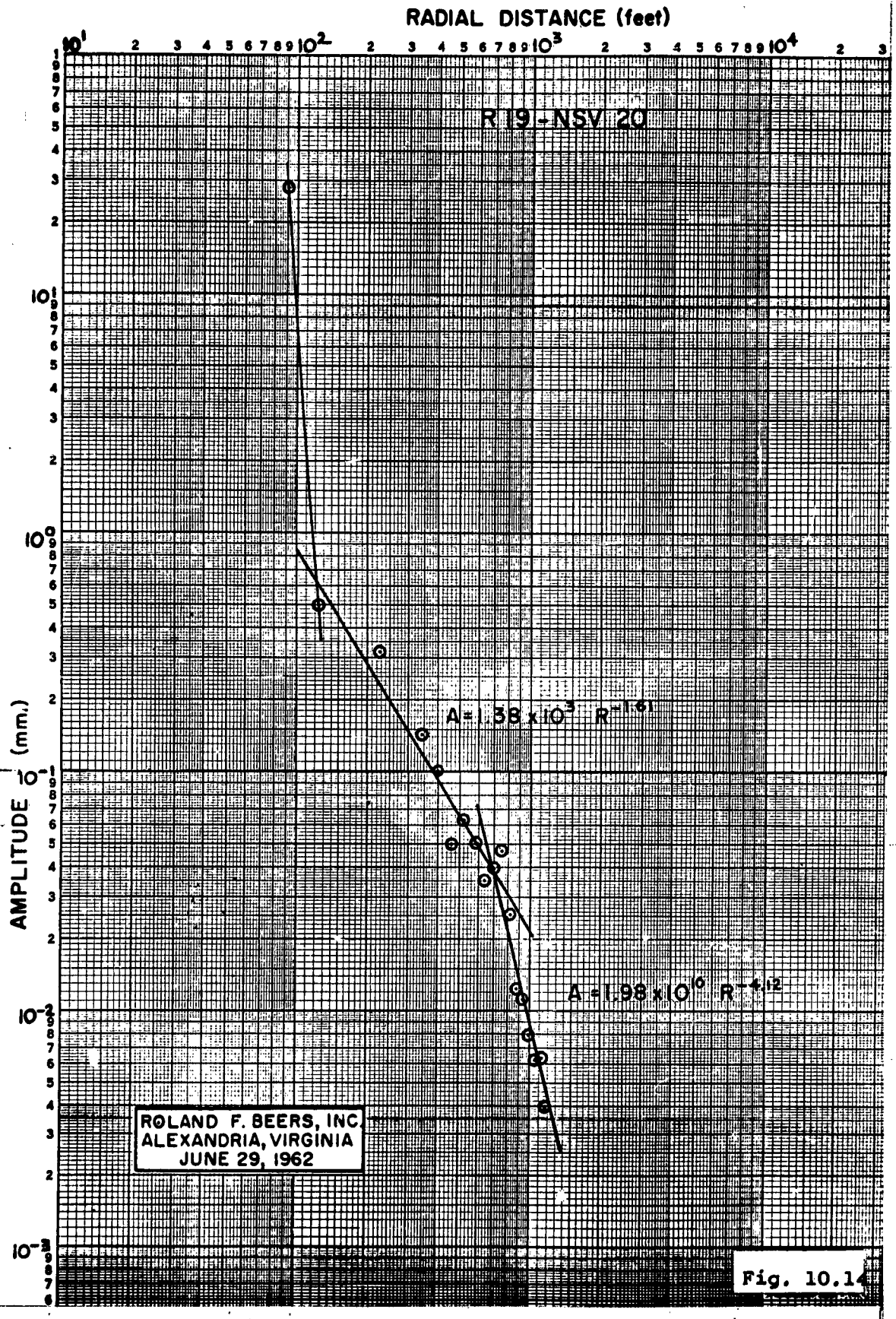
RADIAL DISTANCE (feet)
R 19 - NSV 20
AMPLITUDE (mm.)
A = 1.38 x 10^3 R^-1.61
A = 1.98 x 10^6 R^-4.12
ROLAND F. BEERS, INC.
ALEXANDRIA, VIRGINIA
JUNE 29, 1962

Fig. 10.14

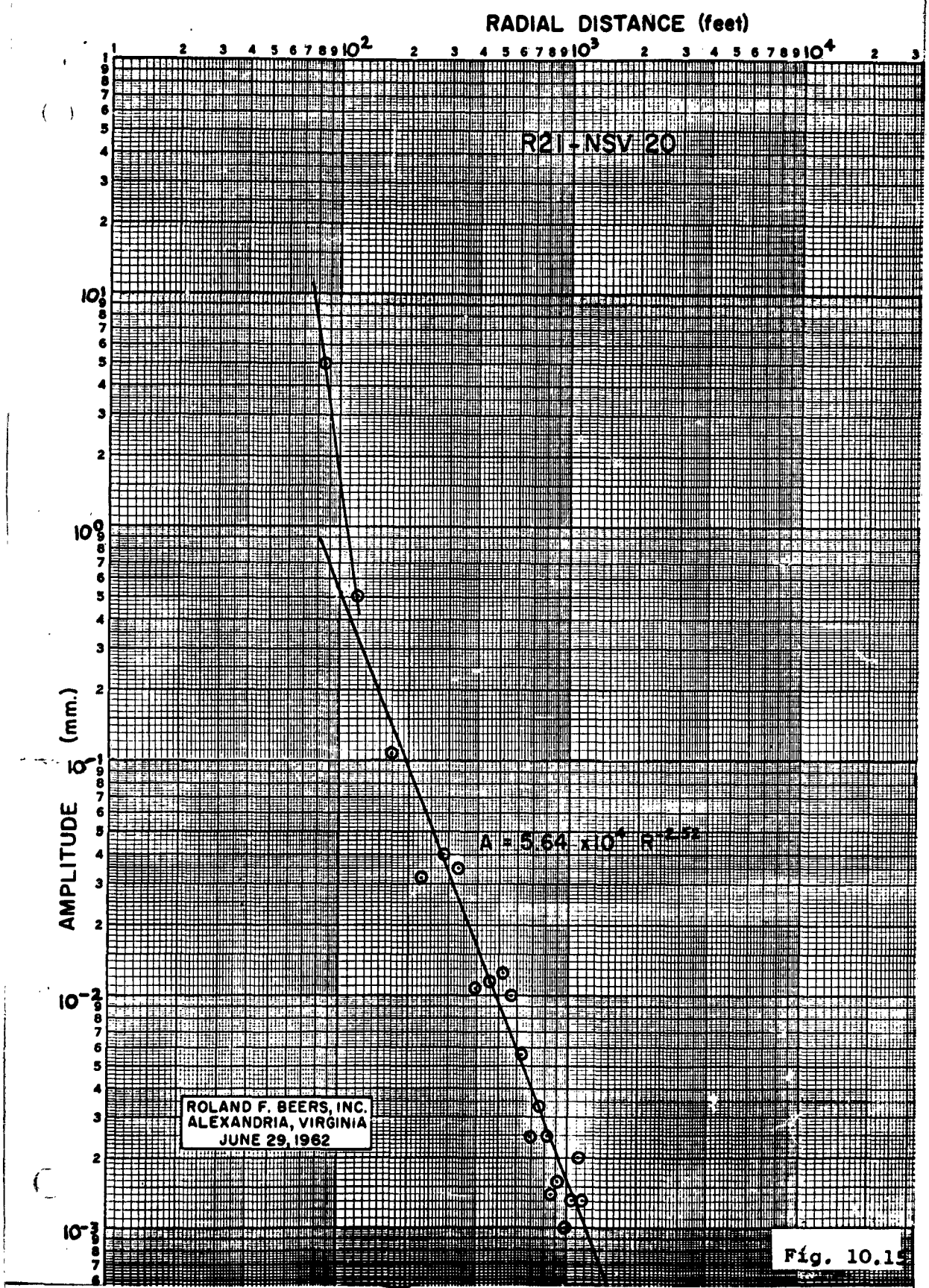
RADIAL DISTANCE (feet)
R21-NSV 20
AMPLITUDE (mm.)
A = 5.64 x10⁴ R^-2.52
ROLAND F. BEERS, INC.
ALEXANDRIA, VIRGINIA
JUNE 29, 1962

Fig. 10.15

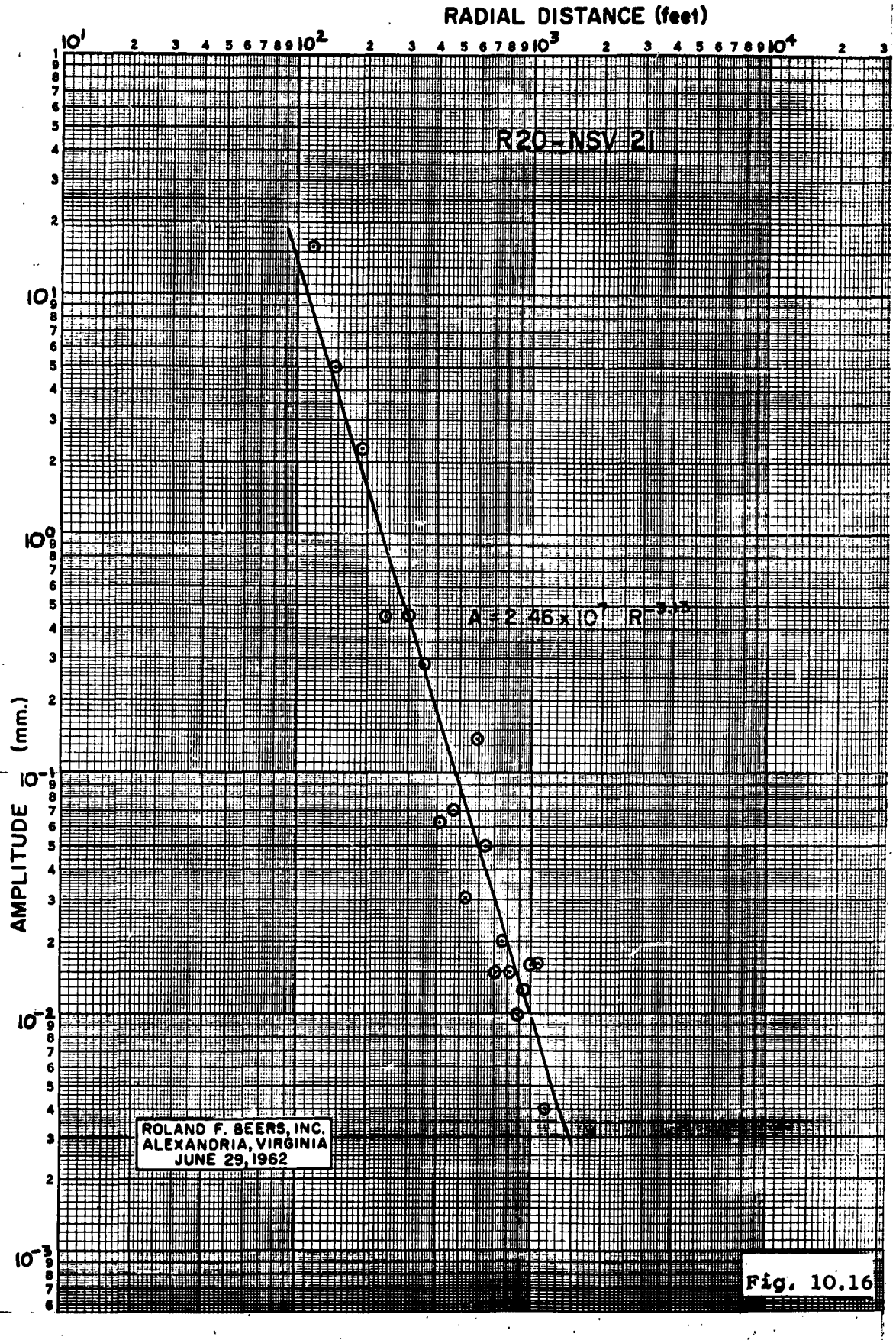
RADIAL DISTANCE (feet)
R20-NSV 21
A = 2.46 x 10^7 R^-3.33
AMPLITUDE (mm.)
ROLAND F. BEERS, INC.
ALEXANDRIA, VIRGINIA
JUNE 29, 1962

Fig. 10.16

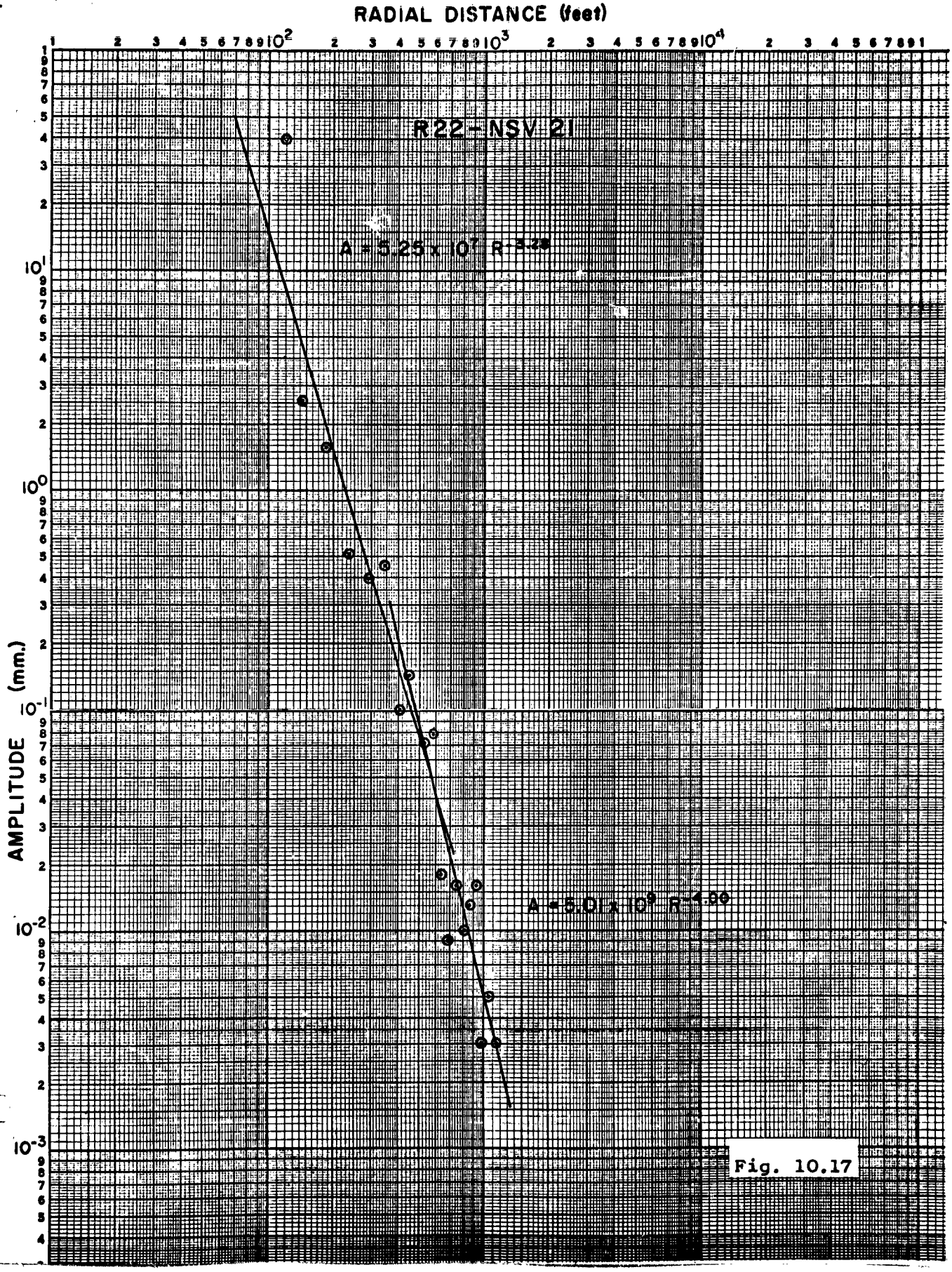
RADIAL DISTANCE (feet)
R22-NSV 21
A = 5.25 x 10^7 R^-3.25
A = 5.01 x 10^9 R^-4.00
AMPLITUDE (mm.)

Fig. 10.17

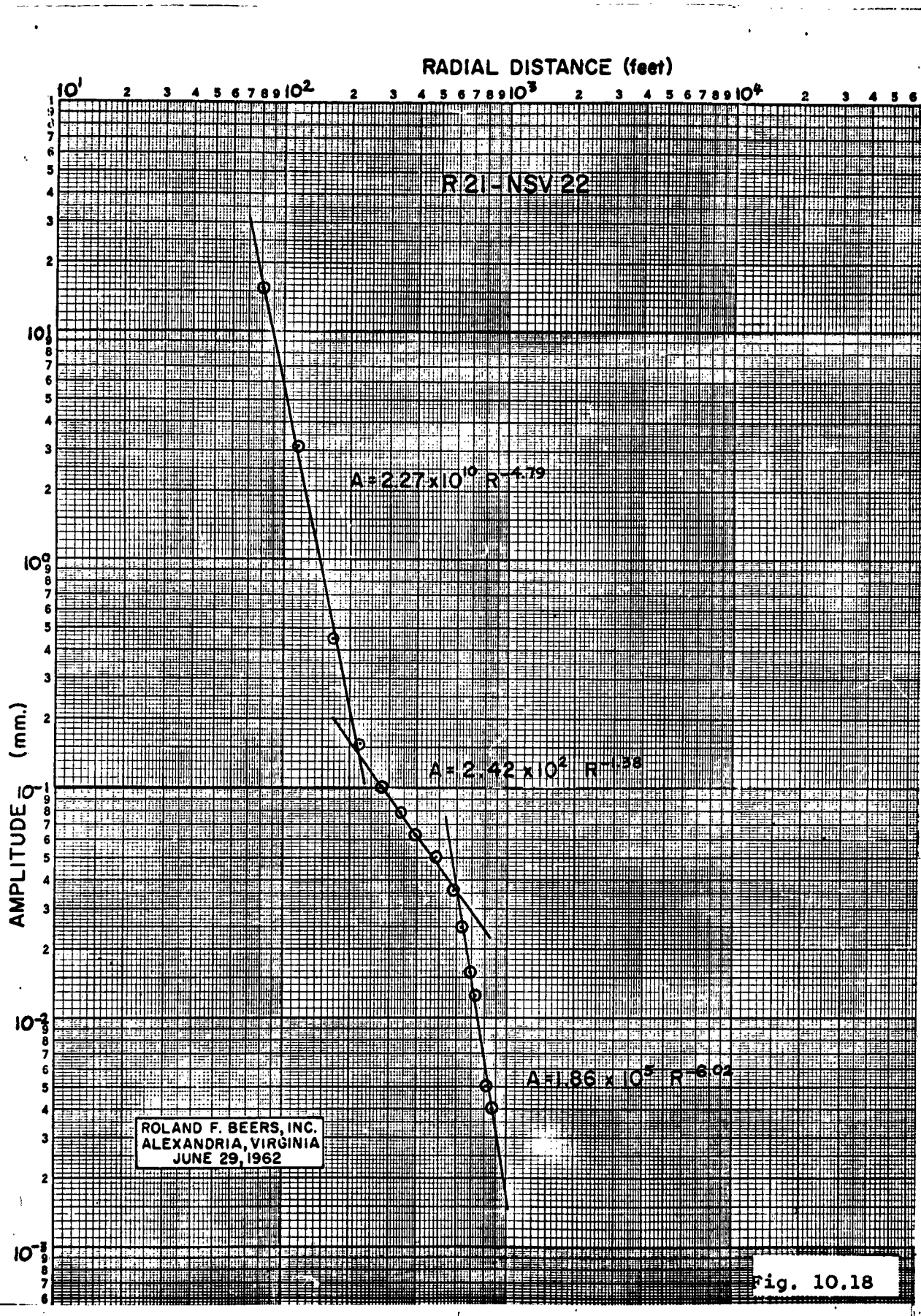
RADIAL DISTANCE (feet)
R 21 - NSV 22
A = 2.27 x 10^0 R^-4.79
A = 2.42 x 10^2 R^-1.38
A = 1.86 x 10^5 R^-6.02
AMPLITUDE (mm.)
ROLAND F. BEERS, INC.
ALEXANDRIA, VIRGINIA
JUNE 29, 1962

Fig. 10.18

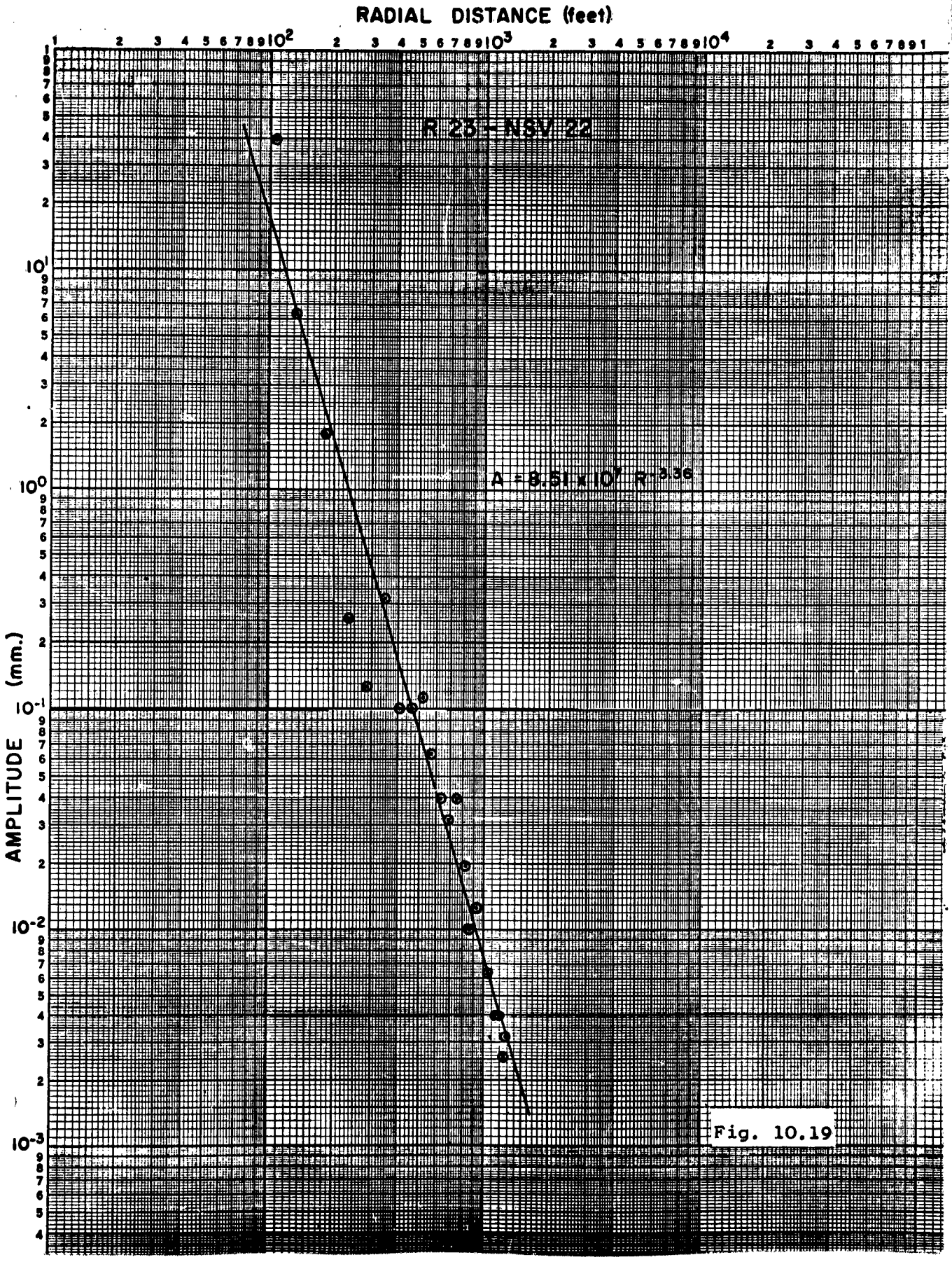

Fig. 10.19

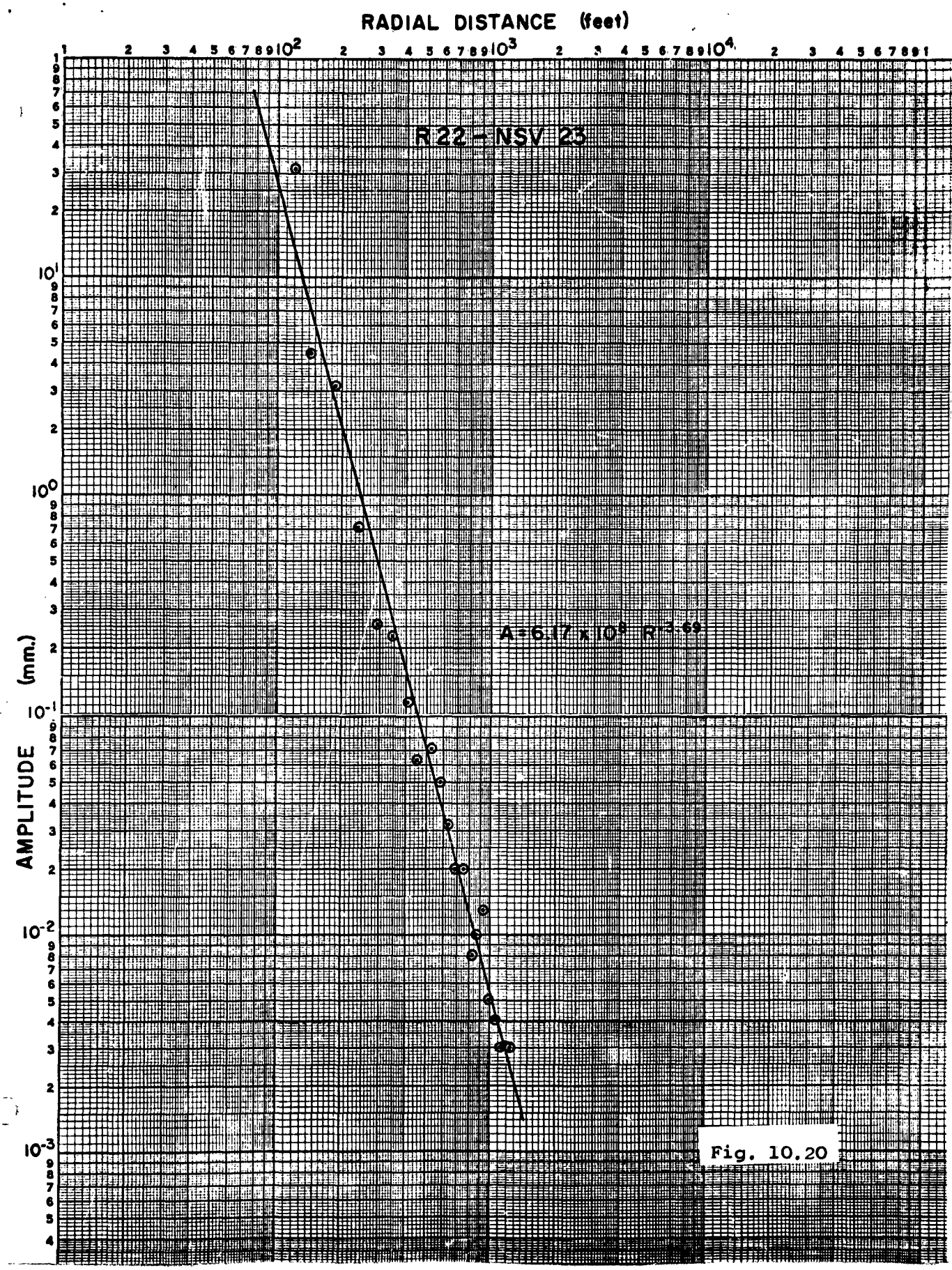

Fig. 10.20

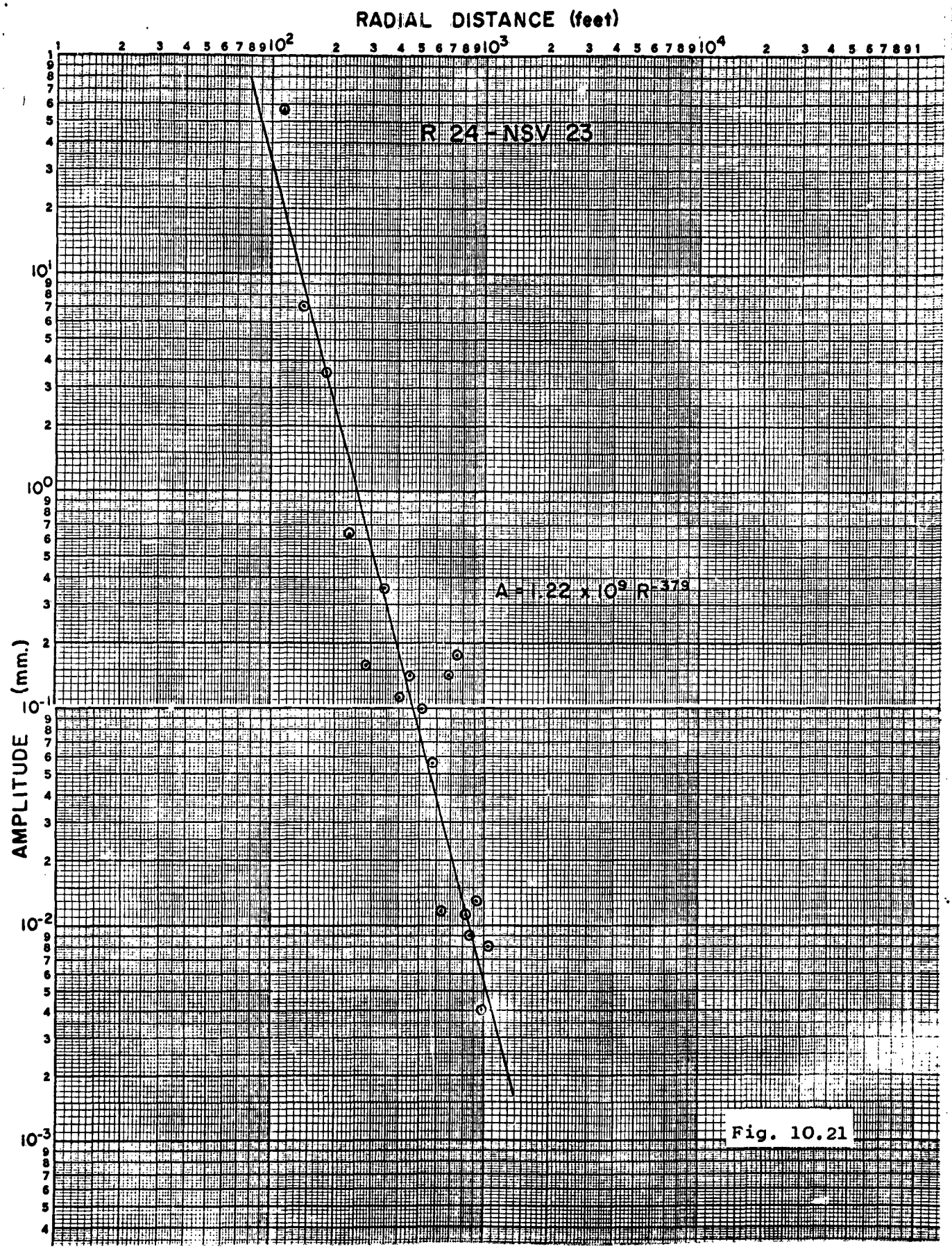

Fig. 10.21

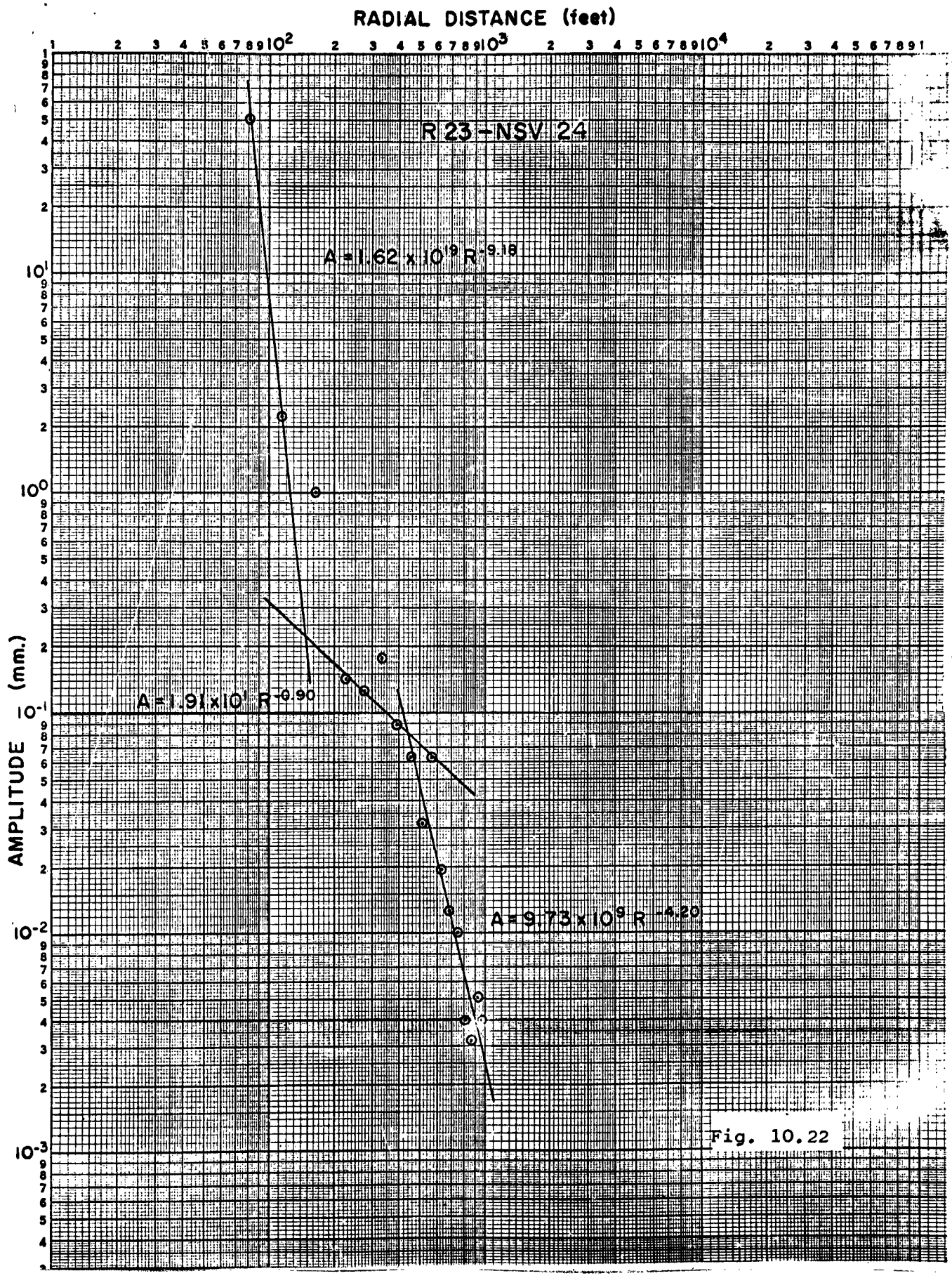
RADIAL DISTANCE (feet)
R 23 - NSV 24
A = 1.62 x 10^19 R^-9.18
A = 1.91 x 10^1 R^-0.90
A = 9.73 x 10^9 R^-4.20
AMPLITUDE (mm.)

Fig. 10.22

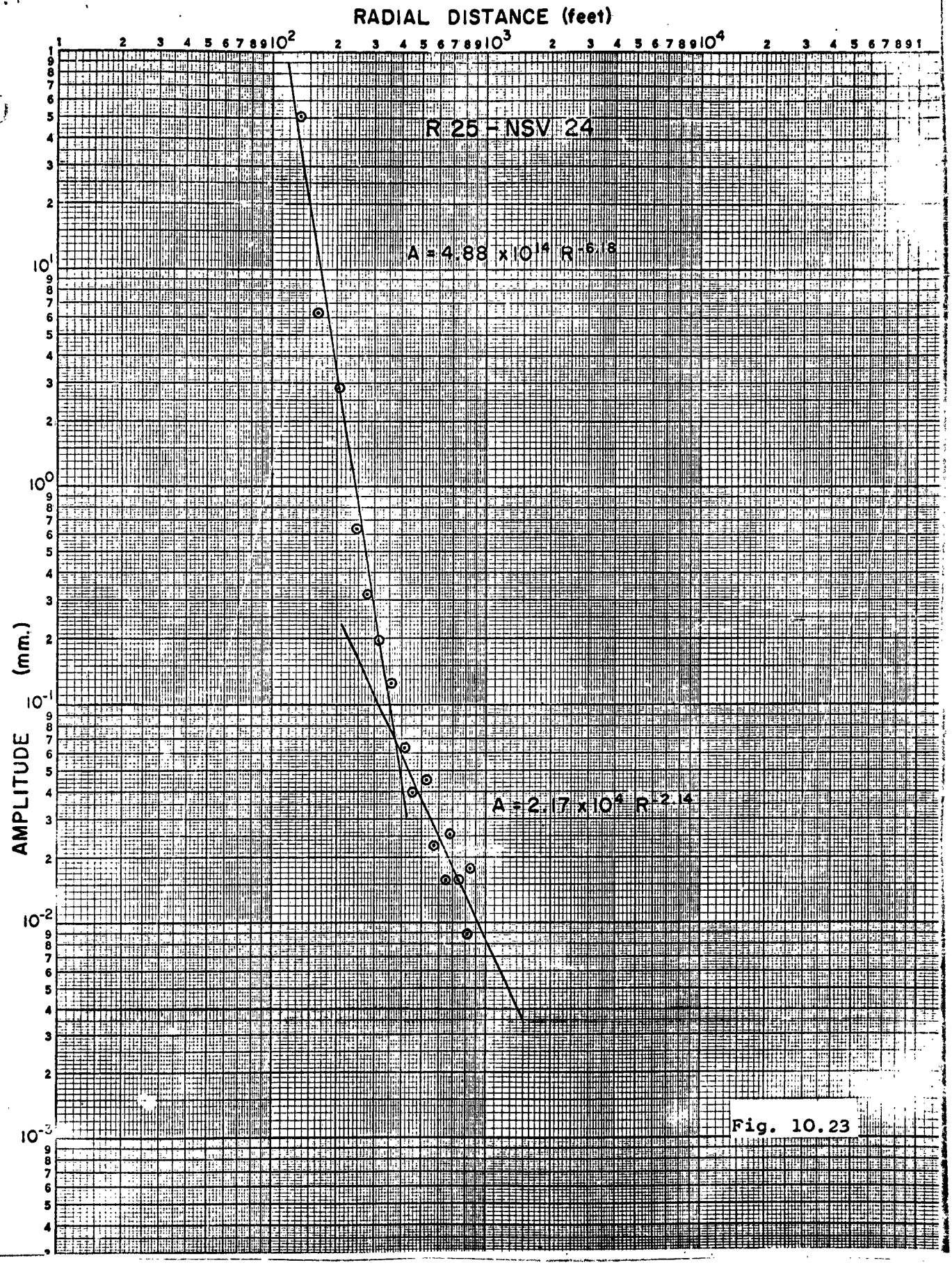
RADIAL DISTANCE (feet)
R 25 - NSV 24
A = 4.88 x 10^14 R^-6.18
A = 2.17 x 10^4 R^-2.14
AMPLITUDE (mm.)

Fig. 10.23

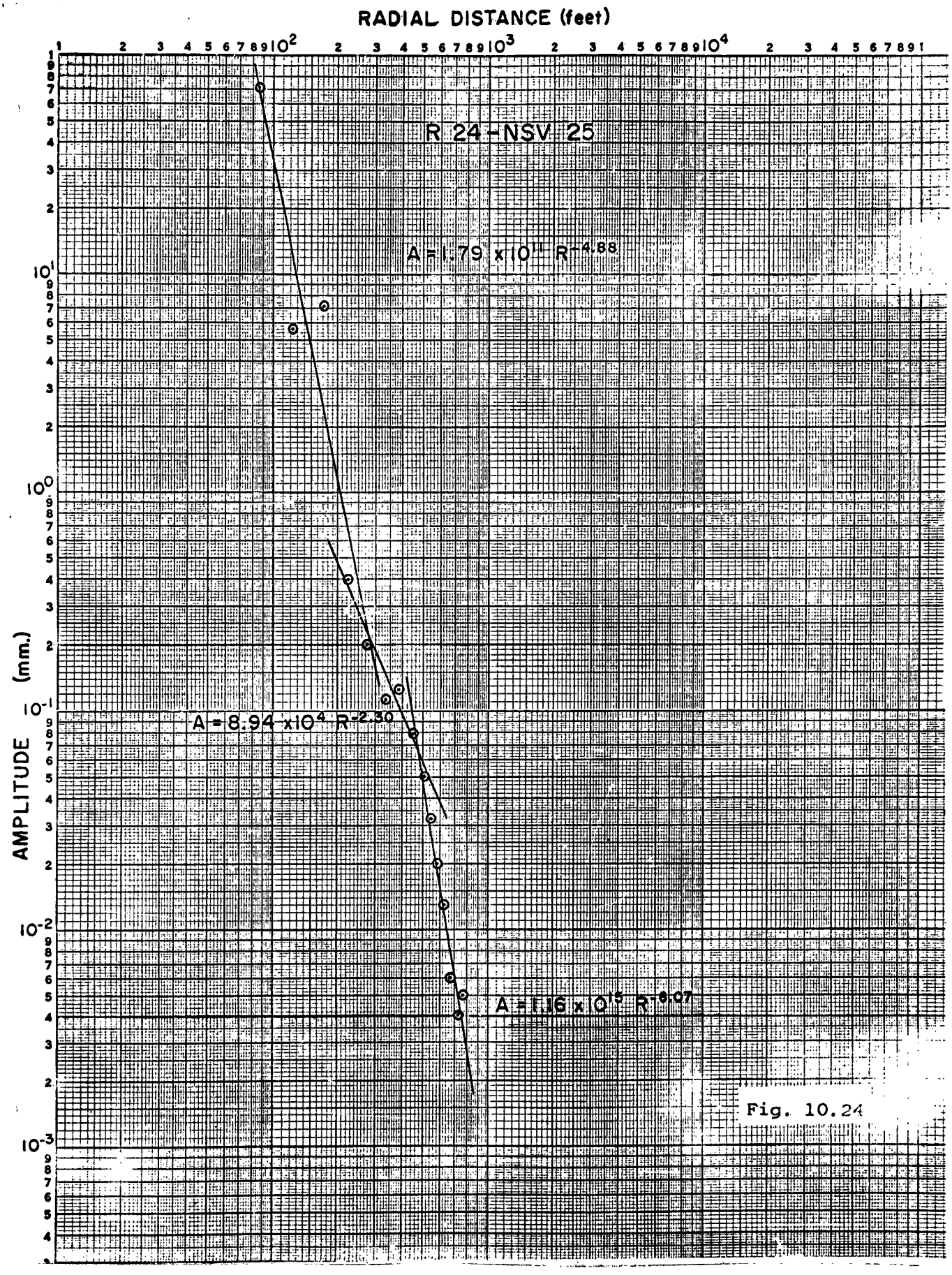
RADIAL DISTANCE (feet)
R 24 - NSV 25
A = 1.79 x 10^11 R^-4.88
A = 8.94 x 10^4 R^-2.30
A = 1.16 x 10^15 R^-6.07
AMPLITUDE (mm.)

Fig. 10.24

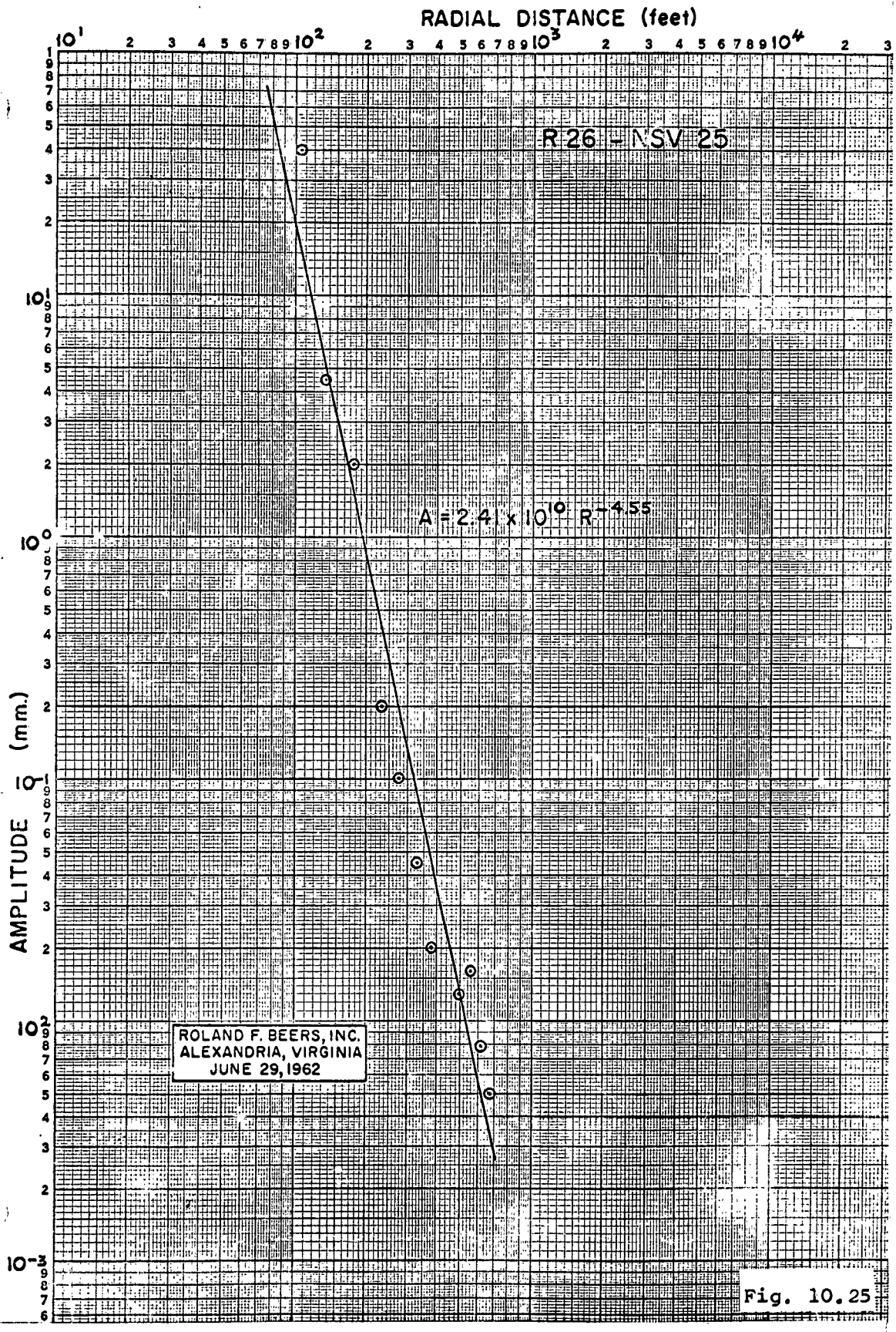
RADIAL DISTANCE (feet)
R 26 - NSV 25
A = 2.41 x 10^10 R^-4.55
AMPLITUDE (mm.)
ROLAND F. BEERS, INC.
ALEXANDRIA, VIRGINIA
JUNE 29, 1962

Fig. 10.25

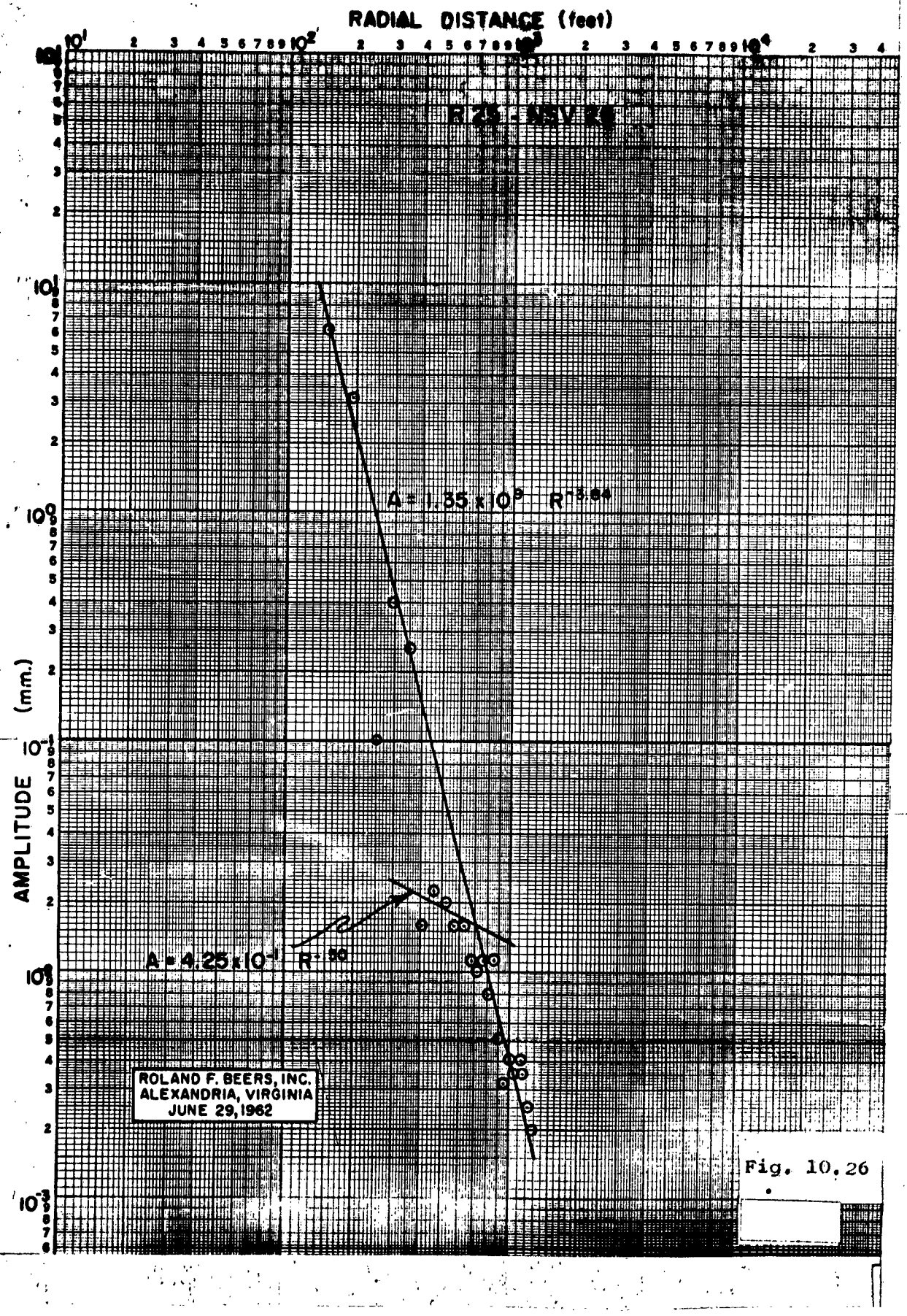
RADIAL DISTANCE (feet)
AMPLITUDE (mm.)
A = 1.35 x 10^3 R^-3.64
A = 4.25 x 10^-1 R^-1.50
ROLAND F. BEERS, INC.
ALEXANDRIA, VIRGINIA
JUNE 29, 1962

Fig. 10, 26

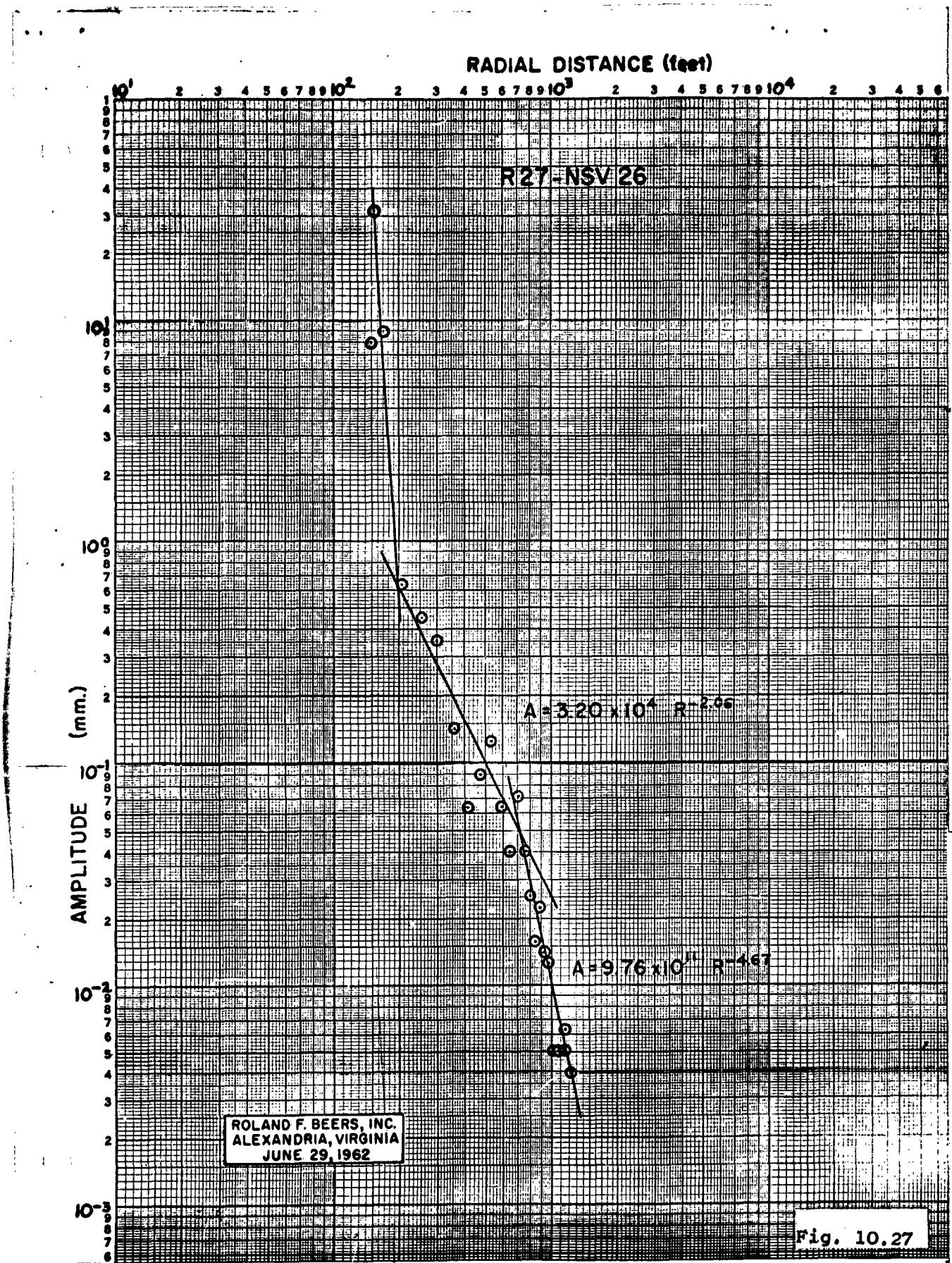
RADIAL DISTANCE (feet)
R27-NSV 26
AMPLITUDE (mm.)
A = 3.20 x 10^4 R^-2.06
A = 9.76 x 10^11 R^-4.67
ROLAND F. BEERS, INC.
ALEXANDRIA, VIRGINIA
JUNE 29, 1962

Fig. 10.27

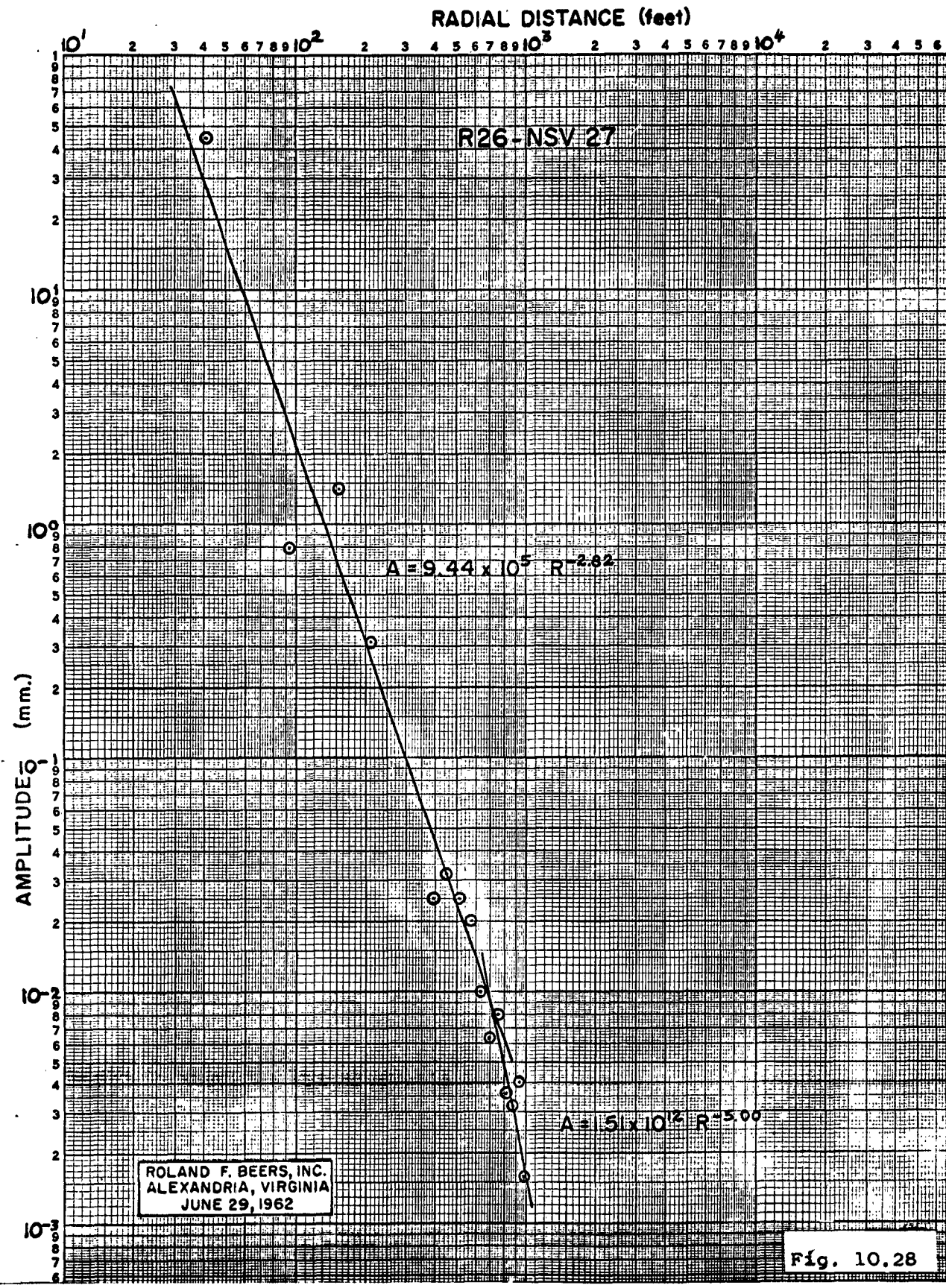
RADIAL DISTANCE (feet)
R26-NSV 27
A = 9.44 x 10^5 R^-2.82
A = 1.51 x 10^12 R^-5.00
AMPLITUDE (mm.)
ROLAND F. BEERS, INC.
ALEXANDRIA, VIRGINIA
JUNE 29, 1962

Fig. 10.28

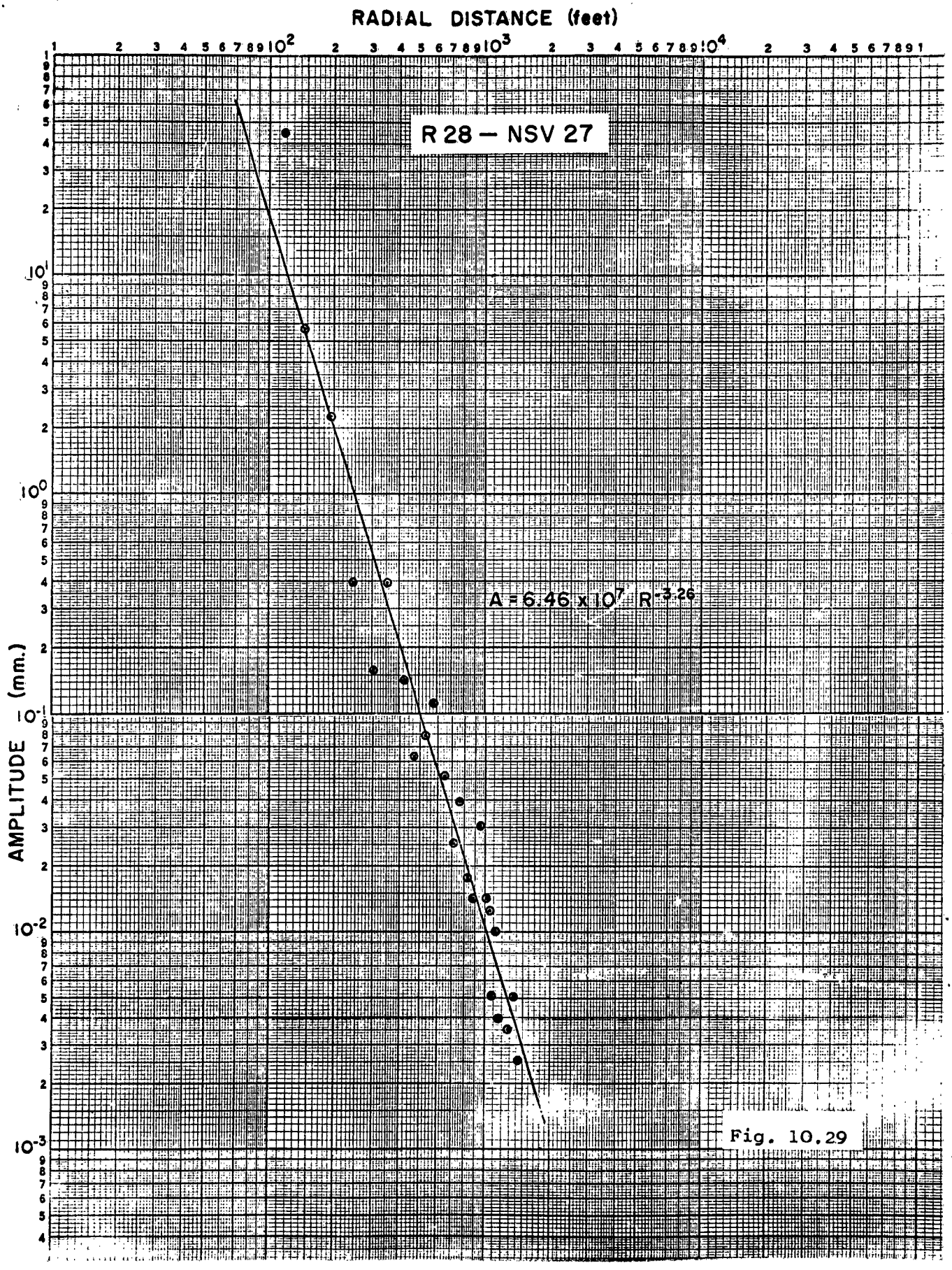
RADIAL DISTANCE (feet)
1 2 3 4 5 6 7 8 9 10^2 2 3 4 5 6 7 8 9 10^3 2 3 4 5 6 7 8 9 10^4 2 3 4 5 6 7 8 9 1
R 28 — NSV 27
A = 6.46 x 10^7 R^-3.26
AMPLITUDE (mm.)
10^1
10^0
10^-1
10^-2
10^-3

Fig. 10.29

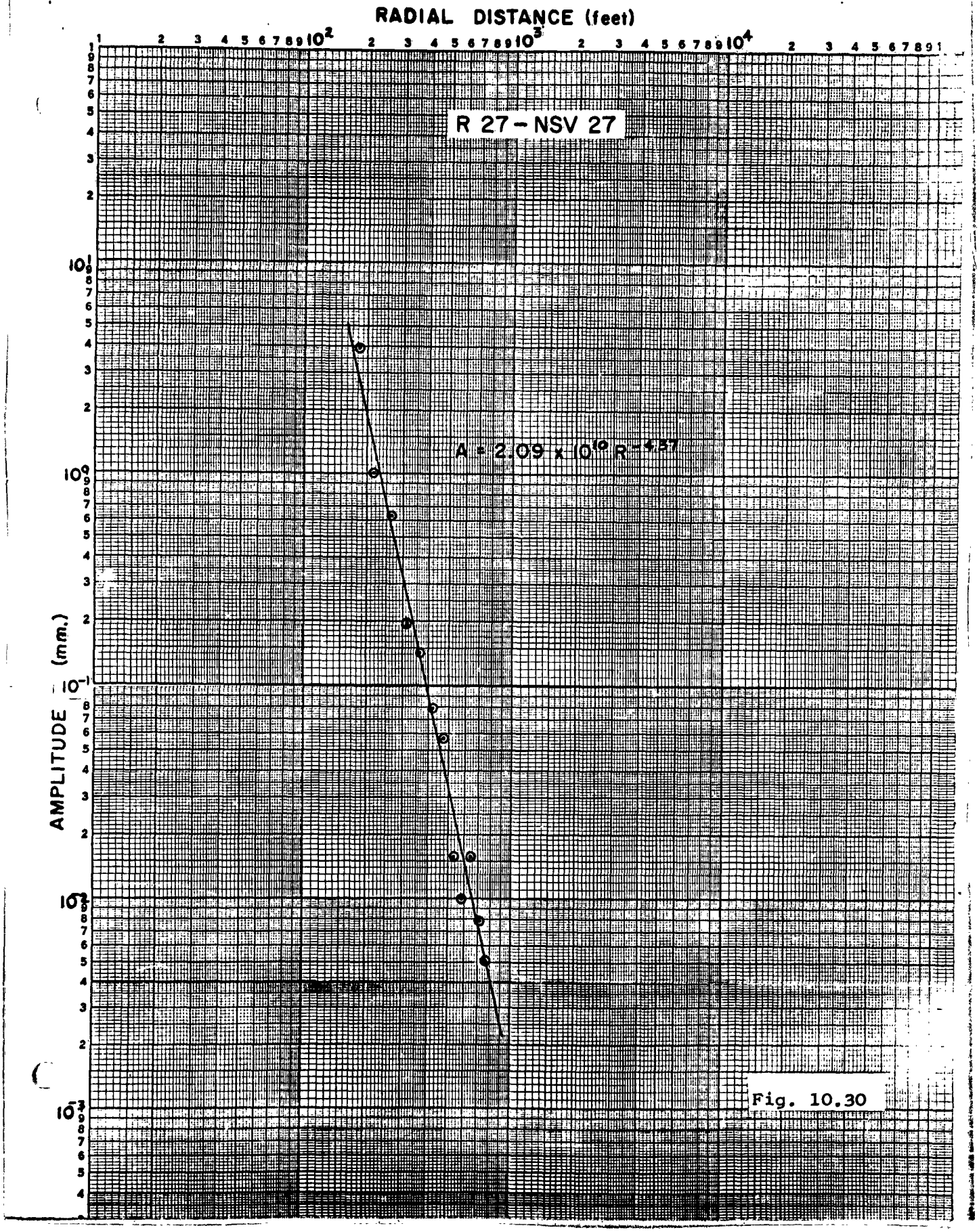
RADIAL DISTANCE (feet)
R 27 – NSV 27
A = 2.09 x 10^10 R^-4.37
AMPLITUDE (mm.)

Fig. 10.30

11.0 Horizontal Seismic Ranging

Horizontal seismic ranging represents an effort to apply the underlying concepts of echo ranging as used in ASW in the ocean to the problem of detecting cavities at long range from the surface of the ground. Conceptually speaking, it is desired to record energy which has been reflected by vertical rather than horizontal interfaces in the ground and propagated essentially in the horizontal plane. To accomplish this it is required to discriminate against energy reflected from the predominant horizontal interfaces which propagates in the vertical direction and which, if not rejected, will saturate the record. The principal innovation in the method employed by U.E.D., Inc., is the development of a recording array with controlled directional response in the horizontal plane (see Figures 11.1, 11.2, and 11.3), high directional response to energy arriving in the horizontal direction as opposed to energy arriving in the vertical direction in the vertical plane (see Figures 11.4 - 11.9), and predetermined band pass characteristics in terms of wave length.

Since the H.S.R. method does not make provision for evaluating the origin of an event in terms of depth, it must be assumed that there is no vertical component to contend with in locating the point of reflection. As a consequence of this assumption, reduction and evaluation of H.S.R. data is largely a problem of identifying valid signals and determining the point of reflection in the plane of the recording array.

Identification of valid signals on the H.S.R. records presents a difficult problem due to the extreme moveouts involved and the uniformity of the recorded amplitudes. On Program A records where maximum response is at right angles, the moveout problem is minimized since recorded energy reaches all of the geophones on the ray at essentially the same time. Examples of Program A recordings illustrating this are shown on Figure 11.10. However, to evaluate Program B recordings, each trace must be displaced by an amount appropriate to remove the moveout from the event. Figures 11.11 and 11.12, show Program B recordings corrected for moveouts based on

estimated apparent velocities. Figure 11.13 shows the uncorrected Program B recording.

The procedure used in locating events was as follows. Apparent events were first located on the Program A records on the basis of alignment. Then the corresponding perpendicular ray on the Program B record was examined to determine if a signal might have been recorded at a commensurate arrival time. This was accomplished by displacing traces according to the estimated suite of moveouts until alignment was obtained. This component of alignment when plotted with the moveout measured on the orthogonal Program A ray was used to determine the total moveout vector and the direction of the source of the event. Velocity was then computed from the ratio of the spread length and total moveout. Using the computed velocity and observed arrival time, the total distance from shot to reflector to array was determined. This distance defines an ellipse whose foci are the shot point and center of the recording array. The computed distance from shot to reflector to array is equal to the sum of focal radii to any point on the ellipse. Since one knows the direction from one focus the location of the reflector may be established.

Enclosure 2 shows the estimated quality of the record alignments picked for analysis and the locations of the reflection points derived from these alignments. Examination of the plotted data discloses no appreciably greater concentration of points in areas of interest than are concentrated in other areas. The same is true of the level of the grades in the different areas. The only seeming correlation, and a tenuous one at that, is with the surface topography and face of the mesa. However, for reasons to be discussed in subsequent paragraphs, it is doubted that any significance can be drawn from the positions of the derived points of reflection.

Horizontal seismic ranging presents many problems amenable to theoretical treatment but resistant to resolution in practice. Much of the difficulty in interpreting the H.S.R. records concerns identification of reliable signals and derivation of their point of origin. In many ways, the problem is not too unlike that often encountered in complex structural areas with conventional reflection seismic surveys when simultaneous arrivals

are recorded with divergent moveouts from many off-side reflections. However, in the case of H.S.R., the number of these arrivals and the resulting interference may be greatly magnified depending upon the orientation of maximum horizontal directional response of the array and geographic variation in the complexity of the medium. If the amplitudes of the recorded energy are generally equivalent for all arrivals, interference may disrupt the continuity of the recorded signals to a point where they are unrecognizable. In the event that such a phenomenon represents the actual situation, corrections for an estimated suite of moveouts would produce completely fallacious results. An assumption which may not be valid here is that coherent signals reached the array regardless of the direction of maximum horizontal response.

An even more difficult problem to resolve is derivation of the true origins of the reflections. In the foregoing analysis of the H.S.R. data it was assumed that the reflections originated at sufficiently shallow depth that the vertical component of position might be ignored. This assumption appears justified on the basis that most of the observed apparent velocities were commensurate with what one might expect for energy propagated in the near surface section. Thus, the distance to the point of reflection may be computed using the apparent velocity determined from the total moveout vector. The weakness in these computations is that they do not encompass the effect of the observed lateral variation in velocity. Consequently, the computed distances may be greatly in error, over and above that which derives from ignoring the vertical component of position.

Since there was no discernible evidence of signals originating below the base of the welded Tos_8 tuff on the recorded H.S.R. data, it should have been worthwhile to modify the directional response of the recording array to permit the reception of reflected refractions. Figure 11.14 shows the velocity stratification of the Oak Spring formation. It is apparent that reflected refractions may be a means of obtaining measurements which are not available with the horizontal seismic ranging technique.

The term "reflected refraction" used hereafter describes the phenomenon whereby energy is refracted laterally along a high velocity carrier bed until it impinges against some form of discontinuity which will reflect the energy back toward the source. The basis for the concept of reflected refractions is that ray theory demands that some energy be refracted into every bed whose velocity is higher than that of any of the beds above it. This is true despite increasing velocity with depth.

Generally speaking, the conditions which appear to be most favorable for reflected refractions are:

A. There must be some form of discontinuity in the carrier bed from which seismic energy can be reflected, diffracted or scattered so as to return it to its source.

B. The carrier bed must be able to transmit the refracted energy. Among the factors which must be considered here are absorption, scattering and "peeloff". The loss of energy due to absorption and scattering of refracted waves within the carrier bed should be about the same as or less than that for a wave transmitted an equal distance perpendicular to the bedding. The most uncertain factor is the loss of energy by refraction out of the carrier bed in directions other than toward the source. This phenomenon appears to be governed by the thickness and physical properties of the carrier bed. Generally, one should expect to observe detectable refraction energy over distances of a few miles. This is governed to a considerable extent by the thickness of the carrier bed, as thick beds are better carriers than thin beds.

C. It is also required to know the directional sensitivity of source-receiver system. Energy reflected from bedding planes approaches the recording array at a much different angle than that of reflected refractions. The directional sensitivity of the source receiver system may, therefore, have an appreciable effect on the relative amplitude of the

two types of events. When a charge is detonated in a homogeneous semi-infinite medium, the longitudinal energy is not radiated uniformly in all directions. The amplitude measured at a given point, and angle from the shot of θ degrees from the vertical will be approximately cos θ times the amplitude measured directly below the shot an equal distance. Since most of the seismometers in use are sensitive only to the vertical component of ground motion, waves of a given amplitude arriving at angle θ will give a response cos θ times the wave arriving vertically. Consequently, the seismic event which arrives at an angle θ from the vertical will be recorded with an amplitude cos θ times that of an event with a vertical path when the reflection time and reflection coefficient are the same for both events. This is true only for a homogeneous semi-infinite media. Polar plots of the directional sensitivity pattern for cos θ are shown in Figures 11.15a and 11.15b. It should be noted, however, that the cos θ pattern is not as directional as the patterns most generally used.

Figure 11.15a illustrates the case for a nigh speed carrier bed with no dip located in a homogeneous semi-infinite medium. Heavy ray paths show the relative sensitivity of a very simple source receiver system to reflections and reflected refractions. In this example the sensitivity to reflected refractions is approximately 25% of the sensitivity to reflections. When, however, the carrier bed is dipping as shown in Figure 11.15b, the sensitivity to reflected refractions becomes 0.87 times as great as that to reflections.

The geometrical theory of reflected refractions assumes a truncated high speed carrier bed located at some arbitrary depth and dipping at an arbitrary angle δ. See Figure 11.16. The truncation may be any feature capable of returning detectable amounts of energy. The strike of the truncation differs from that of the carrier bed by an angle τ (measured in the plane of the bed). It is also assumed that between the point of refraction and truncation, the velocity of the carrier bed is essentially constant at V_2, while the velocity of the adjacent medium is essentially constant at V_1, where $V_2 > V_1$. Consider

V_1 and V_2 to be the average velocities of the medium and carrier bed between the point of refraction and truncation. Within this region, the incident and refracted rays should be essentially straight and should define a plane which is perpendicular to the trace of the truncation that passes through the point of refraction. This plane is shown in Figure 11.17 with the dip of the bedding and the anomalous dips chosen to correspond to those which might be observed in practice. The ray which strikes the carrier bed at the critical angle

$$i_c = \sin^{-1} (V_1 / V_2)$$

at the distance "d" from the truncation should proceed undeflected until it is reflected. The time "t_d", is assumed to have been spent traveling the distance

$$b = V_1 t_d$$

Since

$$t_d = d / V_2$$

the event will appear to occupy a position along the dashed line at the distance

$$b = d (V_1 / V_2)$$

beyond the point of refraction. Substituting $t_d = d / V_2$ into $b = V_1 t_d$ gives the projection "p" of "d" on the ray path. The perpendicular dropped from the truncation to the ray path should meet the carrier bed at an angle equal to the critical angle, i_c, and $p = d \sin i_c$. Making use of this equation and

$$i_c = \sin^{-1} (V_1 / V_2) \text{ and } b = d (V_1 / V_2)$$

it is found that

$$p = d \sin i_c = d (V_1 / V_2) = b$$

This shows that the dip of the event coincides with the line drawn from the truncation perpendicular to the undeflected ray path.

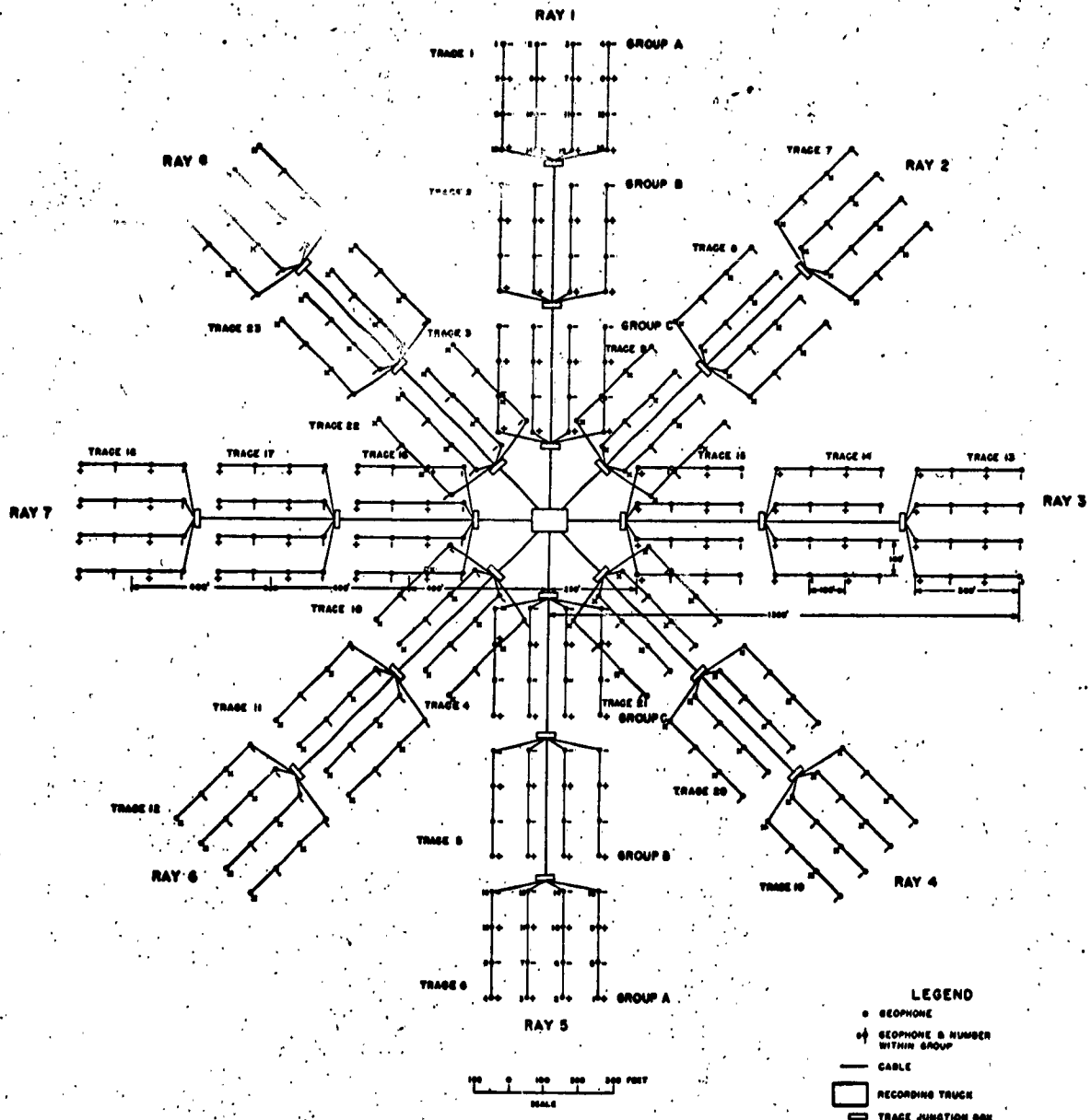

HORIZONTAL SEISMIC RANGING ARRAY

Program B

Fig. 11.1

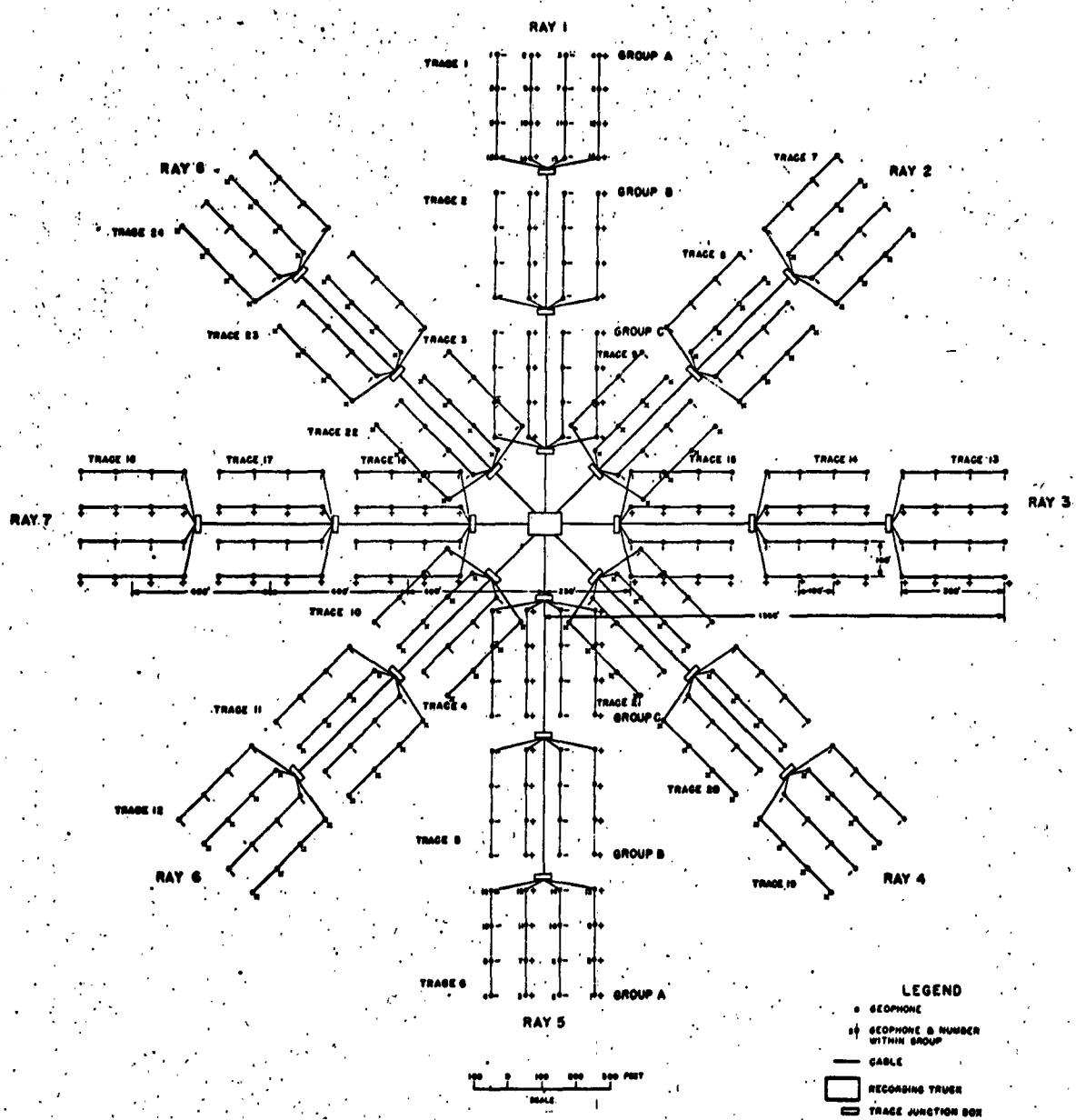

HORIZONTAL SEISMIC RANGING ARRAY

POLARITY ARRANGEMENT FOR

Program A

Fig. 11.2

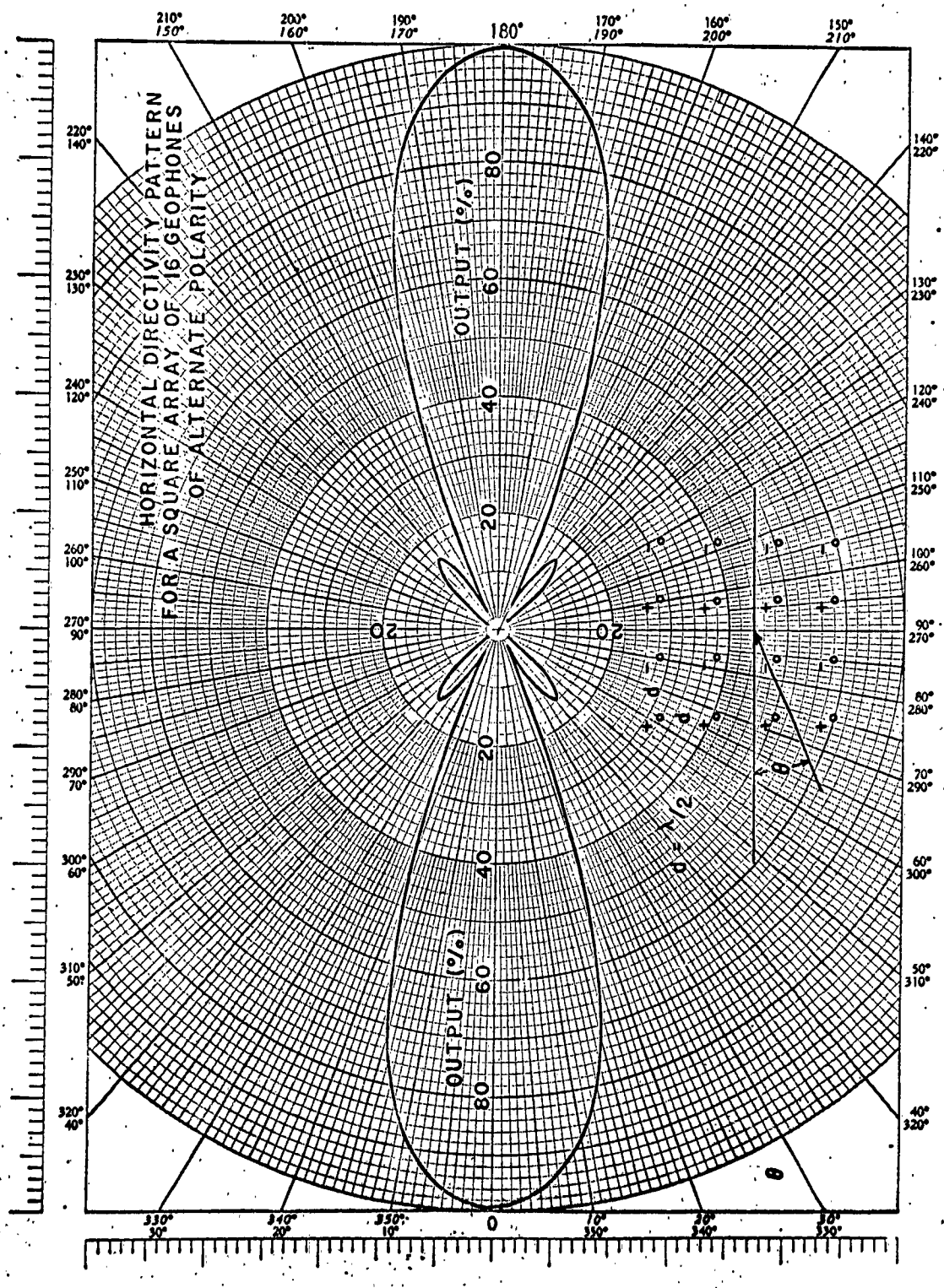
HORIZONTAL DIRECTIVITY PATTERN
FOR A SQUARE ARRAY OF 16 GEOPHONES
OF ALTERNATE POLARITY
OUTPUT (%)
OUTPUT (%)
180°
0
d = λ/2
θ

Fig. 11.3

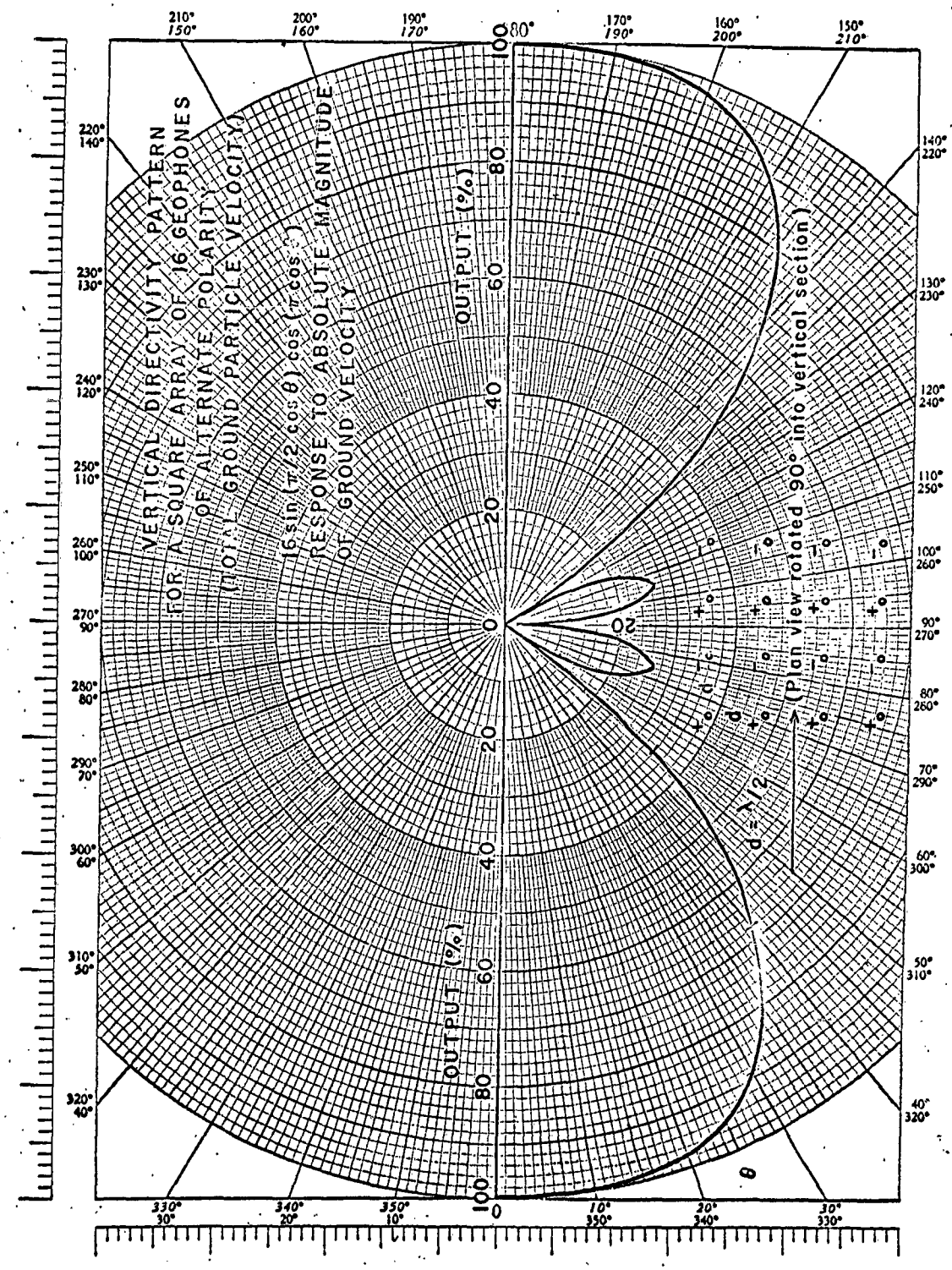
VERTICAL DIRECTIVITY PATTERN
FOR A SQUARE ARRAY OF 16 GEOPHONES
OF ALTERNATE POLARITY
NOTE: GROUND PARTICLE VELOCITY
16 sin(π/2 cosθ) cos(π cos)
RESPONSE TO ABSOLUTE MAGNITUDE
OF GROUND VELOCITY
OUTPUT (%)
OUTPUT (%)
(Plan view rotated 90° into vertical section)
d = λ/2
θ
210° 150°
200° 160°
190° 170°
180°
170° 190°
160° 200°
150° 210°
220° 140°
230° 130°
240° 120°
250° 110°
260° 100°
270° 90°
280° 80°
290° 70°
300° 60°
310° 50°
320° 40°
330° 30°
340° 20°
350° 10°
0
10° 350°
20° 340°
30° 330°
40° 320°
50° 310°
60° 300°
70° 290°
80° 280°
90° 270°
100° 260°
110° 250°
120° 240°
130° 230°
140° 220°
0
20
40
60
80
100
20
40
60
80
100

Fig. 11.4

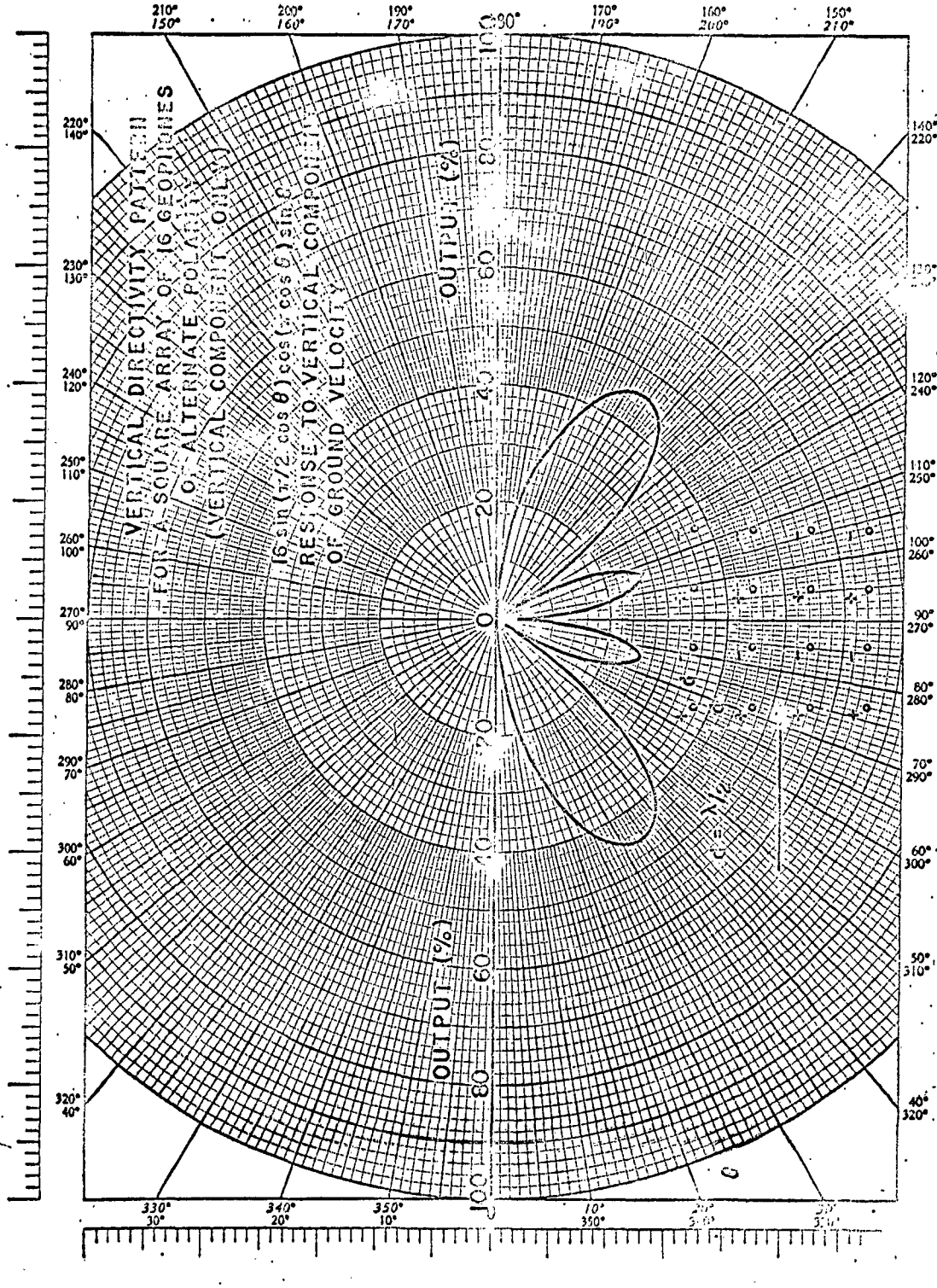
VERTICAL DIRECTIVITY PATTERN
FOR A SQUARE ARRAY OF 16 GEOPHONES
OF ALTERNATE POLARITY
(VERTICAL COMPONENT ONLY)
16 sin (π/2 cos θ) cos (π/2 cos θ) sin θ
RESPONSE TO VERTICAL COMPONENT
OF GROUND VELOCITY
OUTPUT (%)
OUTPUT (%)
210° 150°
200° 160°
190° 170°
180°
170° 190°
160° 200°
150° 210°
220° 140°
230° 130°
240° 120°
250° 110°
260° 100°
270° 90°
280° 80°
290° 70°
300° 60°
310° 50°
320° 40°
140° 220°
120° 240°
110° 250°
100° 260°
90° 270°
80° 280°
70° 290°
60° 300°
50° 310°
40° 320°
330° 30°
340° 20°
350° 10°
10° 350°
0
20
40
60
80
100

Fig. 11.5

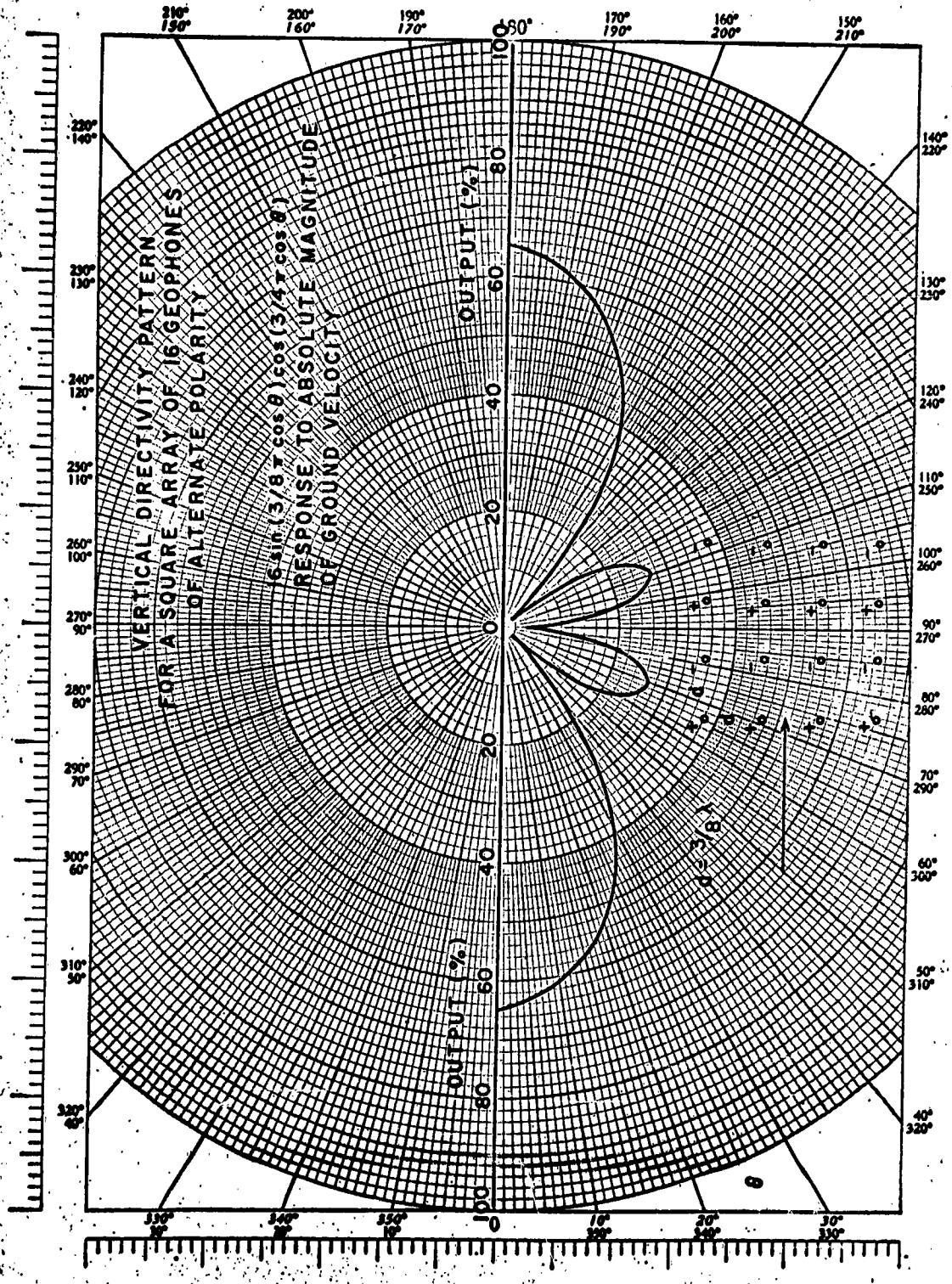
VERTICAL DIRECTIVITY PATTERN
FOR A SQUARE ARRAY OF 16 GEOPHONES
OF ALTERNATE POLARITY
16 sin (3/8 π cos θ) cos (3/4 π cos θ)
RESPONSE TO ABSOLUTE MAGNITUDE
OF GROUND VELOCITY
OUTPUT (%)
OUTPUT (%)
d = 3/8 λ
θ

Fig. 11.6

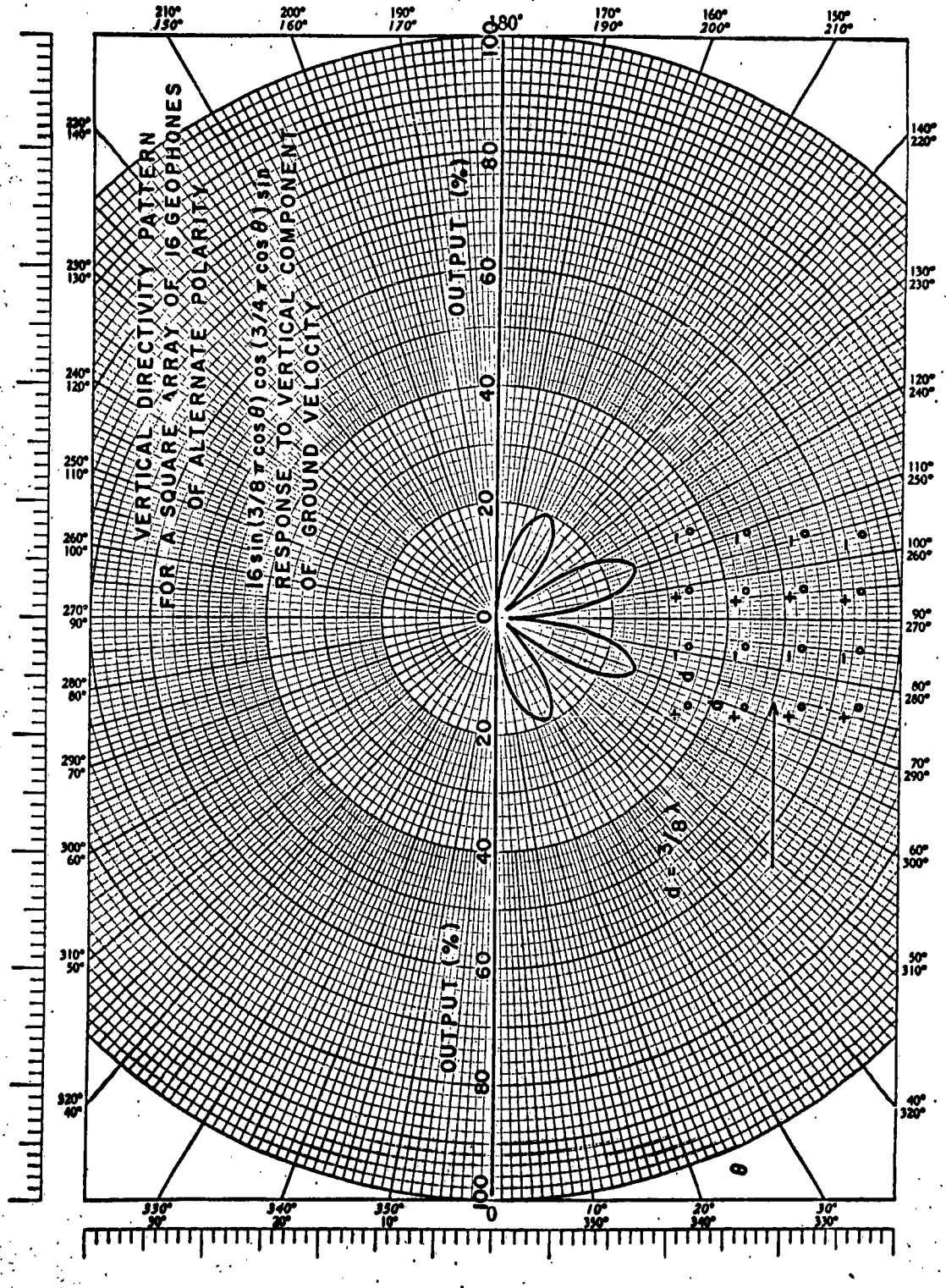
VERTICAL DIRECTIVITY PATTERN
FOR A SQUARE ARRAY OF 16 GEOPHONES
OF ALTERNATE POLARITY
16 sin (3/8 π cos θ) cos (3/4 π cos θ) sin
RESPONSE TO VERTICAL COMPONENT
OF GROUND VELOCITY
OUTPUT (%)
OUTPUT (%)
d = 3/8 λ
θ

Fig. 11.7

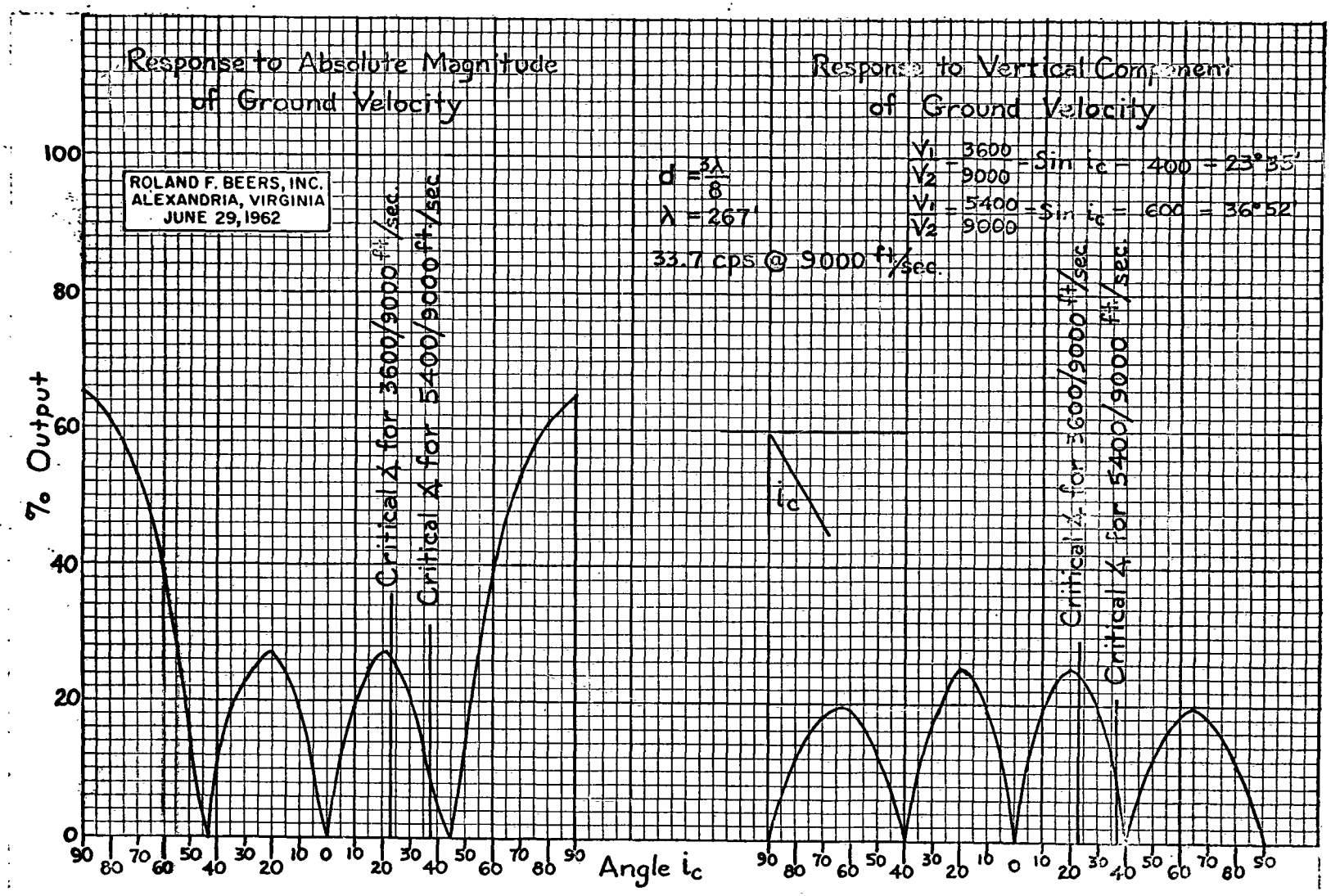
Response to Absolute Magnitude of Ground Velocity
ROLAND F. BEERS, INC.
ALEXANDRIA, VIRGINIA
JUNE 29, 1962
d = 3λ/8
λ = 267'
33.7 cps @ 9000 ft/sec
Critical ∠ for 3600/9000 ft/sec
Critical ∠ for 5400/9000 ft/sec
% Output
100
80
60
40
20
0
90 80 70 60 50 40 30 20 10 0 10 20 30 40 50 60 70 80 90
Angle i_c
Response to Vertical Component of Ground Velocity
$\frac{V_1}{V_2} = \frac{3600}{9000} = \sin i_c = .400 = 23°35'$
$\frac{V_1}{V_2} = \frac{5400}{9000} = \sin i_c = .600 = 36°52'$
i_c
Critical ∠ for 3600/9000 ft/sec
Critical ∠ for 5400/9000 ft/sec
90 80 70 60 50 40 30 20 10 0 10 20 30 40 50 60 70 80 90

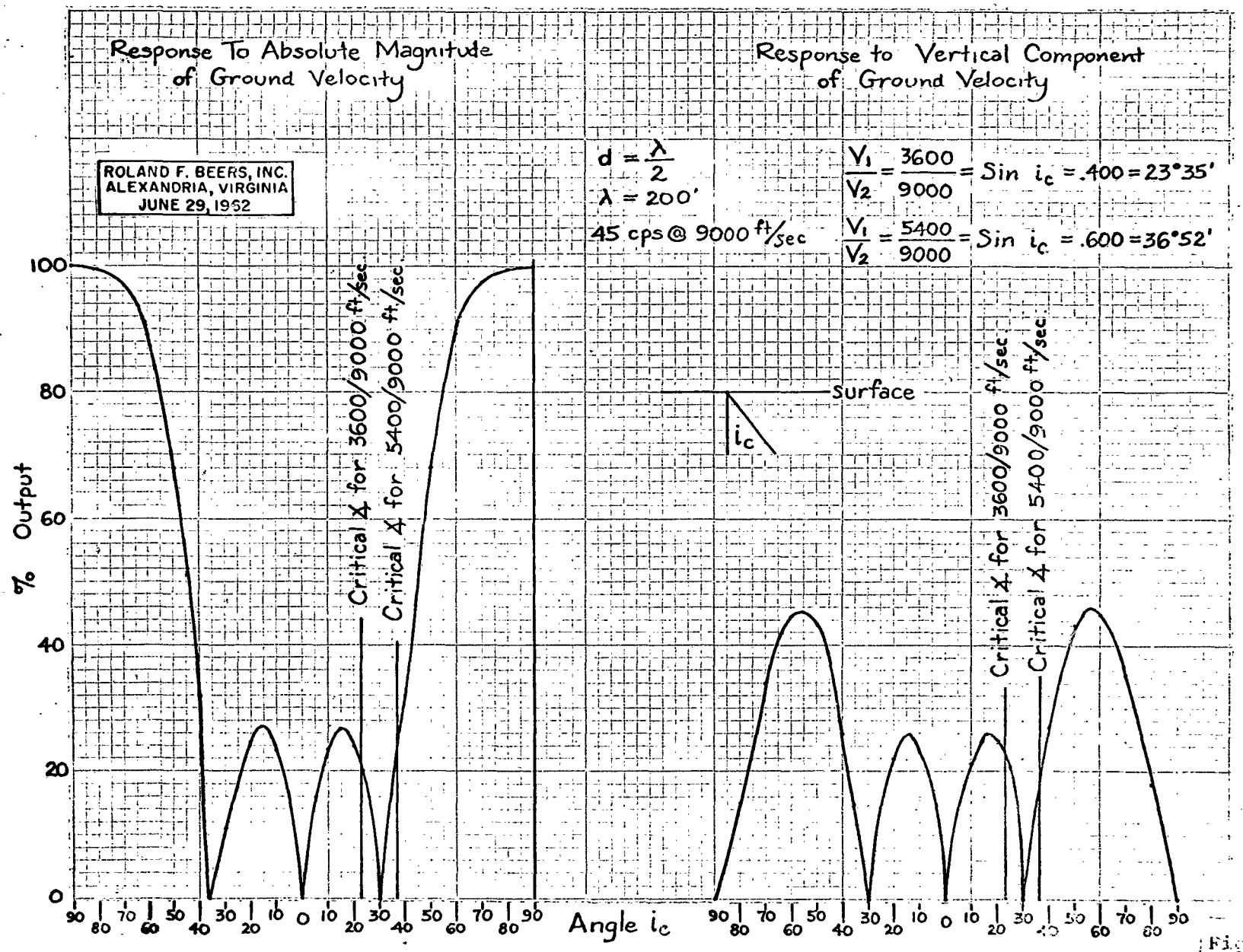
Response To Absolute Magnitude of Ground Velocity
Response to Vertical Component of Ground Velocity
ROLAND F. BEERS, INC.
ALEXANDRIA, VIRGINIA
JUNE 29, 1962
$d = \frac{\lambda}{2}$
$\lambda = 200'$
45 cps @ 9000 ft/sec
$\frac{V_1}{V_2} = \frac{3600}{9000} = \text{Sin } i_c = .400 = 23°35'$
$\frac{V_1}{V_2} = \frac{5400}{9000} = \text{Sin } i_c = .600 = 36°52'$
% Output
100
80
60
40
20
0
Critical ∠ for 3600/9000 ft/sec
Critical ∠ for 5400/9000 ft/sec
Surface
i_c
90 80 70 60 50 40 30 20 10 0 10 20 30 40 50 60 70 80 90
Angle i_c
90 80 70 60 50 40 30 20 10 0 10 20 30 40 50 60 70 80 90
Critical ∠ for 3600/9000 ft/sec
Critical ∠ for 5400/9000 ft/sec

Fig. 11.9

R 7 – HR 2
Rays 3 and 7, Traces 13–18
Program A

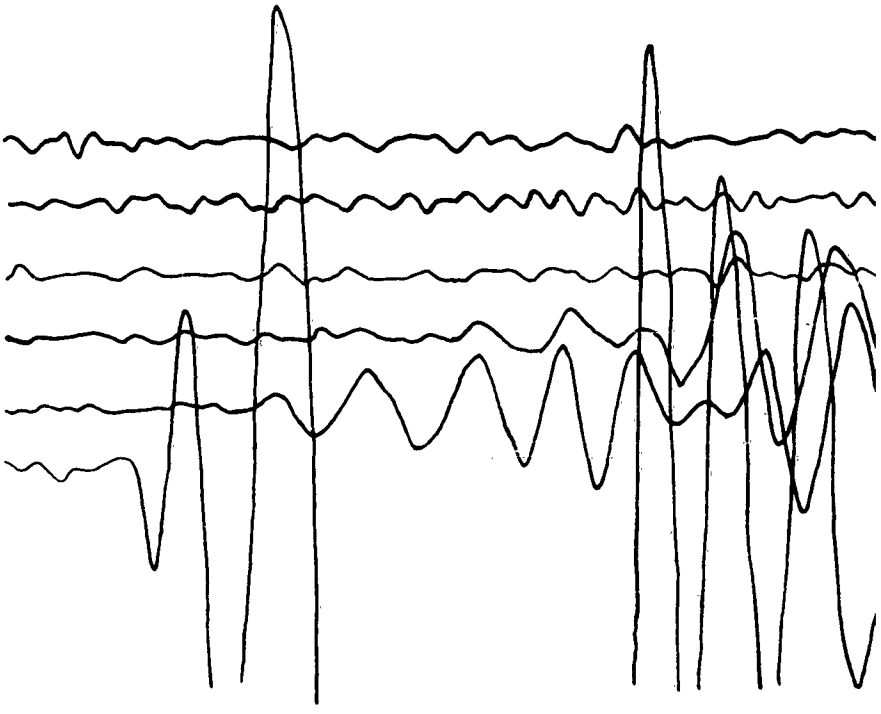

1

R 10 – HR 3
Rays 1 and 5, Traces 1–6
Program A

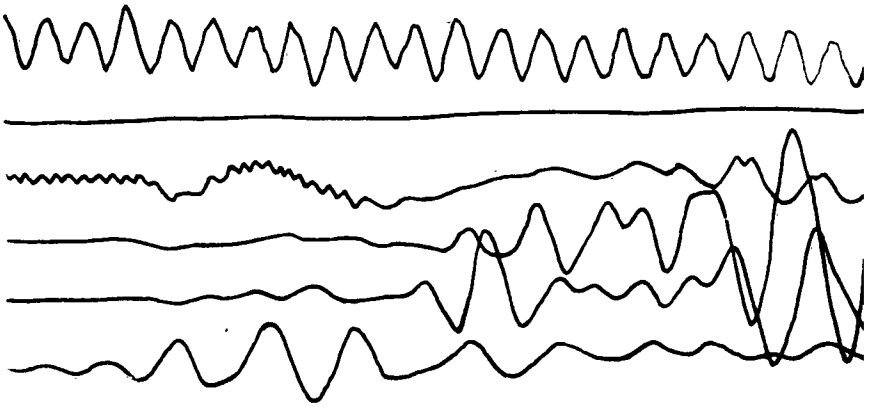

Fig. 11.10 Horizontal Seismic Ranging Recording with Maximum Response Perpendicular to Ray (Program A)

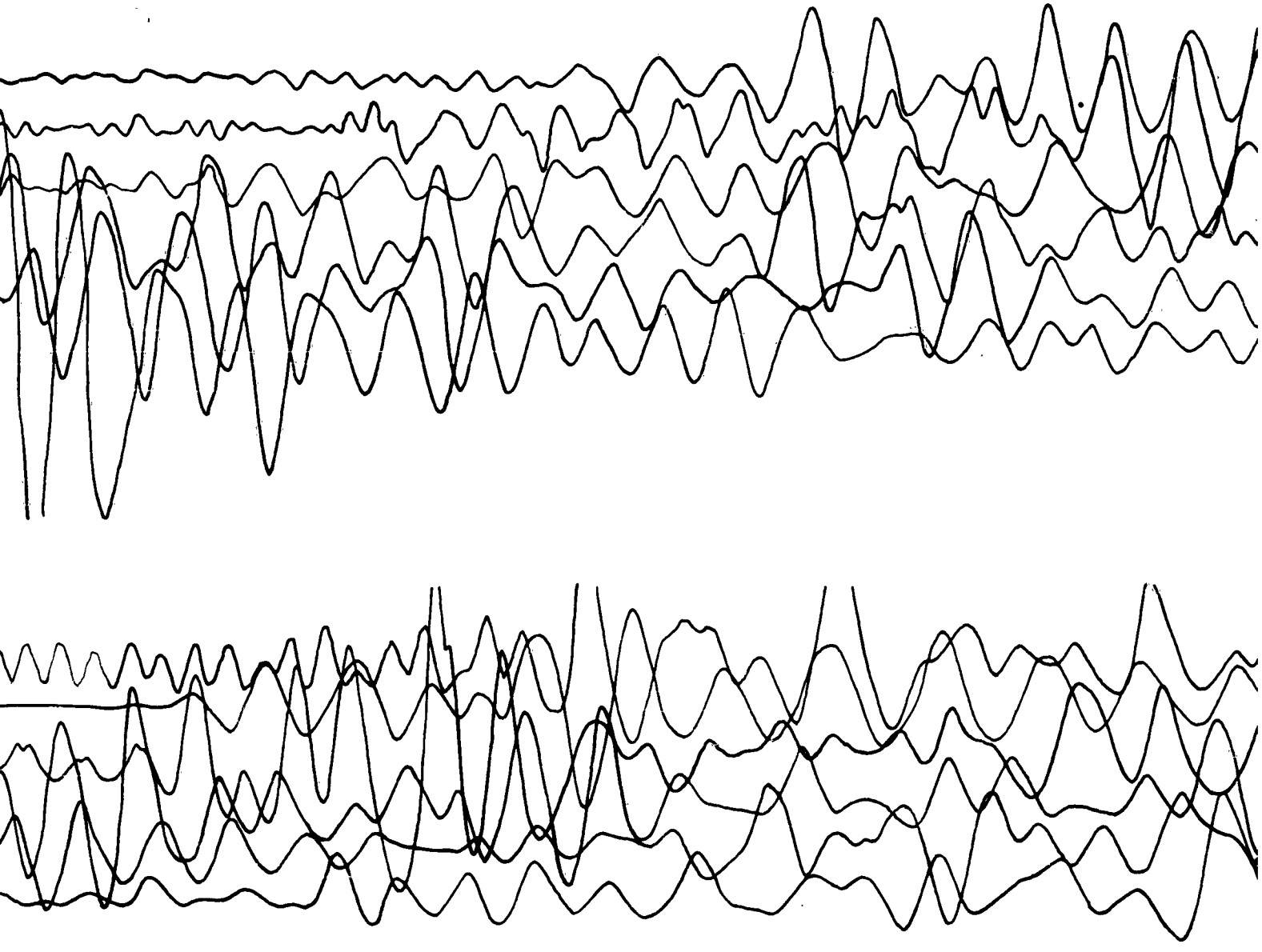

2

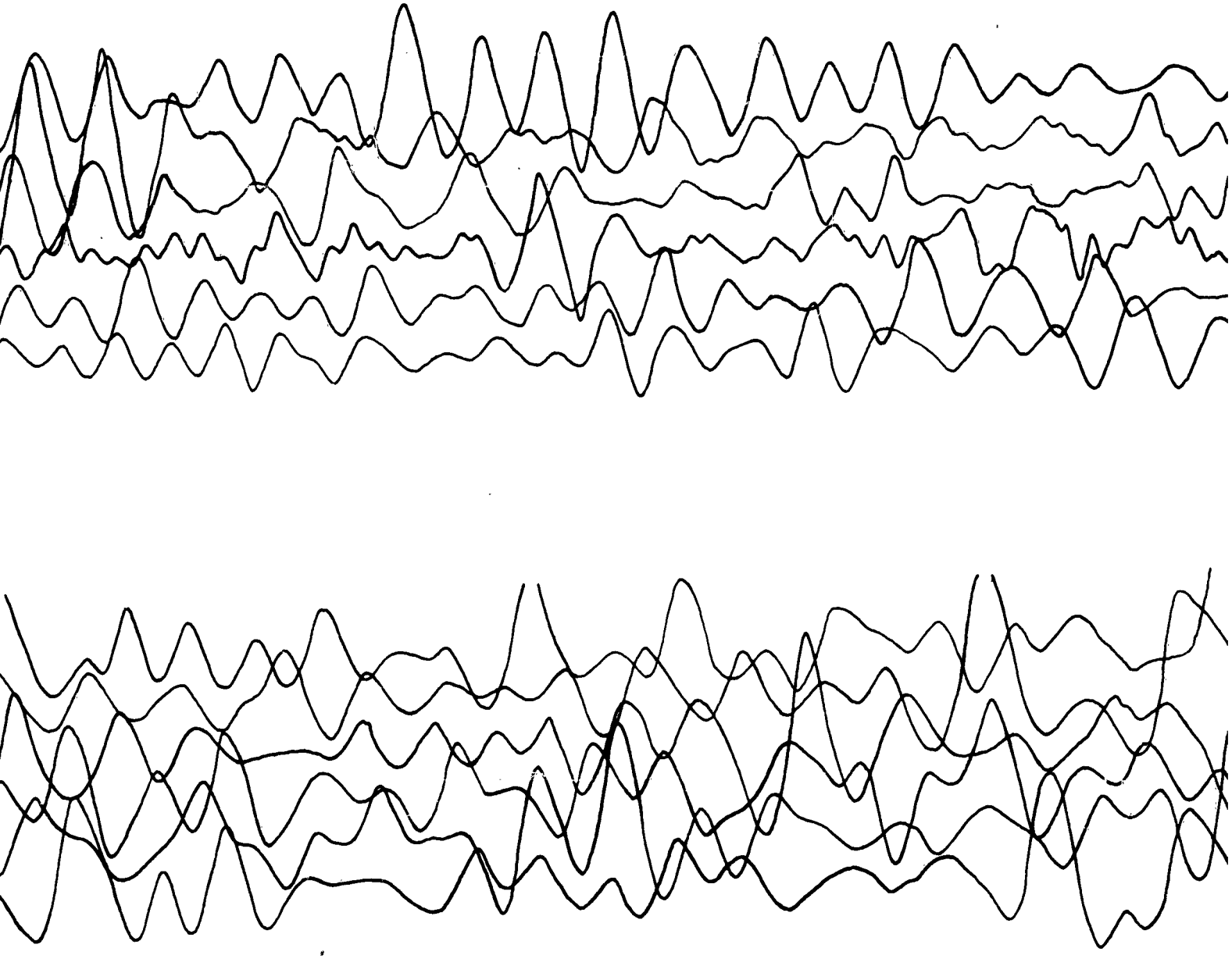

3

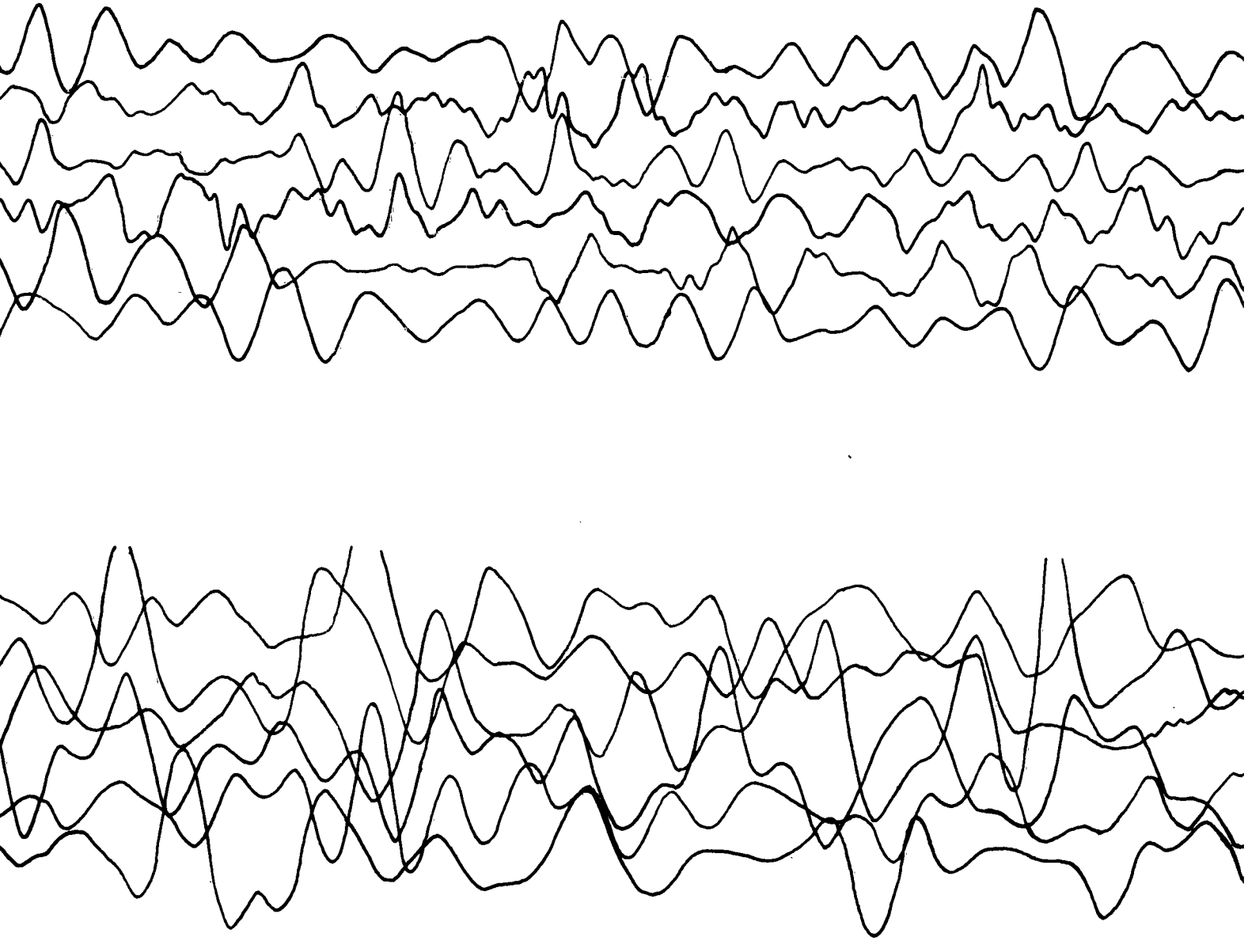

4

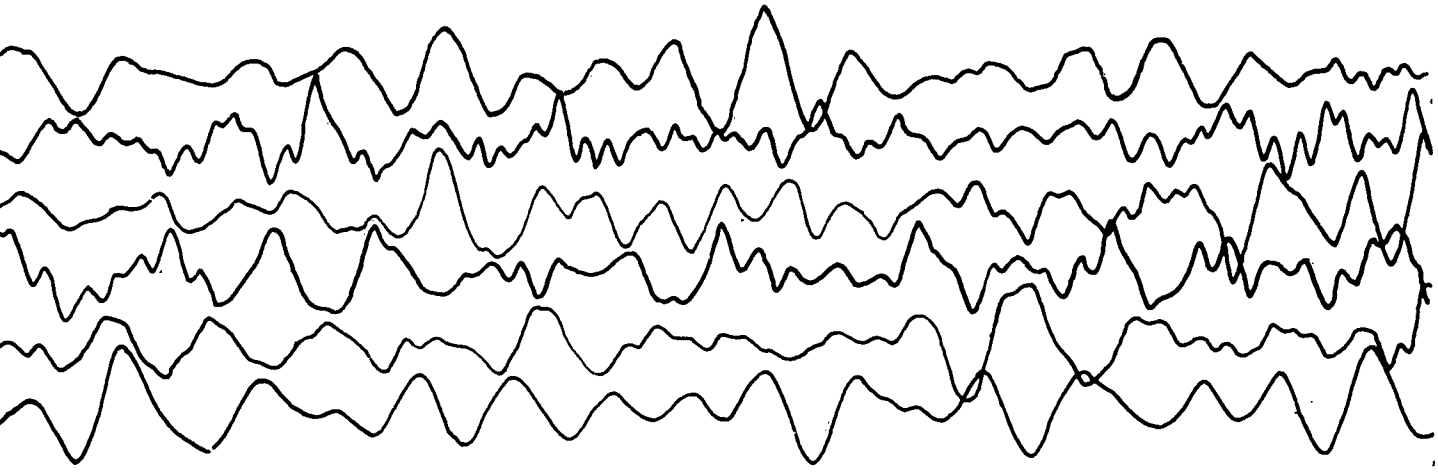

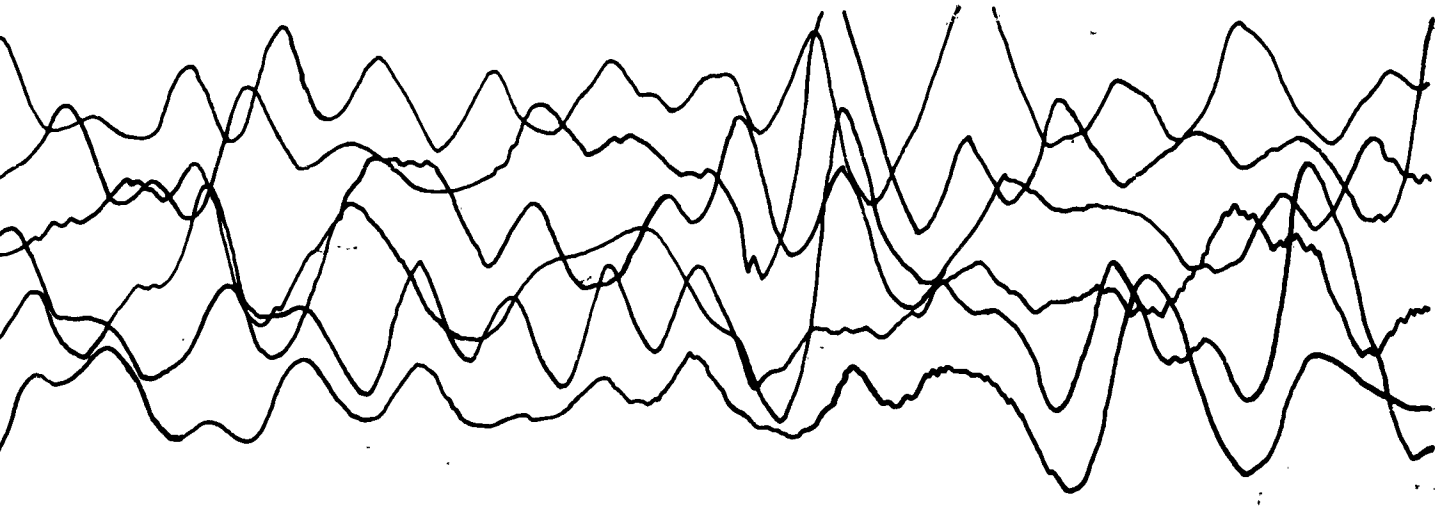

5

11.11

Fig. 11.11 Horizontal Seismic Ranging Recording Corrected for Moveouts Based on Velocities of 6000, 8000, and 10000 feet/second

1

R 10 – HR 3
Rays 3 and 7, Traces 13–18
Program B

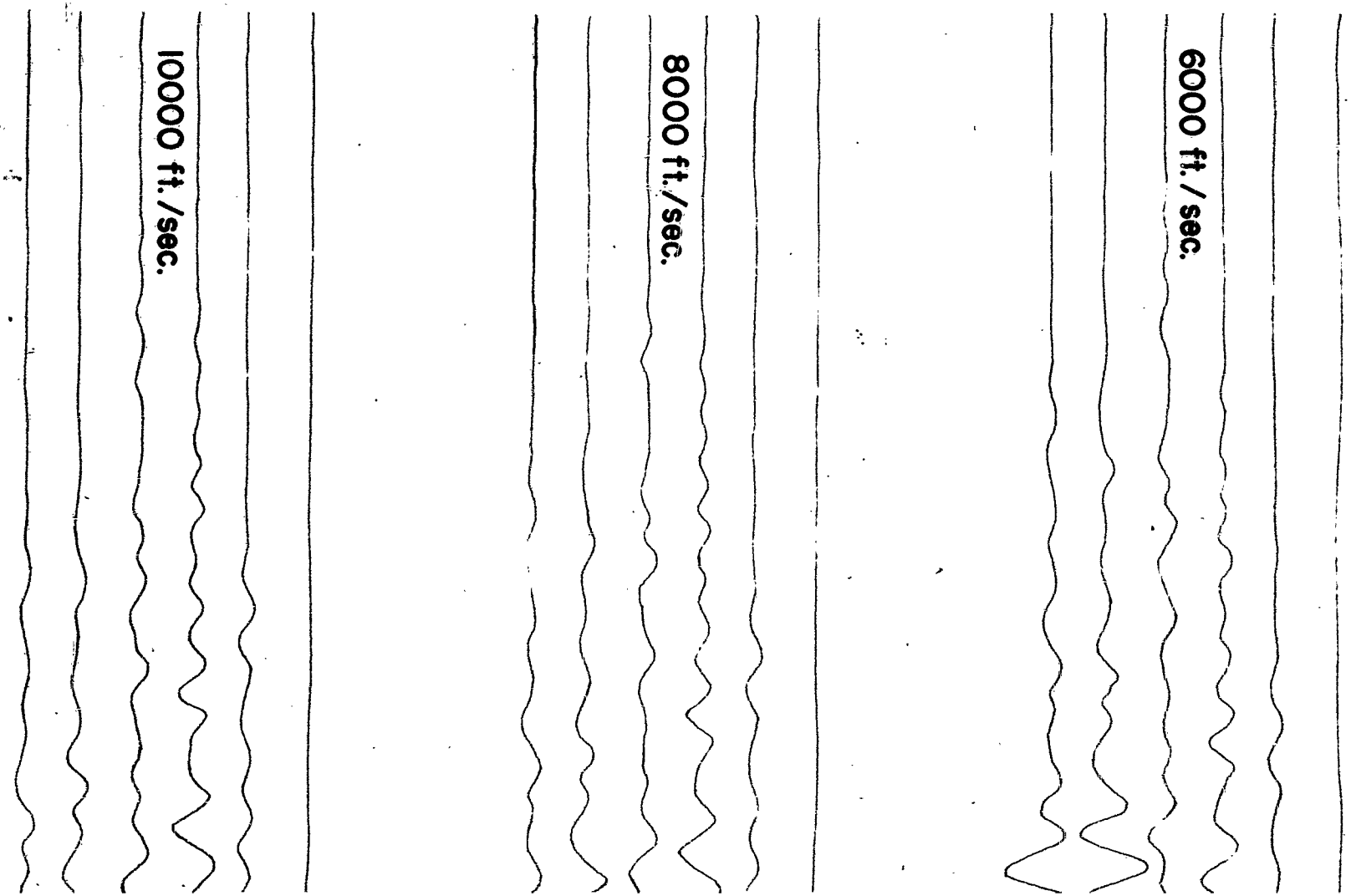

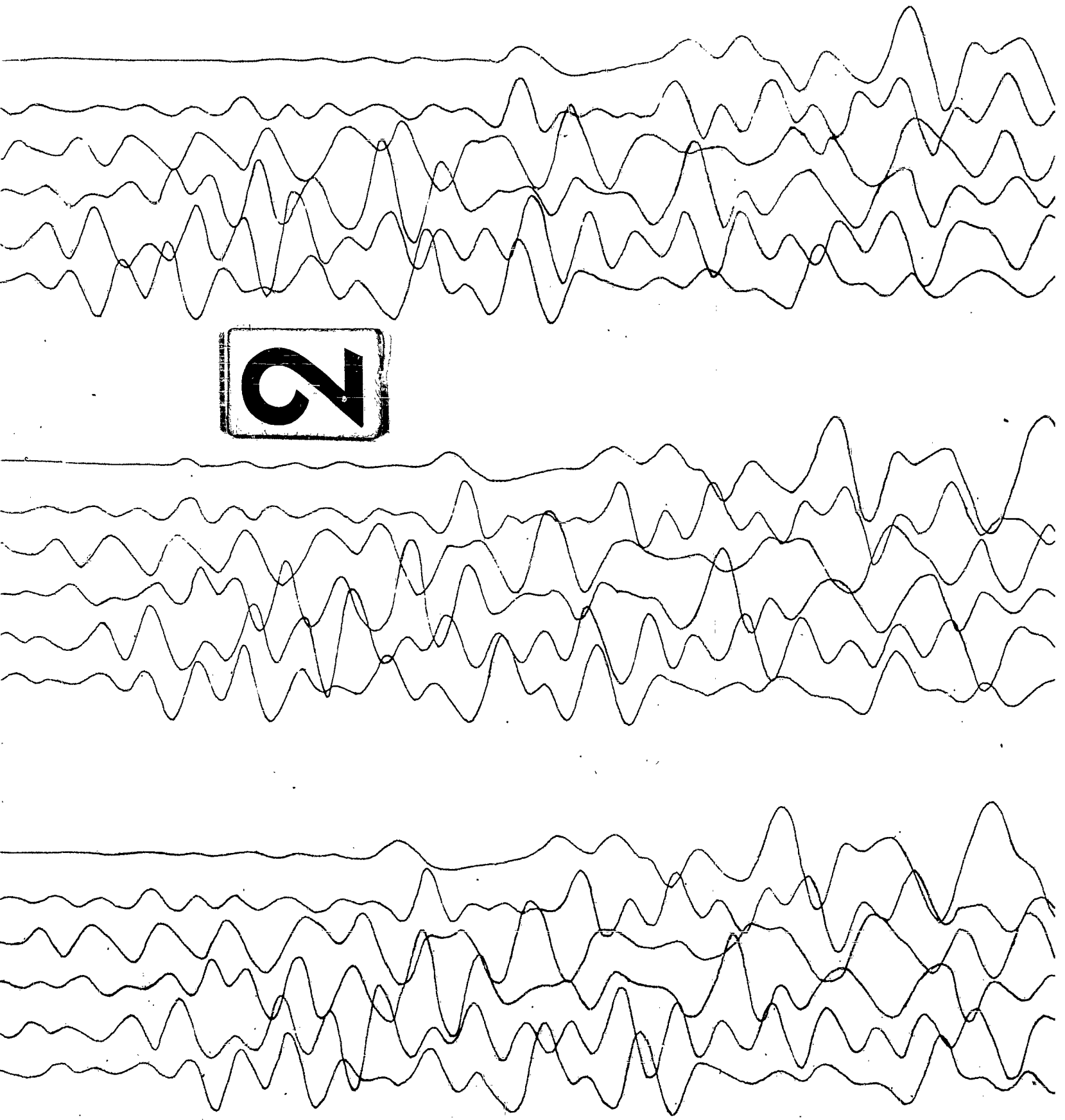

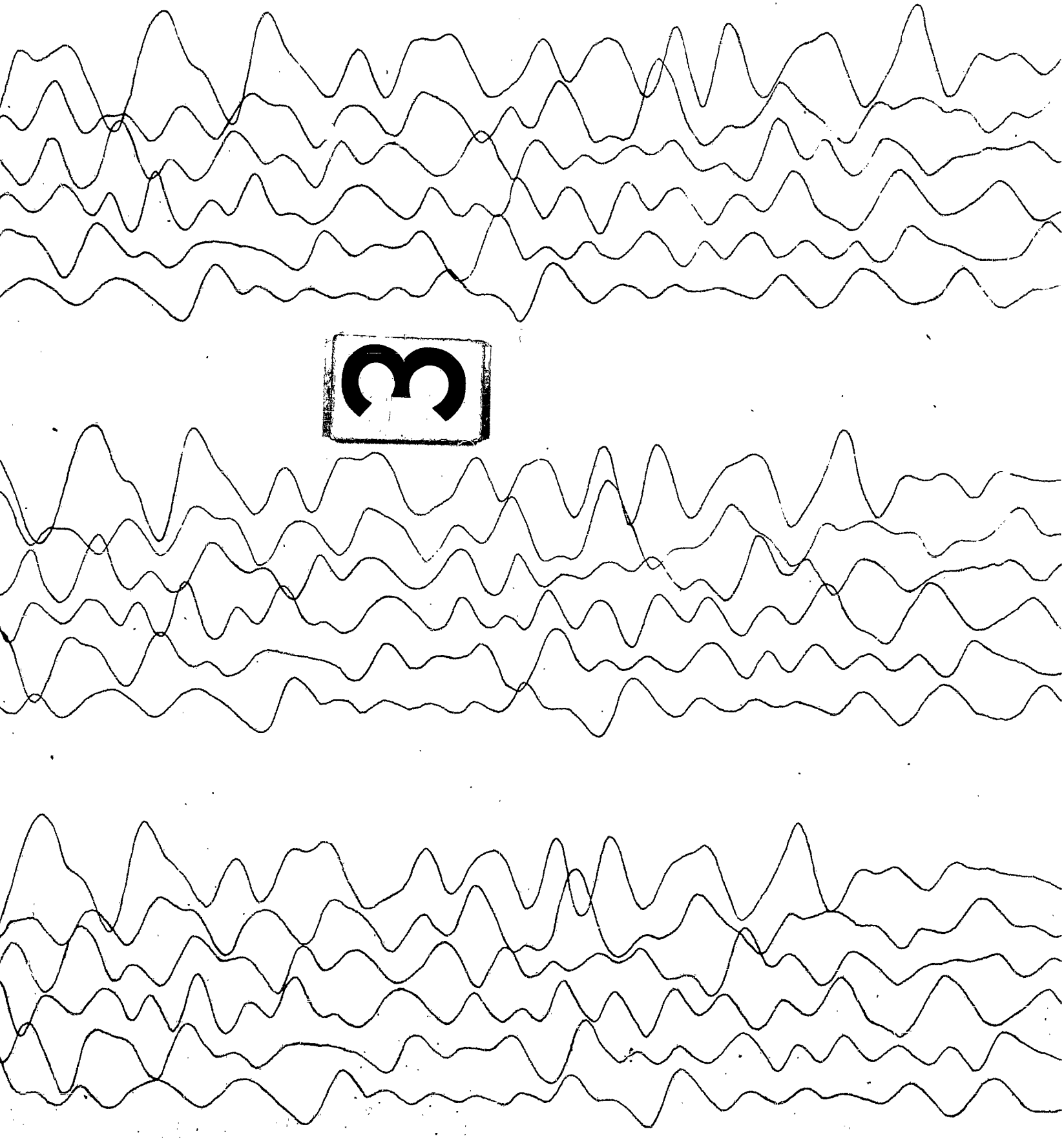

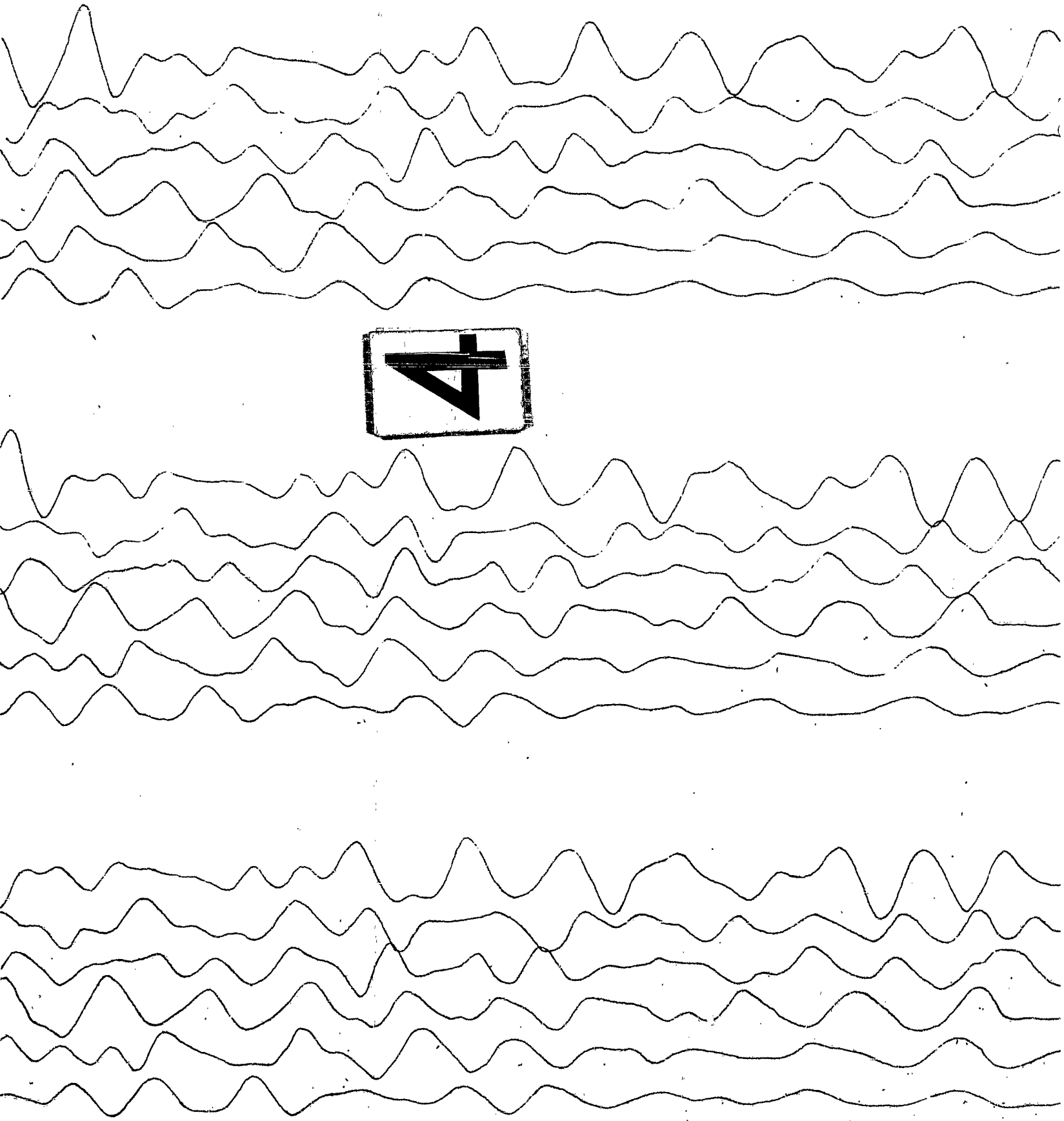

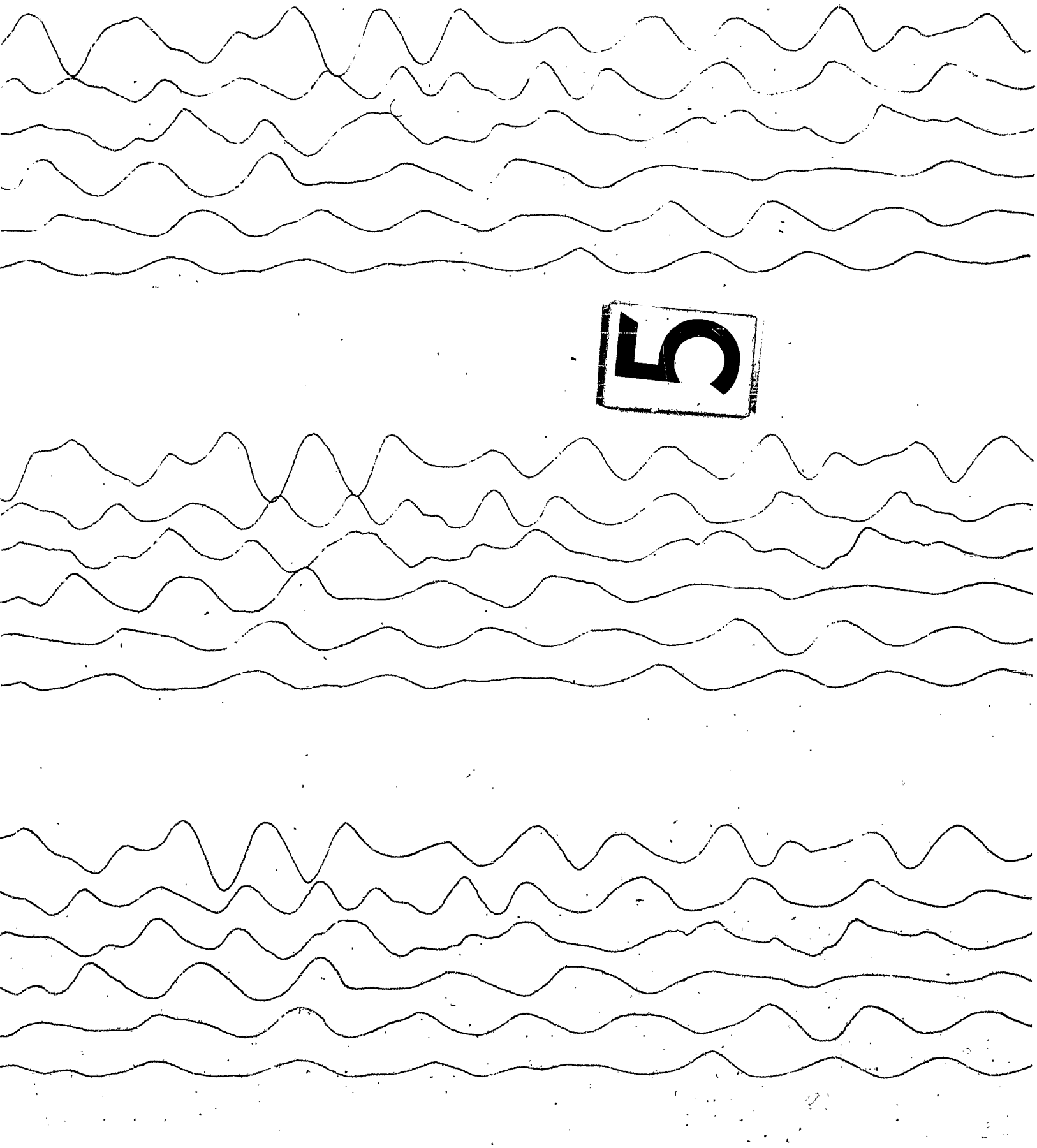

Fig. 11.12 Horizontal Seismic Ranging Recording Corrected for Moveouts Based on Velocities of 6000, 8000, and 10000 feet/second

1

R 7 – HR 2
Rays 1 and 5, Traces 1 – 6
Program B

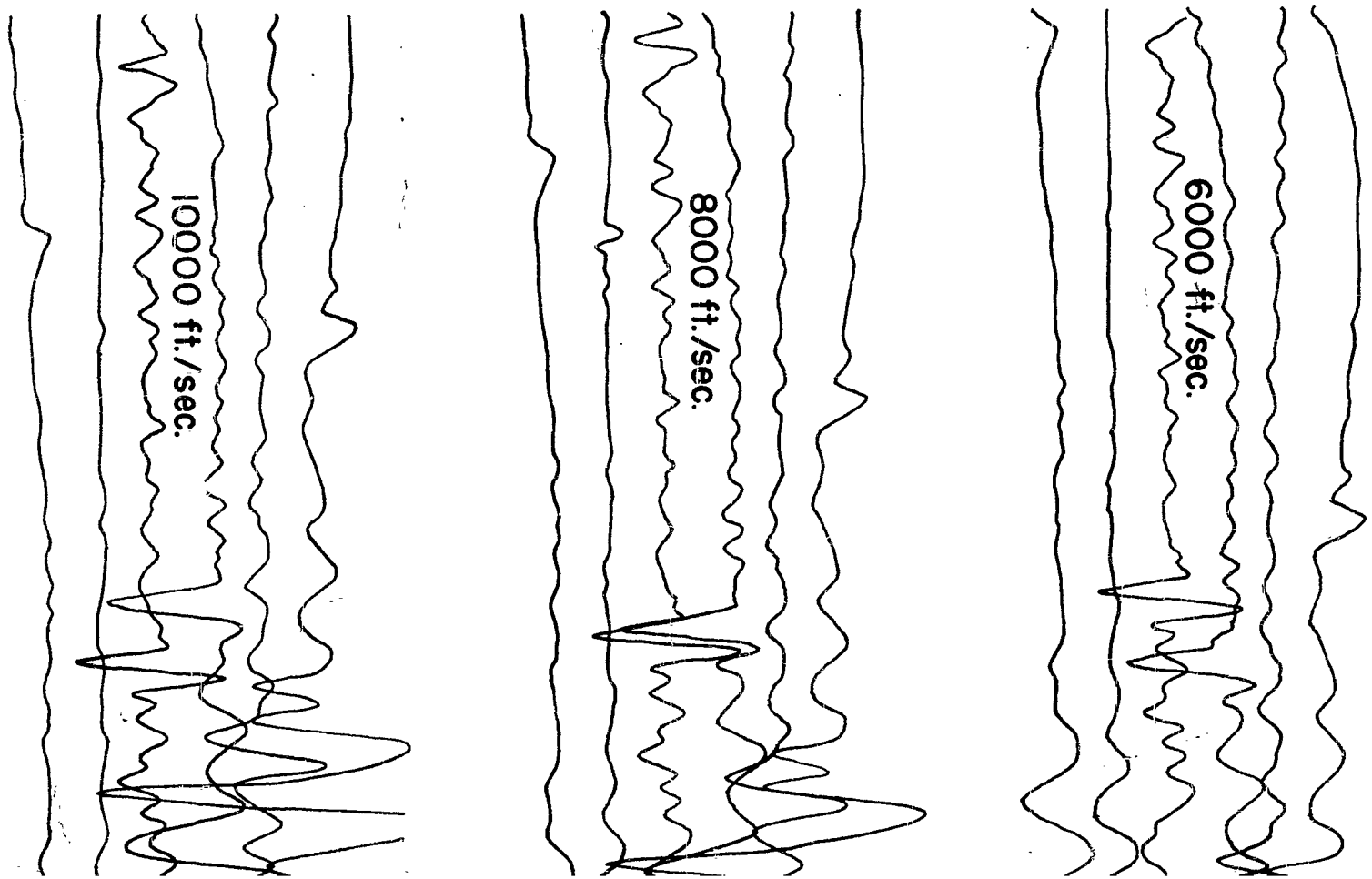

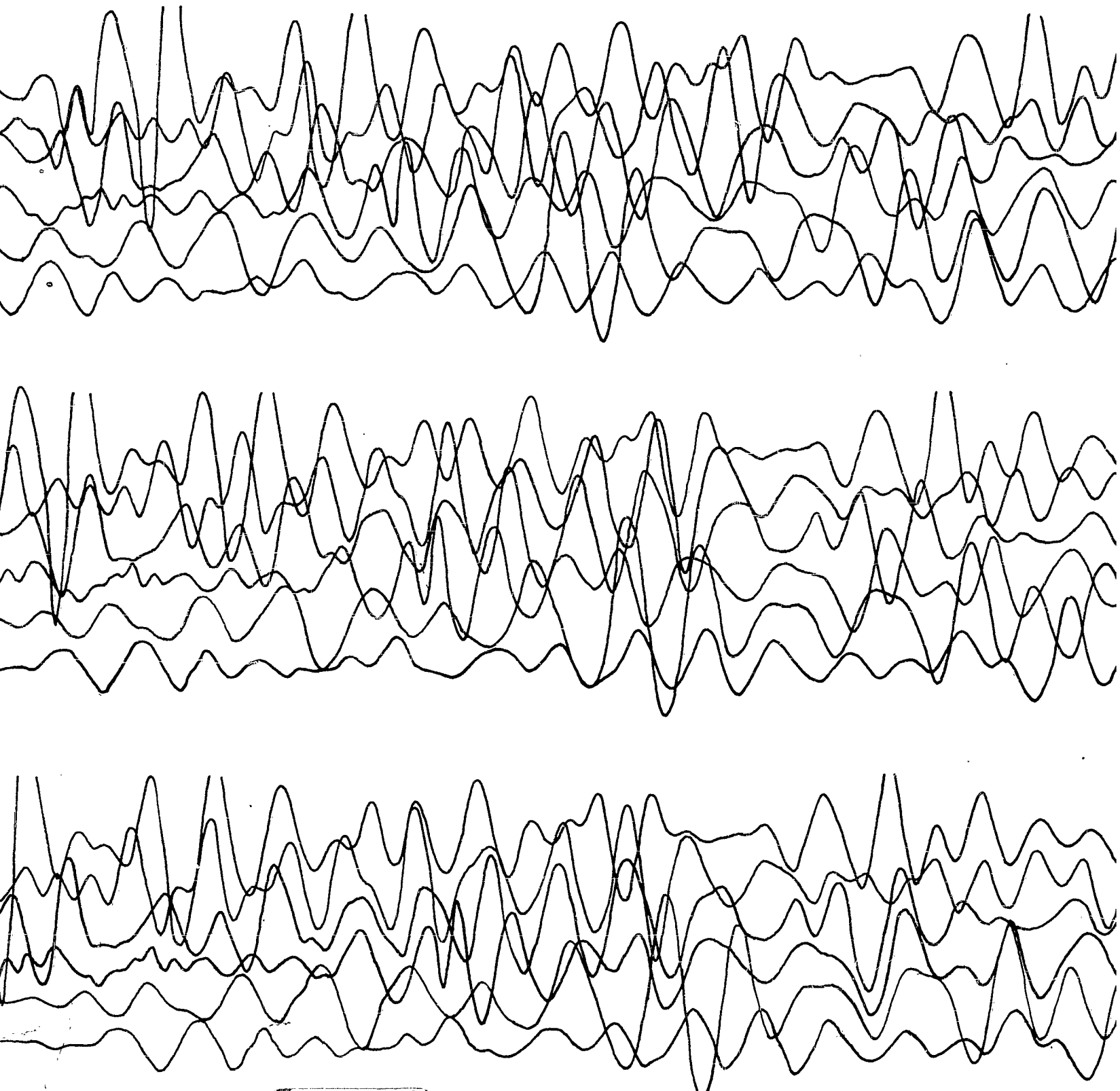

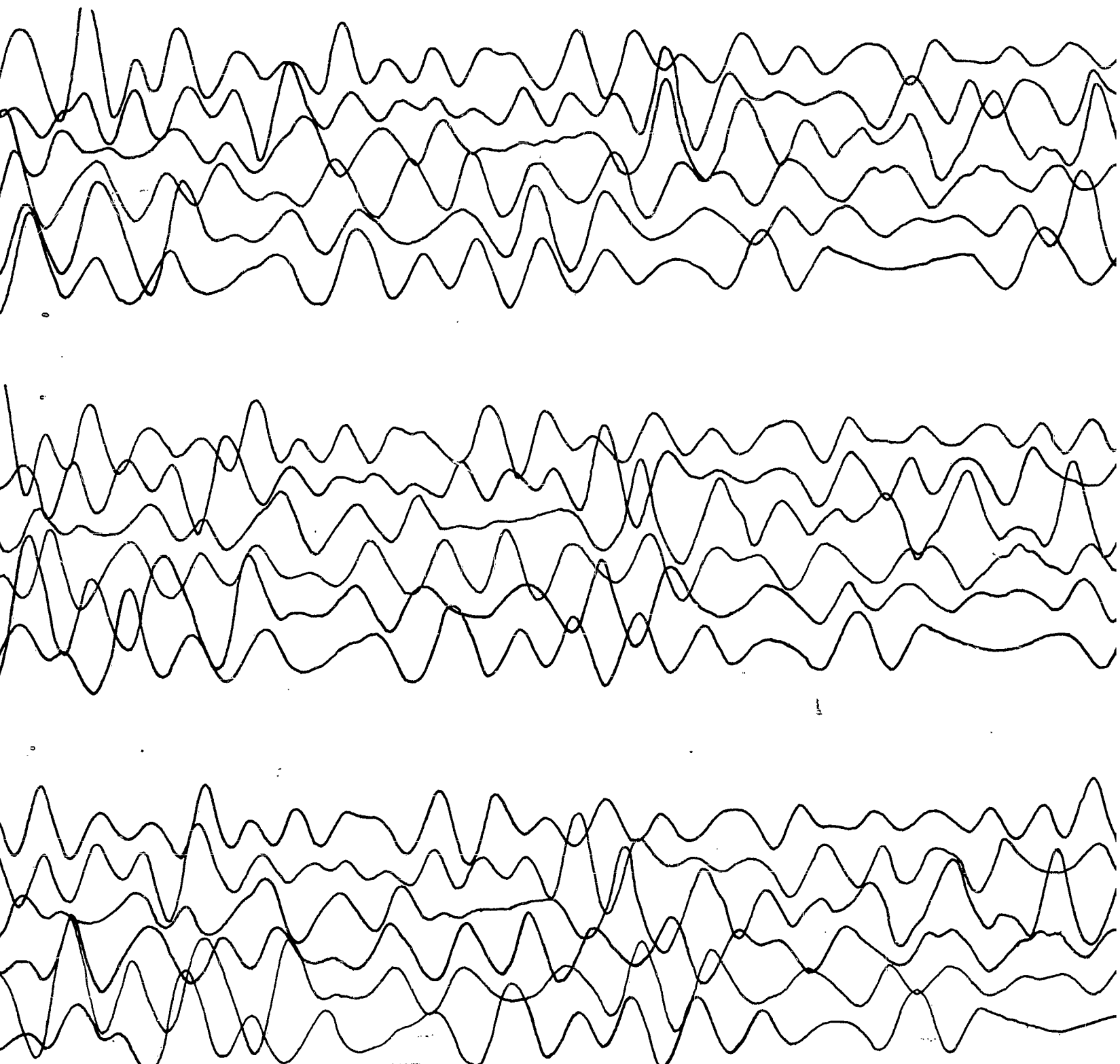

3

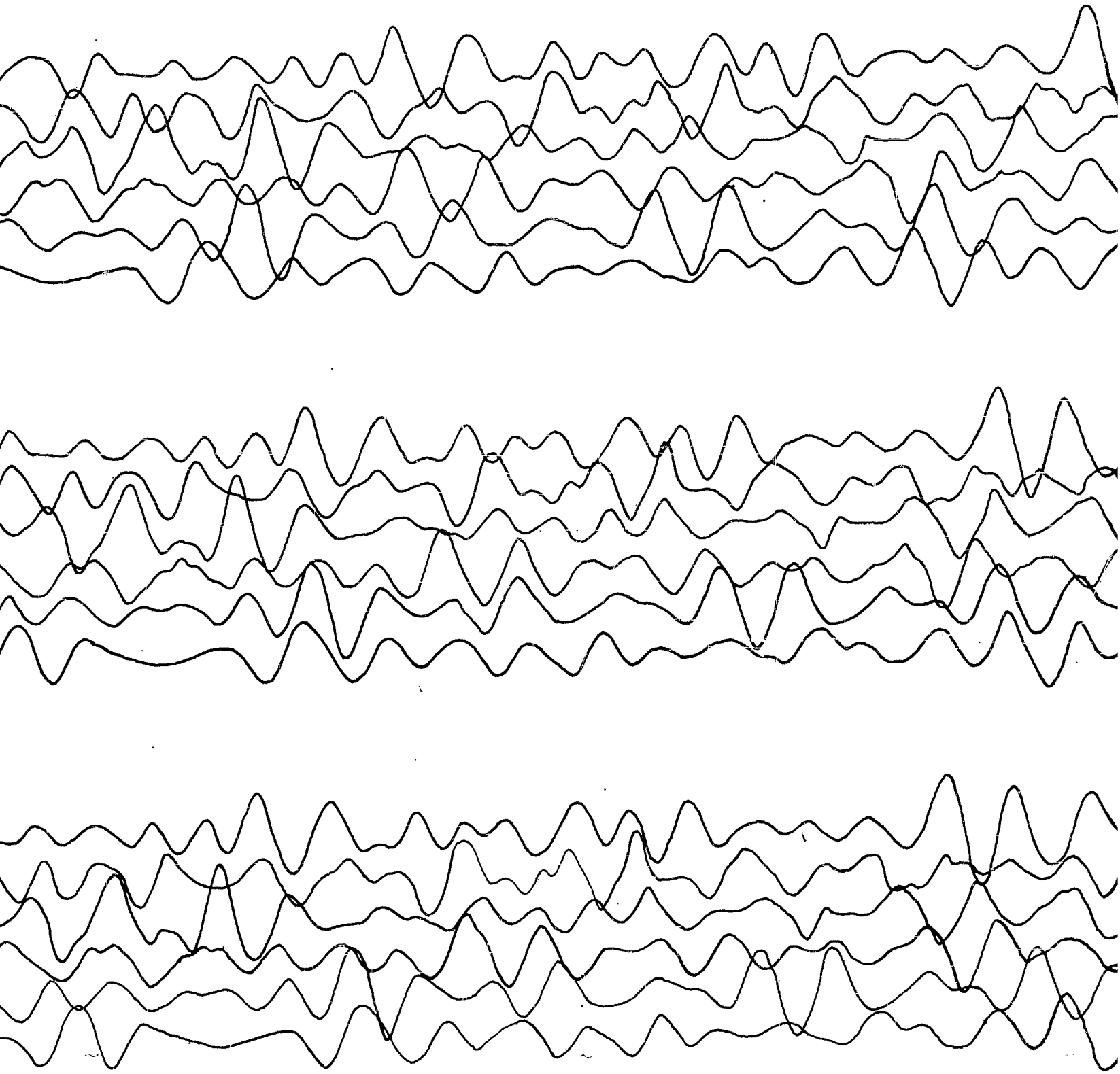

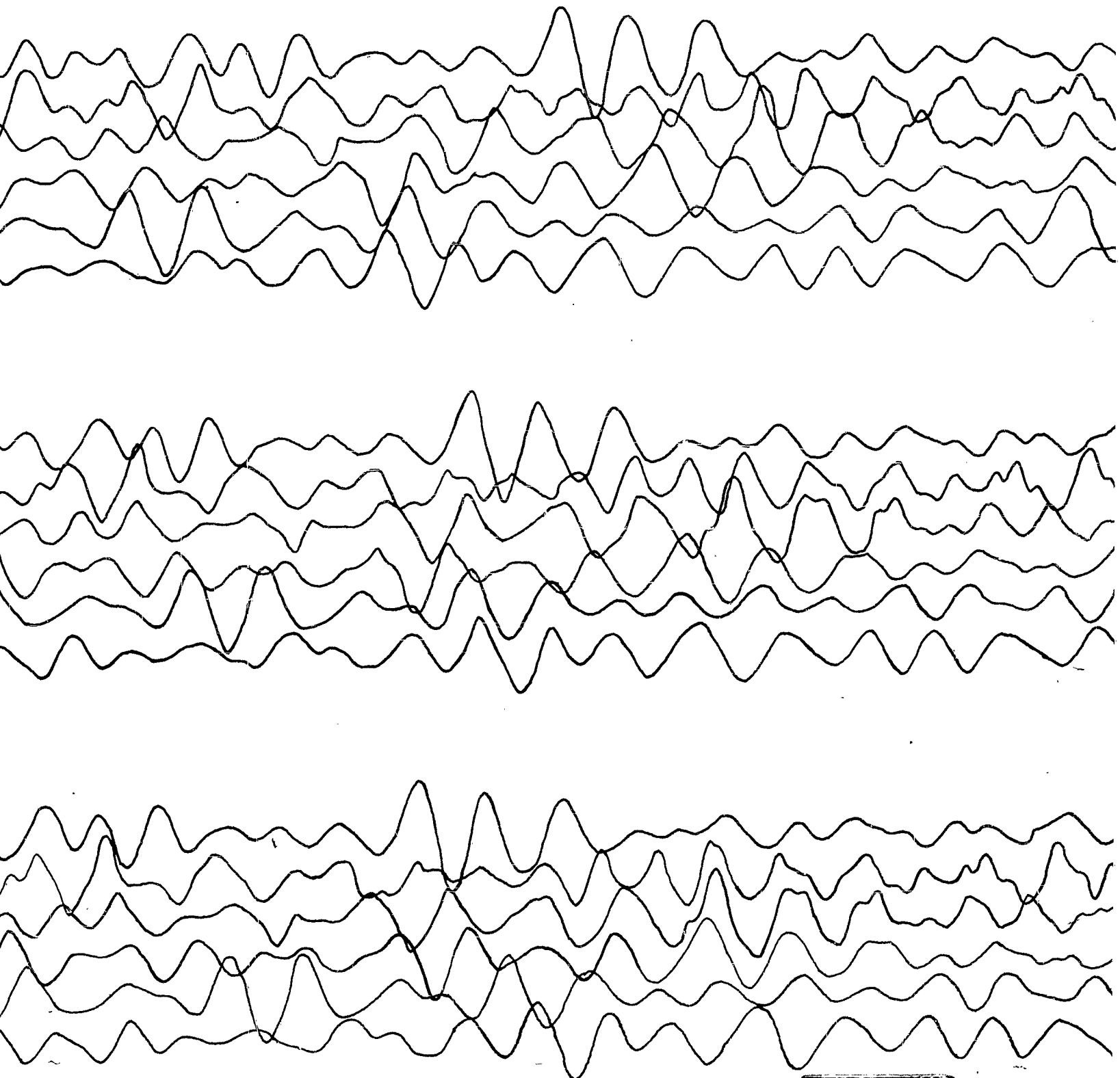

Dry Log

UNITED GEOPHYSICAL

Direction _____ Interlock _____

UNITED GEOPHYSICAL CORPORATION

PROFILE R7-HR2		For AFTAC	
Record A	Date 2-22-61	Location Nye County Nevada	
Party 12	Truck 1110	Inst. 1-32	

Charge		60#	Position	OFFSET DISTANCE	OFFSET DIRECTION	SPREAD DISTANCE	TRACE INTERVAL
Depth of Shot	Top	125	Top Trace				
	Cap	127	Center				
	Bottom	135	Bot. Trace				
Traces	1-24		Shot Point	2390	N7°W		
Mix	none		Tape No.	1292			
Filter Code	1-4		Program	B			
-6db Band	15-85		Rec. Filter	1-4			
Geophone Group	Number	16	Plbk Filt	–			
	Interval	100'	HS-J	28 cps			
	Pattern	4x4	Eccentricity				
t_b			A.R.Number				
t_{sd}							
$t_s = t_b - t_{sd}$							
Filter Corr.							
Ref. Filter							
S.P.G Offset		10'					
Observed t_{uh}							
Corr. to Vert							
Corrected t_{uh}							
V_w							
V_r							
$t_T - t_B$							
$(t_T - t_B)\left(\frac{V_r - V_w}{V_r}\right)$							
$\frac{E_T - E_B}{V_r}$							
D.W.C.							

Sec ____
T ____
R ____

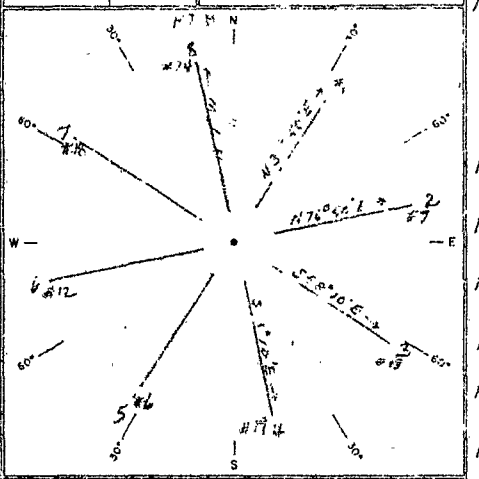

Notes: Wind - 35 Mph., Gusts - 65 M.P.H.
Max. response ∥ to rays.

SHOT POINT GEOPHONE				OFFSET GEOPHONES					
E	7437			E_g			t_f		
D_s				W					
E_s		t_{uh}		E_w			t_w		
D_{sd}		t_{sd}		D_{wd}			t_{wd}		
E_d		t_g		E_d			t_g		

PROSPECT Rainier

PROFILE R7-HR2

1

Pos	Distance From Sat	Elevation
1	[illegible]	7386
2	800	7387
3	400	7400
	-0-	
4	400	7403
5	800	7410
6	1200	7413
7	1200	7368
8	800	7378
9	400	7392
	-0-	
10	400	7400
11	800	7410
12	1200	7421
13	1200	7387
14	800	7385
15	400	7393
	-0-	
16	400	7405
17	800	7423
18	1200	7439
19	1200	7410
20	800	7405
21	400	7404
	-0-	
22	400	7401
23	800	7419
24	1200	7434

t_s	t_g	TOTAL CORR $t_s - t_g$

S13°10'E →

Worked _____ Plotted _____ D.W.C.

Section Ck _____

UNITED

Direction _____ Interlock _____

FIG. 11.13

PRINTED IN U.S.A.

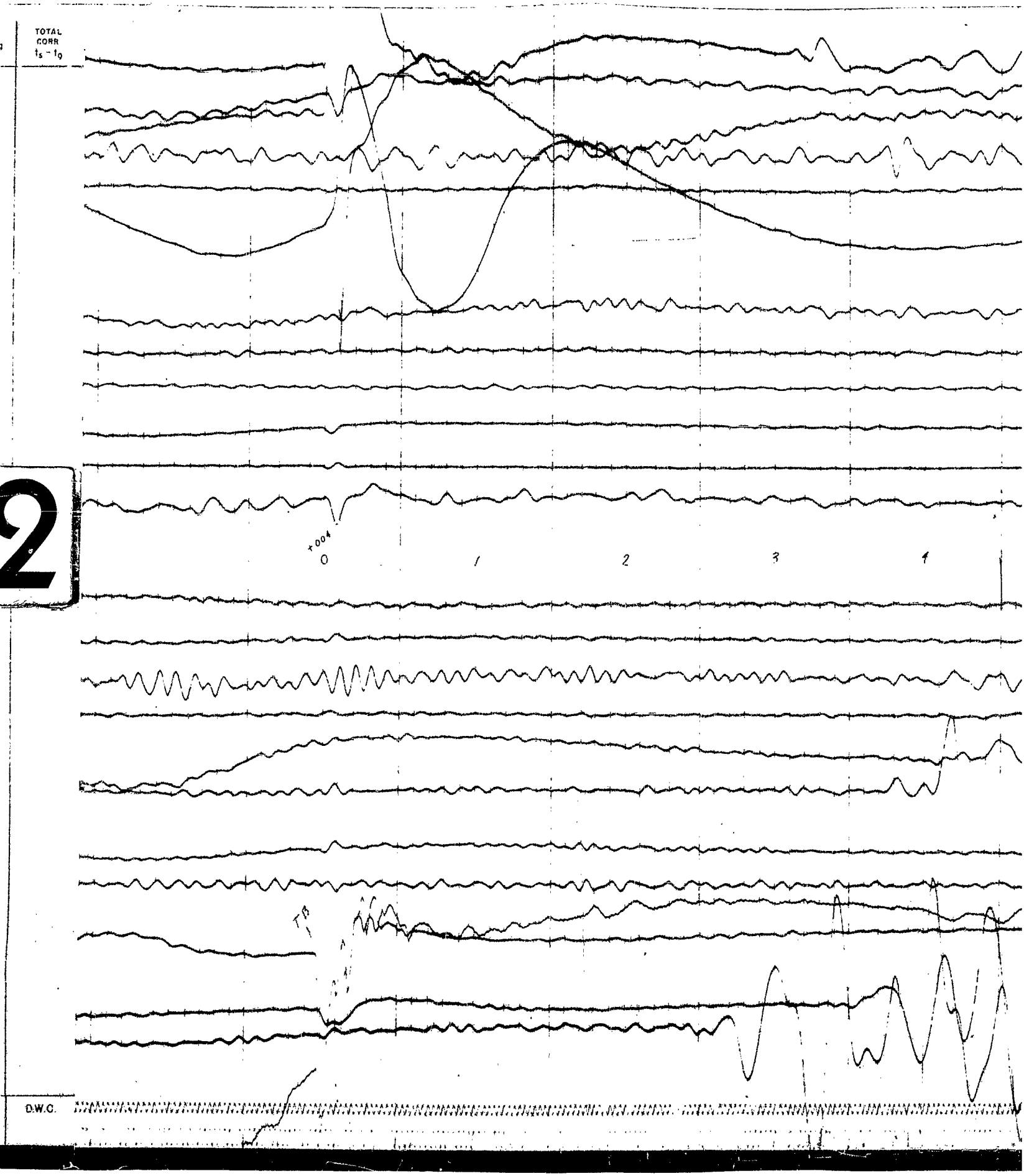
TOTAL
CORR
$t_s - t_g$
+004
0
1
2
3
4
T0
D.W.C.

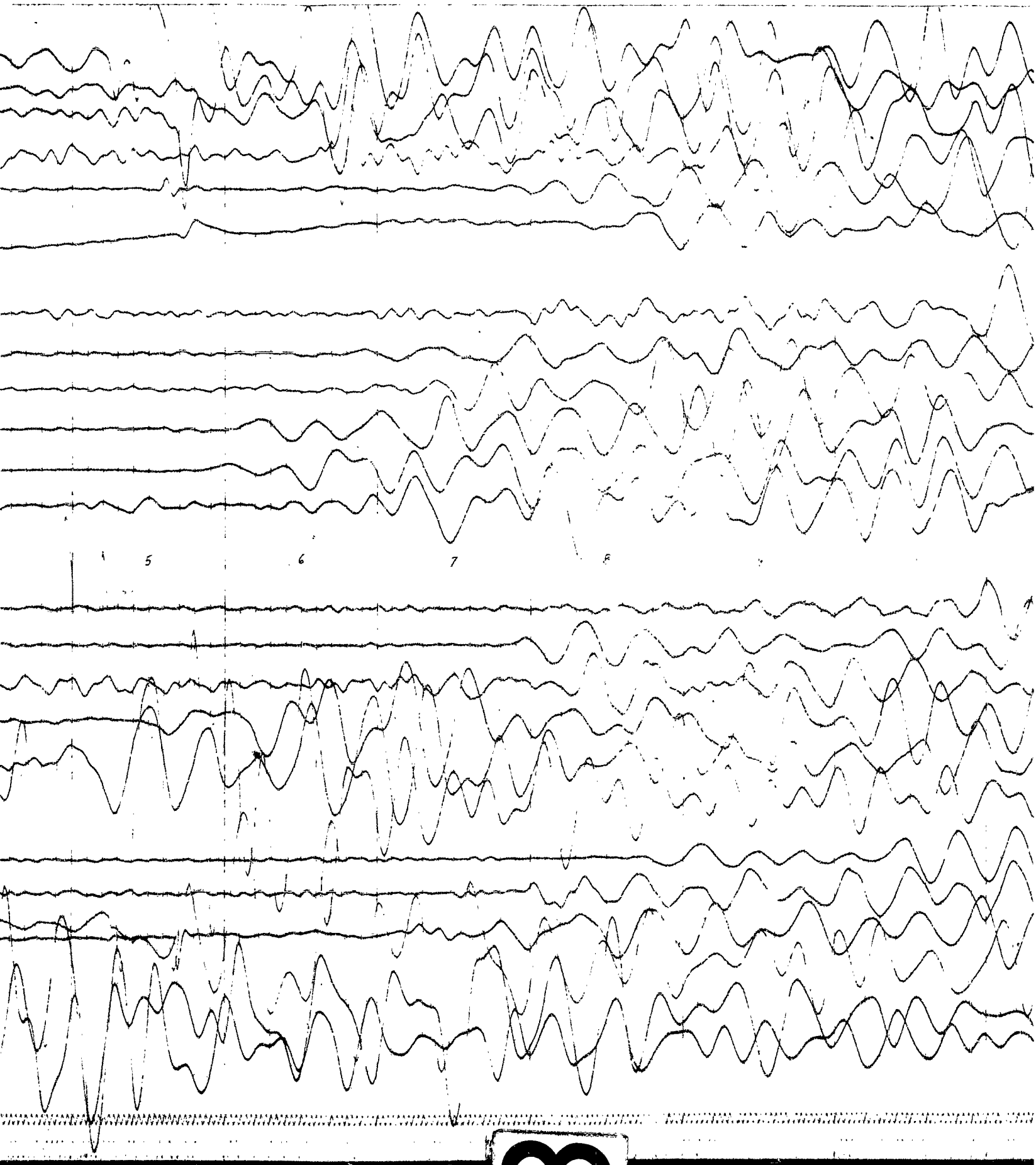
5
6
7
8

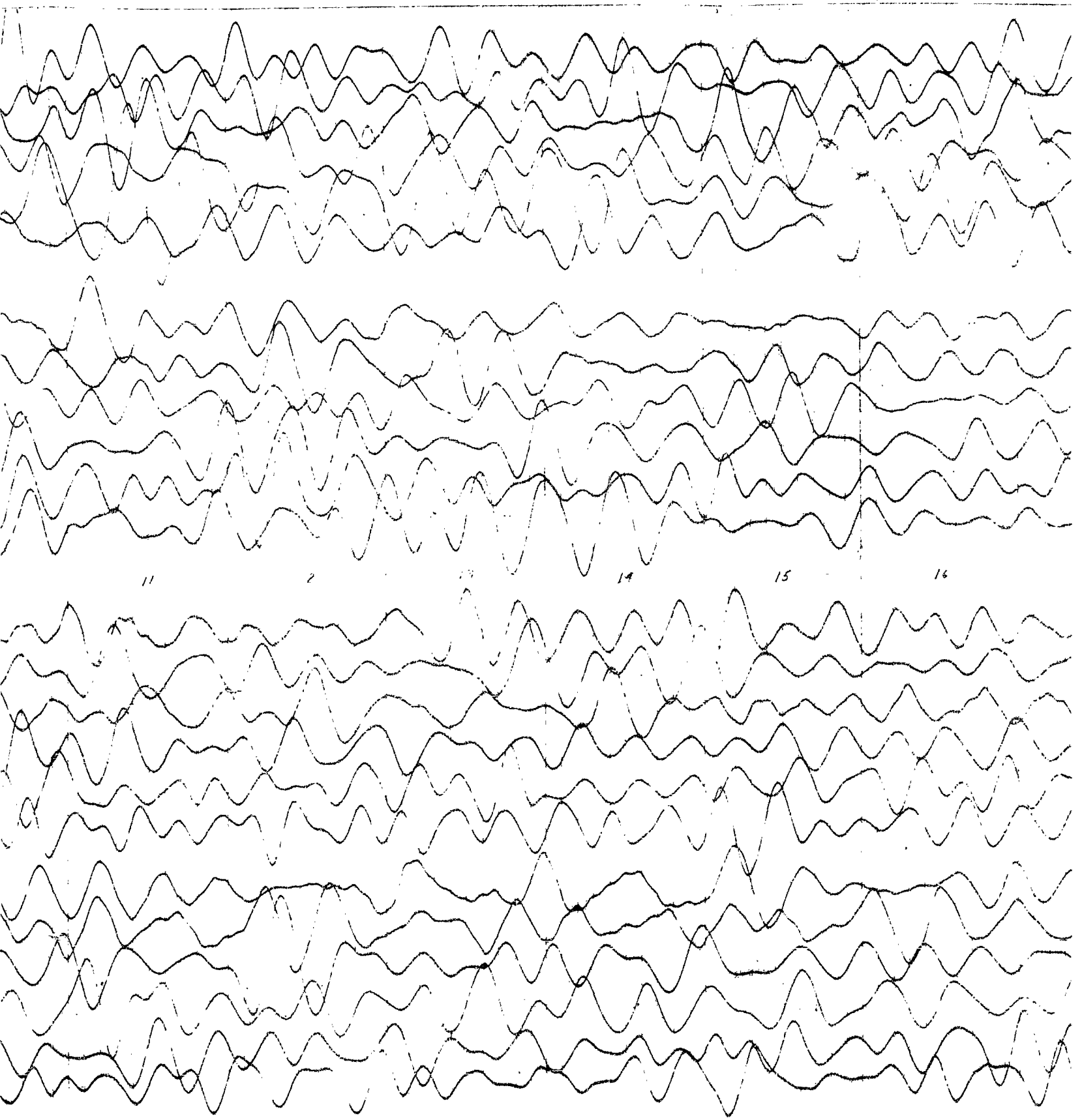
11
14
15
16

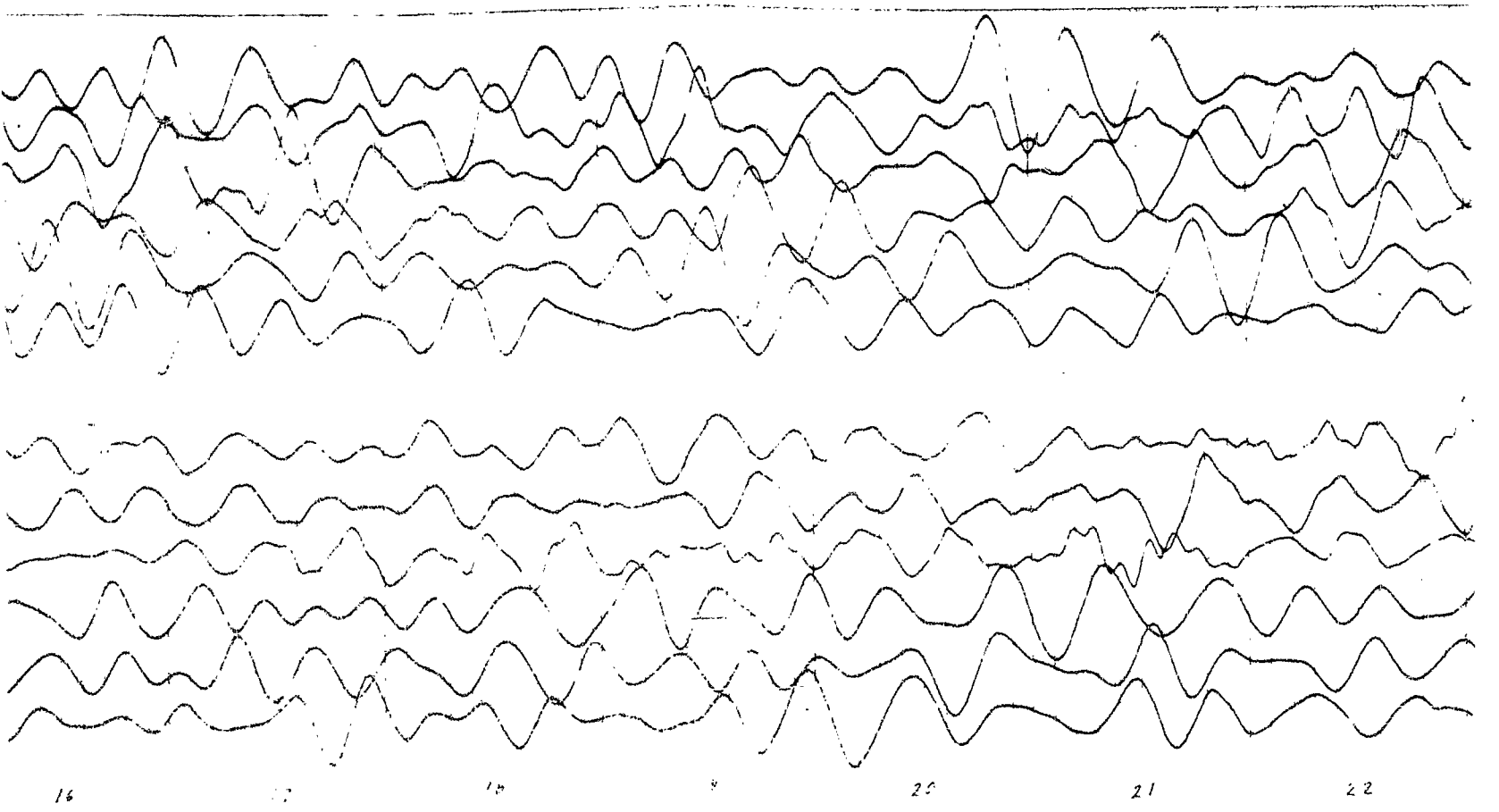

16 17 18 19 20 21 22

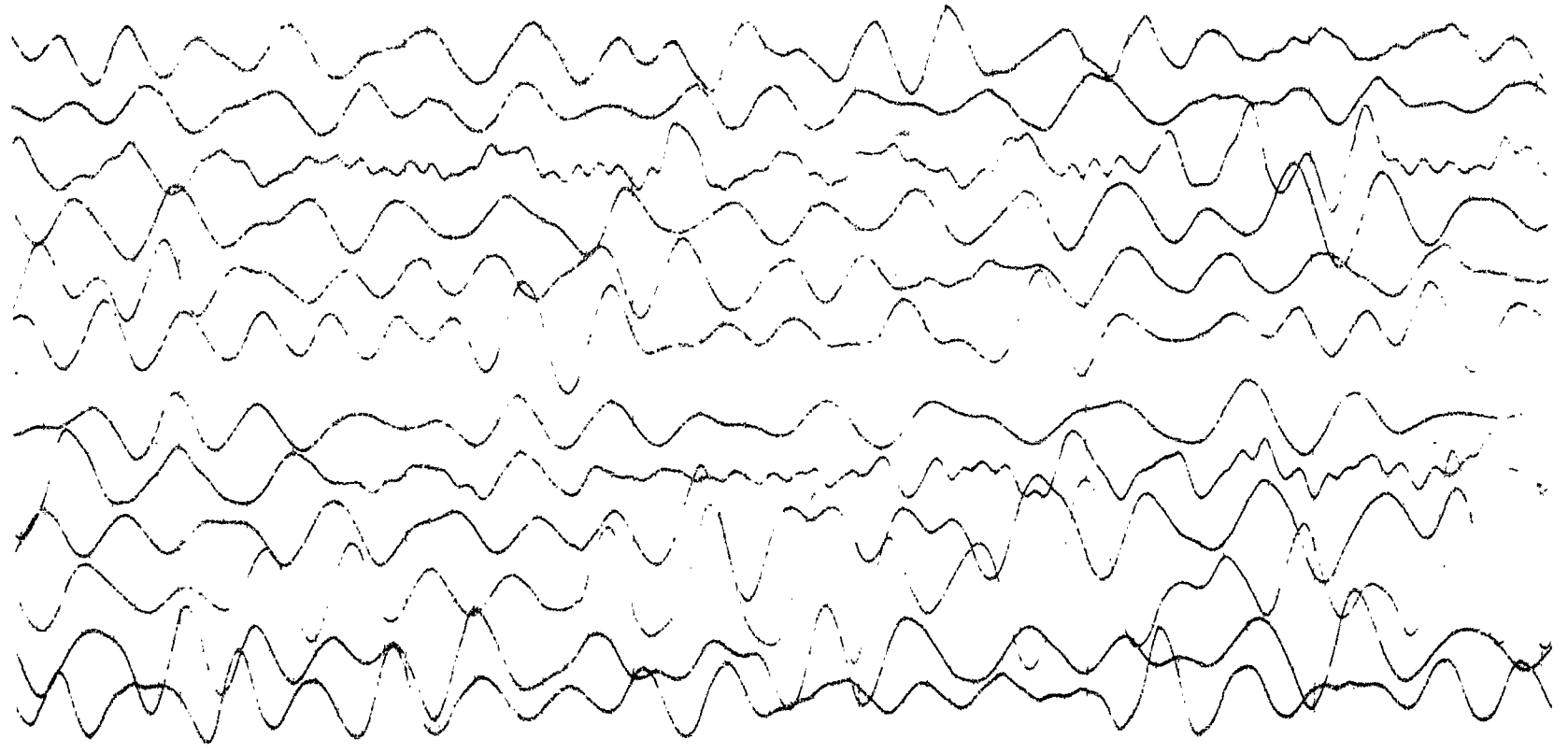

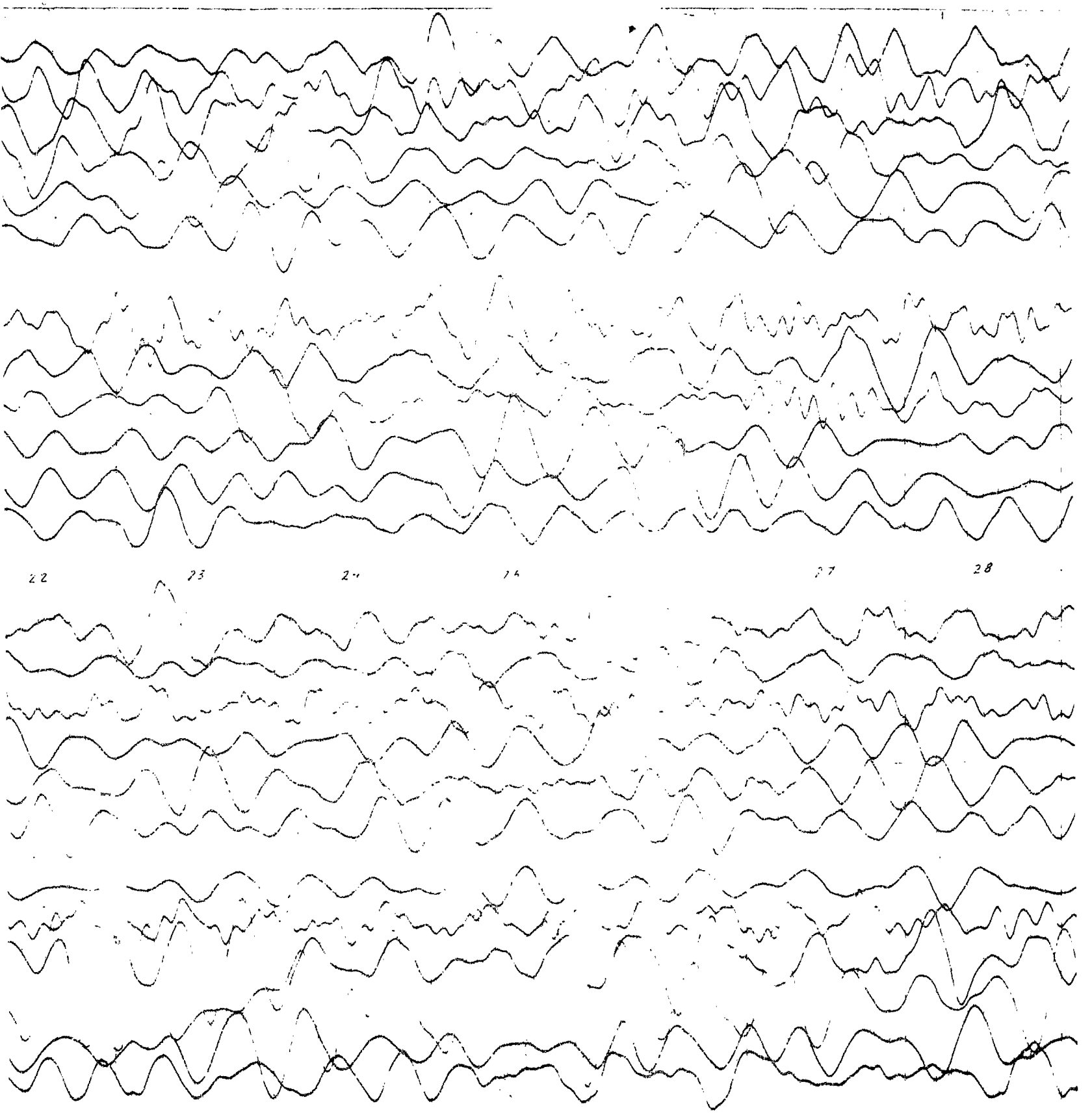
22
23
24
25
27
28

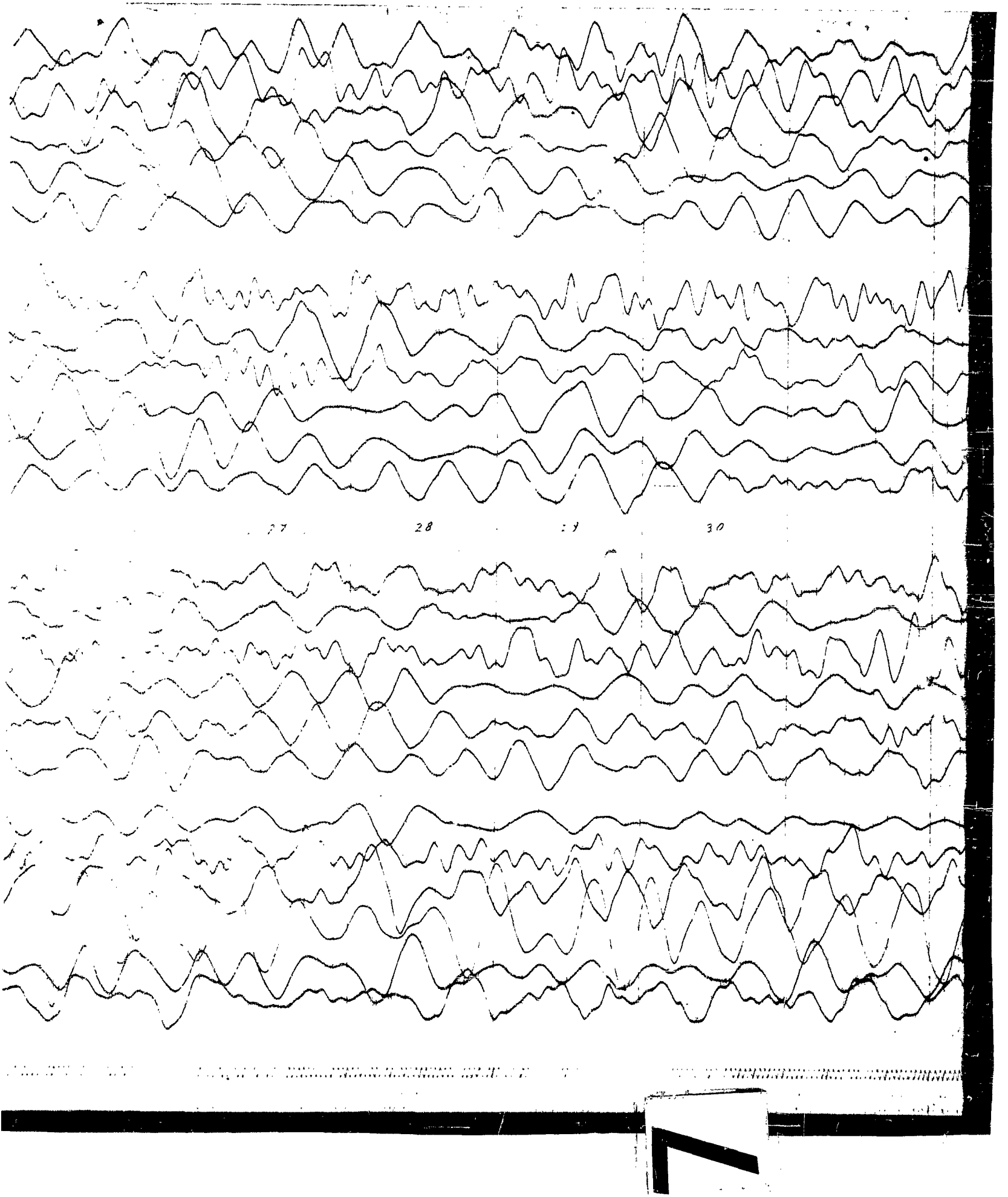
27
28
29
30

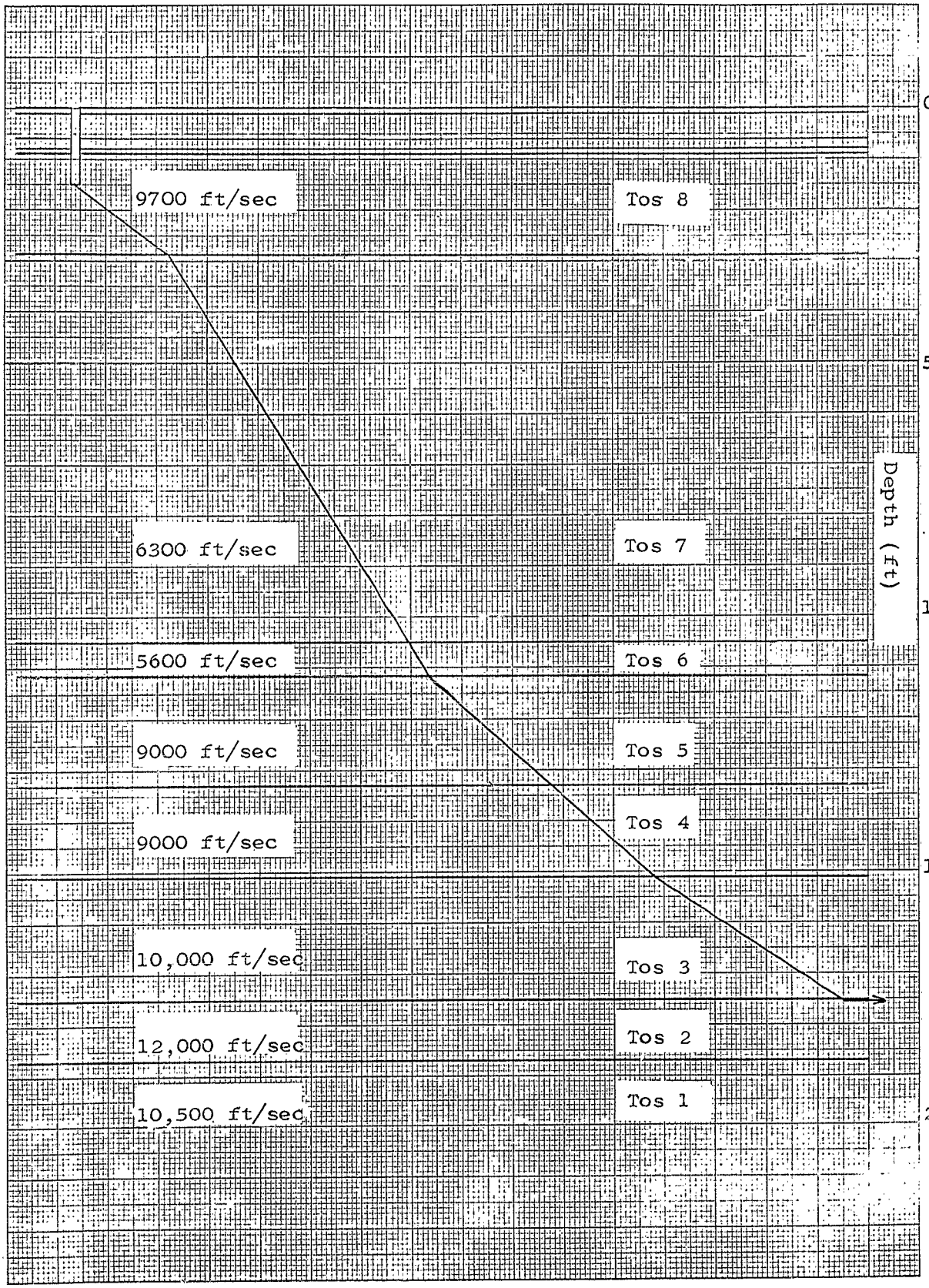

Fig. 11.14

10 X 10 TO THE CM. 358-14
KEUFFEL & ESSER CO. MADE IN U.S.A.

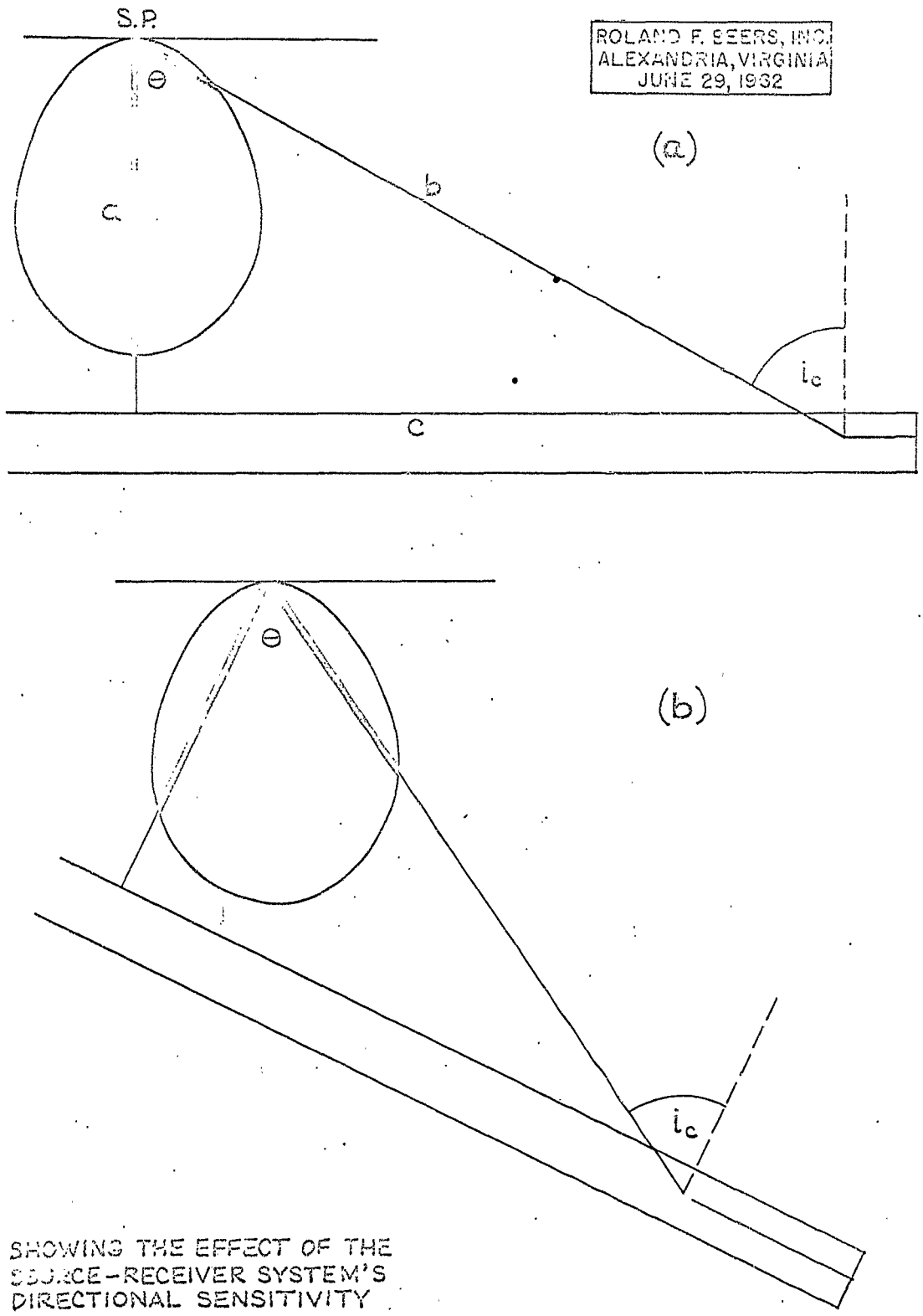

SHOWING THE EFFECT OF THE SOURCE-RECEIVER SYSTEM'S DIRECTIONAL SENSITIVITY

Fig. 11.15

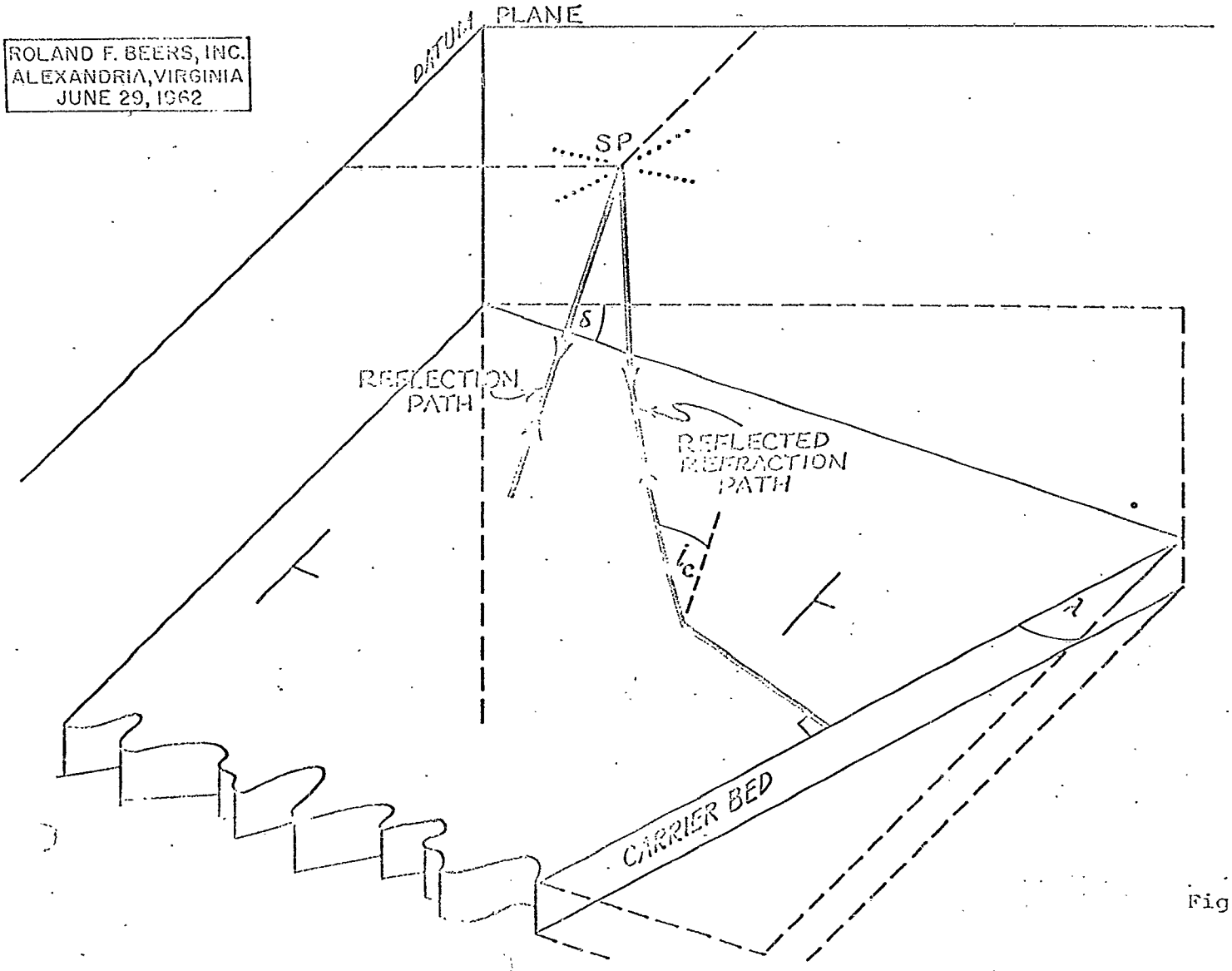
ROLAND F. BEERS, INC.
ALEXANDRIA, VIRGINIA
JUNE 29, 1962
DATUM PLANE
SP
δ
REFLECTION PATH
REFLECTED REFRACTION PATH
i_c
CARRIER BED

Fig. 11.16

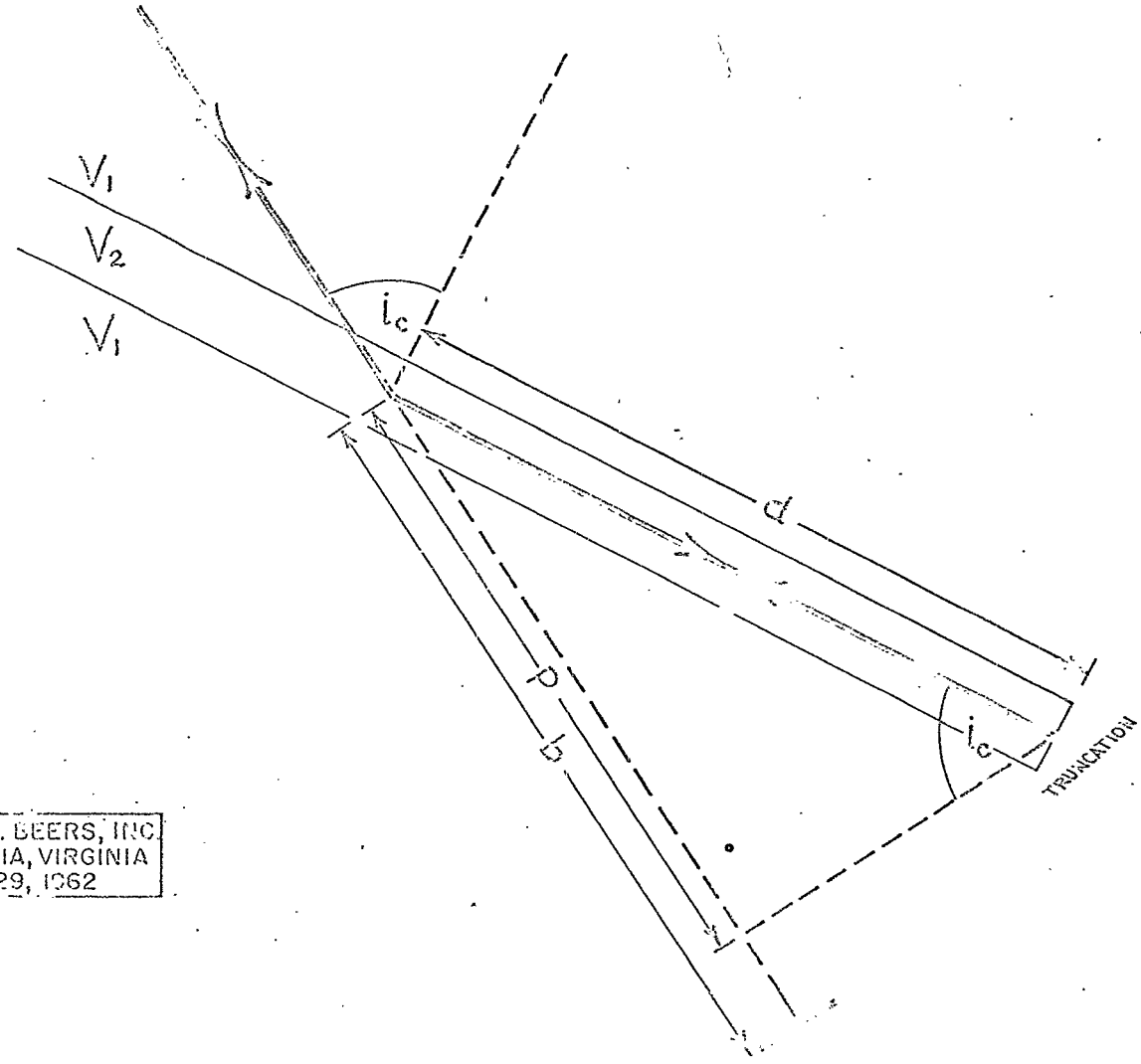

ROLAND F. BEERS, INC.
ALEXANDRIA, VIRGINIA
JUNE 29, 1962

Fig. 11.1

12.0 Tatum Salt Dome

The purpose of the Tatum Salt Dome survey was to provide seismic and geologic data concerning the configuration of the top of the salt, the caprock, and the overlying sediments prior to the execution of an underground nuclear test program. The survey consisted of a total of 110 profiles on two lines, one northwest-southeast, the other northeast-southwest across the top of the dome. Enclosure 3 shows specific locations of all shot points with respect to the dome.

Although individual events range from good to poor in grade, overall record quality is essentially poor when the continuity of events is considered. Extensive phasing inhibits record to record correlation and thereby reduces the reliability with which the configurations of the various horizons can be delineated.

Velocity control on top of and in the immediate vicinity of the salt dome is extensive and of fairly good quality. Examination of the velocity functions obtained at various locations indicates the expected areal variation. No attempt has been made to incorporate this areal variation into the interpretation. Instead, an average velocity function $V_z = 6100 + .7z$ (representative of the applicable velocity data) has been employed to simplify the computations. This function appears to provide an acceptably accurate description of the velocity gradient from the datum (+200') to the top of the limestone caprock. Shot to datum corrections were made using a velocity of 6000 feet per second which is based on five uphole surveys (Figures 12.1 - 12.5). Depth computations for horizons below the limestone caprock are based on velocities taken from sonic logs in the WP-1 and WP-4 holes (on top of the dome proper). The sonic logs in these holes indicate that the average velocity in the limestone caprock and anhydrite is respectively 9,000 and 19,000 feet per second. It should be noted, however, that while the average velocity of the limestone is 9,000 feet per second at these two locations, there is considerable variation in interval velocity which could lead to localized

errors in the depth computations. The velocity in the anhydrite is very uniform and little error in the depth computations is anticipated from this source.

The basis for identifying events on the records was close correlation between core hole depths and the depths obtained for various reflection times, using the foregoing velocity information. Although there is some mistie in depth, this is probably attributable to the difference in time between the onset of a signal and the point of maximum trace deflection.

The strongest reflection on the records correlates with the top of the anhydrite. This is as expected, since the largest velocity contrast is found at the interface between the limestone and anhydrite. Though the limestone and salt reflections are weaker than the anhydrite reflection, it has still been possible to follow these events over the greater part of the survey via record to record correlation.

As expected, very little reflection information was recorded on the records following the arrival of the salt reflection. The few events which were picked and which are shown on the cross-section are of poor to questionable quality. Although these events may have their origin in the salt due to the presence of impurities, it is more likely they originate with multiple or offside reflections.

Shown in cross-section form (see Enclosures 4 and 5) are the configurations in time of the various reflection horizons recorded on the two lines of seismic profiles across the Tatum Salt Dome. Also indicated on these cross-sections are the identities of the principal mapping horizons, beginning with the limestone caprock. Figures 12.6 and 12.7 show the configuration of the three mapping horizons, from the limestone caprock down to the top of the salt in depth.

Examination of the limestone caprock, top of the anhydrite and top of the salt on the depth section shows that the top of the dome and overlying sedimentary section may be considered to be essentially flat. The slight increase in relief with depth, commencing from the top of the anhydrite, is normal.

However, there is also the possibility that the additional relief accrues from the use of an average velocity function and deviation from the 9,000 foot per second velocity used for limestone.

Actual ties between core hole and computed depths are erratic but never appreciably different when all factors are considered. At the top of the limestone caprock, maximum variation between computed and core hole depths is 23 feet and averages 4 feet below actual. At the top of the anhydrite, maximum variation between core hole and computed depth is 34 feet and averages 10 feet above actual. At the top of the salt, maximum variation between core hole and computed depth is 112 feet and averages 78 feet below actual. These results indicate that the velocity used for the limestone is slightly lower than actual and that the velocity used for anhydrite is higher than actual. The depth discrepancy at these horizons may be corrected by application of an areal factor.

It will be noted that the sections have been interrupted at the approximate edges of the dome. This is due to the severe deterioration in the quality of the individual reflections. In lieu of making a questionable interpretation, we have chosen to interrupt the section.

The estimated edges shown on the sections, while agreeing qualitatively with the results of the survey, are based on information presented by the United States Geological Survey in Technical Letter: Dribble I. Quantitative resolution of this problem requires cross-spreads and migration of the data. However, considering the poor quality of the records, it is doubted that a definitive interpretation could be made.

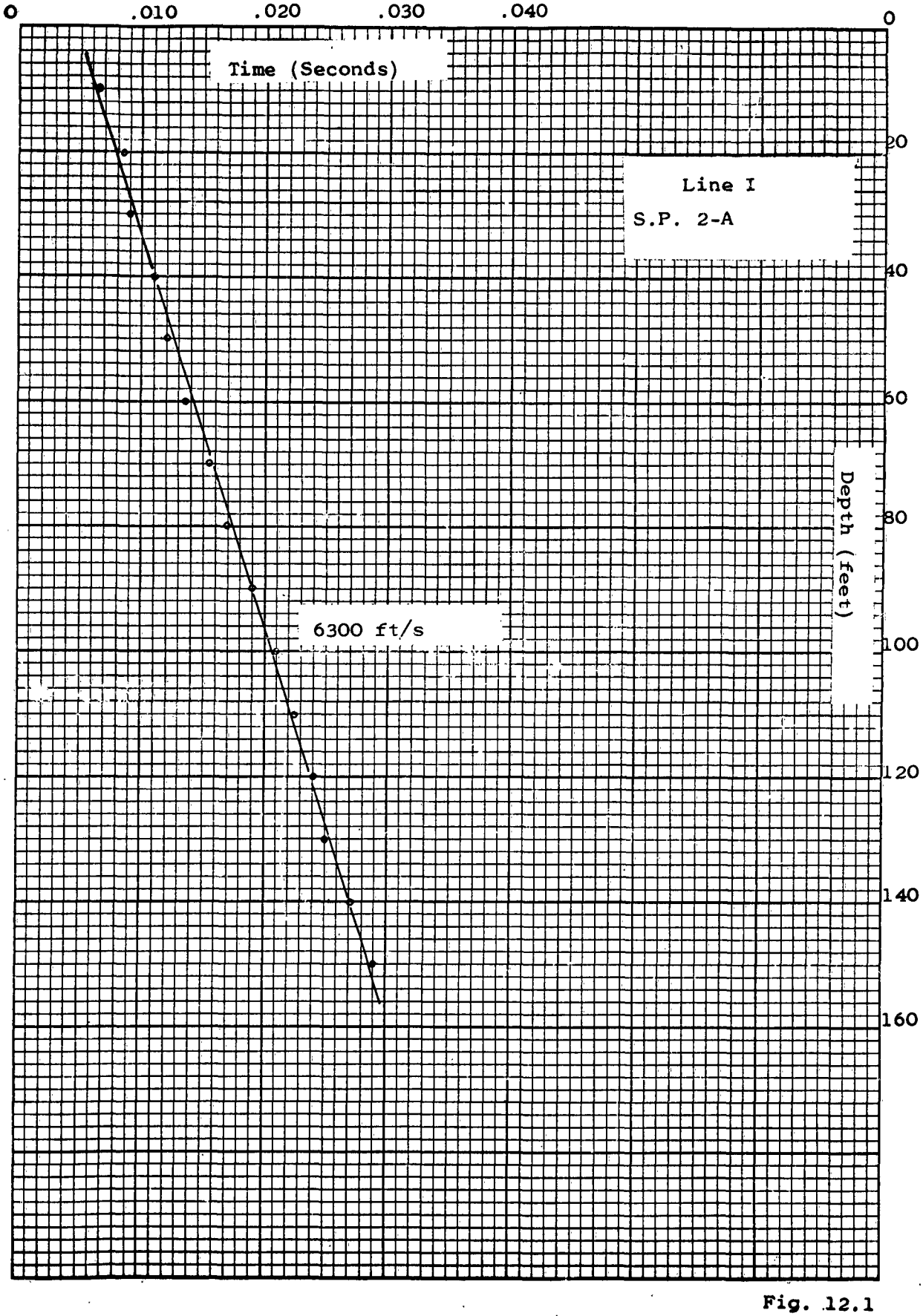
0
.010
.020
.030
.040
0
Time (Seconds)
20
Line I
S.P. 2-A
40
60
Depth (feet)
80
6300 ft/s
100
120
140
160

Fig. 12.1

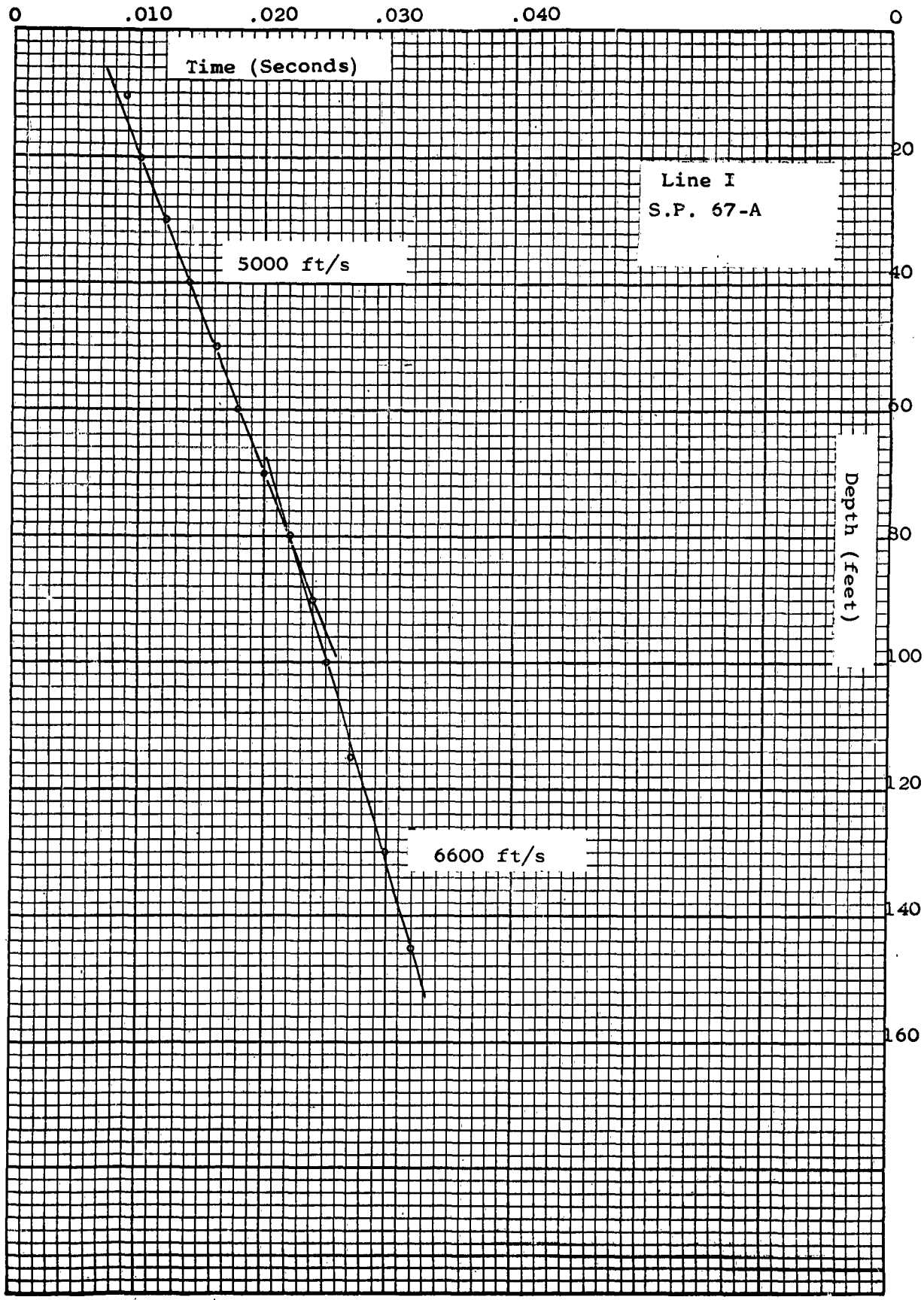
0
.010
.020
.030
.040
0
Time (Seconds)
Line I
S.P. 67-A
5000 ft/s
6600 ft/s
Depth (feet)
20
40
60
80
100
120
140
160
10 X 10 TO THE INCH 359-5
KEUFFEL & ESSER CO.
MADE IN U.S.A.

Fig. 12.2

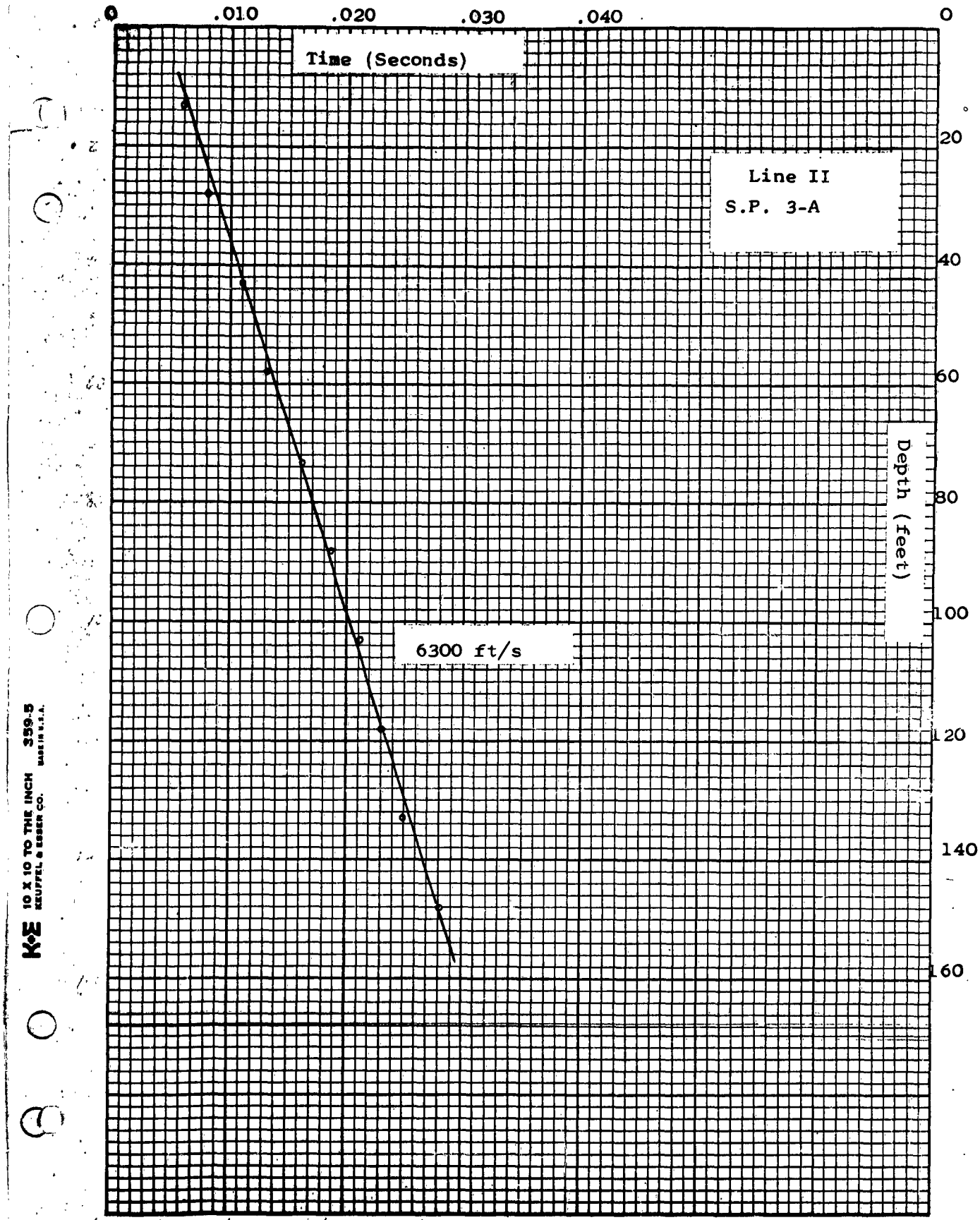
0
.010
.020
.030
.040
0
Time (Seconds)
Line II
S.P. 3-A
20
40
60
80
100
120
140
160
Depth (feet)
6300 ft/s
10 X 10 TO THE INCH 359-5
KEUFFEL & ESSER CO. MADE IN U.S.A.
K&E

Fig. 12.3

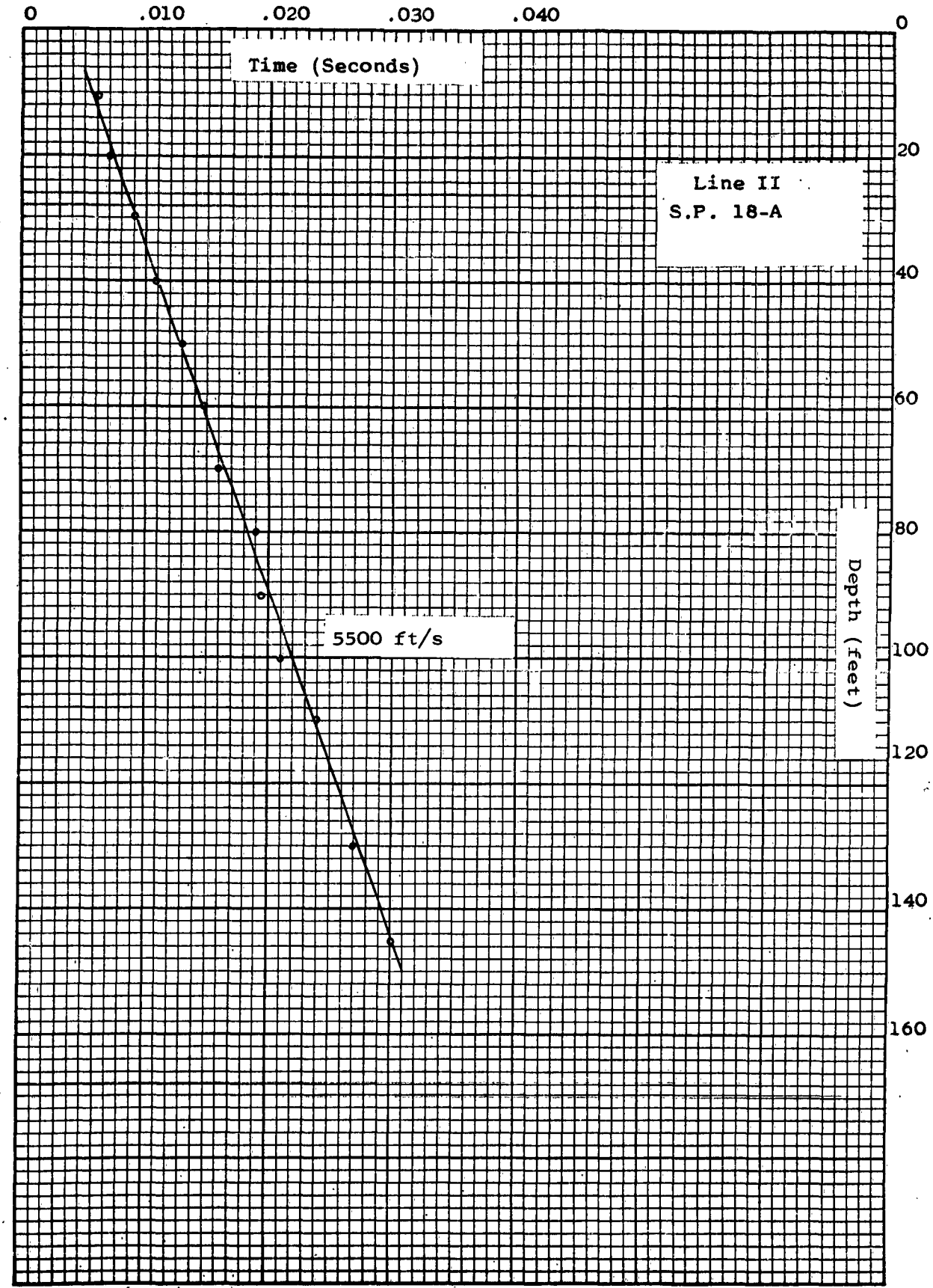
0
.010
.020
.030
.040
Time (Seconds)
Line II
S.P. 18-A
5500 ft/s
Depth (feet)
0
20
40
60
80
100
120
140
160

Fig. 12.4

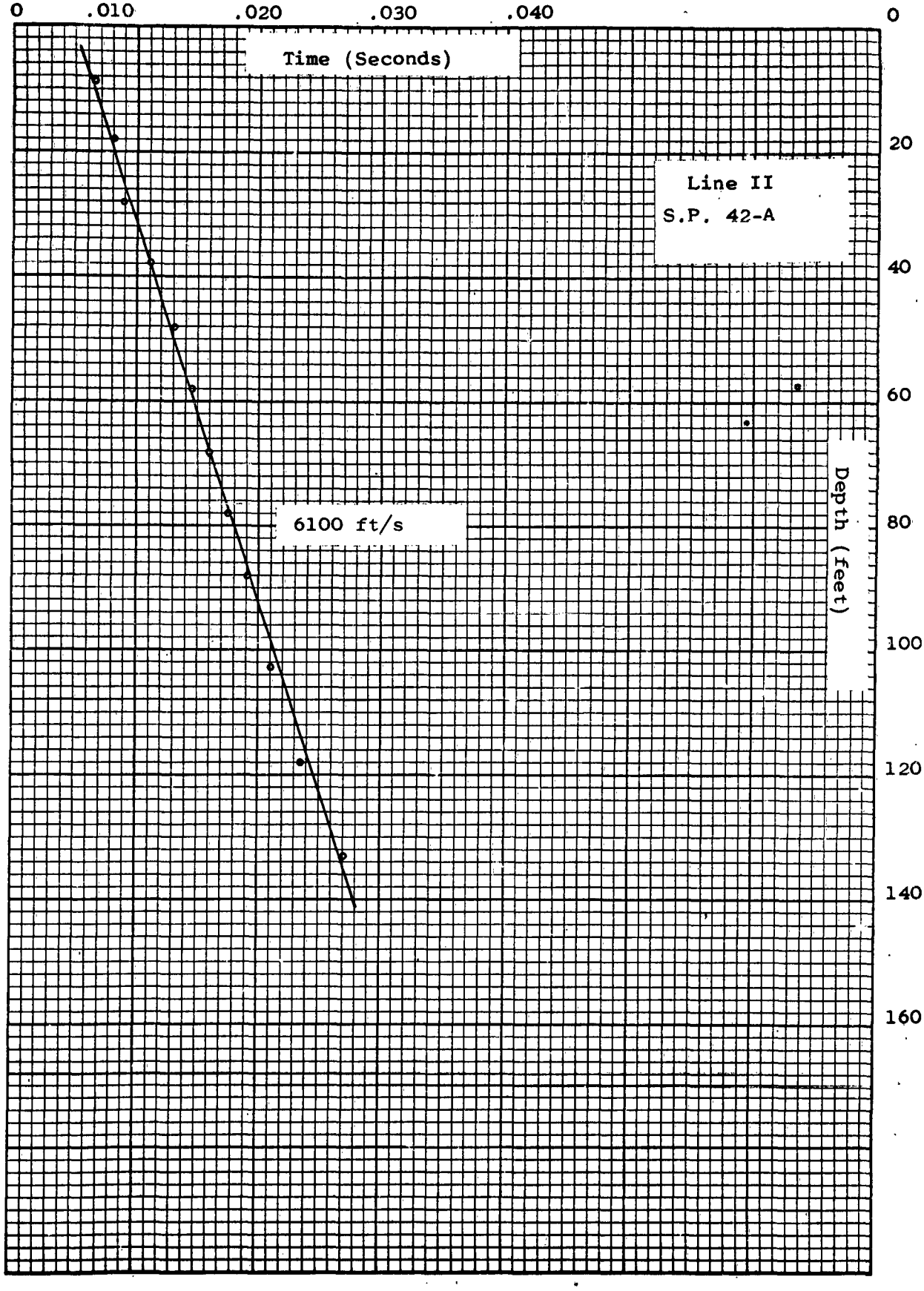
0
.010
.020
.030
.040
0
Time (Seconds)
20
Line II
S.P. 42-A
40
60
Depth (feet)
6100 ft/s
80
100
120
140
160
10 X 10 TO THE INCH 359-5
KEUFFEL & ESSER CO. MADE IN U.S.A.
K&E

Fig. 12.5

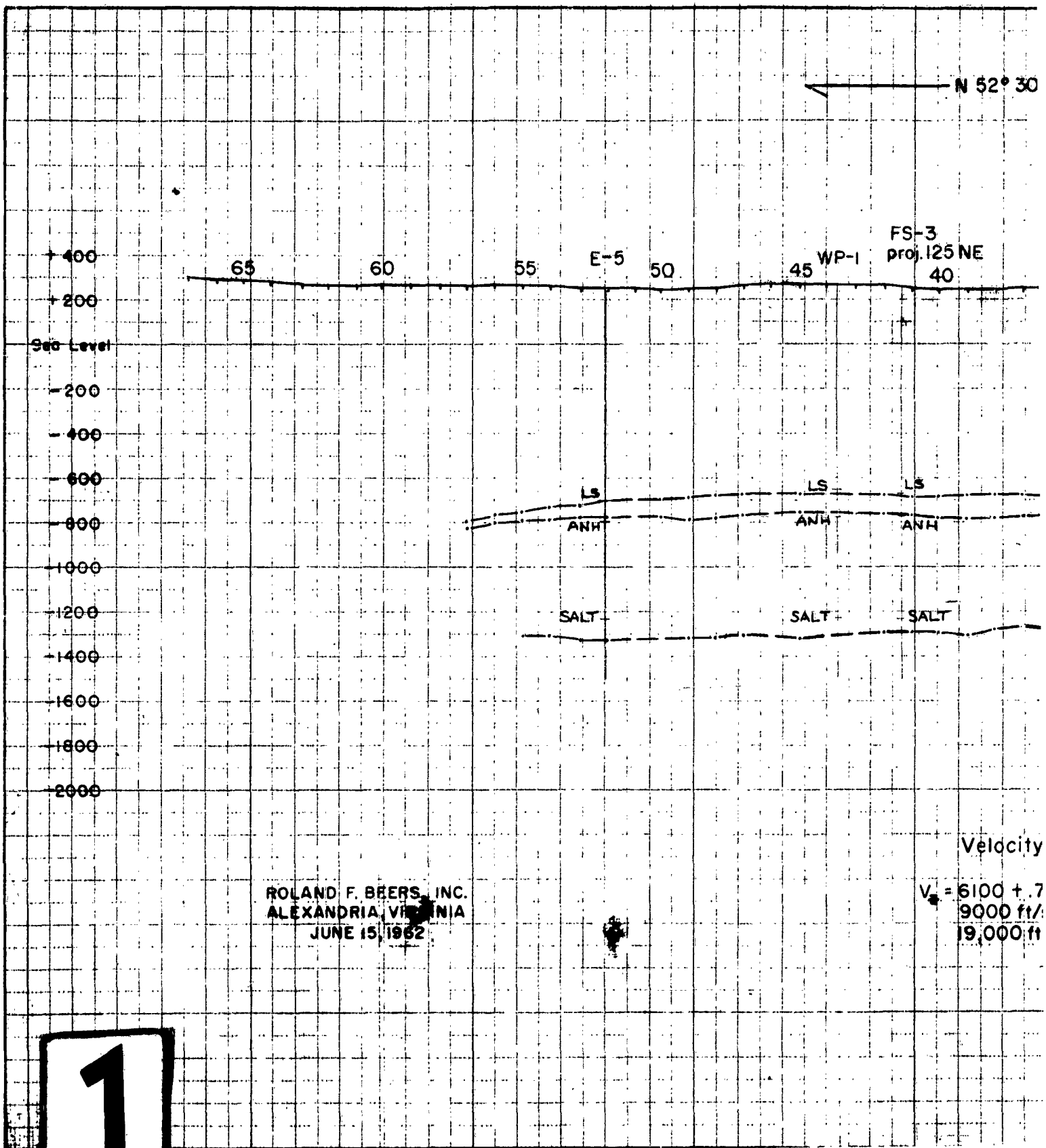
N 52° 30
FS-3
proj. 125 NE
WP-1
E-5
65
60
55
50
45
40
+400
+200
Sea Level
-200
-400
-600
-800
-1000
-1200
-1400
-1600
-1800
-2000
LS
ANH
SALT
Velocity
V = 6100 + .7
9000 ft/
19,000 ft
ROLAND F. BEERS, INC.
ALEXANDRIA, VIRGINIA
JUNE 15, 1962

1

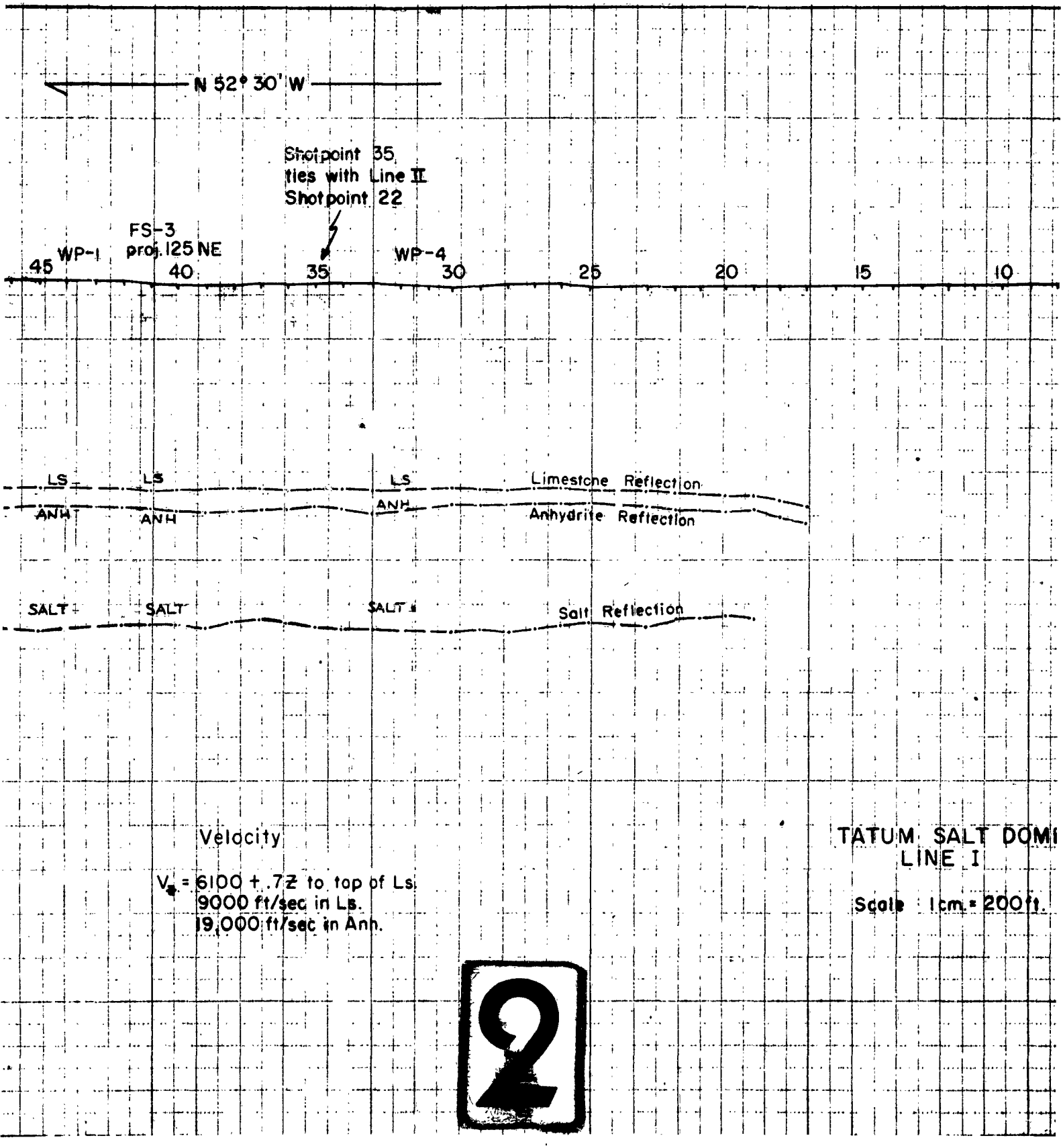

Velocity

V_z = 6100 + .7Z to top of Ls.
9000 ft/sec in Ls.
19,000 ft/sec in Anh.

TATUM SALT DOM
LINE I

Scale 1cm = 200ft.

2

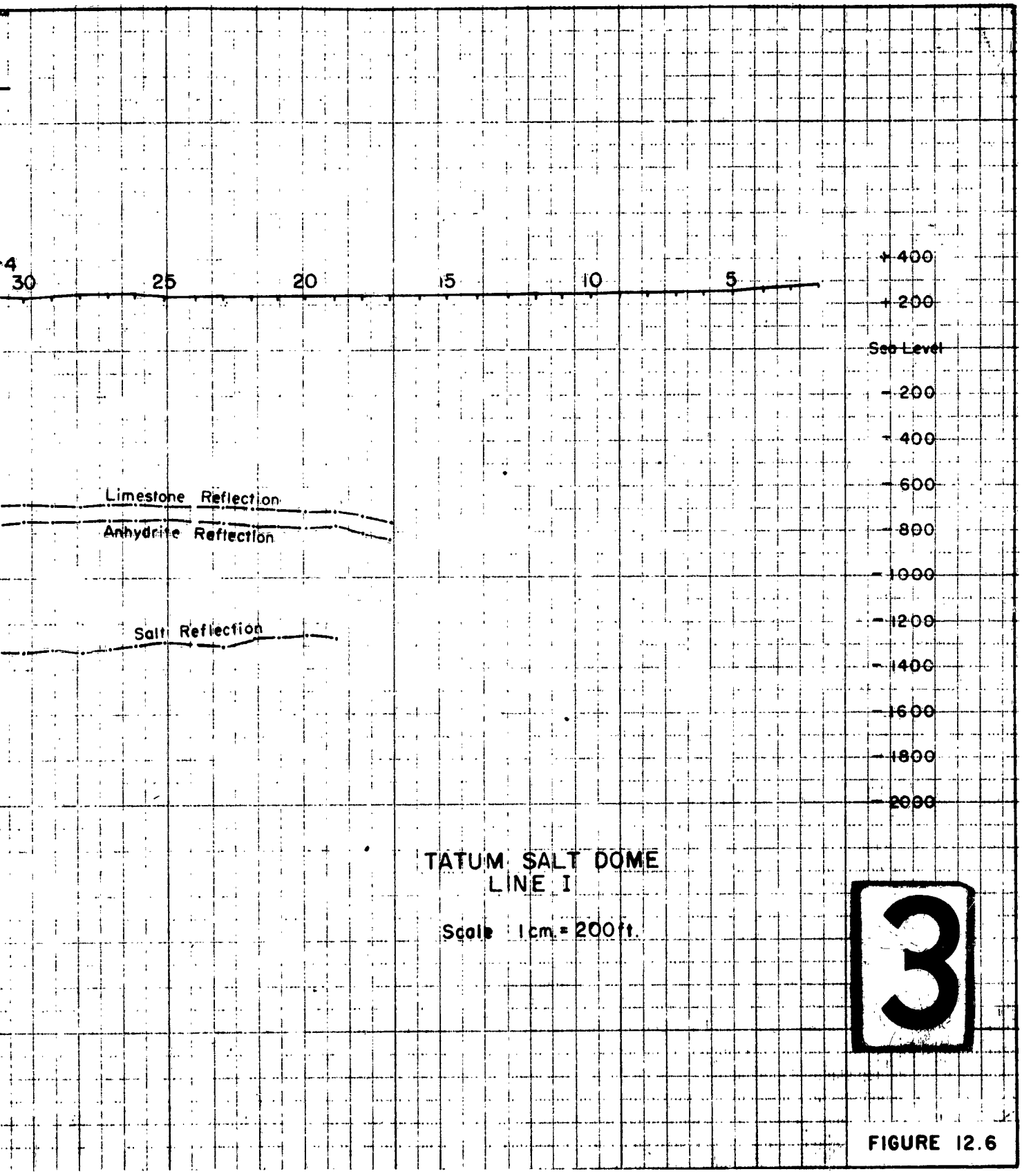
4
30
25
20
15
10
5
+400
+200
Sea Level
-200
-400
-600
-800
-1000
-1200
-1400
-1600
-1800
-2000
Limestone Reflection
Anhydrite Reflection
Salt Reflection
TATUM SALT DOME
LINE I
Scale 1 cm. = 200 ft.
3

FIGURE 12.6

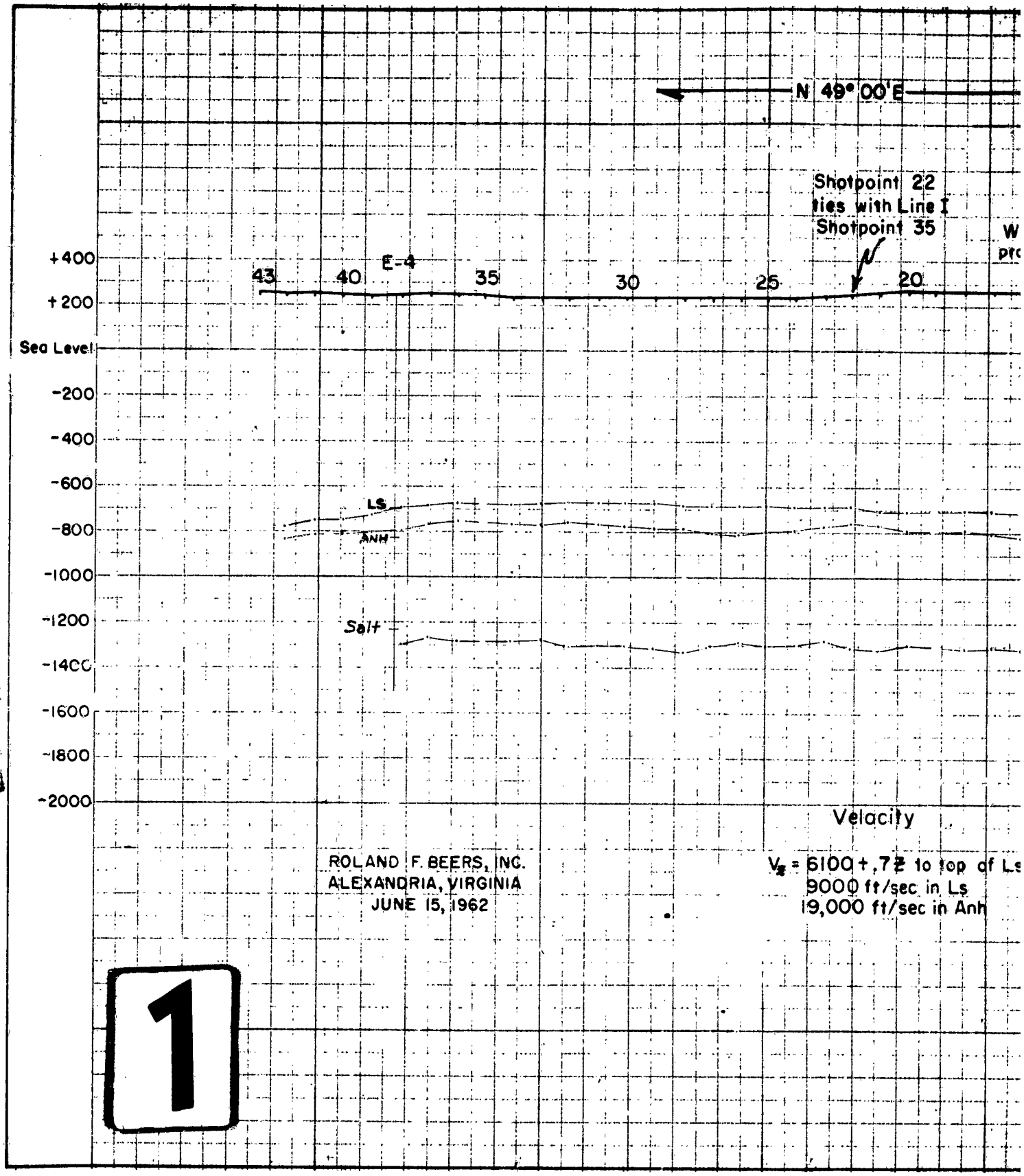
N 49° 00'E
Shotpoint 22
ties with Line I
Shotpoint 35
+400
+200
Sea Level
-200
-400
-600
-800
-1000
-1200
-1400
-1600
-1800
-2000
43
40
E-4
35
30
25
20
LS
ANH
Salt
Velocity
ROLAND F. BEERS, INC.
ALEXANDRIA, VIRGINIA
JUNE 15, 1962
V_E = 6100 + .7Z to top of Ls
9000 ft/sec in Ls
19,000 ft/sec in Anh
1

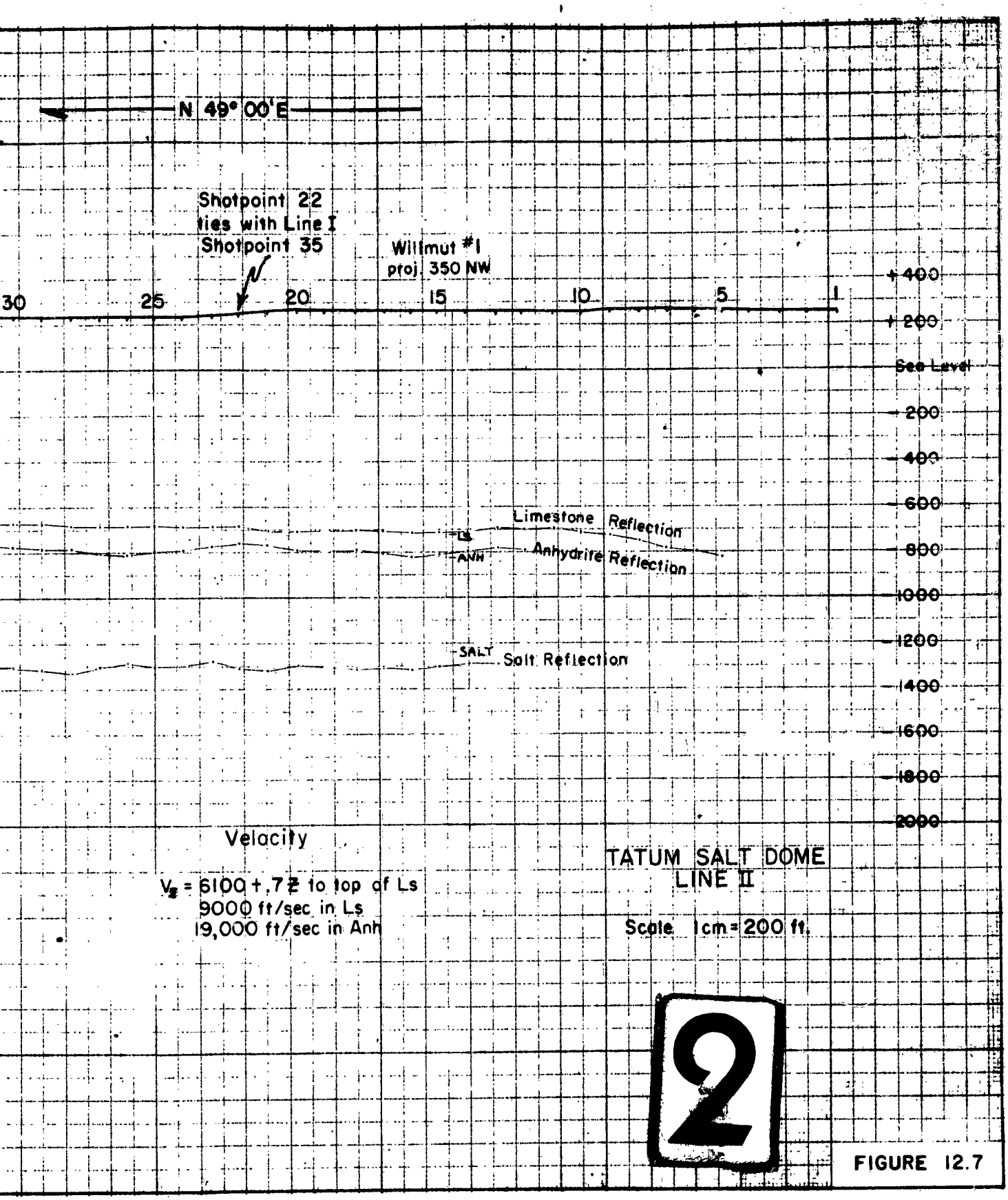
N 49° 00'E
Shotpoint 22
ties with Line I
Shotpoint 35
Wiltmut #1
proj. 350 NW
30
25
20
15
10
5
1
+400
+200
Sea Level
-200
-400
-600
-800
-1000
-1200
-1400
-1600
-1800
-2000
Limestone Reflection
LS
ANH
Anhydrite Reflection
SALT
Salt Reflection
Velocity
V_z = 6100 + .7z to top of Ls
9000 ft/sec in Ls
19,000 ft/sec in Anh
TATUM SALT DOME
LINE II
Scale 1cm = 200 ft.
2

FIGURE 12.7

1

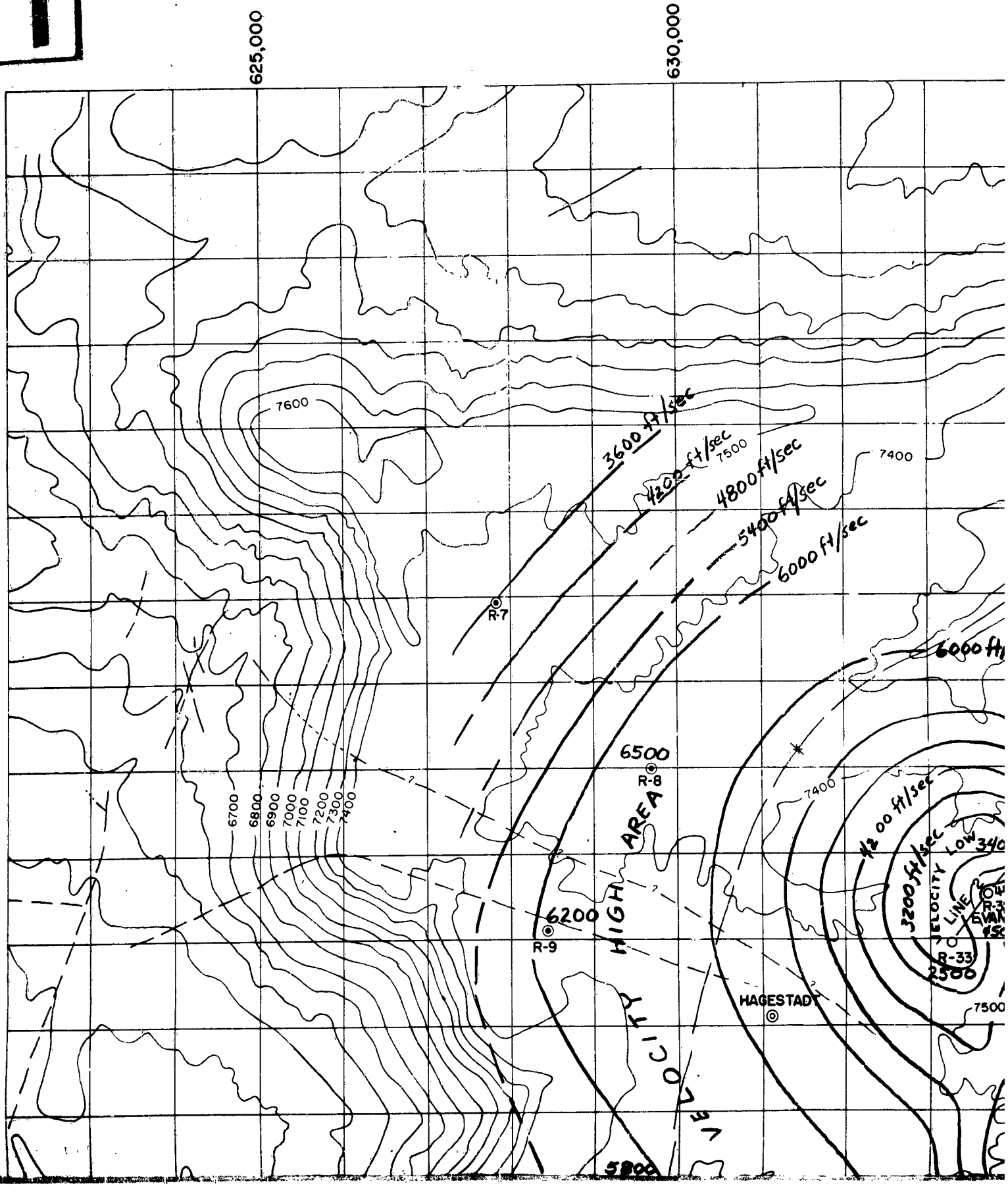
625,000
630,000
7600
7500
7400
3600 ft/sec
4200 ft/sec
4800 ft/sec
5400 ft/sec
6000 ft/sec
R-7
6500
R-8
6200
R-9
HIGH VELOCITY AREA
6700
6800
6900
7000
7100
7200
7300
7400
4200 ft/sec
3200 ft/sec
LOW VELOCITY LINE
R-33
2500
HAGESTADT
5800

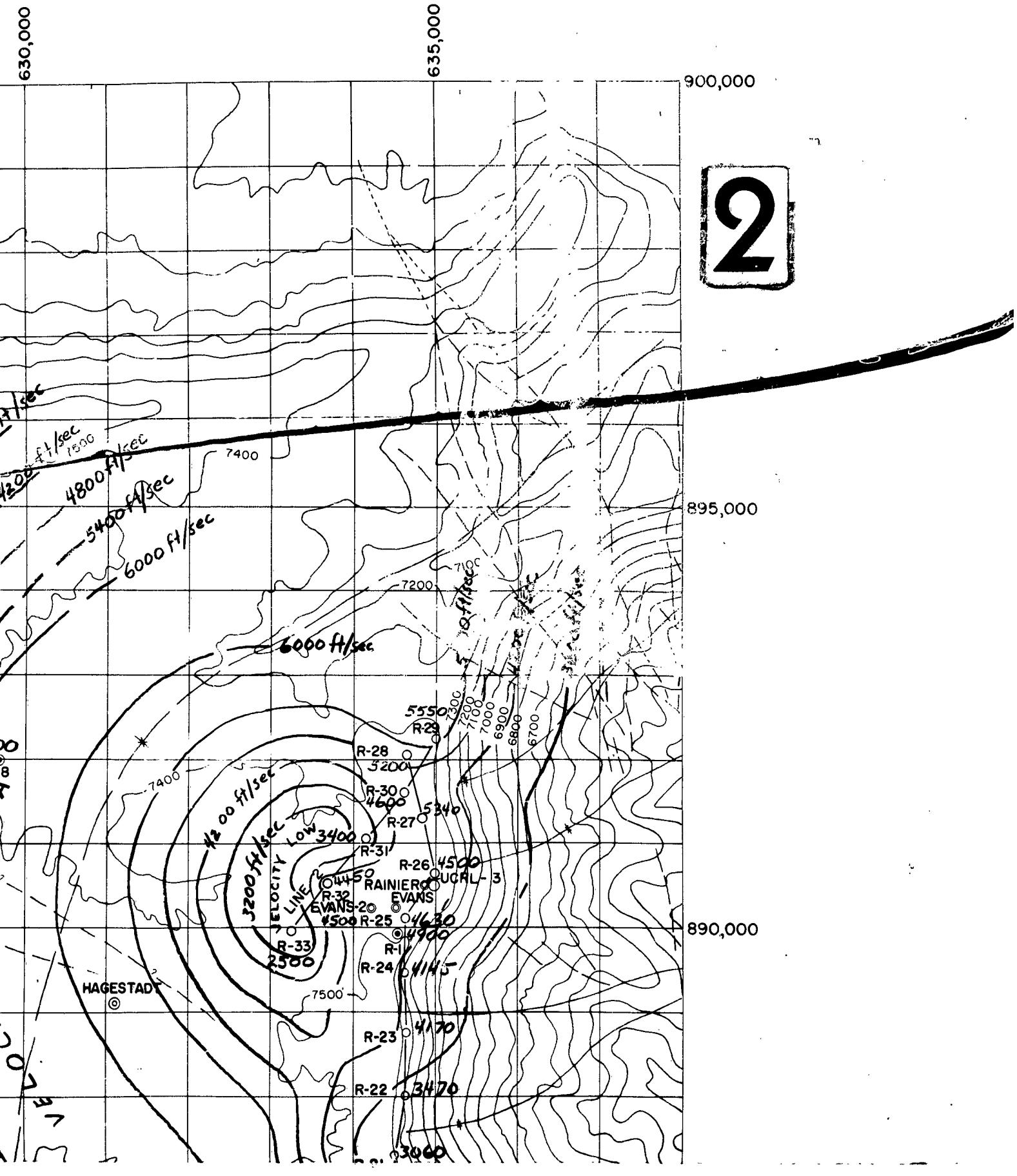
630,000
635,000
900,000
895,000
890,000
2
7400
7500
7200
7100
7000
6900
6800
6700
4800 ft/sec
5400 ft/sec
6000 ft/sec
4200 ft/sec
7500 ft/sec
4200
5550
R-29
R-28
3200
R-30
4600
5340
R-27
3400
R-31
4500
R-26
4450
RAINIER
UCRL-3
R-32
EVANS-20
EVANS
4500
R-25
4630
4900
R-1
R-24
4145
R-33
2500
HAGESTADT
R-23
4170
R-22
3470
3060
VELOCITY LOW
LINE

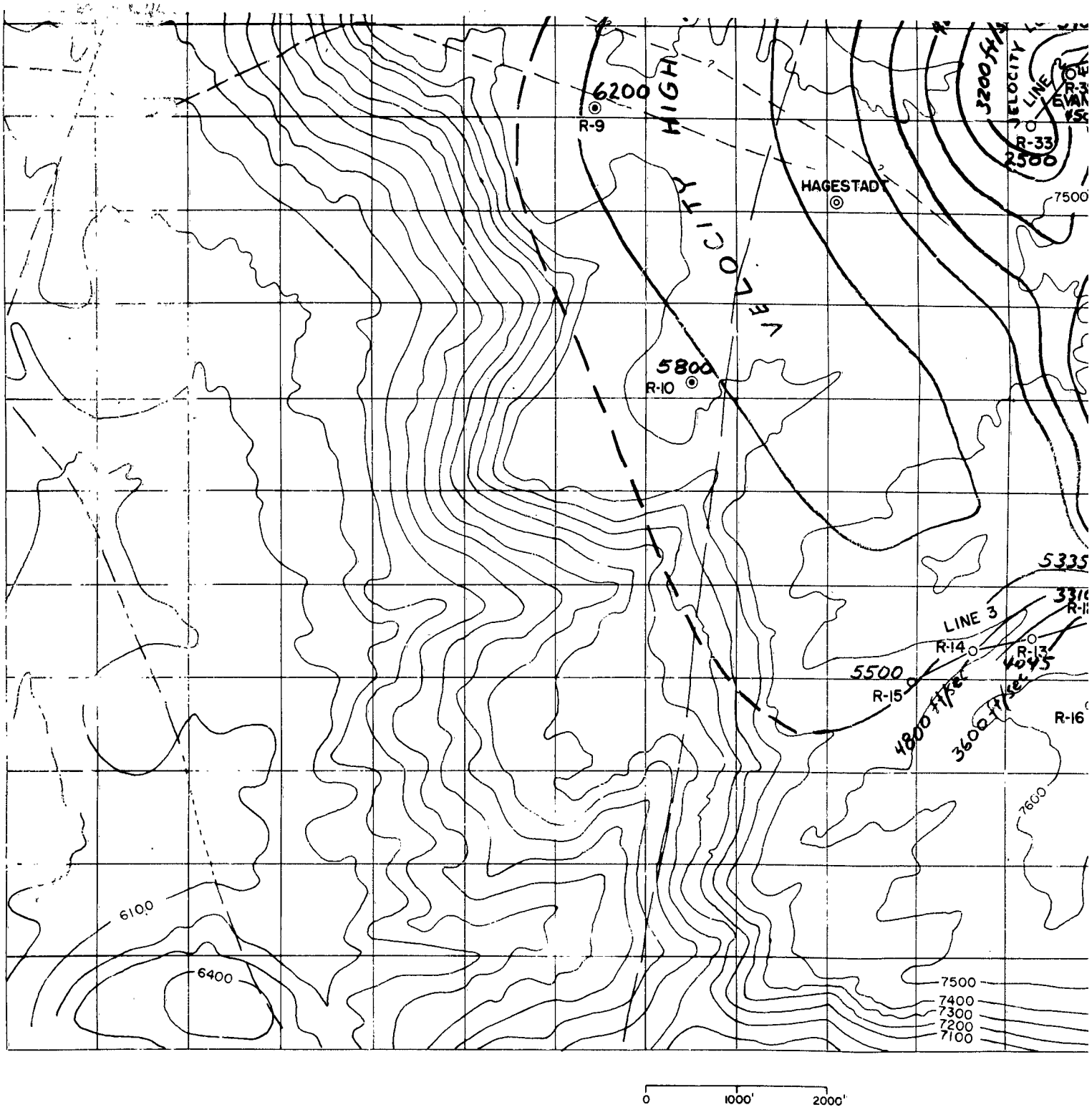

ENCLOSURE I TOPOGRAPHIC MAP OF RAINIER MESA SHOWING LOCATION OF NEAR SURFA
AND UPHOLE VELOCITY SURVEYS AND AVERAGE VERTICAL VELOCITIES OF TI
OF OAK SPRING TUFF

3

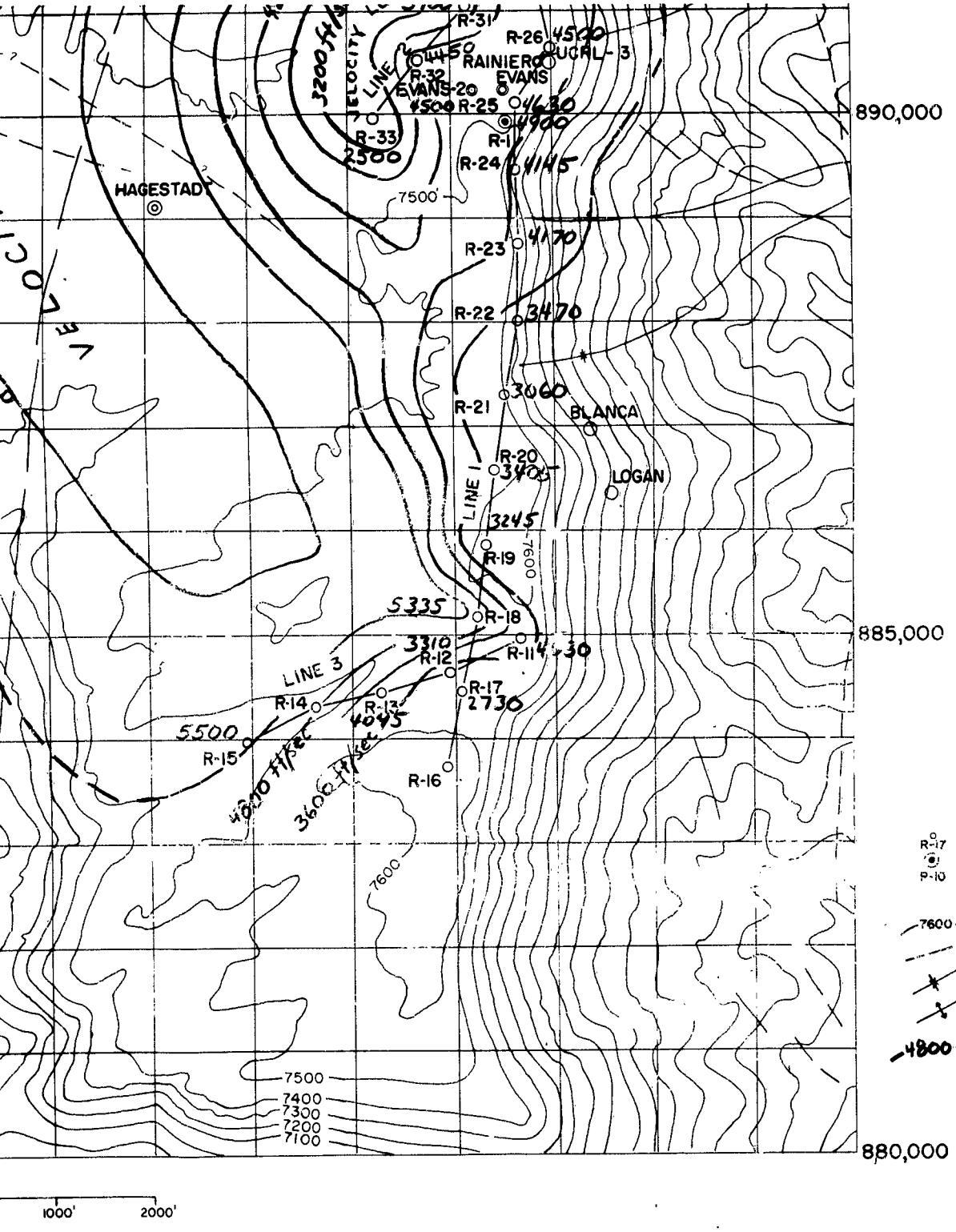

OWING LOCATION OF NEAR SURFACE VELOCITY PROFILES
VERAGE VERTICAL VELOCITIES OF THE UPPER 75 TO 100 FEET

4

1

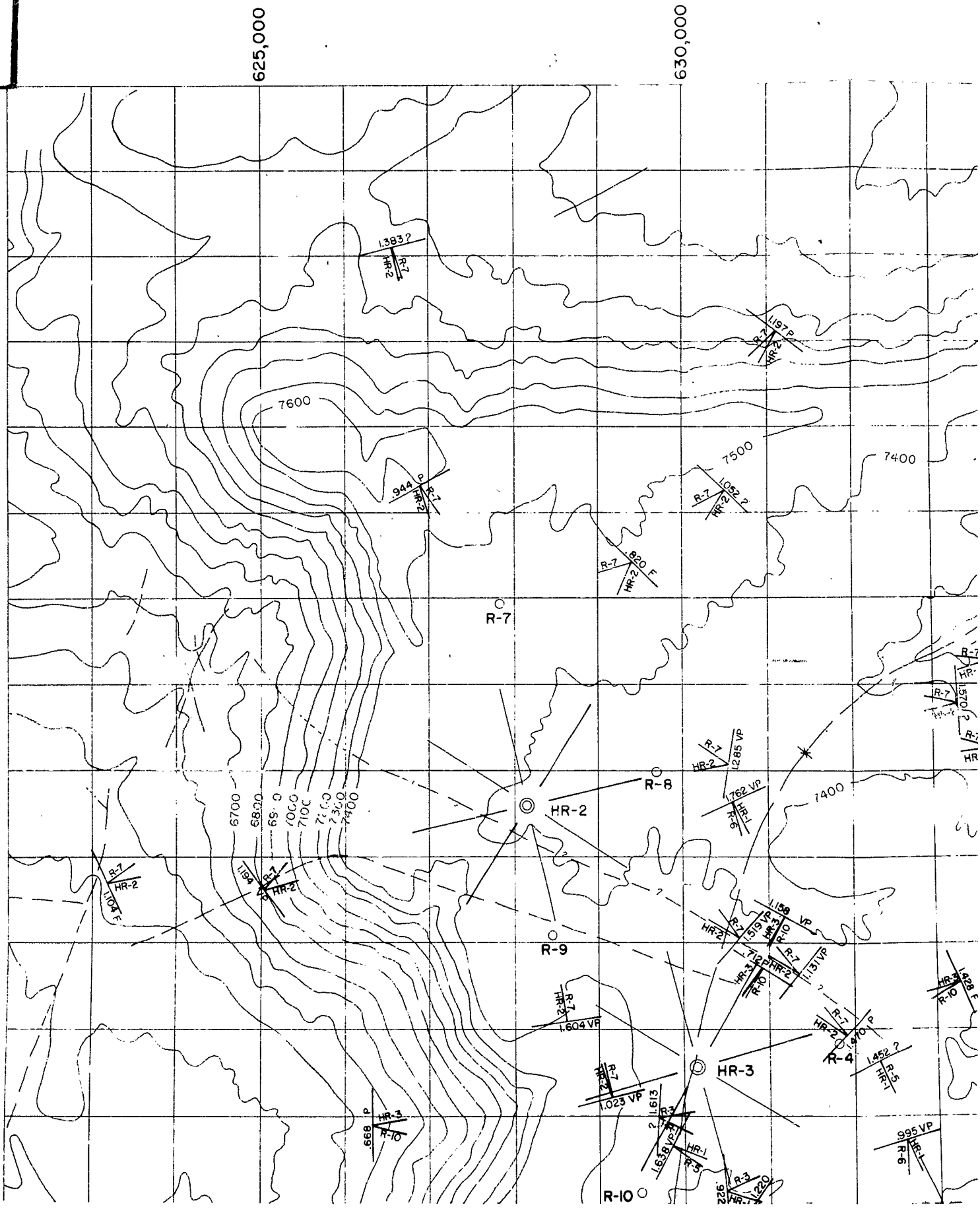

625,000
630,000
7600
7500
7400
7400
6700
6800
R-7
R-8
R-9
R-10
HR-2
HR-3
R-4
1.383 ?
1.197 P
.944 P
1.052 ?
.820 F
1.285 VP
1.762 VP
1.570 ?
1.104 F
1.194
1.158 VP
1.519 VP
1.131 VP
1.604 VP
1.023 VP
1.613
1.638 VP
1.470 P
1.452 ?
.995 VP
.668 P
1.220

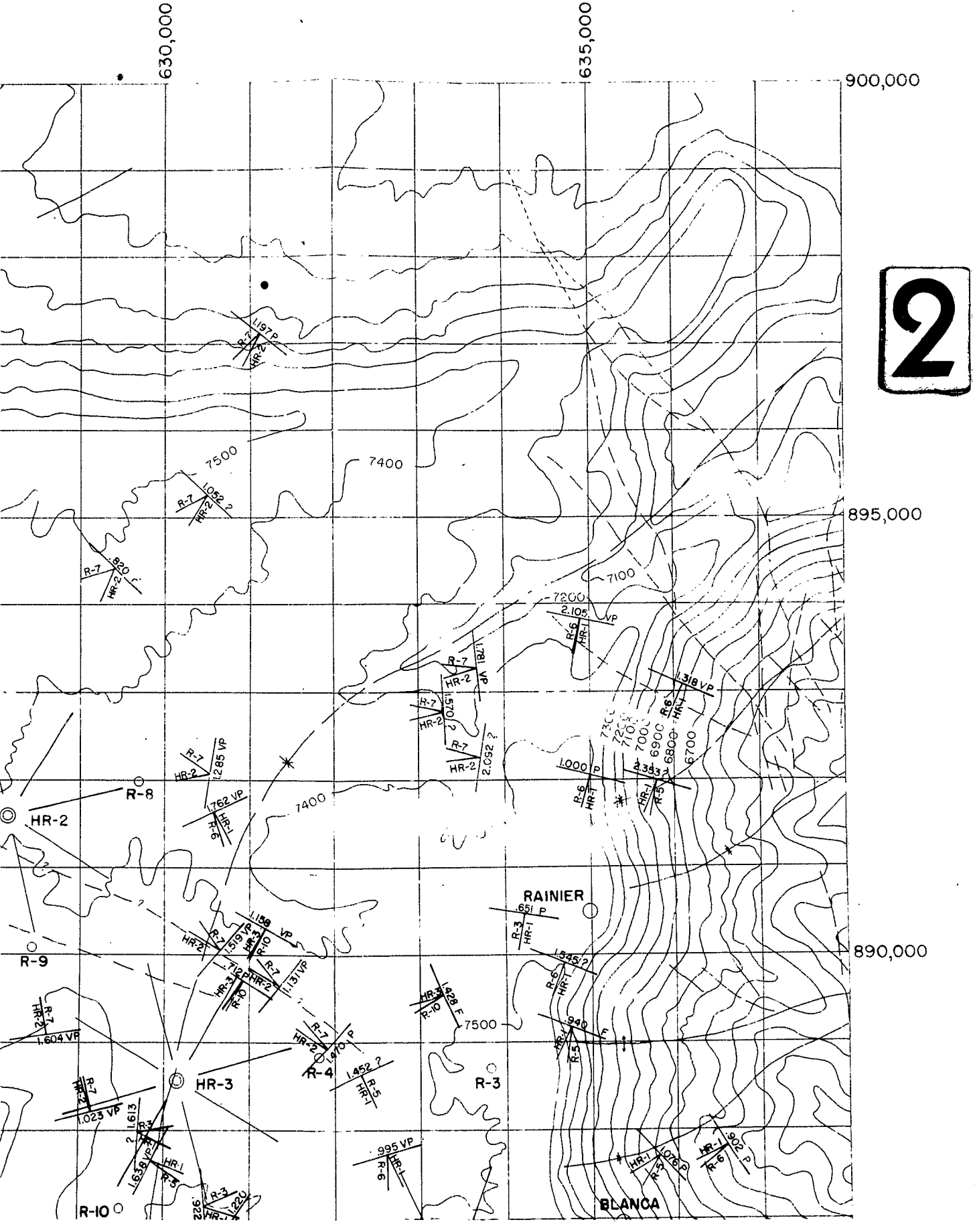
630,000
635,000
900,000
895,000
890,000
2
7500
7400
7100
7200
6900
6800
6700
R-8
HR-2
R-9
HR-3
R-10
R-4
R-3
RAINIER
BLANCA
1.197 P
1.052 ?
.820
1.285 VP
1.762 VP
1.781 VP
1.570 ?
2.092 ?
2.105 VP
1.318 VP
1.000 P
1.383
.651 P
1.345 ?
.940
1.159 VP
1.519 VP
1.712 P
1.131 VP
1.604 VP
1.023 VP
1.613 ?
1.638 VP
1.220
.926
.995 VP
1.470 P
1.452 ?
.428 F
1.076 P
.90 P

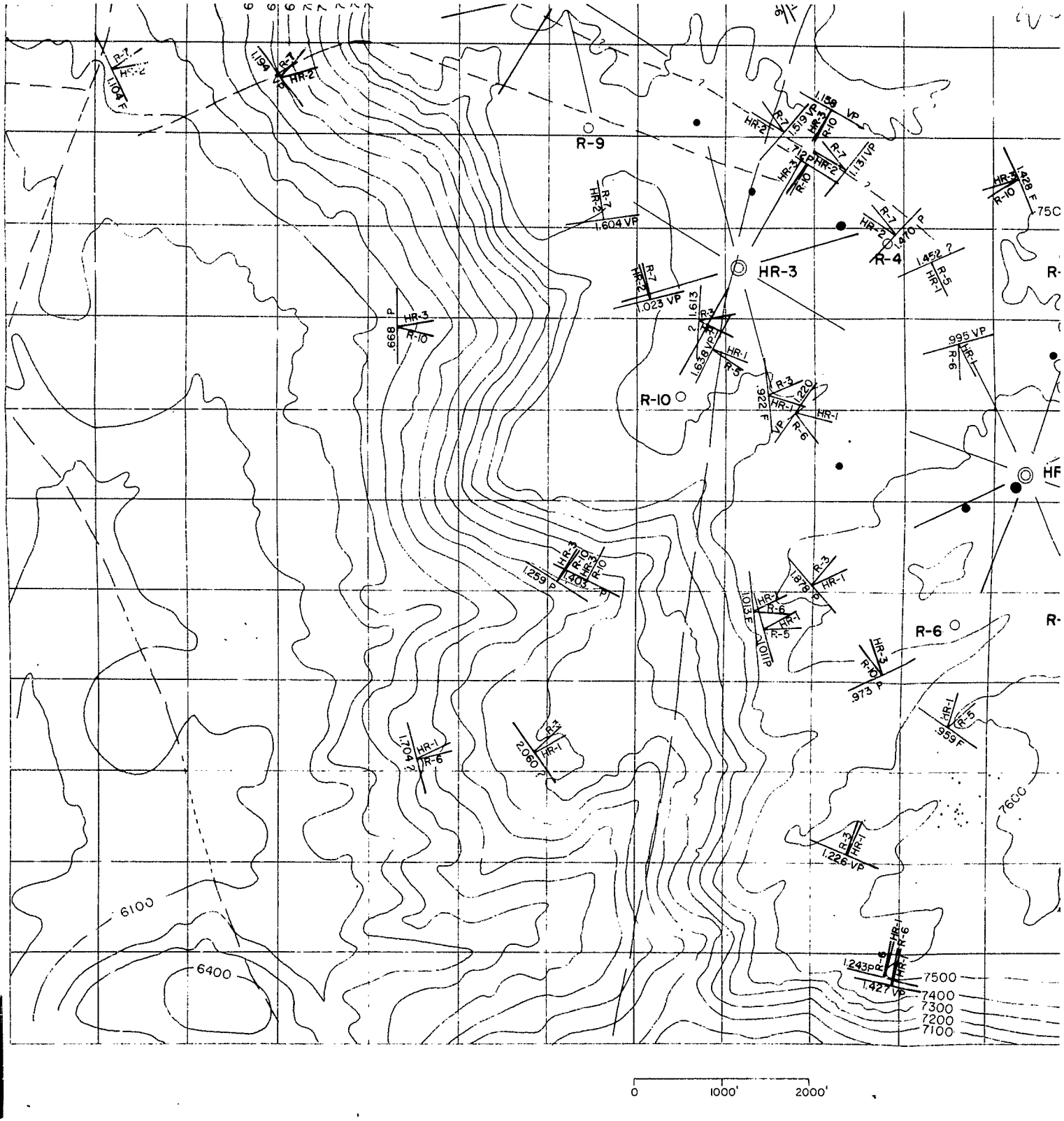

Enclosure 2 TOPOGRAPHIC MAP OF RAINIER MESA SHOWING RESULTS OF HORIZONTA

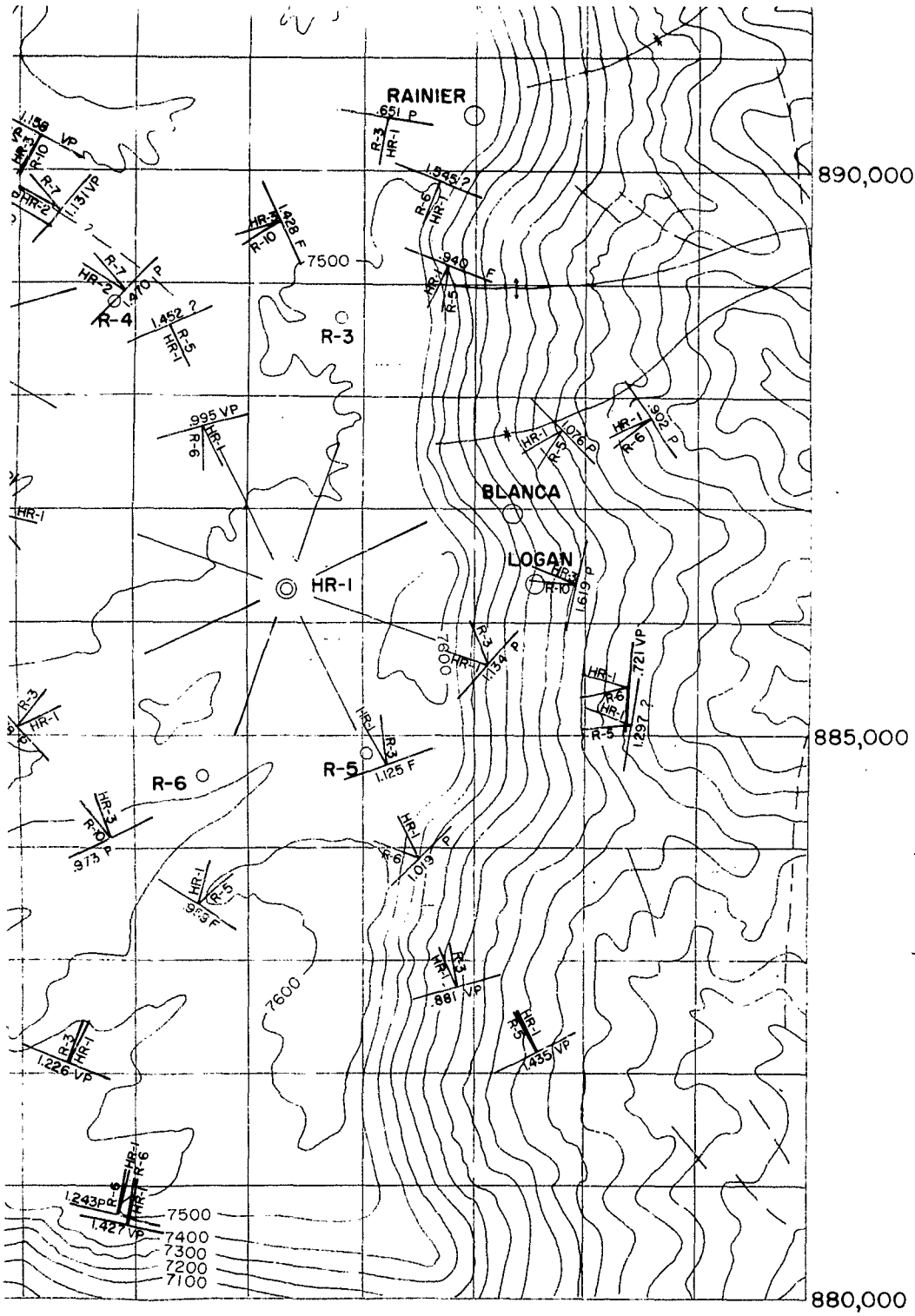

SHOTPOINT

HSR INSTRUMENT ARRAY

REFLECTION POINT SHOWING ARRIVAL TIME, GRADE, SHOTPOINT, AND ARRAY

GRADE DESIGNATIONS

G	GOOD
F	FAIR
P	POOR
VP	VERY POOR
?	QUESTIONABLE

SURFACE CONTOUR, 100' INTERVAL

FAULT

SYNCLINE AXIS

ANTICLINE AXIS

SULTS OF HORIZONTAL SEISMIC RANGING SURVEY

4

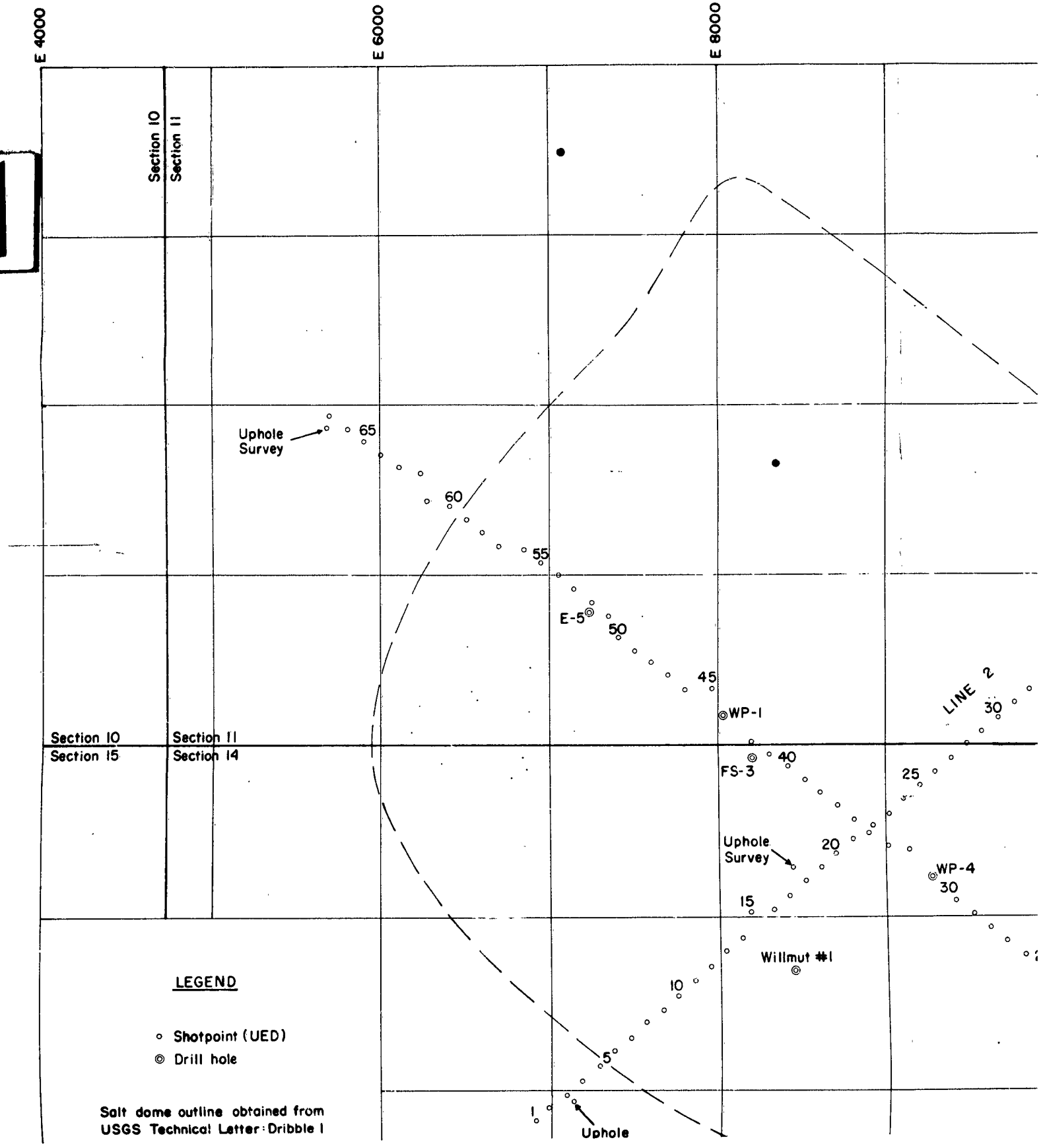
E 4000
E 6000
E 8000
Section 10
Section 11
Section 10
Section 15
Section 11
Section 14
Uphole Survey
65
60
55
E-5
50
45
WP-1
LINE 2
30
40
FS-3
25
Uphole Survey
20
WP-4
30
15
Willmut #1
10
5
1
Uphole
LEGEND
Shotpoint (UED)
Drill hole
Salt dome outline obtained from USGS Technical Letter: Dribble I

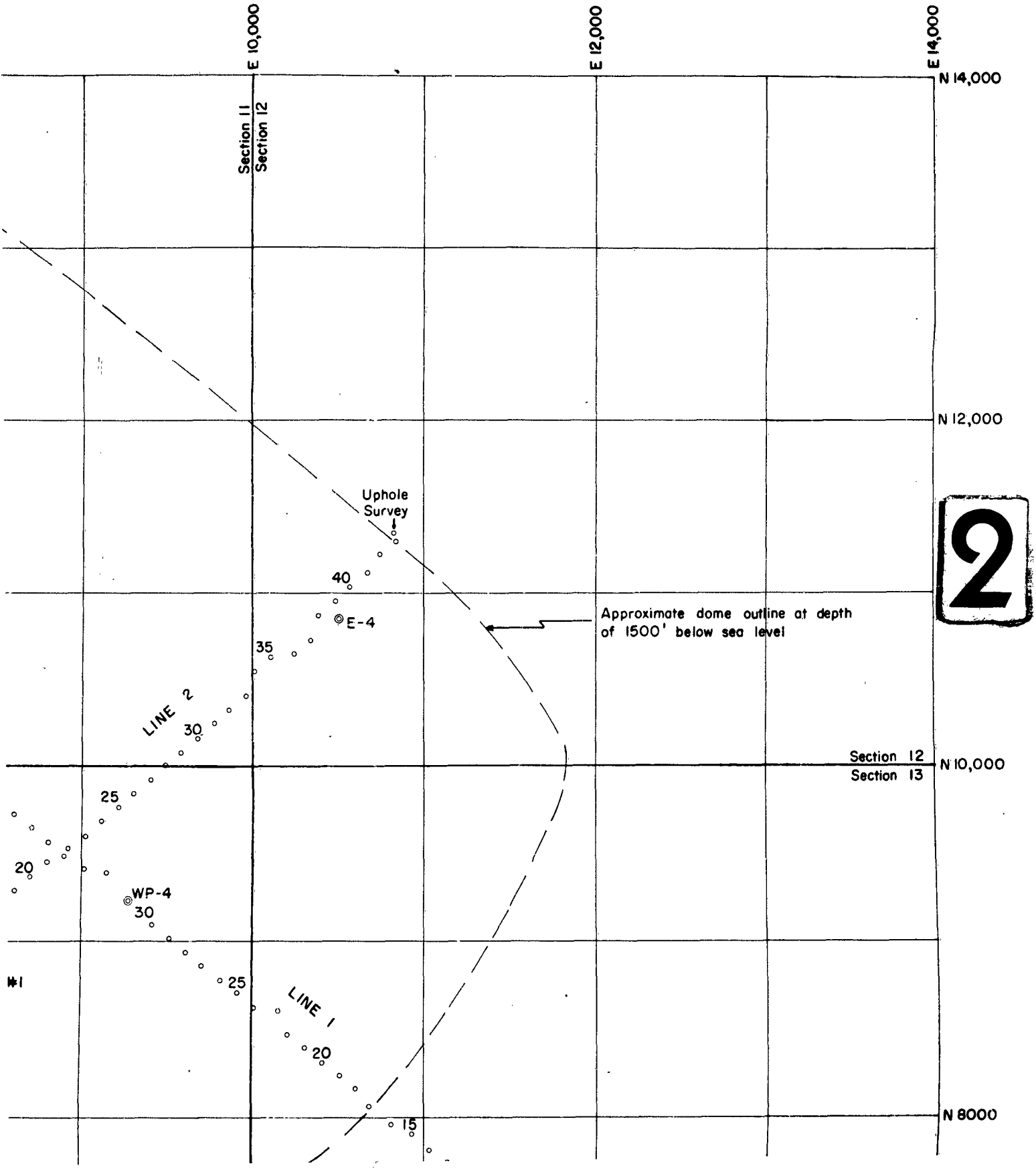
E 10,000
E 12,000
E 14,000
N 14,000
N 12,000
N 10,000
N 8000
Section 11
Section 12
Section 12
Section 13
Uphole Survey
40
E-4
35
LINE 2
30
25
20
WP-4
30
#1
25
LINE 1
20
15
Approximate dome outline at depth of 1500' below sea level
2

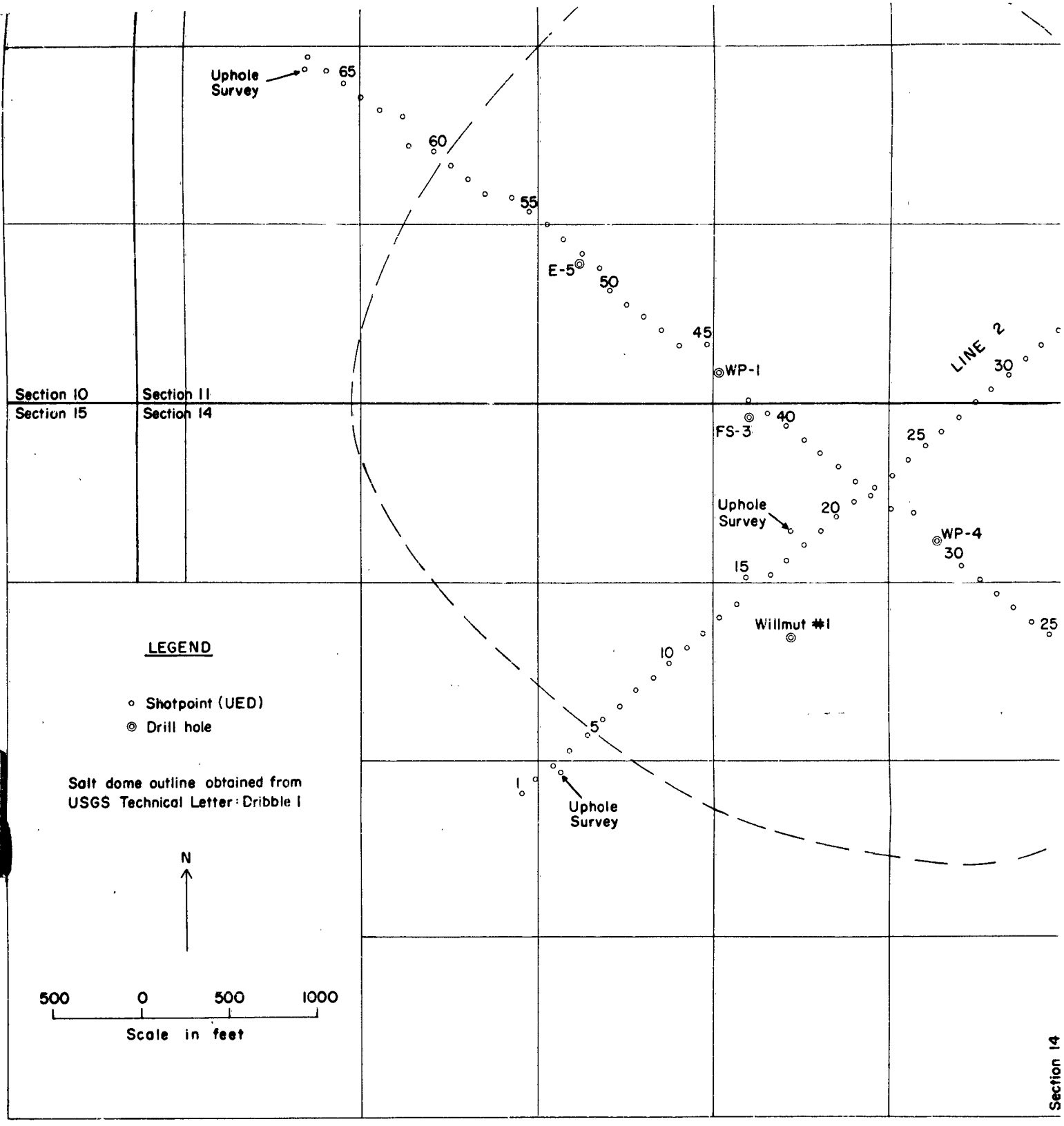

Enclosure 3 UED Seismic Profiles Across Tc

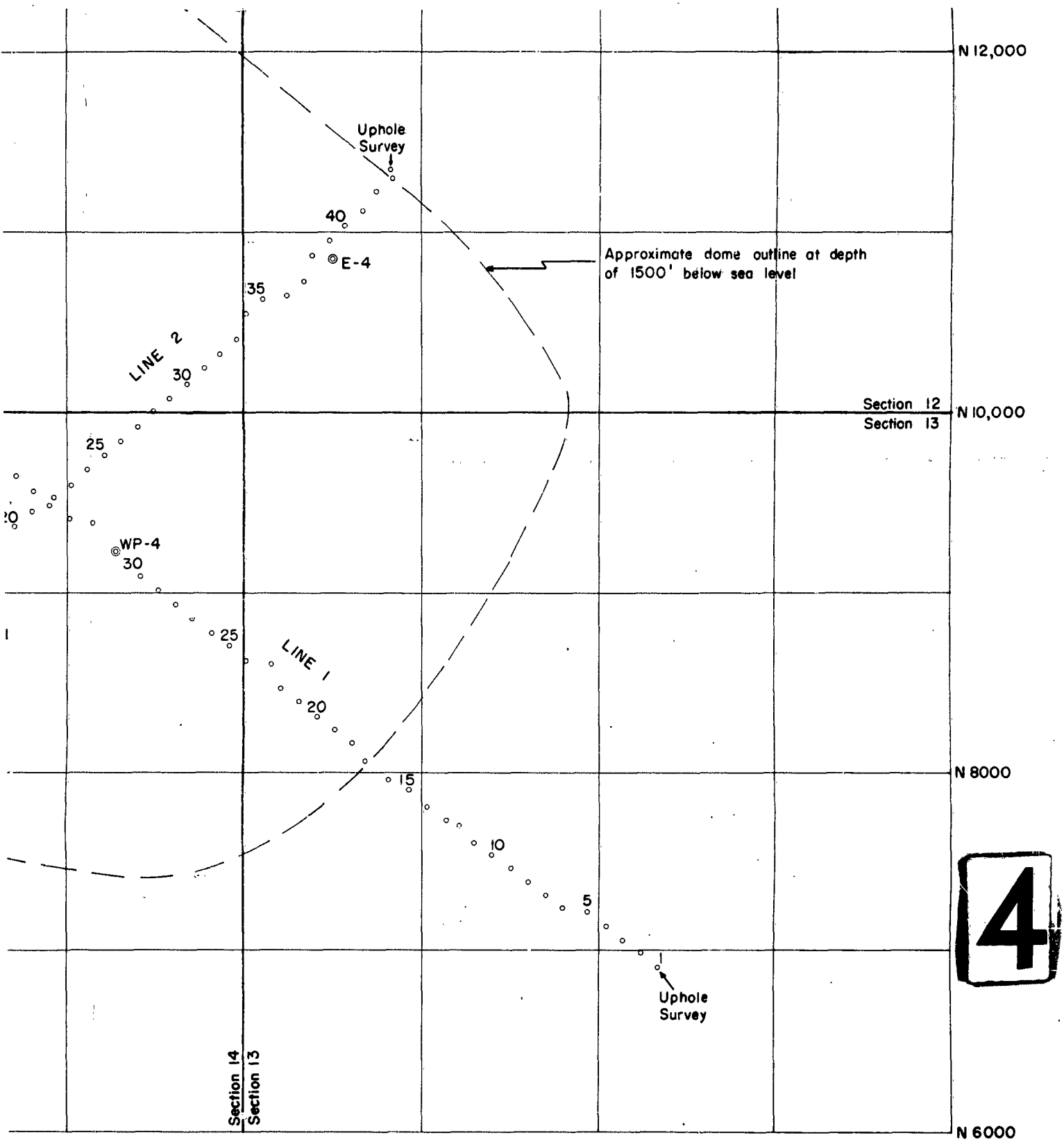

4

: Profiles Across Tatum Salt Dome

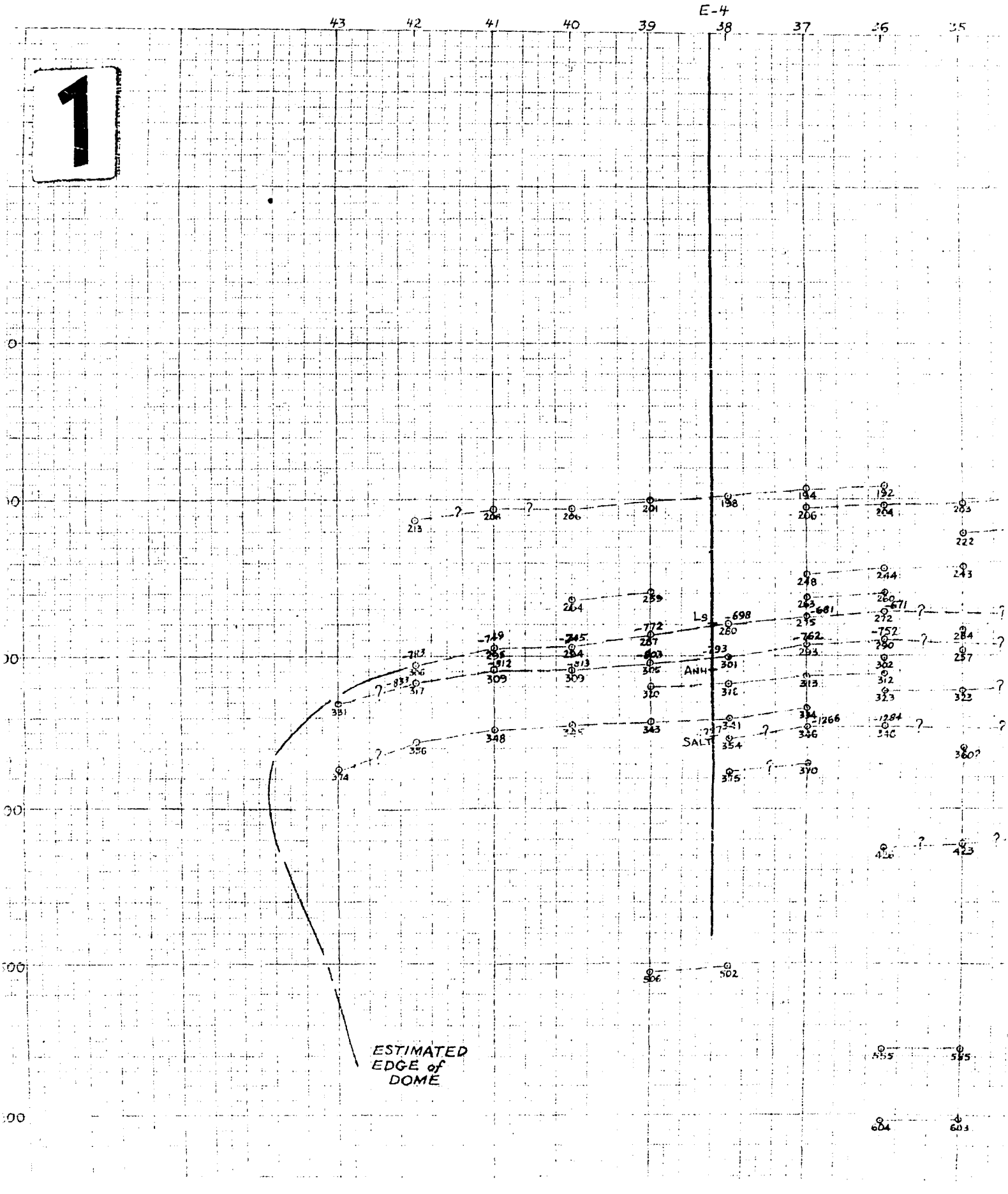
1
E-4
43
42
41
40
39
38
37
36
35
Ls
ANH
SALT
ESTIMATED EDGE of DOME

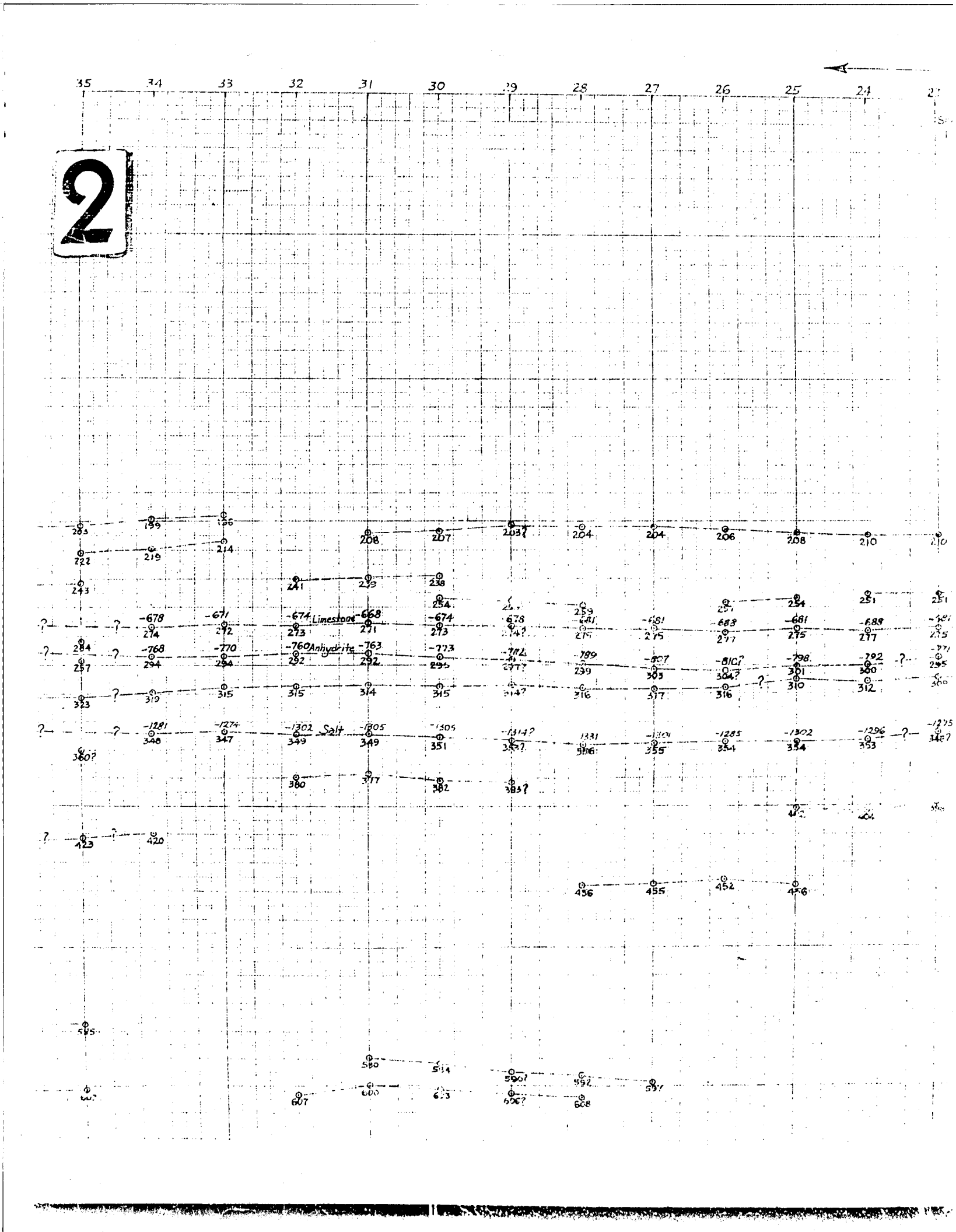
35
34
33
32
31
30
29
28
27
26
25
24
2
Limestone
Anhydrite
Salt

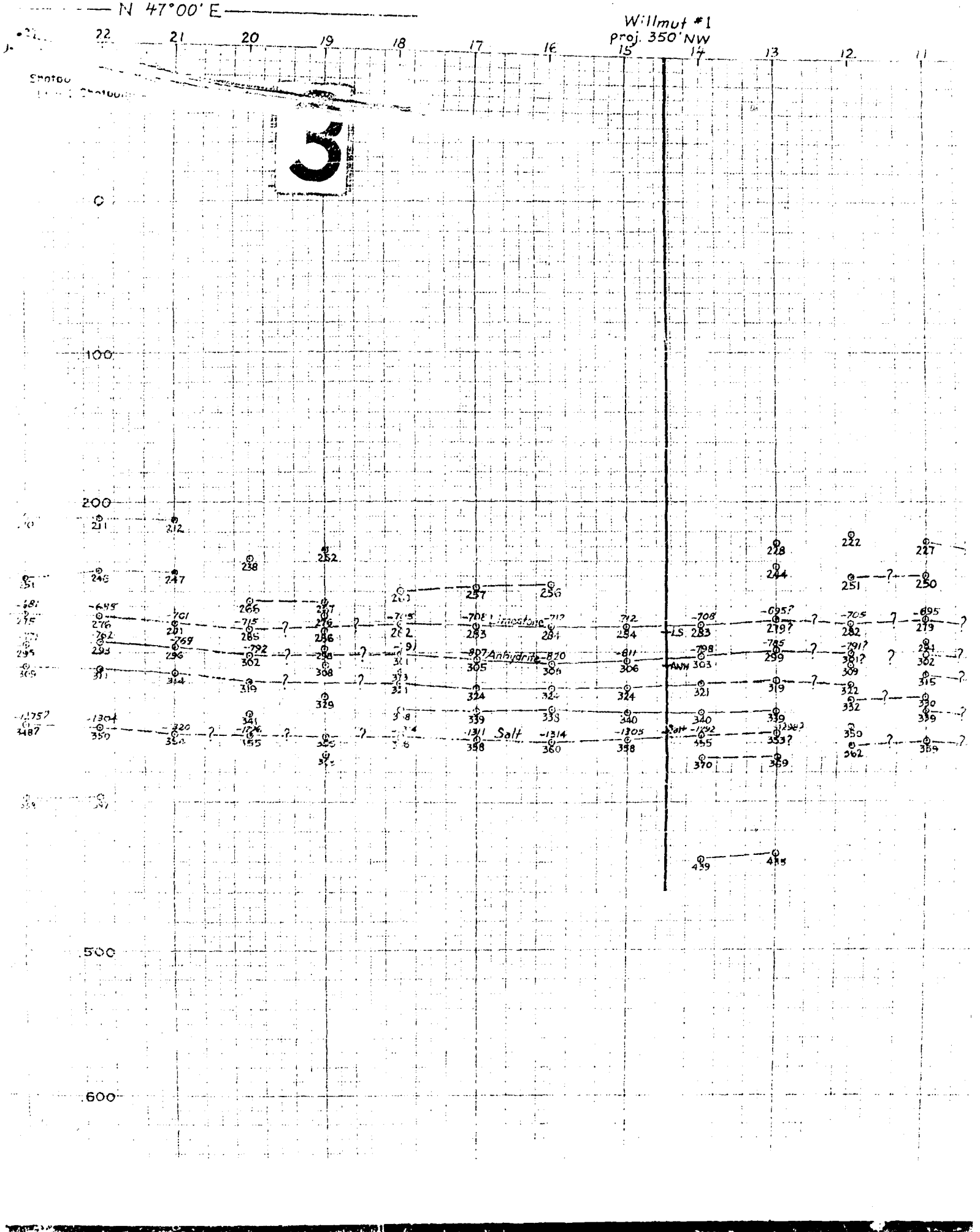
N 47°00' E
Willmut #1
proj. 350' NW
22
21
20
19
18
17
16
15
14
13
12
11
3
0
100
200
500
600
Limestone
Anhydrite
Salt
LS
ANH
Salt

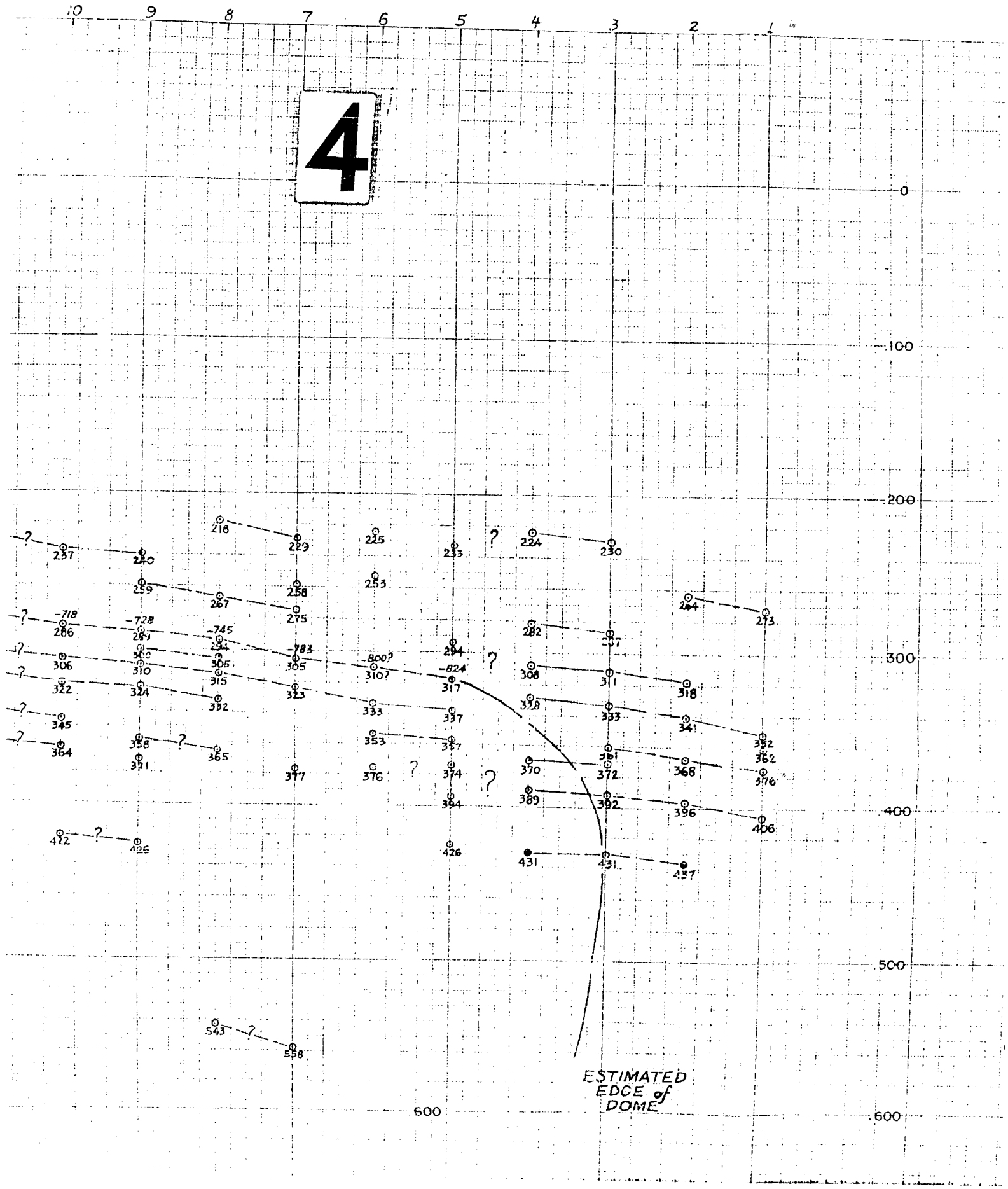
4
10
9
8
7
6
5
4
3
2
1
0
100
200
300
400
500
600
600
ESTIMATED EDGE of DOME

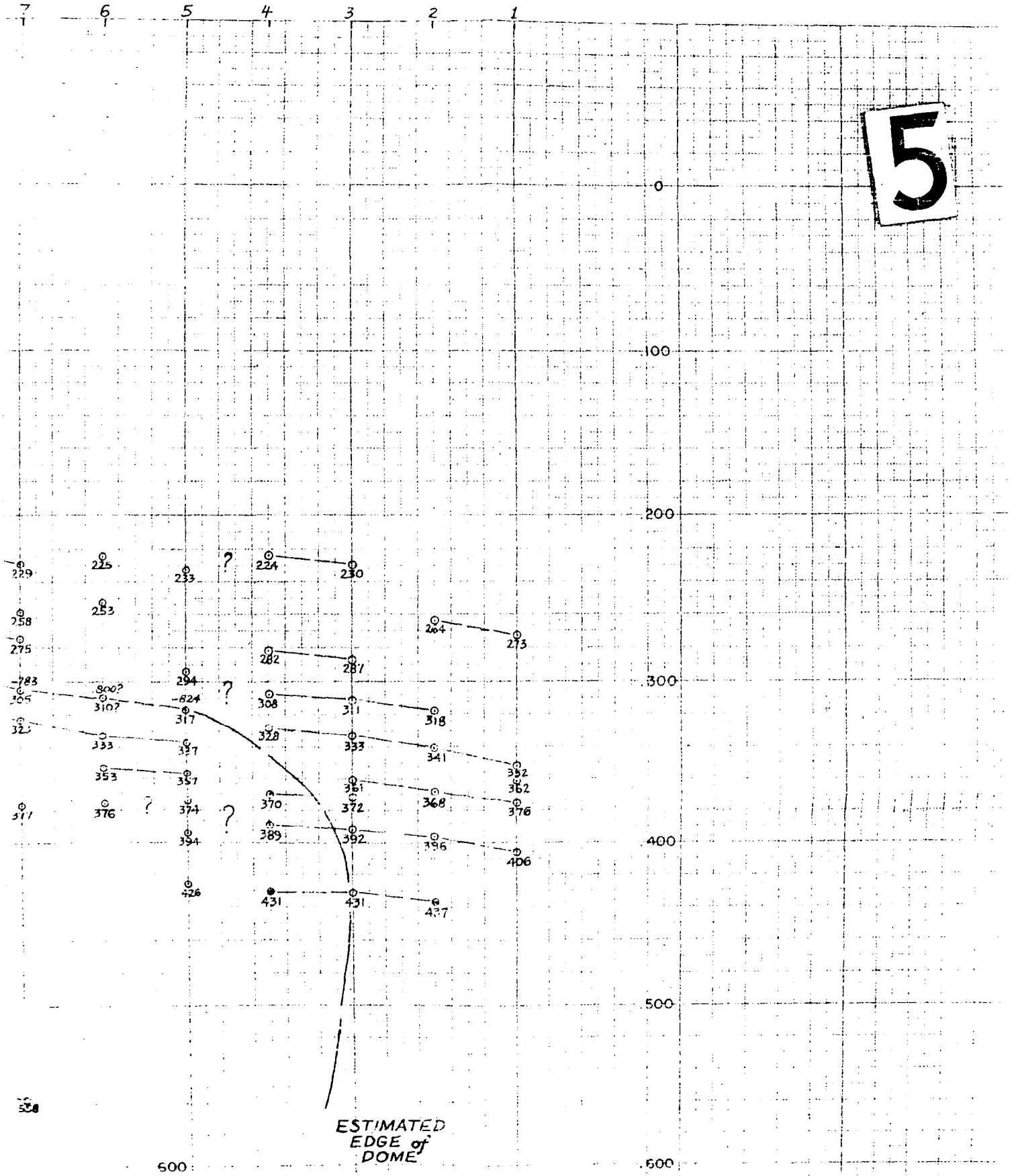

7
6
5
4
3
2
1
0
100
200
300
400
500
600
229
225
233
224
230
258
253
264
273
275
282
287
294
-783
305
800?
310?
-824
317
308
311
318
323
333
327
328
333
341
352
362
353
357
361
368
376
377
376
374
370
372
394
389
392
396
406
426
431
431
437
ESTIMATED EDGE of DOME

5

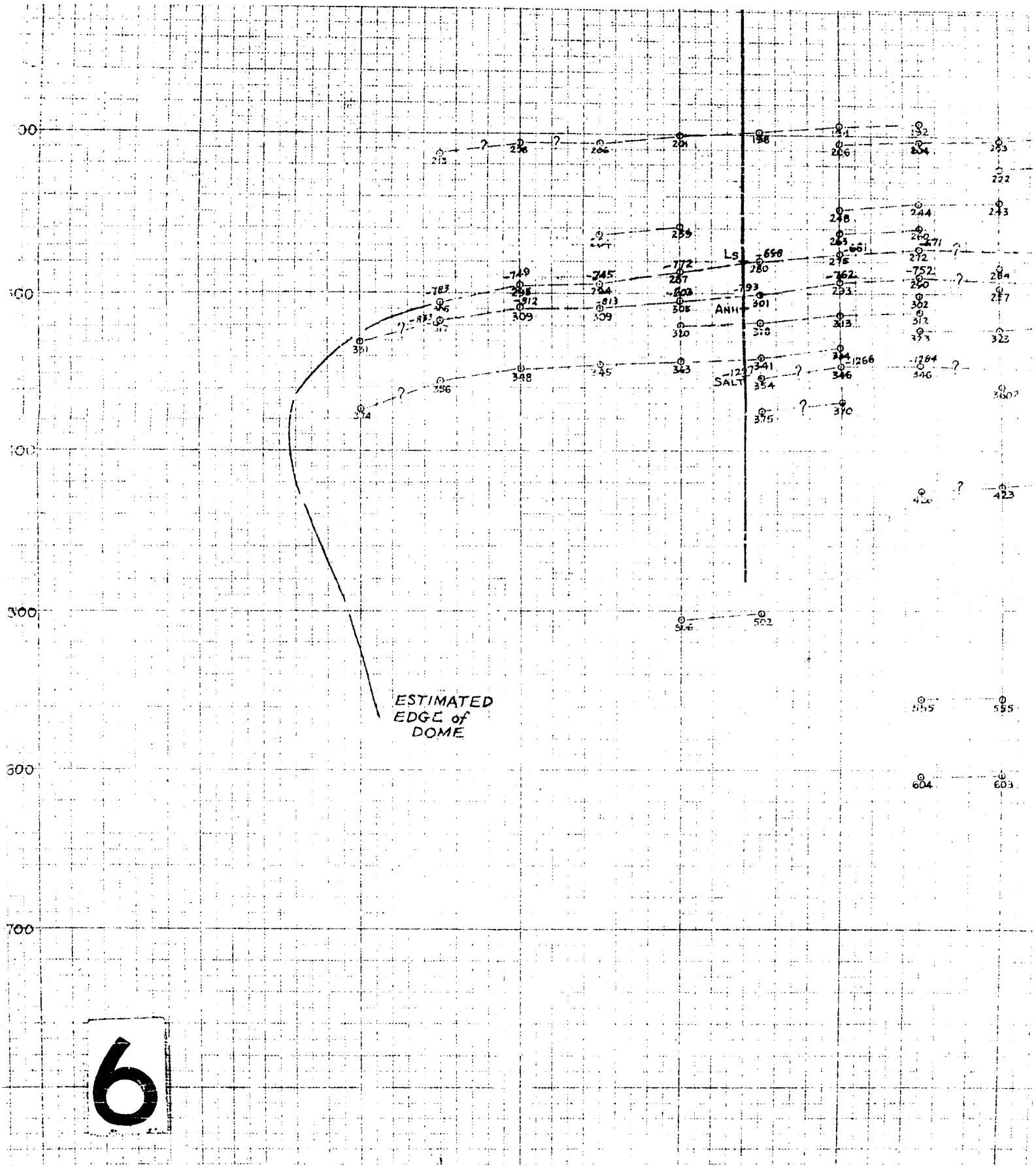

6

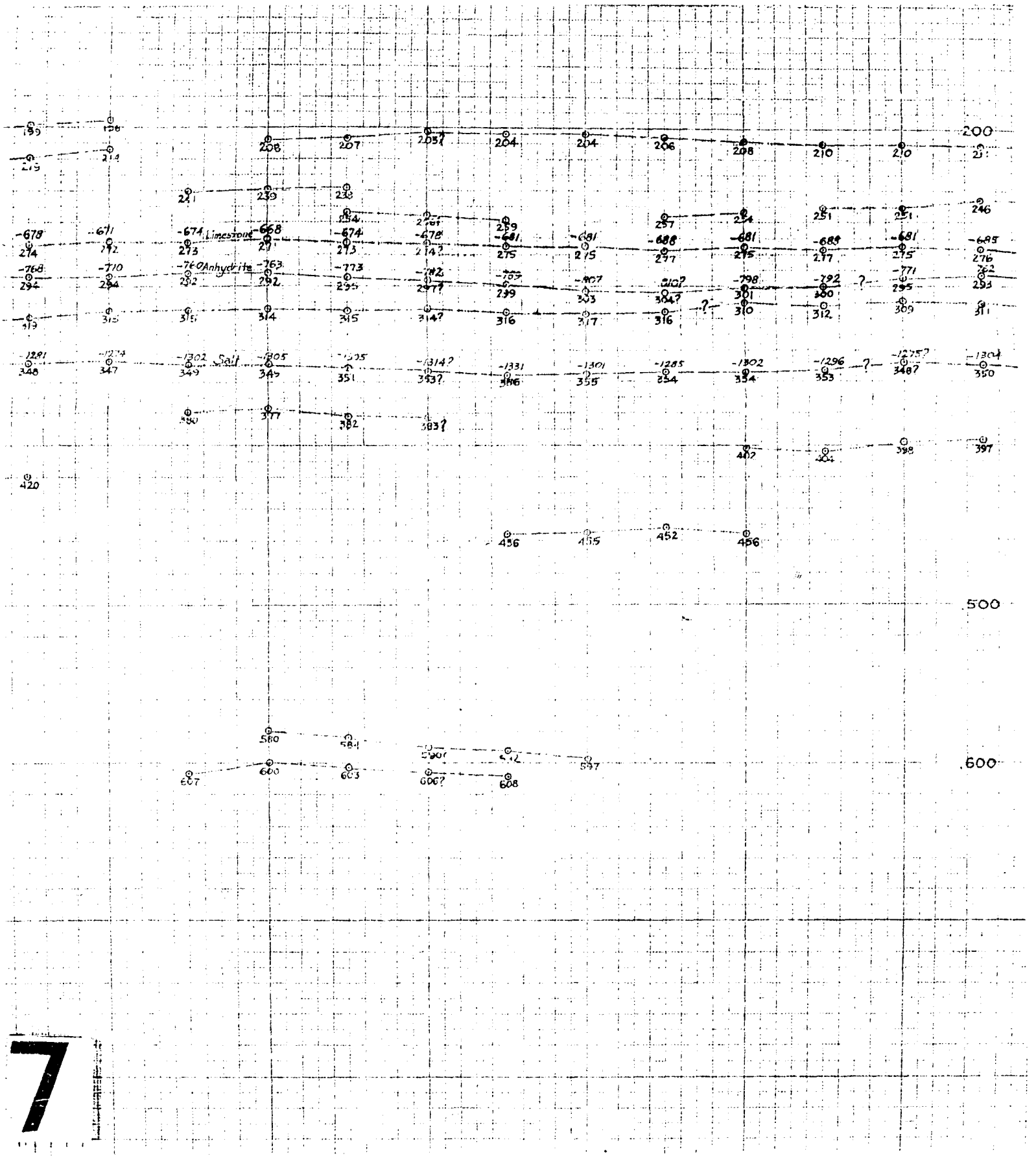
200
500
600
Limestone
Anhydrite
Salt
?

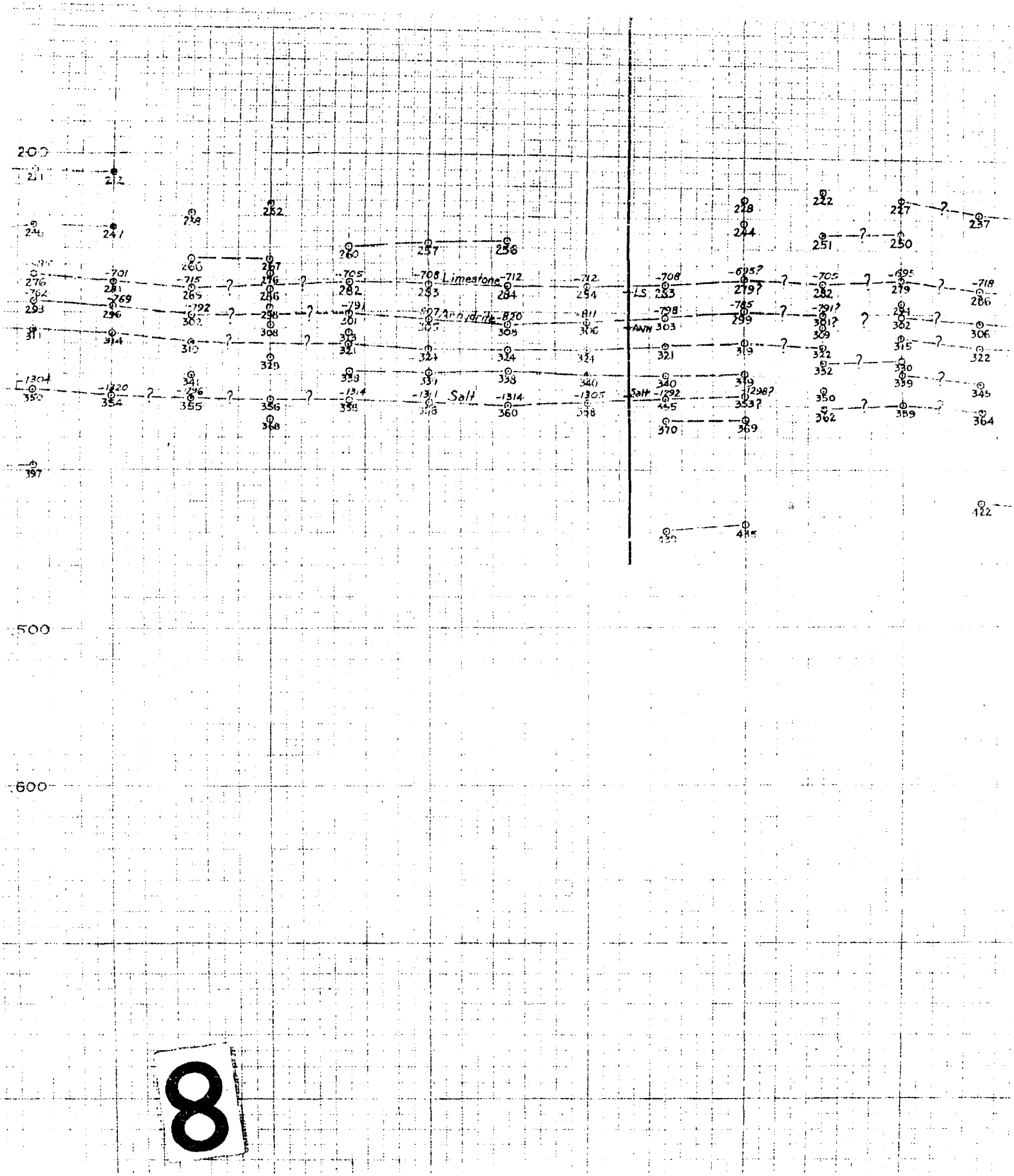

8

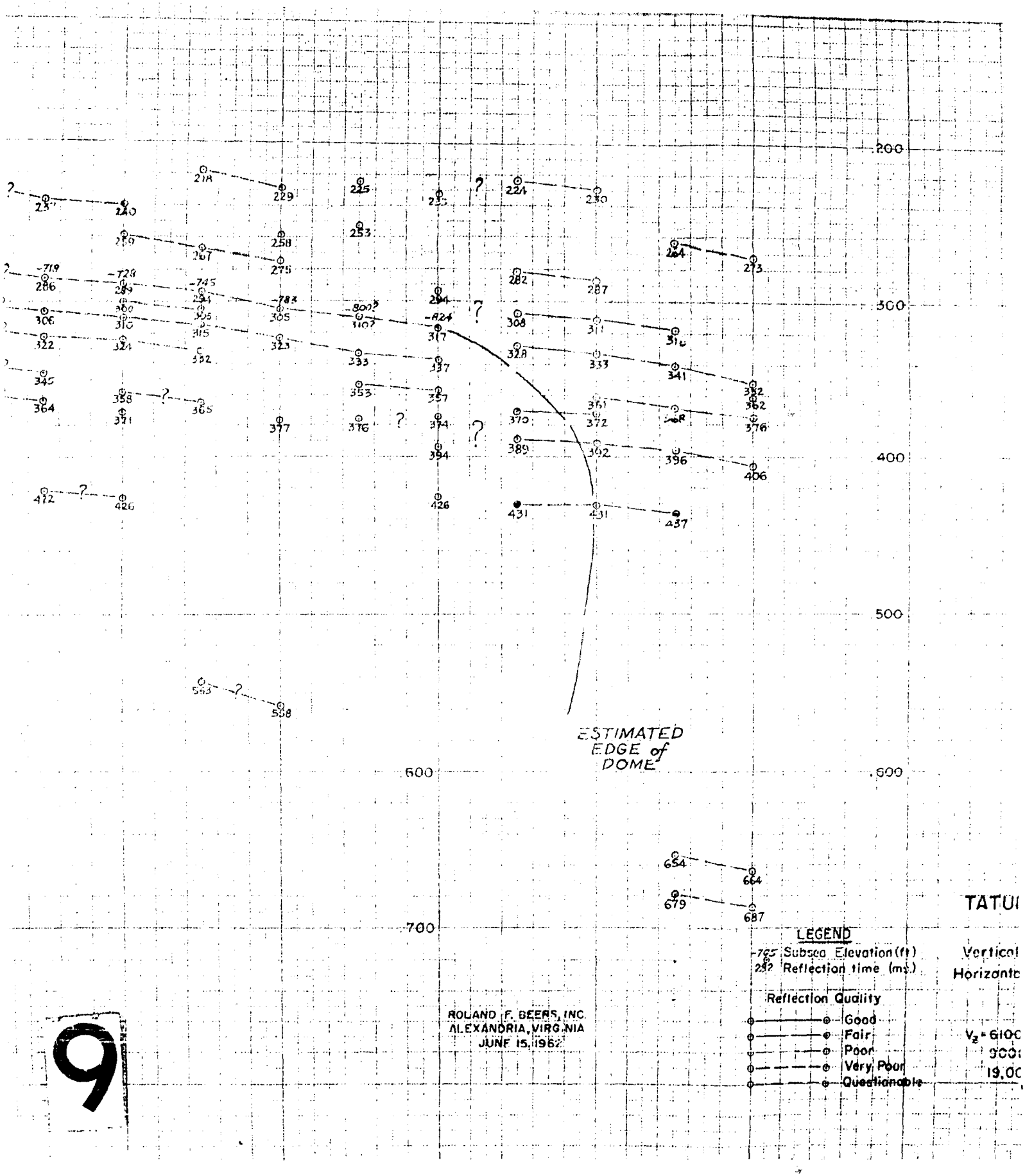
200
300
400
500
600
700
ESTIMATED EDGE of DOME
LEGEND
-725 Subsea Elevation (ft)
252 Reflection time (ms)
Reflection Quality
Good
Fair
Poor
Very Poor
Questionable
ROLAND F. BEERS, INC.
ALEXANDRIA, VIRGINIA
JUNE 15, 1962
TATUI
Vertical
Horizonta
V_2 = 6100
9000
19,00

9

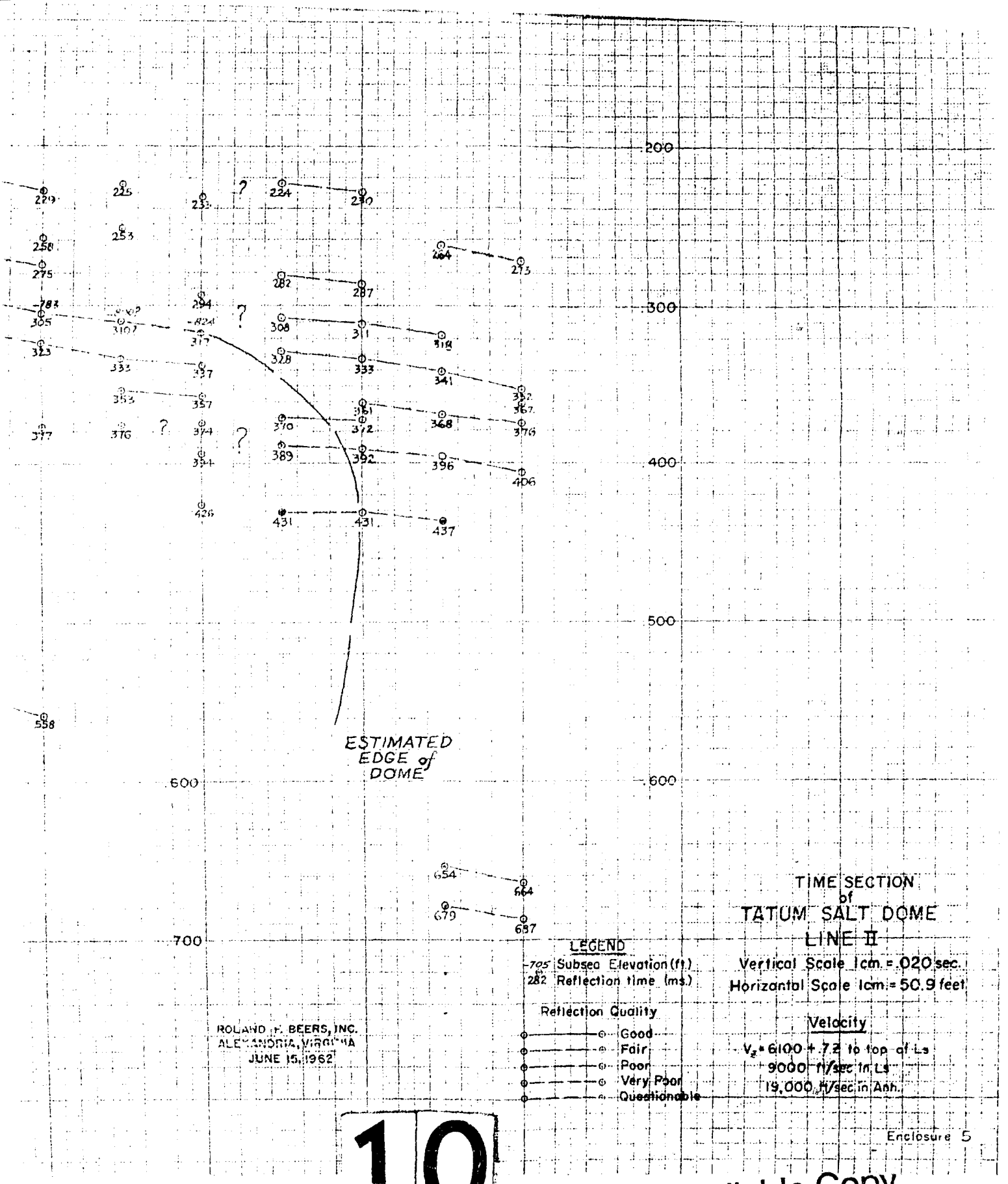

Enclosure 5

10

Best Available Copy

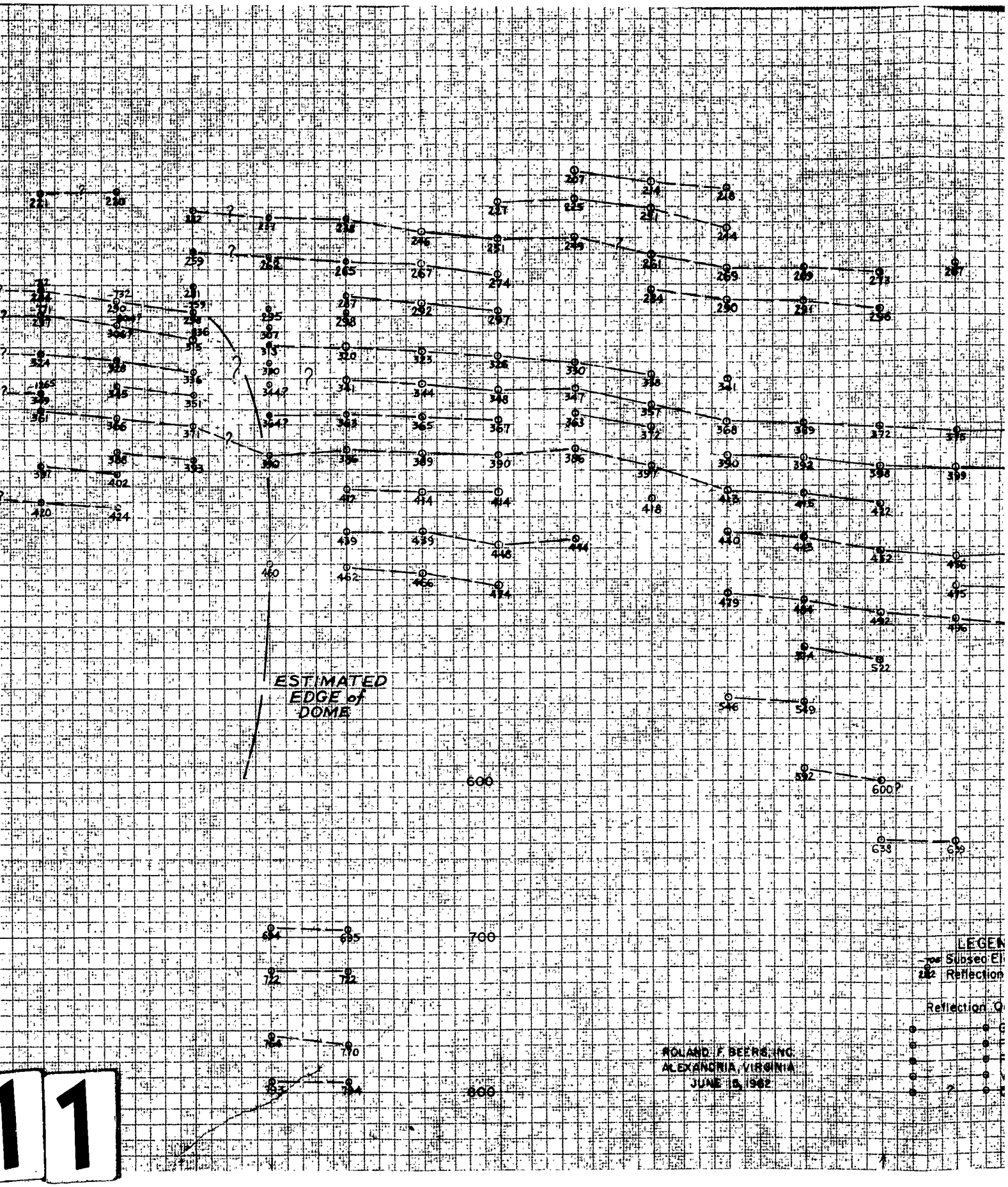
ESTIMATED
EDGE of
DOME
600
700
800
LEGEN
Subsea El
Reflection
Reflection Q
ROLAND F. BEERS, INC.
ALEXANDRIA, VIRGINIA
JUNE 15, 1962

11

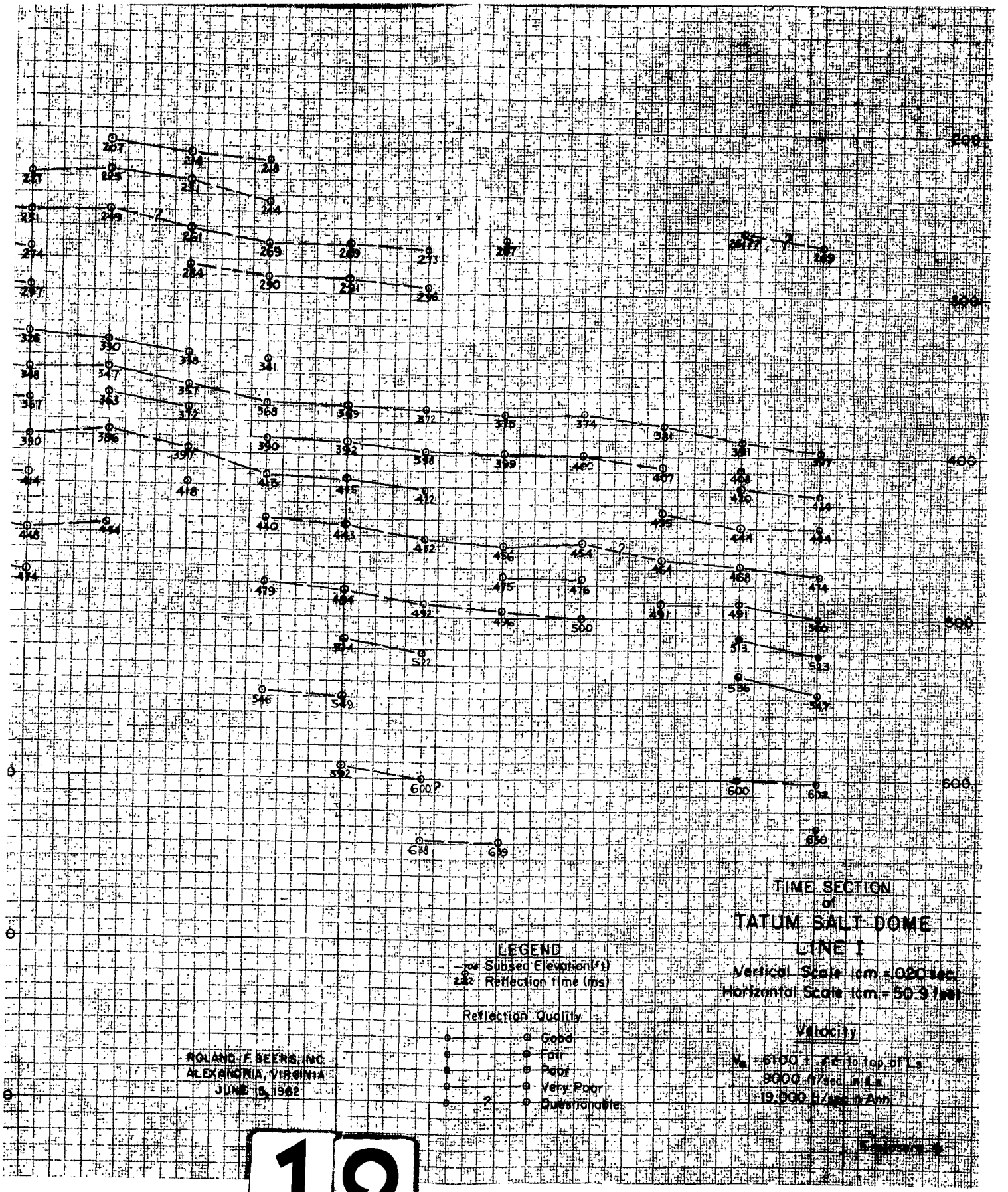
TIME SECTION
of
TATUM SALT DOME
LINE I
Vertical Scale 1cm = .020 sec.
Horizontal Scale 1cm = 50.9 feet
Velocity
V_s = 6100 + .72 to top of Ls
9000 ft/sec in Ls
19,000 ft/sec in Anh.
LEGEND
Subsea Elevation (ft)
Reflection time (ms)
Reflection Quality
Good
Fair
Poor
Very Poor
Questionable
ROLAND F. BEERS, INC.
ALEXANDRIA, VIRGINIA
JUNE 5, 1962
200
300
400
500
600

12

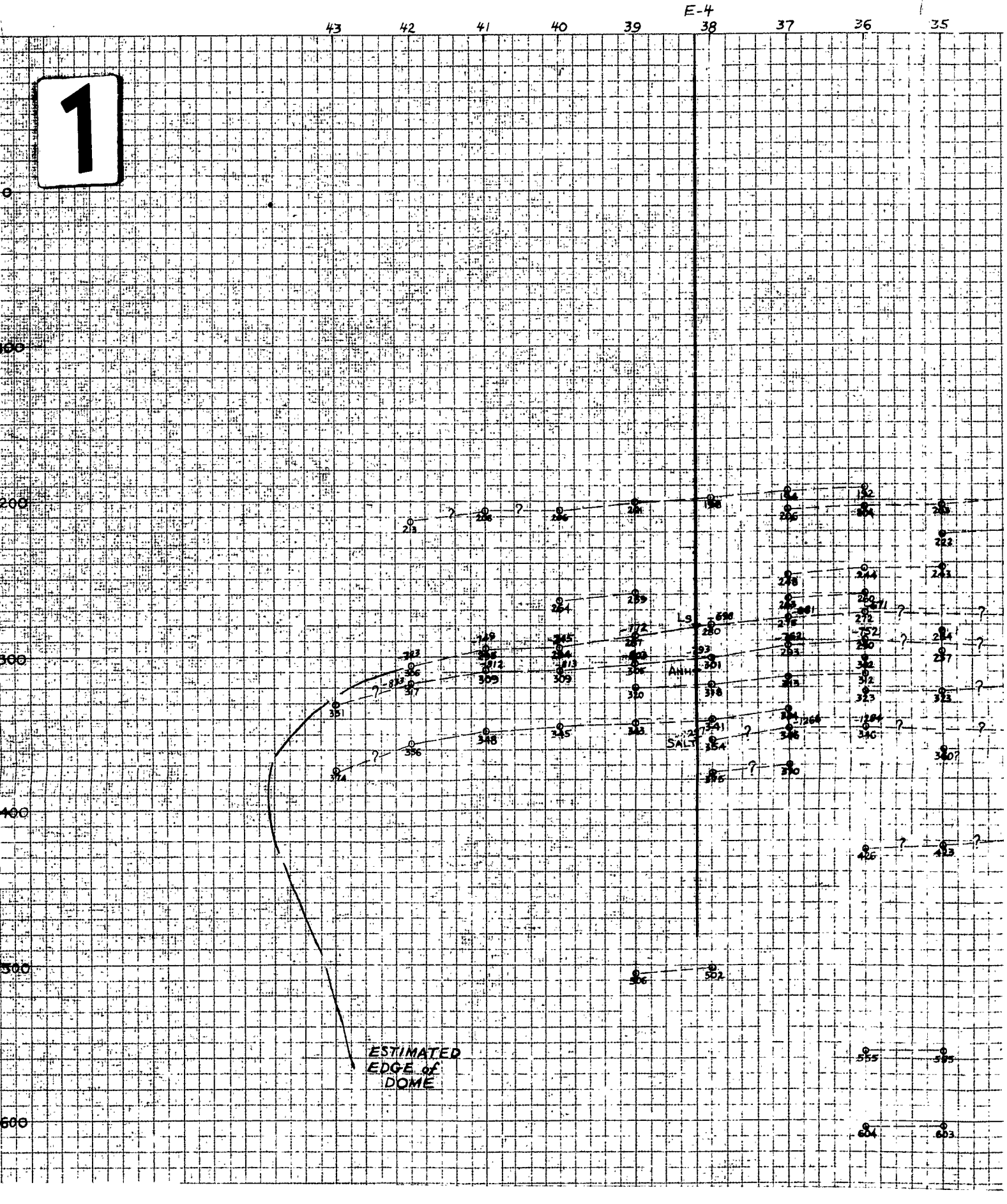
E-4
43
42
41
40
39
38
37
36
35
1
0
200
300
400
500
600
LS
ANH
SALT
ESTIMATED
EDGE of
DOME

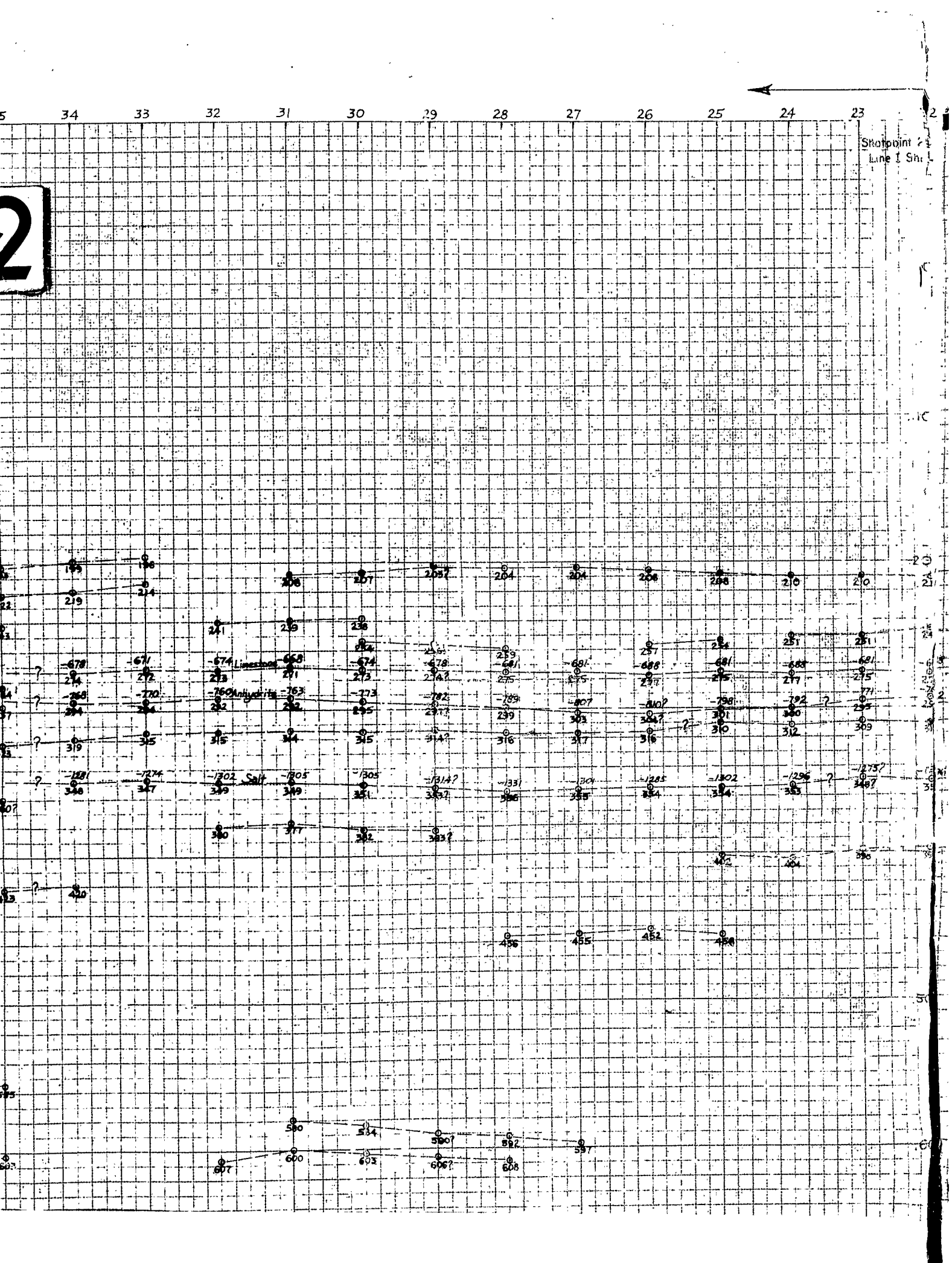
Shotpoint
Line 1 Sh
2
Limestone
Anhydrite
Salt

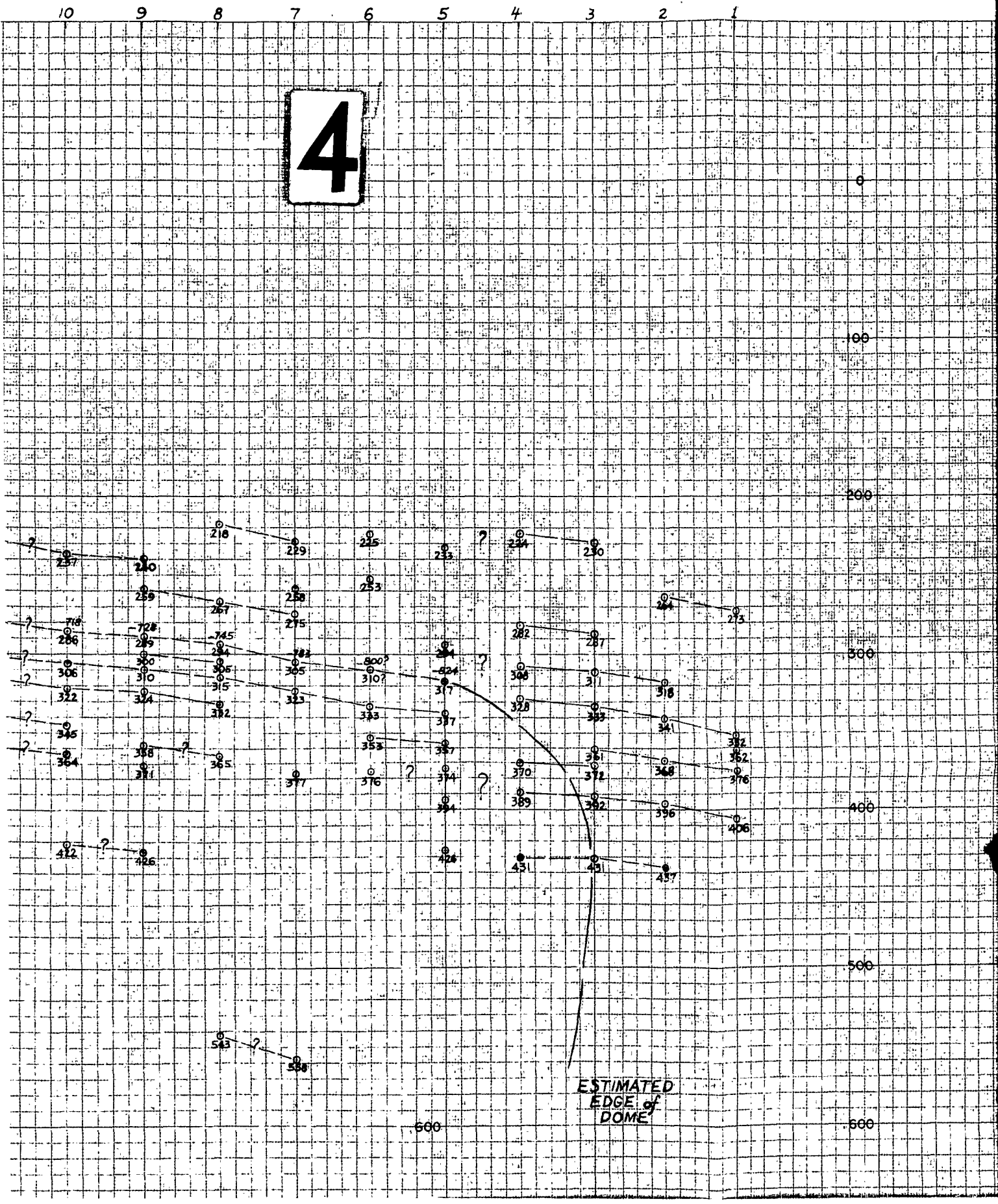
4
10
9
8
7
6
5
4
3
2
1
0
100
200
300
400
500
600
ESTIMATED EDGE of DOME

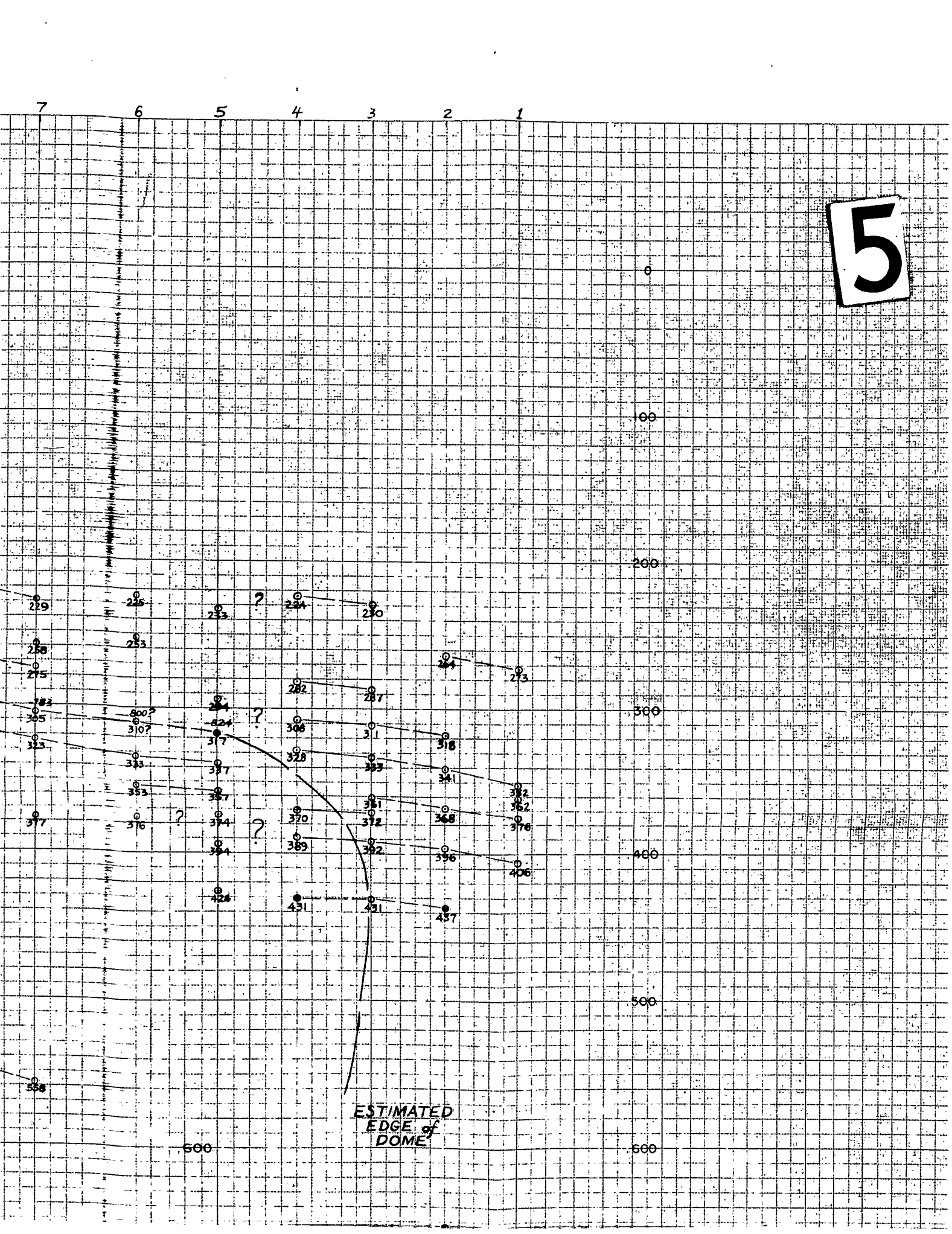

7
6
5
4
3
2
1
5
0
100
200
300
400
500
600
600
229
225
233
?
224
230
258
253
275
264
273
282
287
305
800?
310?
824
?
308
311
318
323
317
328
333
341
333
337
353
357
361
362
377
376
?
374
?
370
372
368
378
394
389
392
396
406
426
431
431
437
558
ESTIMATED EDGE of DOME

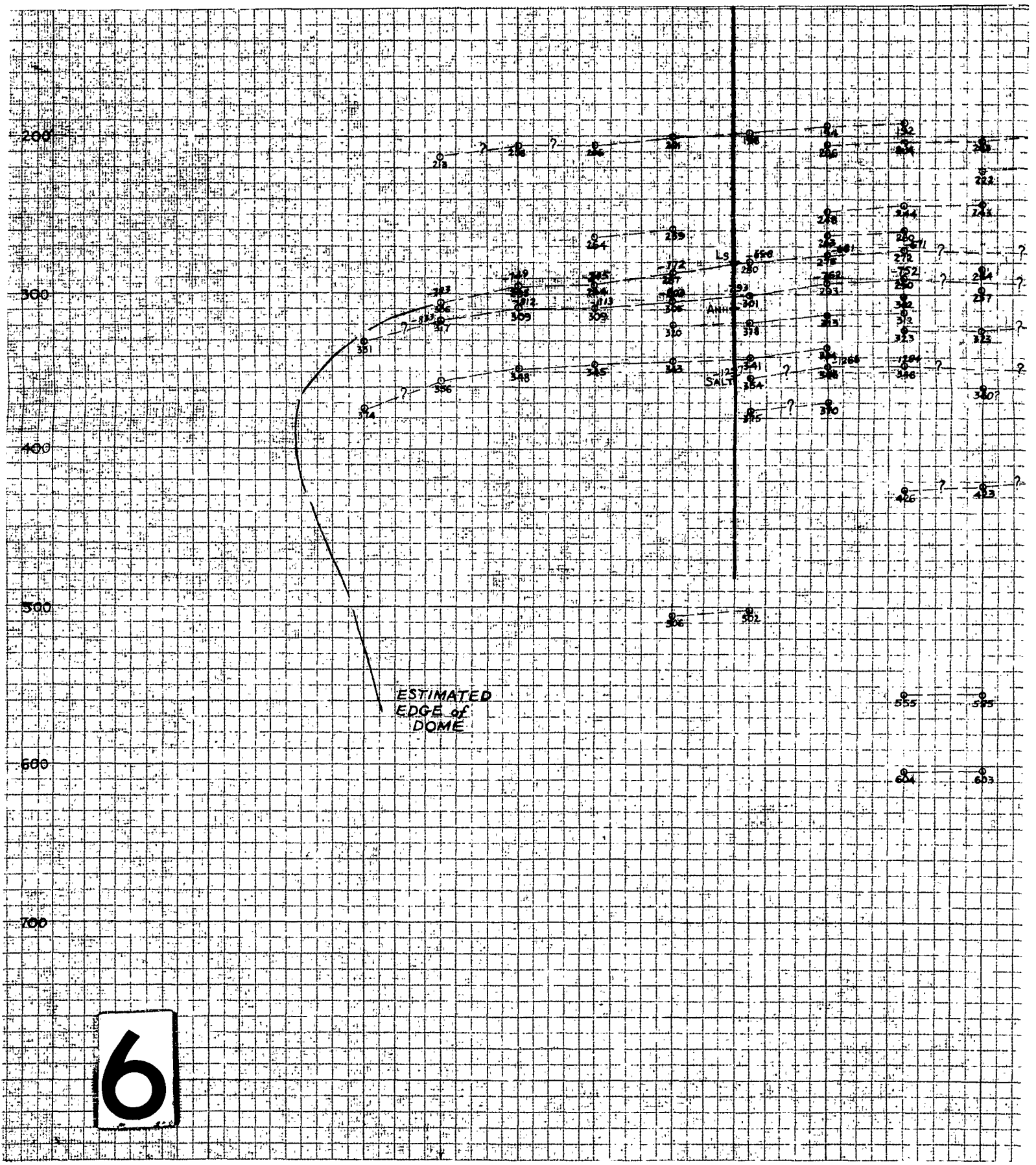

6

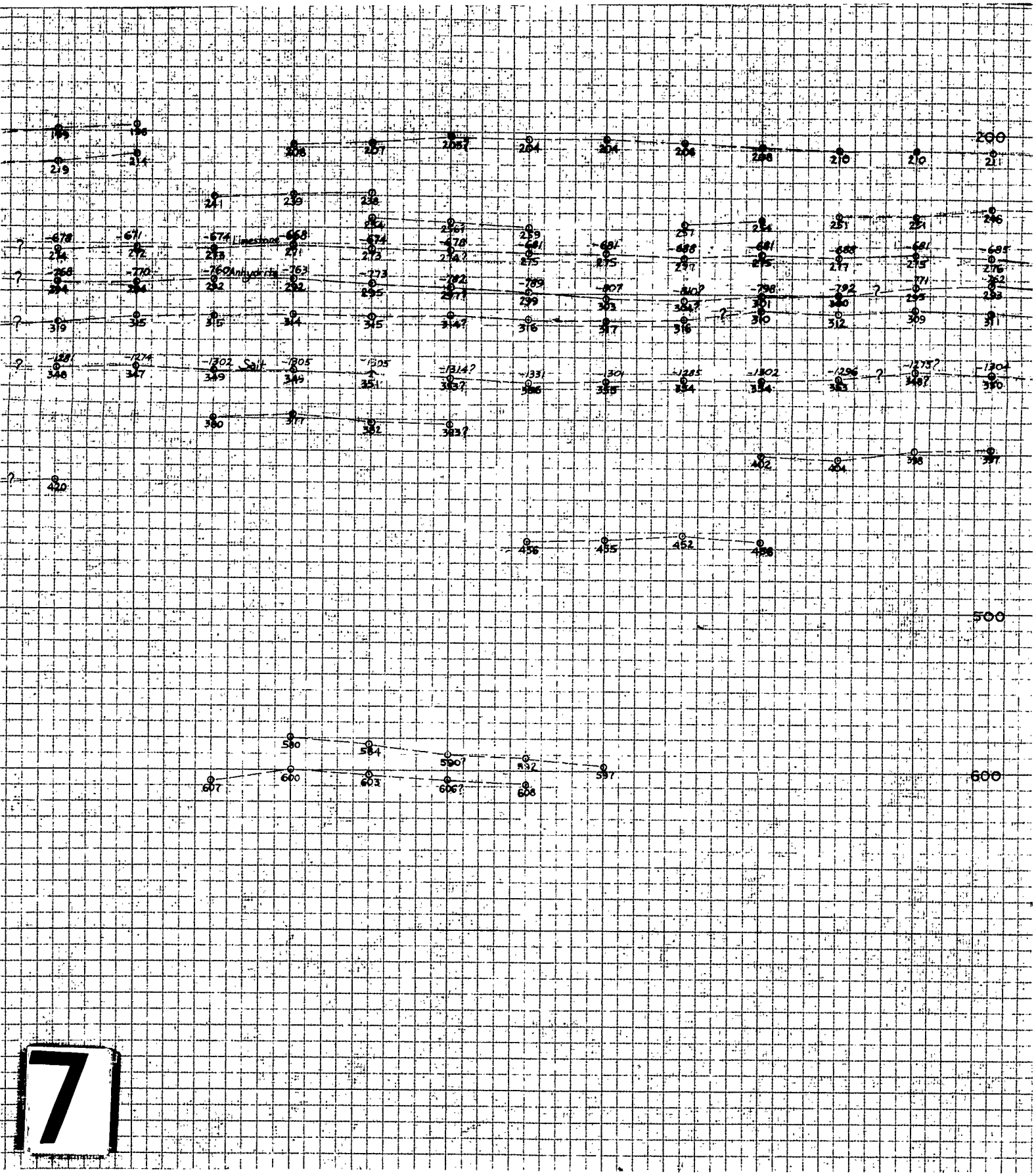
200
500
600
Limestone
Anhydrite
Salt

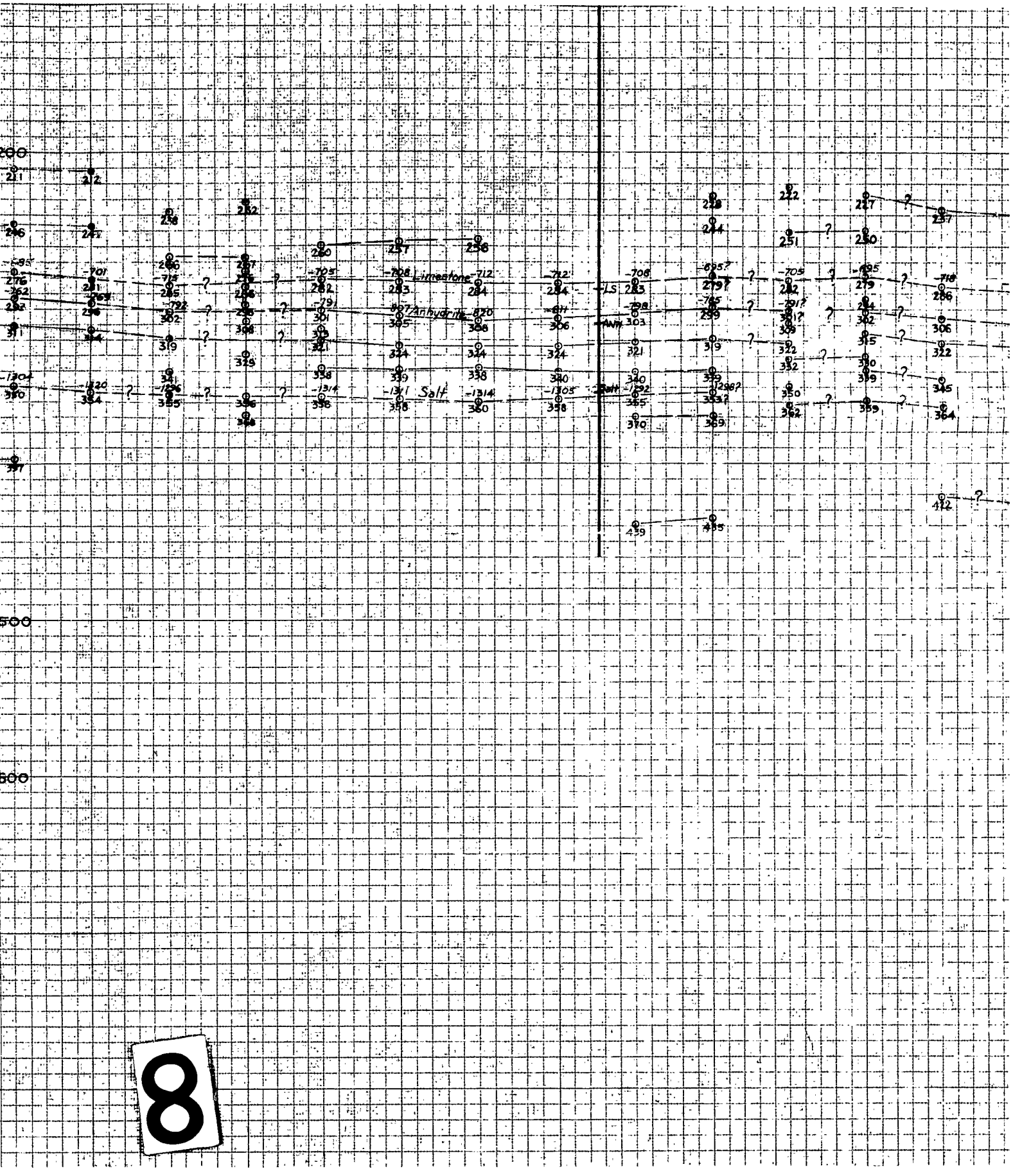
Limestone
Anhydrite
Salt
LS
ANH
500
600

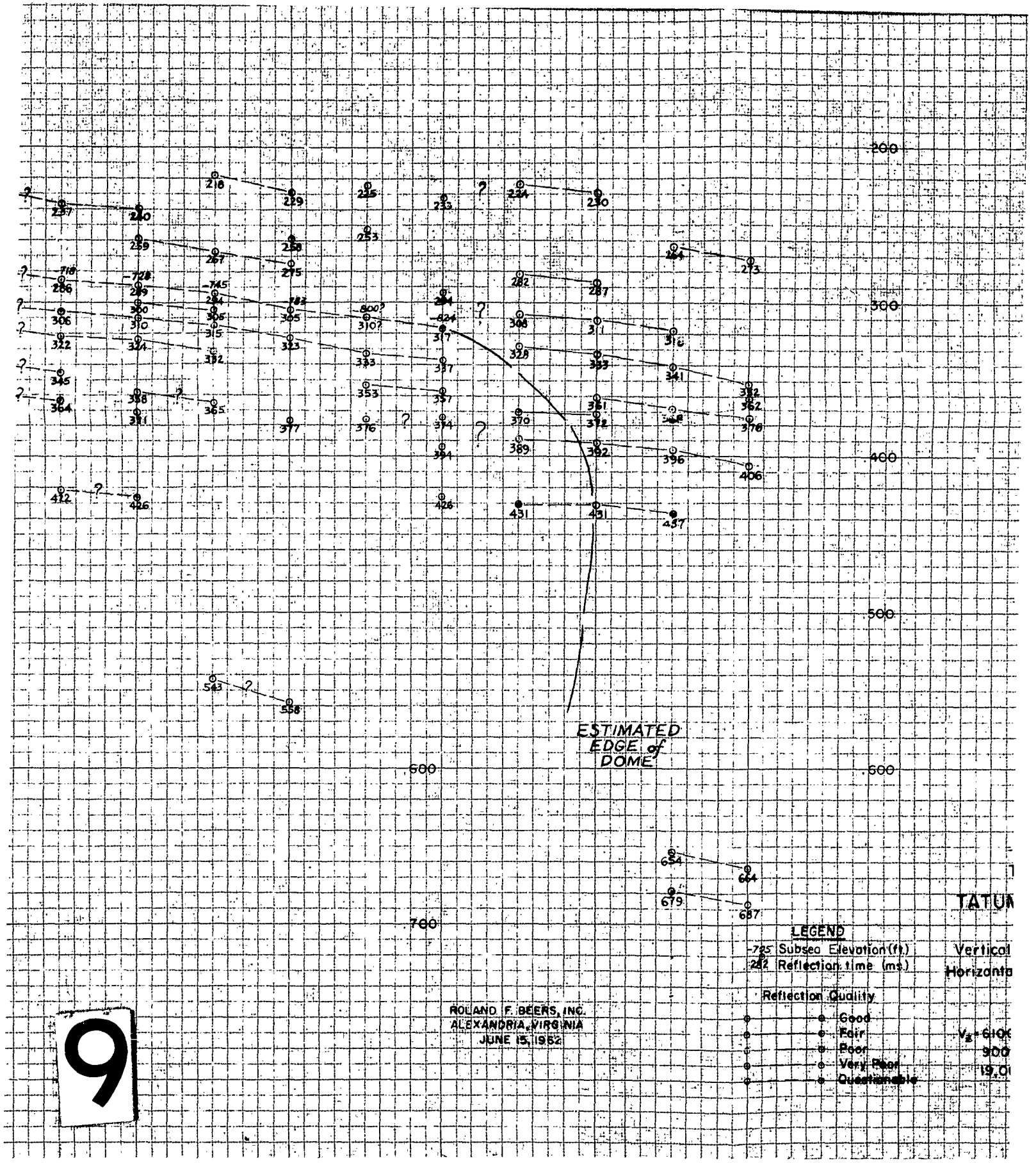
200
300
400
500
600
700
ESTIMATED EDGE of DOME
LEGEND
-725 Subsea Elevation (ft.)
282 Reflection time (ms.)
Reflection Quality
Good
Fair
Poor
Very Poor
Questionable
Vertical
Horizonta
TATUM
ROLAND F. BEERS, INC.
ALEXANDRIA, VIRGINIA
JUNE 15, 1962

9

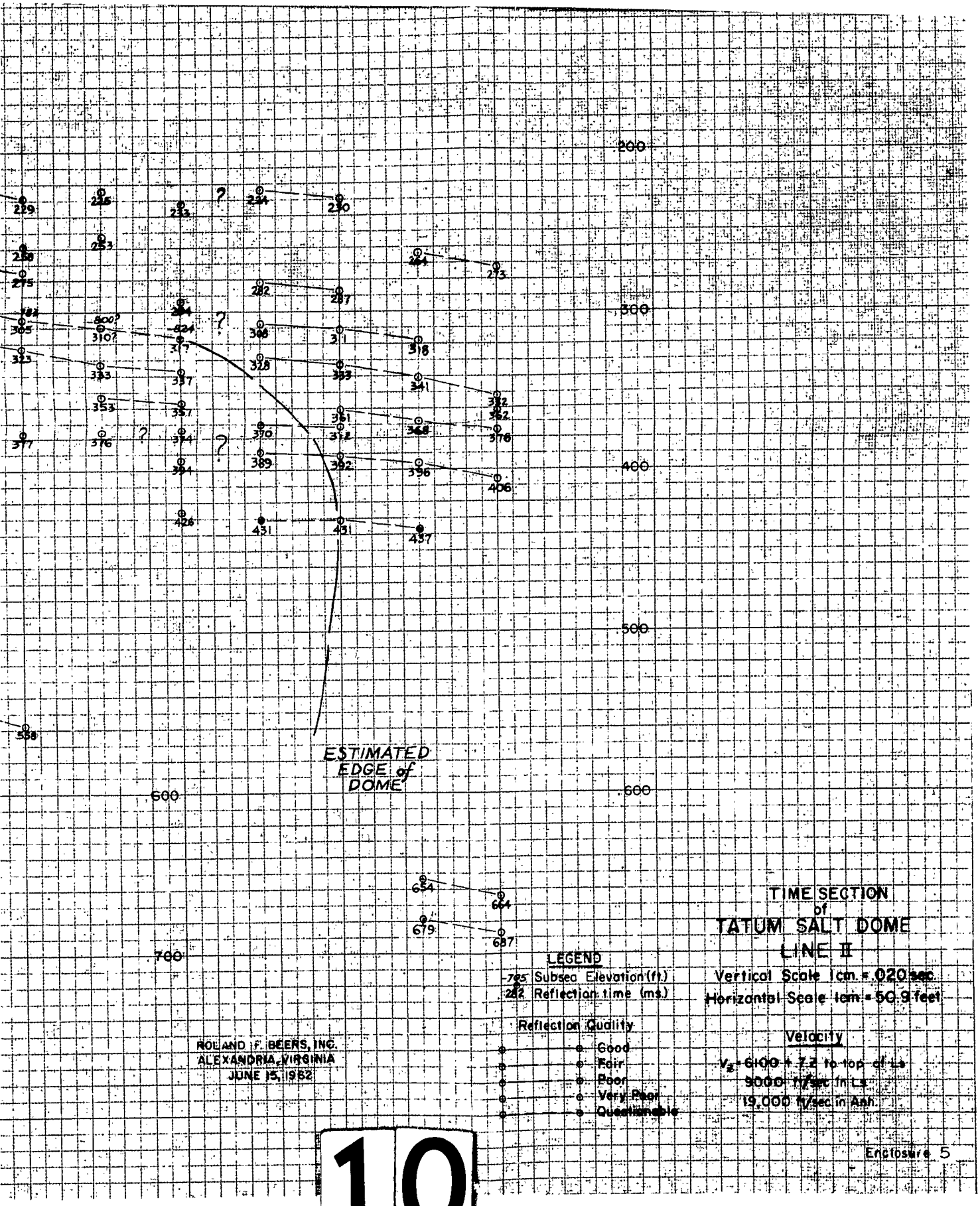

TIME SECTION
of
TATUM SALT DOME
LINE II

Vertical Scale 1cm. = 020 sec.
Horizontal Scale 1cm. = 50.9 feet

Velocity

V_z = 6100 + 7.2 to top of Ls
9000 ft/sec in Ls
19,000 ft/sec in Anh.

LEGEND

-795 Subsea Elevation (ft.)
282 Reflection time (ms.)

Reflection Quality

- Good
- Fair
- Poor
- Very Poor
- Questionable

ROLAND F. BEERS, INC.
ALEXANDRIA, VIRGINIA
JUNE 15, 1962

10

Enclosure 5